



ORNL/TM-12667

**OAK RIDGE  
NATIONAL  
LABORATORY**



## **Validation of the SCALE System for PWR Spent Fuel Isotopic Composition Analyses**

**O. W. Hermann  
S. M. Bowman  
M. C. Brady  
C. V. Parks**

MANAGED AND OPERATED BY  
LOCKHEED MARTIN ENERGY RESEARCH CORPORATION  
FOR THE UNITED STATES  
DEPARTMENT OF ENERGY

ORNL-27 (3-96)

This report has been reproduced directly from the best available copy.

Available to DOE and DOE contractors from the Office of Scientific and Technical Information, P.O. Box 62, Oak Ridge, TN 37831; prices available from (615) 576-8401, FTS 626-8401.

Available to the public from the National Technical Information Service, U.S. Department of Commerce, 5285 Port Royal Rd., Springfield, VA 22161.

This report was prepared as an account of work sponsored by an agency of the United States Government. Neither the United States nor any agency thereof, nor any of their employees, makes any warranty, express or implied, or assumes any legal liability or responsibility for the accuracy, completeness, or usefulness of any information, apparatus, product, or process disclosed, or represents that its use would not infringe privately owned rights. Reference herein to any specific commercial product, process, or service by trade name, trademark, manufacturer, or otherwise, does not necessarily constitute or imply its endorsement, recommendation, or favoring by the United States Government or any agency thereof. The views and opinions of authors expressed herein do not necessarily state or reflect those of the United States Government or any agency thereof.

Computational Physics and Engineering Division

**VALIDATION OF THE SCALE SYSTEM FOR PWR SPENT  
FUEL ISOTOPIC COMPOSITION ANALYSES**

O. W. Hermann  
S. M. Bowman  
M. C. Brady\*  
C. V. Parks

---

\*Sandia National Laboratories, Las Vegas, Nevada.

Date Published: March 1995

Prepared jointly for  
Sandia National Laboratories  
under subcontract AD-4072 with Oak Ridge National Laboratory  
and TRW Environmental Safety Systems  
under subcontract AT7708RT3X  
Oak Ridge National Laboratory

Prepared by the  
OAK RIDGE NATIONAL LABORATORY  
managed by  
MARTIN MARIETTA ENERGY SYSTEMS, INC.  
for the  
U.S. DEPARTMENT OF ENERGY  
under contract DE-AC05-84OR21400



# CONTENTS

	<u>Page</u>
LIST OF FIGURES .....	v
LIST OF TABLES .....	vi
ABSTRACT .....	xi
1. INTRODUCTION .....	1
2. MODEL AND METHODS IN SAS2H .....	3
2.1 BACKGROUND .....	3
2.2 MODULES AND DATA .....	4
2.3 METHOD AND TECHNIQUES .....	5
2.3.1 Neutronics Models .....	5
2.3.2 Burnup-Dependent Cross Sections .....	7
2.3.3 Final Depletion and Decay Analysis .....	10
2.4 INPUT FEATURES .....	10
2.5 HEAT GENERATION VALIDATION .....	11
3. PWR FUEL ASSEMBLY DATA FOR PROBLEMS ANALYZED .....	12
3.1 CALVERT CLIFFS PWR SPENT FUEL DESIGN AND OPERATING DATA .....	12
3.2 H. B. ROBINSON PWR SPENT FUEL DESIGN AND OPERATING DATA .....	23
3.3 OBRIGHEIM PWR SPENT FUEL DESIGN AND OPERATING DATA .....	29
3.4 ADDITIONAL PWR DATA USED FOR SCALE SYSTEM INPUT .....	29
4. PREDICTED AND MEASURED ISOTOPIC COMPOSITIONS .....	38
4.1 CALVERT CLIFFS PWR ANALYSES .....	38
4.2 H. B. ROBINSON PWR ANALYSES .....	38
4.3 OBRIGHEIM PWR ANALYSES .....	38
5. SUMMARY AND DISCUSSION OF RESULTS .....	51
5.1 SUMMARY OF THE RESULTS .....	51
5.2 BASIS FOR DISCUSSION .....	51
5.3 ACTINIDE NUCLIDE RESULTS .....	63
5.4 FISSION-PRODUCT RESULTS .....	64
5.5 COMPARISON OF MEASURED VS PREDICTED DIFFERENCES WITH EXPERIMENTAL UNCERTAINTIES .....	70
6. GENERAL SUMMARY .....	72
6.1 SUMMARY OF THE BENCHMARK COMPARISONS .....	72
6.2 CONCLUSIONS .....	73
REFERENCES .....	75

APPENDIX A. SAS2H INPUT FILES FOR CALVERT CLIFFS, H. B. ROBINSON, AND OBRIGHEIM FUEL ASSEMBLIES . . . . .	79
APPENDIX B. COMPARISONS OF MEASURED ISOTOPIC DATA TO SAS2H CALCULATIONS . . . . .	101
APPENDIX C. INDIVIDUAL LABORATORY OBRIGHEIM FUEL ISOTOPIC MEASUREMENTS, AVERAGES, AND 1 $\sigma$ IN ESTIMATE OF AVERAGES . . .	119
APPENDIX D. STATISTICAL DATA ANALYSIS OF SAS2H PREDICTIONS VS MEASUREMENTS . . . . .	125
APPENDIX E. MISCELLANEOUS SPATIAL FACTORS AFFECTING ASSEMBLY AVERAGED RESULTS . . . . .	129
E.1. RADIAL VARIATION IN $^{239}\text{Pu}$ . . . . .	129
E.2. AXIAL VARIATION IN $^{239}\text{Pu}$ . . . . .	135
E.3. SECONDARY EFFECTS OF VARIATION IN $^{239}\text{Pu}$ ON $^{235}\text{U}$ . . . . .	138

## LIST OF FIGURES

<u>Figure</u>	<u>Page</u>
1. Flow path invoked by SAS2H sequences. . . . .	6
2. Examples of larger unit cell for the model used in the path-B portion of SAS2H. . . . .	8
3. Schematic of successive ORIGEN-S cases used to produce the burnup-dependent number densities for a SAS2H case with two libraries per cycle . . . . .	9
4. Example of fuel depletion SAS2 input. . . . .	11
5. Location of Fuel Rod MKP109 in Assembly D047 . . . . .	16
6. Location of Fuel Rod MLA098 in Assembly D101 . . . . .	17
7. Location of Fuel Rod NBD107 in Assembly BT03 . . . . .	18
8. Location of Fuel Rod N-9 in diagram of Assembly B05 coupled with burnable poison fixture . . . . .	26
9. Fuel temperature versus rod power for Obrigheim . . . . .	28
10. SAS2H "path-B" model for Calvert Cliffs fuel assemblies . . . . .	34
11. Range in calculated vs measured isotopic differences for 19 cases (27BURNUPLIB cross-section data) . . . . .	52
12. Range in calculated vs measured isotopic differences for 10 assembly averages (27BURNUPLIB cross-section data) . . . . .	53
13. Range in calculated vs measured isotopic differences for 13 pellet sample cases (44GROUPNDF5 cross-section data) . . . . .	56
14. Range in calculated vs measured isotopic differences for 6 Obrigheim assemblies (44GROUPNDF5 cross-section data) . . . . .	57
15. ENDF/B Versions V and VI (n,γ) cross sections of <sup>155</sup> Eu at low neutron energies . . . . .	66
16. ENDF/B Versions V and VI (n,γ) cross sections of <sup>155</sup> Eu in a significant part of resonance region . . . . .	67
E.1. Method of simulating the actual rod locations (a) in unit cell (b) to obtain $\phi_1$ and $\phi_2$ . . . . .	131

## LIST OF TABLES

<u>Table</u>	<u>Page</u>
1. List of fuel nuclides automatically included by SAS2 for inclusion in neutronics processing . . . . .	9
2. Basic parameters of the measured spent fuel . . . . .	13
3. Calvert Cliffs general fuel assembly design data . . . . .	14
4. Fuel composition of Calvert Cliffs fuel assemblies . . . . .	15
5. Power histories and boron concentrations Fuel Assembly D047 Rod MKP109 . . . . .	20
6. Operating data for Calvert Cliffs Assembly D047, Rod MKP109, Assembly D101, Rod MLA098, and Assembly BT03, Rod NBD107 . . . . .	22
7. Moderator conditions and effective fuel temperatures for Calvert Cliffs 1 PWR . . . . .	24
8. Design data for H. B. Robinson Fuel Assembly B05 . . . . .	25
9. Operating data for H. B. Robinson Assembly B05, Rod N-9 pellet samples . . . . .	27
10. Moderator conditions and effective fuel temperatures for H. B. Robinson Unit 2 PWR . . . . .	27
11. Borosilicate glass composition in BP assemblies . . . . .	30
12. Borosilicate glass input atom densities . . . . .	30
13. Design data for the analyzed Obrigheim fuel assemblies . . . . .	31
14. Power history of Obrigheim fuel assemblies 168, 170, 171, 172, and 176 . . . . .	32
15. Operating data for the Obrigheim fuel assemblies and dissolved fuel batches . . . . .	33
16. Light-element mass per unit of fuel for SAS2H input . . . . .	36
17. Effective parameters of the 21 nonfuel positions—20 guide tubes (12 with BPRs) and 1 instrument tube . . . . .	36
18. Fuel, fuel activation, fission product, and light-element nuclides for which cross sections were updated in SAS2H cases . . . . .	37
19. Measured irradiated composition, in g/g UO <sub>2</sub> , of Calvert Cliffs Assembly D047 Rod MKP109 . . . . .	39
20. Measured irradiated composition, in g/g UO <sub>2</sub> , of Calvert Cliffs Assembly D101 Rod MLA098 . . . . .	40
21. Measured irradiation composition, in g/g UO <sub>2</sub> , of Calvert Cliffs Assembly BT03 Rod NBD107 . . . . .	40
22. Measured irradiation composition, in Ci/g UO <sub>2</sub> , of Calvert Cliffs Assembly D047 Rod MKP109 . . . . .	41
23. Measured irradiation composition, in Ci/g UO <sub>2</sub> , of Calvert Cliffs Assembly D101 Rod MLA098 . . . . .	41
24. Measured irradiation composition, in Ci/g UO <sub>2</sub> , of Calvert Cliffs Assembly BT03 Rod NBD107 . . . . .	42
25. Percentage difference between measured and computed nuclide compositions for Calvert Cliffs PWR pellet samples (27BURNUPLIB library) . . . . .	43
26. Percentage difference between measured and computed nuclide compositions for Calvert Cliffs PWR pellet samples (44GROUPNDF5 library) . . . . .	44
27. Average percentage difference between measured and computed nuclide compositions for each Calvert Cliffs PWR assembly, using two ENDF/B data versions . . . . .	45



28.	Measured irradiation composition, in g/g UO <sub>2</sub> , of H. B. Robinson Assembly B05 Rod N-9	46
29.	Measured irradiation composition, in Ci/g UO <sub>2</sub> , of H. B. Robinson Assembly B05 Rod N-9	46
30.	Percentage difference between measured and computed nuclide compositions for H. B. Robinson PWR pellet samples and average from Assembly B05 Rod N-9 (27BURNUPLIB library)	47
31.	Percentage difference between measured and computed nuclide compositions for H. B. Robinson PWR pellet samples and average from Assembly B05 Rod N-9 (44GROUPNDF5 library)	47
32.	Obrigheim average measured nuclide composition relative to time of unloading, in g/MTU	48
33.	Obrigheim average measured isotopic atomic ratios relative to time of unloading	48
34.	Percentage difference between measured and computed nuclide compositions and atomic ratios for Obrigheim PWR assembly samples (using 27BURNUPLIB cross sections)	49
35.	Percentage difference between measured and computed nuclide compositions and atomic ratios for Obrigheim PWR assembly samples (using 44GROUPNDF5 cross sections)	50
36.	Average percentage difference between measured and computed nuclide compositions or atom ratios for each PWR fuel assembly examined and averages of all assemblies (27BURNUPLIB library)	54
37.	Average percentage difference between measured and computed nuclide compositions or atom ratios for each PWR fuel assembly examined and averages of all assemblies (44GROUPNDF5 library)	58
38.	Summary of percentage difference averages and spreads relative to the separate cases and the assembly evaluations	60
39.	Percentage differences for each element averaged over the absolute values of percentage differences for all isotopes of the element	62
40.	Examples of differences between SCALE derived actinide cross sections processed from ENDF/B-IV and ENDF/B-V data	65
41.	Summary of experimental uncertainties compared with average percentage differences in measured and computed compositions	71
A.1.	Calvert Cliffs Assembly D047 Rod MKP109, 27.35 GWd/MTU, ENDF/B-IV	80
A.2.	Calvert Cliffs Assembly D047 Rod MKP109, 37.12 GWd/MTU, ENDF/B-IV	80
A.3.	Calvert Cliffs Assembly D047 Rod MKP109, 44.34 GWd/MTU, ENDF/B-IV	81
A.4.	Calvert Cliffs Assembly D101 Rod MLA098, 18.68 GWd/MTU, ENDF/B-IV	81
A.5.	Calvert Cliffs Assembly D101 Rod MLA098, 26.62 GWd/MTU, ENDF/B-IV	82
A.6.	Calvert Cliffs Assembly D101 Rod MLA098, 33.17 GWd/MTU, ENDF/B-IV	82
A.7.	Calvert Cliffs Assembly BT03 Rod NBD107, 31.40 GWd/MTU, ENDF/B-IV	83
A.8.	Calvert Cliffs Assembly BT03 Rod NBD107, 37.27 GWd/MTU, ENDF/B-IV	83
A.9.	Calvert Cliffs Assembly BT03 Rod NBD107, 46.46 GWd/MTU, ENDF/B-IV	84
A.10.	H. B. Robinson Assembly B05 Rod N-9, 16.02 GWd/MTU, ENDF/B-IV	84
A.11.	H. B. Robinson Assembly B05 Rod N-9, 23.81 GWd/MTU, ENDF/B-IV	85
A.12.	H. B. Robinson Assembly B05 Rod N-9, 28.47 GWd/MTU, ENDF/B-IV	85
A.13.	H. B. Robinson Assembly B05 Rod N-9, 31.66 GWd/MTU, ENDF/B-IV	86

A.14.	Obrigheim (KWO) Assembly 170 Batch 94, 25.93 GWd/MTU, ENDF/B-IV	86
A.15.	Obrigheim (KWO) Assembly 172 Batch 92, 26.54 GWd/MTU, ENDF/B-IV	87
A.16.	Obrigheim (KWO) Assembly 176 Batch 91, 27.99 GWd/MTU, ENDF/B-IV	87
A.17.	Obrigheim (KWO) Assembly 168 Batch 86, 28.40 GWd/MTU, ENDF/B-IV	88
A.18.	Obrigheim (KWO) Assembly 171 Batch 89, 29.04 GWd/MTU, ENDF/B-IV	88
A.19.	Obrigheim (KWO) Assembly 176 Batch 90, 29.52 GWd/MTU, ENDF/B-IV	89
A.20.	Calvert Cliffs Assembly D047 Rod MKP109, 27.35 GWd/MTU, ENDF/B-V	89
A.21.	Calvert Cliffs Assembly D047 Rod MKP109, 37.12 GWd/MTU, ENDF/B-V	90
A.22.	Calvert Cliffs Assembly D047 Rod MKP109, 44.34 GWd/MTU, ENDF/B-V	90
A.23.	Calvert Cliffs Assembly D101 Rod MLA098, 18.68 GWd/MTU, ENDF/B-V	91
A.24.	Calvert Cliffs Assembly D101 Rod MLA098, 26.62 GWd/MTU, ENDF/B-V	91
A.25.	Calvert Cliffs Assembly D101 Rod MLA098, 33.17 GWd/MTU, ENDF/B-V	92
A.26.	Calvert Cliffs Assembly BT03 Rod NBD107, 31.40 GWd/MTU, ENDF/B-V	92
A.27.	Calvert Cliffs Assembly BT03 Rod NBD107, 37.27 GWd/MTU, ENDF/B-V	93
A.28.	Calvert Cliffs Assembly BT03 Rod NBD107, 46.46 GWd/MTU, ENDF/B-V	93
A.29.	H. B. Robinson Assembly B05 Rod N-9, 16.02 GWd/MTU, ENDF/B-V	94
A.30.	H. B. Robinson Assembly B05 Rod N-9, 23.81 GWd/MTU, ENDF/B-V	94
A.31.	H. B. Robinson Assembly B05 Rod N-9, 28.47 GWd/MTU, ENDF/B-V	95
A.32.	H. B. Robinson Assembly B05 Rod N-9, 31.66 GWd/MTU, ENDF/B-V	95
A.33.	Obrigheim (KWO) Assembly 170 Batch 94, 25.93 GWd/MTU, ENDF/B-V	96
A.34.	Obrigheim (KWO) Assembly 172 Batch 92, 26.54 GWd/MTU, ENDF/B-V	97
A.35.	Obrigheim (KWO) Assembly 176 Batch 91, 27.99 GWd/MTU, ENDF/B-V	97
A.36.	Obrigheim (KWO) Assembly 168 Batch 86, 28.40 GWd/MTU, ENDF/B-V	98
A.37.	Obrigheim (KWO) Assembly 171 Batch 89, 29.04 GWd/MTU, ENDF/B-V	98
A.38.	Obrigheim (KWO) Assembly 176 Batch 90, 29.52 GWd/MTU, ENDF/B-V	99
B.1.	Calvert Cliffs Assembly D047 Rod MKP109, 27.35 GWd/MTU	102
B.2.	Calvert Cliffs Assembly D047 Rod MKP109, 37.12 GWd/MTU	103
B.3.	Calvert Cliffs Assembly D047 Rod MKP109, 44.34 GWd/MTU	104
B.4.	Calvert Cliffs Assembly D101 Rod MLB.98, 18.68 GWd/MTU	105
B.5.	Calvert Cliffs Assembly D101 Rod MLB.98, 26.62 GWd/MTU	106
B.6.	Calvert Cliffs Assembly D101 Rod MLB.98, 33.17 GWd/MTU	107
B.7.	Calvert Cliffs Assembly BT03 Rod NBD107, 31.40 GWd/MTU	108
B.8.	Calvert Cliffs Assembly BT03 Rod NBD107, 37.27 GWd/MTU	109
B.9.	Calvert Cliffs Assembly BT03 Rod NBD107, 46.46 GWd/MTU	110
B.10.	H. B. Robinson Assembly B05 Rod N-9, 16.02 GWd/MTU	111
B.11.	H. B. Robinson Assembly B05 Rod N-9, 23.81 GWd/MTU	111
B.12.	H. B. Robinson Assembly B05 Rod N-9, 28.47 GWd/MTU	112
B.13.	H. B. Robinson Assembly B05 Rod N-9, 31.66 GWd/MTU	112
B.14.	Obrigheim (KWO) Assembly 170 Batch 94, 25.93 GWd/MTU	113
B.15.	Obrigheim (KWO) Assembly 172 Batch 92, 26.54 GWd/MTU	114
B.16.	Obrigheim (KWO) Assembly 176 Batch 91, 27.99 GWd/MTU	115
B.17.	Obrigheim (KWO) Assembly 168 Batch 86, 28.40 GWd/MTU	116
B.18.	Obrigheim (KWO) Assembly 171 Batch 89, 29.04 GWd/MTU	117
B.19.	Obrigheim (KWO) Assembly 176 Batch 90, 29.52 GWd/MTU	118
C.1.	Obrigheim fuel composition measurements, their averages, and 1 $\sigma$ in the averages for $^{235}\text{U}$ (milligrams/gram U)	120

C.2.	Obrigheim fuel composition measurements, their averages, and 1 $\sigma$ in the averages for $^{236}\text{U}$ (milligrams/gram U) . . . . .	120
C.3.	Obrigheim fuel composition measurements, their averages, and 1 $\sigma$ in the averages for $^{238}\text{Pu}$ (milligrams/gram U) . . . . .	121
C.4.	Obrigheim fuel composition measurements, their averages, and 1 $\sigma$ in the averages for $^{239}\text{Pu}$ (milligrams/gram U) . . . . .	121
C.5.	Obrigheim fuel composition measurements, their averages, and 1 $\sigma$ in the averages for $^{240}\text{Pu}$ (milligrams/gram U) . . . . .	122
C.6.	Obrigheim fuel composition measurements, their averages, and 1 $\sigma$ in the averages for $^{241}\text{Pu}$ (milligrams/gram U) . . . . .	122
C.7.	Obrigheim fuel composition measurements, their averages, and 1 $\sigma$ in the averages for $^{242}\text{Pu}$ (milligrams/gram U) . . . . .	123
D.1.	Statistics for SAS2H vs measurements, actinide data from ENDF/B-IV . . . . .	126
D.2.	Statistics for SAS2H vs measurements, actinide data from ENDF/B-V . . . . .	127
E.1.	Example of effective cross sections, $\sigma(n,\gamma)_{\text{U}238}$ and $\sigma(n,f)_{\text{U}235}$ , derived from group values and flux $\phi_1$ and $\phi_2$ at unit cell locations $d_1$ and $d_2$ . . . . .	133
E.2.	Fuel-rod-dependent $^{239}\text{Pu}$ production rate ratio from XSDRNPM computed activities $\Sigma(n,\gamma)_{\text{U}238} \phi$ and $\Sigma(n,f)_{\text{Total}} \phi$ . . . . .	134
E.3.	Differences between measured and computed $^{239}\text{Pu}$ contents over the range in burnup along the fuel rods . . . . .	136
E.4.	PWR $^{235}\text{U}$ enrichments for different burnups . . . . .	137
E.5.	Measured fissionable nuclide contents and computed neutron multiplication constant ( $k_\infty$ ) of Assembly D047 Rod MKP109 . . . . .	137



## ABSTRACT

The validity of the computation of pressurized-water-reactor (PWR) spent fuel isotopic composition by the SCALE system depletion analysis was assessed using data presented in the report. Radiochemical measurements and SCALE/SAS2H computations of depleted fuel isotopics were compared with 19 benchmark-problem samples from Calvert Cliffs Unit 1, H. B. Robinson Unit 2, and Obrigheim PWRs. Even though not exhaustive in scope, the validation included comparison of predicted and measured concentrations for 14 actinides and 37 fission and activation products.

The basic method by which the SAS2H control module applies the neutron transport treatment and point-depletion methods of SCALE functional modules (XSDRNPM-S, NITAWL-II, BONAMI, and ORIGEN-S) is described in the report. Also, the reactor fuel design data, the operating histories, and the isotopic measurements for all cases are included in detail. The underlying radiochemical assays were conducted by the Materials Characterization Center at Pacific Northwest Laboratory as part of the Approved Testing Material program and by four different laboratories in Europe on samples processed at the Karlsruhe Reprocessing Plant.

Comparisons are given in terms of percentage differences of computed minus measured compositions of the fuel. The SCALE depletion analyses for all cases applied two different cross-section libraries. One was the 27-energy-group SCALE-4 library, which has light-element and actinide data processed from ENDF/B-IV and fission-product data processed from ENDF/B-V. The second library applied was a 44-energy-group library derived entirely from the latest ENDF/B-V files with the exception that data for  $^{16}\text{O}$ ,  $^{154}\text{Eu}$ , and  $^{155}\text{Eu}$  were taken from ENDF/B-VI. Almost all the total average percentage differences for the actinide isotopes and for the isobaric mass values 154 and 155 were significantly better in cases using the latter library, whereas other fission-product comparisons with measurements were essentially the same in using either library. The final fuel rod and batch average differences for nuclides  $^{235}\text{U}$  and  $^{239}\text{Pu}$  were  $-3.1$  and  $5.4\%$  for the former library and  $-2.2$  and  $-0.4\%$  for the latter library, respectively. Except for  $^{237}\text{Np}$ , only  $^{242}\text{Cm}$  and  $^{244}\text{Cm}$  had excessive differences ( $>15\%$ ); these isotopes had similarly large uncertainties in their measurements. The percentage differences exceeded 15% for fission products  $^{99}\text{Tc}$ ,  $^{126}\text{Sn}$ ,  $^{148}\text{Sm}$ ,  $^{149}\text{Sm}$ ,  $^{151}\text{Sm} + ^{151}\text{Eu}$ ,  $^{152}\text{Sm}$ ,  $^{154}\text{Sm} + ^{154}\text{Eu} + ^{154}\text{Gd}$  (for the former library only) and  $^{155}\text{Eu} + ^{155}\text{Gd}$ . Although the spread of the percentage differences for all cases of each nuclide were large (particularly for comparisons of pellet sample results), reasons why the pellet-location-dependence of reactor flux affect significant nuclide reaction rates were briefly investigated and discussed. It was concluded by the authors that the SCALE depletion analysis properly qualifies as a basic tool for predicting isotopic compositions of spent fuel from PWR power plants. Also, it was evident that cross sections of actinide isotopes processed from ENDF/B-V were superior to those taken from ENDF/B-IV.



## 1. INTRODUCTION

The radionuclide characteristics of light-water-reactor (LWR) spent fuel play key roles in the design and licensing activities for radioactive waste transportation systems, interim storage facilities, and the final repository site. Several areas of analysis require detailed information concerning the time-dependent behavior of radioactive nuclides including (1) neutron/gamma-ray sources for shielding studies, (2) fissile/absorber concentrations for criticality safety determinations, (3) residual decay heat predictions for thermal considerations, and (4) curie and/or radiological toxicity levels for materials assumed to be released into the ground/environment after long periods of time. One of the functions of the SCALE (Standardized Computer Analyses for Licensing Evaluation) code system<sup>1</sup> is to predict the radionuclide composition of depleted fuel discharged from a pressurized-water reactor (PWR). Recent applications of calculated isotopic contents for depleted reactor fuel include several criticality safety analyses for investigation of storage or shipment of spent fuel.<sup>2-6</sup> The ANSI/ANS 8.1 criticality safety standard<sup>7</sup> requires validation<sup>8</sup> of the analytical methods used in these spent fuel criticality analyses. Although this study focuses on isotopes important for criticality studies, the results should be of sufficient scope to apply to other areas such as radiation shielding and heat transfer as well. The purpose of this report is to present and discuss a set of problems to be used in the validation of the SCALE modular code system for computing the isotopic content of PWR spent fuel.

The spent fuel isotopic predictions reported in this document were computed by the SAS2H control module<sup>1,9,10</sup> contained in Version 4.2 of the SCALE system (SCALE-4.2) except for an additional application of the more recently developed 44-group cross-section library noted below. All further references to SCALE-4 in this document refer generically to Version 4 of the SCALE system, although all calculations herein were performed with SCALE-4.2. The major portion of the radiochemical assays of PWR spent fuel included in this study were conducted<sup>11-14</sup> by the Material Characteristics Center (MCC) at Pacific Northwest Laboratory (PNL) using discharged PWR fuel from Calvert Cliffs Unit 1 and H. B. Robinson Unit 2. Additional spent fuel characterizations<sup>15,16</sup> presented herein were conducted by four research laboratories in Europe using fuel elements from the Obrigheim (KWO) PWR.

A wide range of parameters was included in the problems analyzed for this study. The fuel exposures, or burnups, are in the range 16.02 to 46.46 gigawatt days per metric ton uranium (GWd/MTU). The PWR designs are substantially different. Also, there are significant variations in fuel <sup>235</sup>U enrichments (2.45 to 3.04 wt %), assembly power histories, material temperatures (743 to 923 K), specific powers (13.1 to 44.7 MW/MTU), and other pertinent operational conditions among the cases considered.

The source of the neutron cross-section data used in fuel depletion analyses by the SCALE system is a significant aspect of the validation. Two different cross-section libraries were applied. The SCALE "27BURNUPLIB" cross-section library (Vol. III, Sect. M4.2.8 of ref. 1) has actinide and light-element data derived from Version IV of the Evaluated Nuclear Data Files (ENDF) and fission-product data processed from early ENDF/B-V files. The second library, "44GROUPNDF5,"<sup>17</sup> applied in the analyses reported here, is a 44-energy-group library derived entirely from the latest ENDF/B-V files with the exception of data for three nuclides. The cross sections for <sup>16</sup>O, <sup>154</sup>Eu, and <sup>155</sup>Eu in this library were taken from ENDF/B-VI;<sup>18</sup> the cross sections of the latter two nuclides were expected to substantially improve the computation of <sup>154</sup>Eu, <sup>155</sup>Eu, and <sup>155</sup>Gd inventories.

The model and methods applied in SAS2H are discussed in the next section. The benchmark problems used in this analysis are given in the subsequent section, including the reactor fuel assembly design and operating data required for input to the SCALE fuel depletion cases. Comparisons of predicted and measured isotopic compositions of the problems for the three reactors are then presented, discussed, and summarized. Finally, the reliability of the basic data and computation techniques based on comparisons of predicted and measured isotopics is discussed in the general summary of this report.



## 2. MODEL AND METHODS IN SAS2H

The SAS2H control module of the SCALE code system has been documented extensively elsewhere (Sect. S2, ref. 1). A concise description of the model is included in this section.

### 2.1 BACKGROUND

The SAS2H control module of the SCALE-4 system was designed to provide an automated, yet highly flexible, analysis sequence for determining the characteristics of spent fuel (i.e., isotopics, decay heat, radiation sources, etc.). The SAS2 control module was originally developed for earlier versions of SCALE to provide a sequence that generates radiation source terms for spent fuel and to utilize these sources within a one-dimensional (1-D) shielding analysis of a shipping cask. Although the shielding portion of the sequence can still be accessed, the principal use of SAS2(H) over its history has been fuel depletion and decay analyses to obtain spent fuel characteristics needed for subsequent analyses. Because earlier SAS2 versions used an infinite lattice pin-cell model for the neutronics analysis, only variations in lattice design and composition could be considered. This simple procedure has been shown to produce conservative actinide inventories for PWR spent fuel, but does not provide the versatility required for depletion analysis of boiling-water-reactor (BWR) fuel.<sup>19</sup> Thus, the original SAS2 sequence has been enhanced considerably to produce the SCALE-4 version that is denoted as SAS2H. With the SAS2H model, the presence of water holes, control rods, burnable poison rods (BPRs) orifice tubes, and other assembly design features can be considered in an approximate fashion. This new capability allows a more accurate evaluation of isotopic concentrations and source terms at long cooling times (>10 years), where actinide contributions are more important.

The criteria originally applied in developing the SAS2 module have not changed over its continual evolution. These criteria are the following:

1. predict, using first principles, the nuclear characteristics for spent fuel assemblies having a specified reactor history;
2. predict radiation dose rates for a radial model of a shipping cask containing spent fuel with the calculated characteristics;
3. permit the user to supply a minimal quantity of input using the relatively convenient format of the SCALE system;
4. apply standard analytical models using well-established computer codes to represent the physics of the system being analyzed within the 1-D limits of the codes;
5. apply acceptable and documented data bases, which can be updated in the future;
6. automate the use of known methods in calculating some of the input parameters and the selection of appropriate control options for the various codes applied in the analysis;
7. document extensively the analytical techniques, limitations, program flow, sample cases, and user's guide; and
8. make both the code and the manual easily available to the technical community.

In noting the more general value of the module, the neutron and photon spectral sources produced by SAS2H can now be conveniently accessed by the SCALE shielding analysis modules.

The remainder of this section describes the SAS2H analysis sequence used to calculate the characteristics of spent LWR fuel. Previous limited validation/verification efforts for the SAS2H models and results will also be discussed.

## 2.2 MODULES AND DATA

The SAS2H control module performs the depletion/decay analysis using the well-established codes (or functional modules) and data libraries provided in the SCALE system. The applicable modules and data libraries are reviewed briefly in this section. More detail can be found in ref. 1.

Problem-dependent resonance processing of neutron cross sections is performed by SAS2H using the BONAMI-S and NITAWL-II modules. BONAMI-S applies the Bondarenko method of resonance self-shielding for nuclides that have Bondarenko data included with their cross sections. NITAWL-II is an updated version of the NITAWL code and performs resonance self-shielding corrections using the Nordheim Integral Treatment for nuclides that have resonance parameters included with their cross sections.

The XSDRNPM-S module, as applied by SAS2H, is used to produce weighted and collapsed cross sections for the fuel-depletion calculations. XSDRNPM-S performs a 1-D discrete-ordinates transport calculation based on various specified geometries requested in the data supplied by SAS2H. Data from the weighted cross-section library and spectra produced by XSDRNPM-S are used by the COUPLE module to update an ORIGEN-S nuclear data library and modify the ORIGEN-S spectral parameters (THERM, RES, and FAST).

The ORIGEN-S module is used for the depletion/decay portion of SAS2H. ORIGEN-S is referred to as a point-depletion code and contains no explicit spatial dependence. Therefore, all data provided to ORIGEN-S (i.e., cross sections or spectral data) are effective values weighted over the spatial region of interest. ORIGEN-S is used to compute time-dependent concentrations and source terms for a large number of isotopes that are simultaneously generated or depleted through neutronic transmutation, fission, radioactive decay, input feed rates, and physical or chemical removal rates. The time dependence of the nuclide concentrations is solved by using the matrix exponential expansion technique. A generalized form of the Bateman equation is used to solve for concentrations of short-lived nuclides to ensure better accuracy.

Any master AMPX cross-section library<sup>20</sup> with SCALE nuclide identifiers can be used by the SAS2H module. Of the available SCALE libraries, the hybrid 27-group neutron cross-section library is typically applied. This library primarily has ENDF/B-IV data, but early ENDF/B-V data have been added for the needed fission products. Also, a 44-group neutron cross-section library prepared with the latest revised ENDF/B-V data files, with the exception that <sup>16</sup>O, <sup>154</sup>Eu, and <sup>155</sup>Eu cross sections were prepared with ENDF/B-VI data files, has recently been processed and is used in this study. A fission-product evaluation conducted at ORNL and reported<sup>17</sup> in 1990 showed a significant difference between ENDF/B-V and ENDF/B-VI capture cross-section evaluations of both <sup>154</sup>Eu and <sup>155</sup>Eu. The resonance integral for <sup>155</sup>Eu in the ENDF/B-VI evaluation was greater than an order of magnitude higher than that in the corresponding ENDF/B-V evaluation. The reason for this extreme difference is that <sup>155</sup>Eu resonance parameters were not available in the ENDF/B-V data files.

The ORIGEN-S data libraries (Sect. M7 of ref. 1) are accessed for the half-lives, decay constants, fission yields, and Q-values. One modification to the ORIGEN-S decay data base in Version 4.2 of SCALE was required in this study. The half-life of <sup>79</sup>Se was corrected from 33,000 to 330,000 years. The <sup>79</sup>Se spent fuel content was measured in units of curies. The conversion of the calculated <sup>79</sup>Se mass to curies applies the half-life. Preliminary results were an order of magnitude too high. An inspection of the progress report in which the upper limit of the <sup>79</sup>Se half-life

was first reported indicated that instead of using the correct factor of  $1.68 \times 10^8$  for converting  $\mu\text{g}/(\text{d}/\text{s})$  to half-life in years, a value of approximately  $1.68 \times 10^7$  was applied, which is too low by a factor of 10. The larger half-life was updated in the ORIGEN-S library for local use and will be included in future releases of SCALE.

Input data for each SCALE module are prepared by SAS2H based on a single set of input consisting of basic engineering parameters (e.g., fuel pin-cell dimensions and compositions) and keywords cast in a simple, free-form format. The SAS2H program uses this basic information to derive additional parameters (e.g., number densities or associated physics data) and to prepare the input for each of the functional modules in the sequence. Nuclide densities required by the codes are prepared by the SCALE Material Information Processor Library (MIPLIB) from both the user input (e.g., material densities or volume fractions) and the contents of the SCALE Standard Composition Library. MIPLIB is also an essential tool in calculating applicable physics parameters (e.g., Dancoff factors) for the neutronics modules.

## 2.3 METHOD AND TECHNIQUES

The method applied by SAS2H utilizes data describing a fuel assembly as it is initially loaded into a particular reactor. The geometry, initial material composition, average zone temperatures, and time-dependent specific power of the fuel assembly are required input. Fundamentally, the chief function of the SAS2H program is to convert this user input data, plus data available within the SCALE system, into the input required by functional modules and transfer the data onto the interface units read by these codes. A diagram of the basic flow path invoked by SAS2H and the SCALE driver for depletion and decay analyses is shown in Fig. 1. Appropriate parameters are returned to the SCALE driver to properly invoke the functional modules in the SAS2H method. The methods and techniques employed by SAS2H through the execution of the final ORIGEN-S case are discussed in the remainder of this section.

### 2.3.1 Neutronics Models

The flow chart of Fig. 1 indicates two computational paths (path A and path B) for the neutronics portion of the depletion analysis. Although the neutronics modules used in these sequential flow paths are similar (both access BONAMI-S, NITAWL-II, and XSDRNPM-S), the models analyzed are quite different. Path A evaluates a model similar to that used in earlier SAS2 versions. The addition of flow path B and its model distinguishes the new version of the SAS2 control module that is denoted SAS2H.

Basically, the model used in path A represents the fuel as an infinite lattice of fuel pins. Cross-section processing is followed by a 1-D discrete-ordinates transport computation of the neutron flux in a unit cell with white boundary conditions. The cell-weighted cross sections produced by this path-A model are then applied to the fuel zone of the path-B model. The model applied in path B is a larger unit cell model used to represent part or all of an assembly within an infinite lattice. The concept of using cell-weighted data in the 1-D XSDRNPM-S analysis of path B is an approximate method for evaluating heterogeneity effects found in fuel-pin lattices containing different types of rods or water "holes." The path-B model is used by SAS2H to generate few-group, cell-weighted cross sections for ORIGEN-S and to calculate the neutron flux for an "assembly-averaged" fuel region that is used to update the ORIGEN-S spectral parameters for isotopes not explicitly included in the cell model.

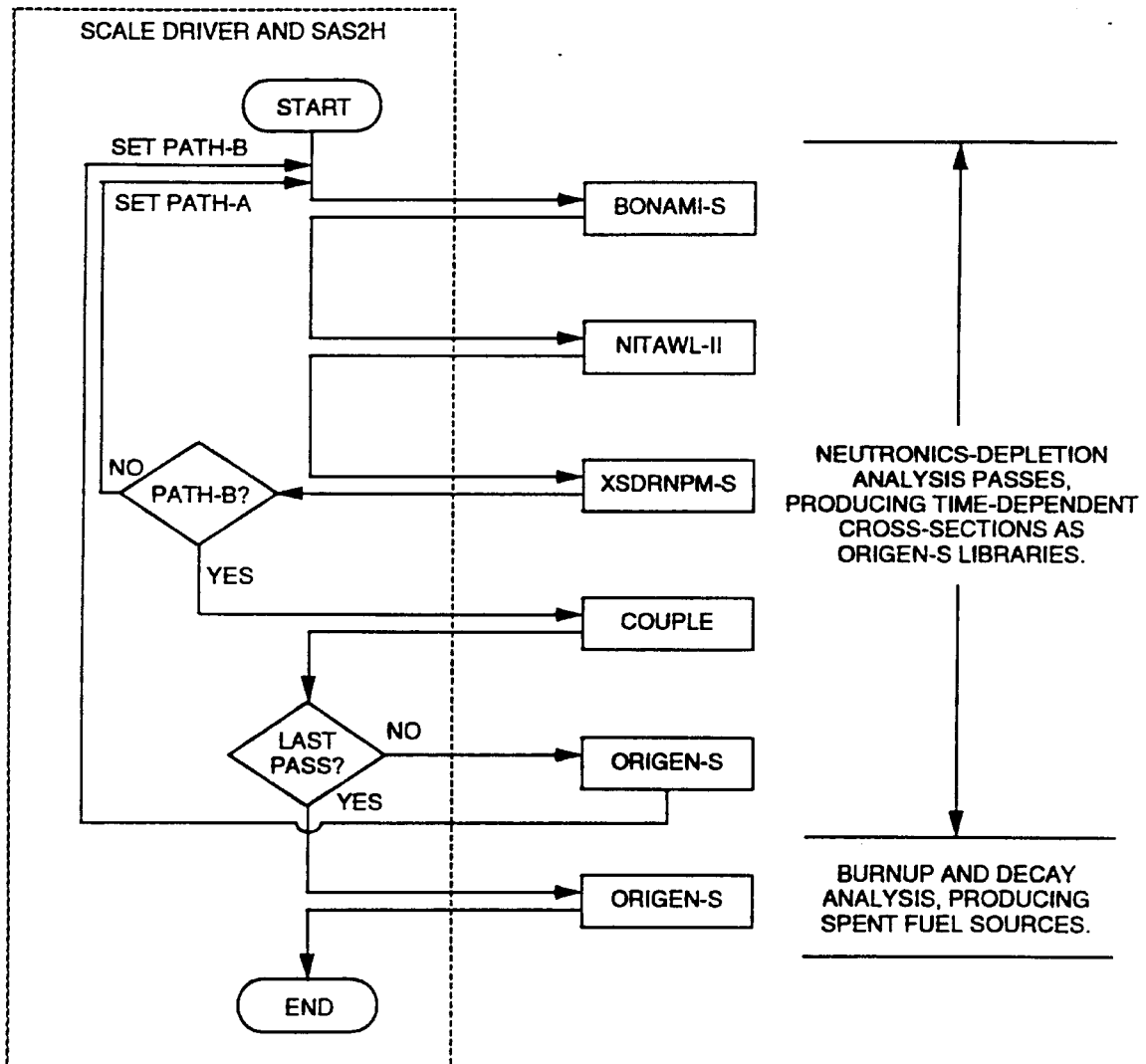


Fig. 1. Flow path invoked by SAS2H sequences.

Two examples of the larger unit cells are depicted in Fig. 2, where diagram (a) applies to a PWR control rod assembly and diagram (b) applies to a burnable poison assembly in a BWR. Variations to diagram (b) (e.g., omitting the casing and channel moderator) would apply to different types of BWR or PWR assemblies. The essential rule in deriving the zone radii is to maintain the relative volumes in the actual assembly. The central region of the larger cell can be modeled as an assembly guide tube, a BPR containing no fuel, an orifice rod, an axial peaking rod, a fuel rod containing a burnable poison, or almost any other pin-cell type rod. A fuel region surrounds the central region moderator with a radius that conserves the relative volumes of fuel and moderator for the entire assembly. Also, the fuel assembly housing material, or casing, and channel moderator between assemblies may be added by conserving volumes. Assembly rod spacers and other hardware that may be present are usually ignored. However, if their effects are estimated to be significant, they may be input by using zone average or effective densities.

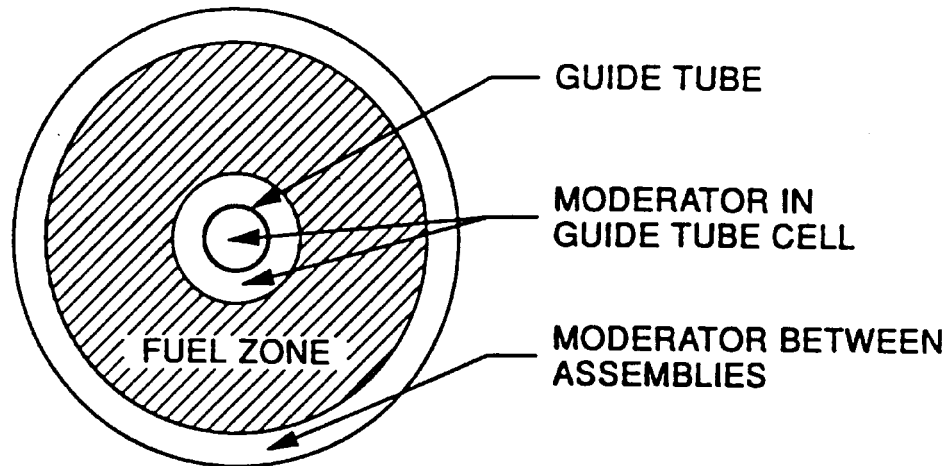
During normal reactor operation, there are axial variations in moderator density and power in all assemblies. The approximation used to determine the average water density may have a significant effect upon the results. A frequent and acceptable practice in using SAS2H for PWR assemblies is to derive the average density using the water pressure and the average core temperature.

### 2.3.2 Burnup-Dependent Cross Sections

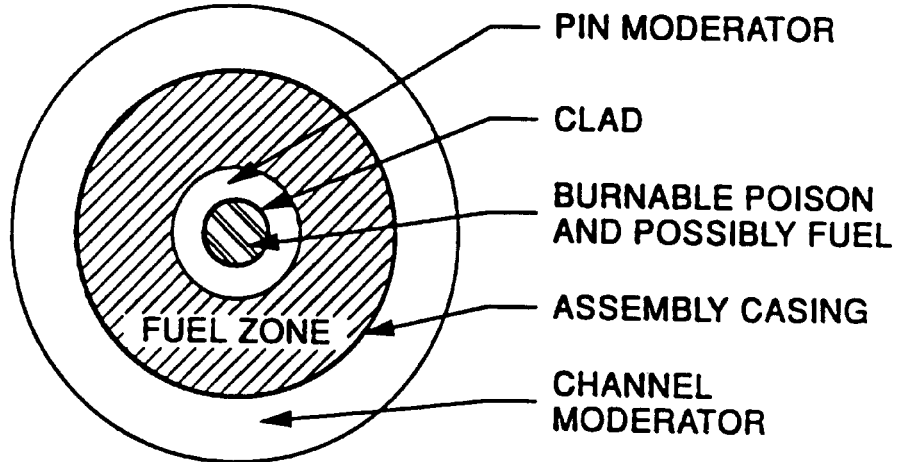
Fuel cross sections vary with burnup because of the change in nuclide concentration and because of the resulting shift in the energy spectrum of the neutron flux. The neutronics-depletion procedure of Fig. 1 is applied repeatedly by SAS2H to produce cross-section libraries for the irradiation intervals requested in the input. The major data differences for the sequential "passes" are in the nuclide densities and reactor history parameters.

The user input specifies the number of reactor power cycles, the number of libraries to make per cycle, the specific power in each cycle, and both the total operation time and downtime of each cycle. The irradiation-time interval associated with each library is derived from this input. With the exception of the initial fresh-fuel library, each cross-section library is based on number densities obtained for the midpoint of the irradiation-time interval. The midpoint number densities for an irradiation interval are computed from an ORIGEN-S case that uses the library from the previous irradiation interval. Collapsed cross sections for all nuclides included in the path-B XSDRNPM-S analysis are explicitly updated and included on each new ORIGEN-S working library. Other nuclide cross sections on the ORIGEN-S library are updated using broad-group, flux-weight factors from the path-B XSDRNPM-S analysis. Trace amounts of the selected nuclides shown in Table 1 are automatically included by SAS2H in the XSDRNPM-S analysis to ensure that appropriate cross sections are available for important nuclides that build up in the fuel during depletion. Additional trace nuclides (e.g., major fission products) can be input by the user.

The procedure is illustrated schematically in Fig. 3 for a two-cycle case where two libraries per cycle are requested. The first step is to produce the "PASS 0" library prepared using the fresh fuel isotopes. This initial library is used in the first ORIGEN-S case to generate number densities at the midpoint of the first irradiation interval. Next, the SAS2H module performs the necessary data processing and rewrites all code interfaces. Then, the "PASS 1" library is produced by executing path A and path B of Fig. 1 a second time with the new input interfaces. Each additional pass applies the same procedure as used for "PASS 1" [i.e., (1) isotopic densities at the midpoint of the  $N$ th irradiation interval are obtained using the library from the  $N-1$  interval and the isotopic densities at the start of the  $N-1$  interval, and (2) the "PASS  $N$ " library is obtained using the neutronics procedure with the midpoint isotopic densities].



(a) FOR PWR CONTROL ROD ASSEMBLY, AFTER CONTROL RODS WITHDRAWN.



(b) FOR BWR BURNABLE POISON ASSEMBLY WITH LARGE CHANNEL ZONE.

Fig. 2. Examples of larger unit cell for the model used in the path-B portion of SAS2H.

Table 1. List of fuel nuclides automatically included by SAS2 for neutronics processing<sup>a</sup>

<sup>135</sup> Xe	<sup>238</sup> Pu	<sup>242m</sup> Am
<sup>133</sup> Cs	<sup>239</sup> Pu	<sup>243</sup> Am
<sup>234</sup> U	<sup>240</sup> Pu	<sup>242</sup> Cm
<sup>235</sup> U	<sup>241</sup> Pu	<sup>243</sup> Cm
<sup>236</sup> U	<sup>242</sup> Pu	<sup>244</sup> Cm
<sup>238</sup> U	<sup>241</sup> Am	1/v-absorber <sup>b</sup>
<sup>237</sup> Np		

<sup>a</sup>Unless overridden by user input, these nuclides are added to the initial fuel mixture with a number density of 10<sup>-20</sup> atoms/b-cm.

<sup>b</sup>Used to calculate the THERM parameters applied in ORIGEN-S (see Sect. F7 of ref. 1).

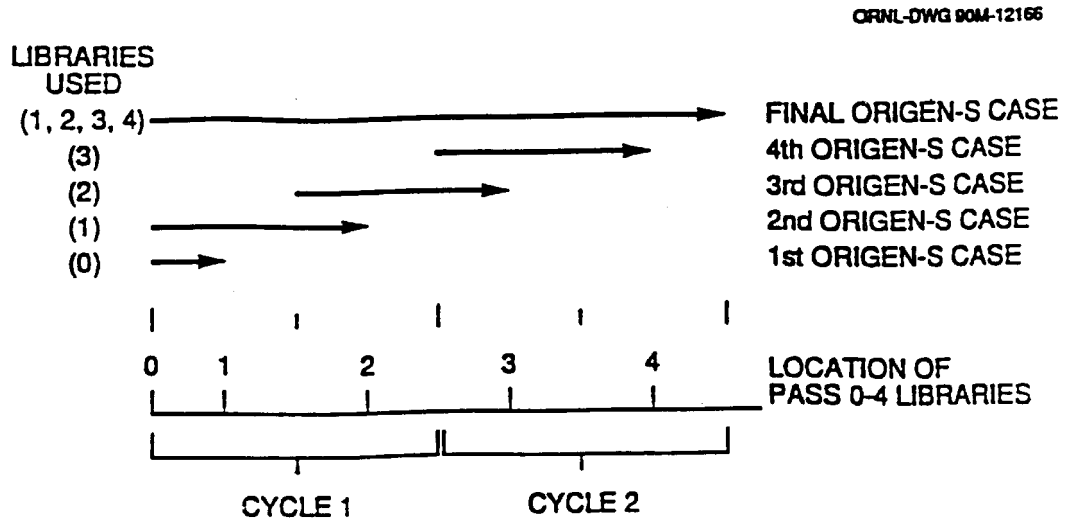


Fig. 3. Schematic of successive ORIGIN-S cases used to produce the burnup-dependent number densities for a SAS2H case with two libraries per cycle.

Number densities for the heavy nuclides of the fuel, together with their activation products and fission products, are all computed by ORIGEN-S. In addition, ORIGEN-S calculates the depletion of the burnable poisons boron, gadolinium, and cadmium, and some of the specified structural materials or light elements (e.g., lithium). As noted earlier, the moderator density does not change from the initial material specification unless requested by the user. The fraction of the first-cycle (initial material specification) density of the water or soluble boron may be specified by the user for each cycle.

### 2.3.3 Final Depletion and Decay Analysis

The purpose of the neutronics-depletion method was to produce a set of ORIGEN-S working libraries that apply to the specified fuel assembly at various points during its irradiation history. These libraries and the initial nuclide densities form the input to the final ORIGEN-S depletion case. All the nuclides in the ORIGEN-S binary library<sup>1</sup> are available for the analysis. These nuclides presently include 689 light elements, such as clad and structural materials, 129 actinides, including fuel nuclides and their decay and activation products, and 879 fission-product nuclides. All depletion/decay transitions are automatically provided in the ORIGEN-S library and can be updated easily by COUPLE.

The first step of the final ORIGEN-S case is the nuclide generation and depletion computation using the "PASS 1" library. The first-cycle power and "PASS 1" time interval are applied. Four equal-size time steps are used during the irradiation time, followed by a single downtime interval. If no downtime is specified, a zero-time interval is applied. Next, a similar computation is performed using the compositions determined at the end of the "PASS 1" calculation and the cross-section data on the "PASS 2" library. The analysis proceeds with each succeeding library and corresponding assembly power and time interval. Ultimately, the nuclide inventories (actinides, fission products, and light elements) are computed at the burnup corresponding to the discharge of the assembly from the reactor. Finally, a decay-only subcase (six equal-size time steps) is computed for the requested spent fuel cooling time. The calculated compositions from this last decay subcase are applied in the determination of other spent fuel characteristics (e.g., radiation sources and heat generation).

## 2.4 INPUT FEATURES

Basic engineering data, in free-form input, are required to perform the SAS2H analysis. An example of the input for the fuel-depletion data in a sample case is shown in Fig. 4. The input provided in Fig. 4 is for a three-cycle depletion of a  $17 \times 17$  PWR assembly to 33 MWd/kgU. The first part through the line giving the square-pitch dimensions defines the reactor materials and lattice cell design, the next part describes the power operating history and other data on the fuel assembly, and the final part gives the light-element contents. Even though all the data are available at reactor sites, nominal data can be found in various reactor fuel characterization compilations (see various references in Sect. 3).



```

-SAS2H      PARM='SKIPSHIPDATA'
SAS2 SAMPLE CASE 3: 33 MWD/KGU, 17*17 PIN, PWR, 3 CYC, DRY-FUEL CASK
27GROUPNDF4      LATTICECELL
UO2 1 0.9018 811 92234 0.028 92235 3.2 92236 0.015 92238 96.757 END
ZIRCALLOY 2 1          620 END
H2O          3 DEN-0.733 1 570 END
ARBM-BORMOD 0.733 1 1 0 0 5000 100 3 550.0E-6 570 END
CO-59        3 1-20          570 END
END COMP
SQUAREPITCH 1.25984 0.83566 1 3 0.94996 2 END
NFIN/ASSM-264 FUELNTH-365.76 NCYCLES-3 NLIB/CYC-1
PRINTLEVEL-4
LIGHTEL-16
POWER-18.3025 BURN-290 DOWN-30 END
POWER-17.3025 BURN-300 DOWN-60 BFRAC-0.95 END
POWER-16.3025 BURN-290 DOWN-1826.25 BFRAC-0.92 END
C 0.05999 N 0.03377 O 62.14 AL 0.04569
SI 0.06586 P 0.1422 TI 0.04983 CR 2.340
MN 0.1096 FE 4.599 CO 0.03344 NI 4.402
ZR 100.8 NB 0.3275 MO 0.1816 SN 1.652
END

```

Fig. 4. Example of fuel depletion SAS2 input.

## 2.5 HEAT GENERATION VALIDATION

Reference 21 describes work performed to validate the SAS2H analysis sequence for use in calculating heat generation rates for PWR and BWR spent fuel. The validation study involved comparing calorimetric measurements of spent fuel assembly heat rates with computed values. In this study, results were compared for ten PWR and ten BWR spent fuel assemblies obtained from three reactors: Point Beach Unit 2 (PWR), Turkey Point Unit 3 (PWR), and Cooper Nuclear Station (BWR). Measured and computed decay heat rates and percentage differences for each measurement are documented. The average differences for the three reactors indicated the computed values of the Point Beach PWR assemblies to be greater than the measurements and the opposite relationship for data of the other two reactors. Specifically, the assembly average percentage differences were  $3.0 \pm 1.9\%$ ,  $-0.7 \pm 1.7\%$ , and  $-0.7 \pm 2.6\%$  for the Point Beach, Turkey Point, and Cooper Nuclear Station analyses, respectively. The report concluded that SAS2H gave valid results for spent fuel heat generation for a wide range of burnups, initial enrichments, and reactor power history. The validation performed here provides a more strenuous test of the analysis sequence since heat generation is a global quantity that could mask compensating errors in individual isotopics.

### 3. PWR FUEL ASSEMBLY DATA FOR PROBLEMS ANALYZED

The problems selected for validation of depletion and decay analysis using the SAS2H control module of the SCALE code system are based on post-irradiation measurements performed with PWR spent fuel from the Calvert Cliffs Unit 1, H. B. Robinson Unit 2, and Obrigheim reactors. The Materials Characterization Center at Pacific Northwest Laboratory selected three  $14 \times 14$  Combustion Engineering (CE) assemblies from Calvert Cliffs and one  $15 \times 15$  Westinghouse assembly from H. B. Robinson for the Approved Testing Material (ATM) program that was designed to provide a source of well-characterized spent fuels.<sup>11-14</sup> For a specific rod within each assembly, radiochemical measurements were made on fuel pellets from either three or four axial positions with each position corresponding to a different burnup. For each pellet, measured data were obtained for the major actinides, cesium isotopes, and <sup>99</sup>Tc. Other fission products of importance to burnup credit (i.e., high neutron absorbers) have recently been measured for one Calvert Cliffs assembly [D047 (ATM-104)].<sup>22</sup> Isotopic measurements of the Obrigheim  $14 \times 14$  assemblies were performed in Europe.<sup>15,16</sup> For these measurements, each assembly was cut in half lengthwise and dissolved separately at the Karlsruhe Reprocessing Plant in Germany. The radiochemical analysis for a number of actinide and fission products was subsequently carried out by four independent institutes. The Obrigheim measurements thus provide "assembly average" isotopic values that, in comparison with individual pellet measurements, are more consistent with the spatially independent (i.e., assembly average) point-depletion techniques typically used to characterize spent fuel for away-from-reactor applications. Some pellets were also selected from the Obrigheim assemblies for radiochemical assay, but these measurements have not been included in this evaluation.

The initial <sup>235</sup>U fuel enrichment, the accumulated burnup, and the cooling time are very important parameters in characterizing the nuclide inventory of spent PWR fuel. Table 2 provides these basic characterization parameters for the three Calvert Cliffs assemblies, the single H. B. Robinson assembly and the five Obrigheim assemblies considered in this report. The enrichments, burnups, and cooling times in Table 2 are representative of a very large percentage of the spent fuel inventory in the United States and thus provide appropriate data for validating nuclide depletion, buildup, and decay models. The following subsections provide the detailed descriptions necessary to perform a calculational prediction of the spent fuel isotopic compositions for each assembly and pellet location. Listings of the actual input data to SAS2H for all of the validation cases are shown in Appendix A. Comparisons of the measured data against isotopic compositions predicted using the SAS2H/ORIGEN-S sequence of SCALE-4 code system are given in Sect. 4.

#### 3.1 CALVERT CLIFFS PWR SPENT FUEL DESIGN AND OPERATING DATA

The Calvert Cliffs Unit 1 PWR uses CE fuel assemblies with a  $14 \times 14$  pin lattice. A general description of the standard Calvert Cliffs fuel assembly design is presented in Table 3. The initial fuel compositions for the assemblies are listed in Table 4. The locations within the  $14 \times 14$  assembly lattice of the specific fuel rods examined from each assembly are shown in Figs. 5 through 7.

The assembly designated D047 was loaded in Calvert Cliffs Unit 1 during cycles 2 through 5, inclusive. D101 was only loaded during cycles 2 through 4, inclusive. BT03 was loaded during cycles 1 through 4, inclusive. The operating data (e.g., cumulative burnups) on

Table 2. Basic parameters of the measured spent fuel

Pressurized water reactor	Test assembly (ATM No.)	Enrichment (wt % <sup>235</sup> U)	Axial <sup>a</sup> location (cm)	Burnup (GWd/MTU)	Cooling time (d)
Calvert Cliffs Unit 1	D047 (ATM-104)	3.038	13.20	27.35	1870 <sup>b</sup>
			27.70	37.12	
			165.22	44.34	
Calvert Cliffs Unit 1	D101 (ATM-103)	2.72	8.90	18.68	2374
			24.30	26.62	
			161.70	33.17	
Calvert Cliffs Unit 1	BT03 (ATM-106)	2.453	11.28	31.40	2447
			19.92	37.27	
			161.21	46.46	
H. B. Robinson Unit 2	B05 (ATM-101)	2.561	11	16.02	3936
			26	23.81	3936
			199	28.47	3631
			226	31.66	3631
Obrigheim	170	3.13	N/A. <sup>c</sup>	25.93	0 <sup>d</sup>
Obrigheim	172	3.13	N/A. <sup>c</sup>	26.54	0 <sup>d</sup>
Obrigheim	176, batch 91	3.13	N/A. <sup>c</sup>	27.99	0 <sup>d</sup>
Obrigheim	168	3.13	N/A. <sup>c</sup>	28.40	0 <sup>d</sup>
Obrigheim	171	3.13	N/A. <sup>b</sup>	29.04	0 <sup>d</sup>
Obrigheim	176, batch 90	3.13	N/A. <sup>b</sup>	29.52	0 <sup>d</sup>

<sup>a</sup>Distance from bottom of fuel.

<sup>b</sup>Radiochemical analyses of additional fission products at 3817 d, with reported values adjusted to 1870 d.

<sup>c</sup>Not applicable. Assembly average isotopic measurements and burnup.

<sup>d</sup>Measured data converted to time of shutdown for discharge.

Table 3. Calvert Cliffs general fuel assembly design data

Parameter	Data	
	Assembly ID	D047 and D101
Assembly general data		
Designer	Combustion Engineering	Combustion Engineering
Lattice	14 × 14	14 × 14
Number of fuel rods	176	176
Number of guide tubes	5	5
Assembly pitch, cm	20.78	20.78
Fuel rod data		
Type fuel pellet	UO <sub>2</sub>	UO <sub>2</sub>
UO <sub>2</sub> density, g/cm <sup>3</sup>	10.413	10.175
Pellet end dishing, vol %	3.539 <sup>a</sup>	1.366 <sup>a</sup>
Pellet stack density, g/cm <sup>3</sup>	10.045	10.036
Rod pitch, cm (in.)	1.4732 (0.580)	1.4732 (0.580)
Rod OD, cm (in.)	1.1176 (0.440)	1.1176 (0.440)
Rod ID, cm (in.)	0.9855 (0.388)	0.9855 (0.388)
Pellet diameter, cm (in.)	0.9563 (0.3765)	0.9639 (0.3795)
Active fuel length, cm (in.)	347.22 (136.7)	347.22 (136.7)
Clad material	Zircaloy-4	Zircaloy-4
Guide tube data		
Inner radius, cm (in.)	1.314 (0.5175)	1.314 (0.5175)
Outer radius, cm (in.)	1.416 (0.5575)	1.416 (0.5575)
Tube material	Zircaloy-4	Zircaloy-4

<sup>a</sup>Calculated from design dimensions of pellet.

Sources: refs. 12 through 14 and ref. 23.

Table 4. Fuel composition of Calvert Cliffs fuel assemblies

Parameter	D047 <sup>a</sup> (ATM-104)	D101 <sup>b</sup> (ATM-103)	BT03 <sup>c</sup> (ATM-106)
Enrichment,			
wt % <sup>235</sup> U	3.038	2.72	2.453
wt % <sup>234</sup> U <sup>a</sup>	0.027	0.024	0.022
wt % <sup>236</sup> U <sup>a</sup>	0.014	0.013	0.011
Total uranium, wt %	88.14	88.14	88.14
Oxygen, wt %	11.86	11.86	11.86
Carbon, ppm	18	12	19
Nitrogen, ppm	23	24	44
Fluorine, ppm	<5	<5	<5
Chlorine, ppm	<10	<10	<10
Iron, ppm	<45	52	<45
Silver, ppm	<1	<1	<1
Aluminum, ppm	<115	<121	<115
Nickel, ppm	<25	<25	<25

<sup>a</sup>Data taken from ref. 13.

<sup>b</sup>Data taken from ref. 12.

<sup>c</sup>Data taken from ref. 14.

<sup>d</sup>Not part of fuel certification data; calculated according to the following equations:<sup>24</sup>

$$^{234}\text{U wt \%} = 0.0089 \times ^{235}\text{U wt \%}$$

$$^{236}\text{U wt \%} = 0.0046 \times ^{235}\text{U wt \%}$$

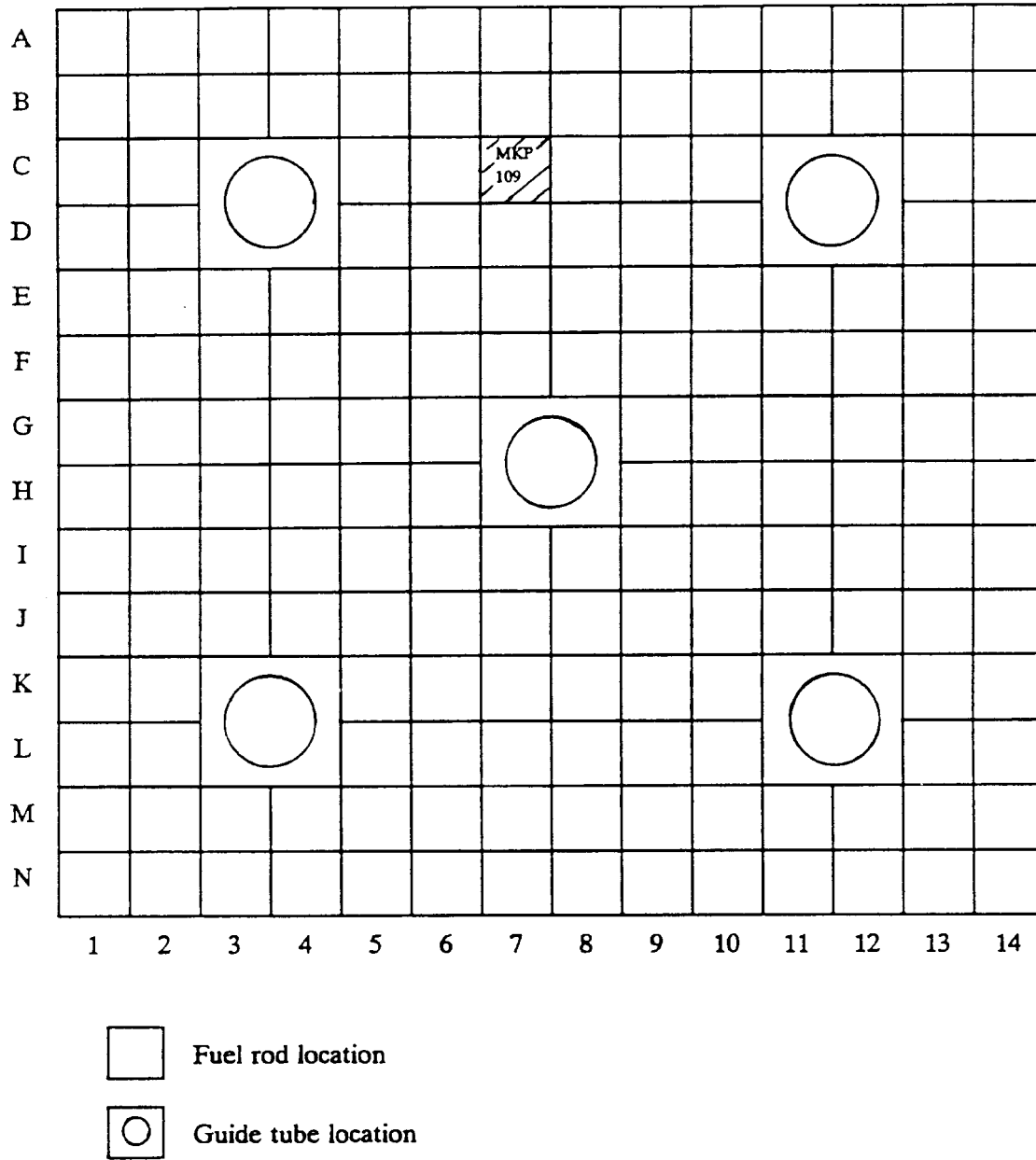


Fig. 5. Location of Fuel Rod MKP109 in Assembly D047.

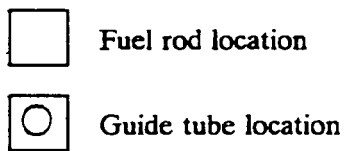
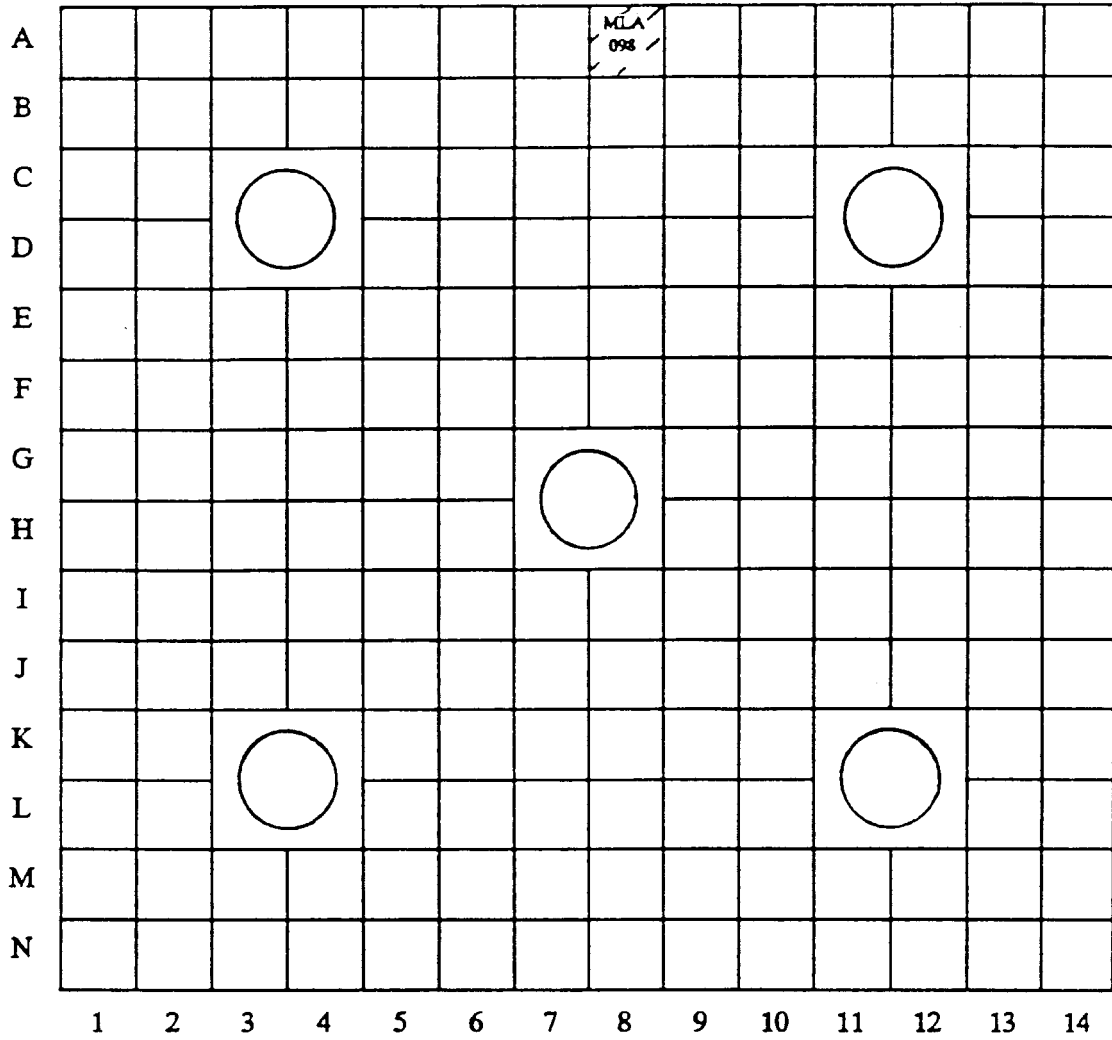
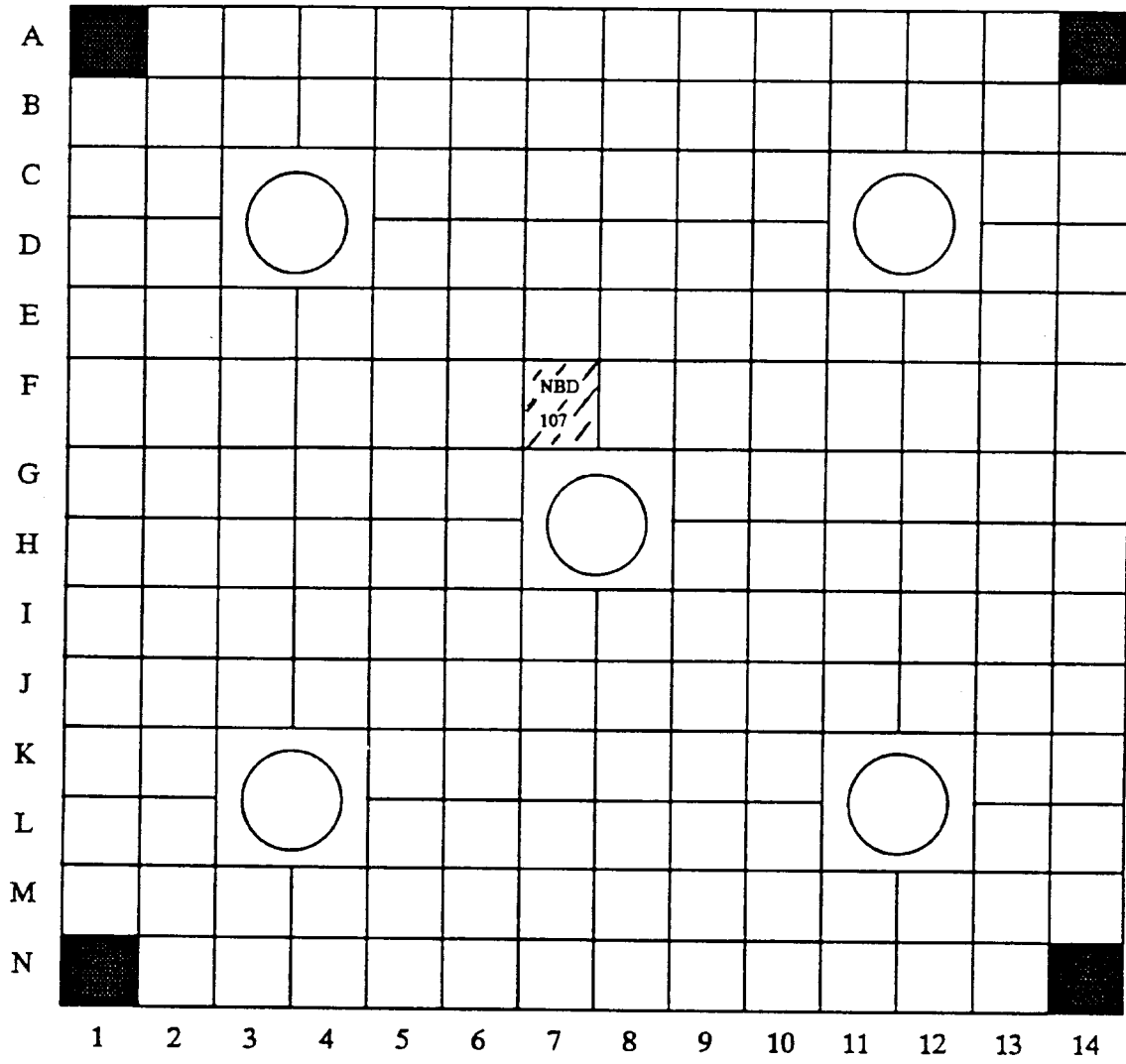


Fig. 6. Location of Fuel Rod MLA098 in Assembly D101.






-  Fuel rod location
-  Guide tube location
-  Nonfuel rods

Fig. 7. Location of Fuel Rod NBD107 in Assembly BT03.



the samples taken from the D047 assembly were available in greater detail<sup>25</sup> than the data for the D101 and BT03 assemblies. Linear heat generation rates (LHGRs) for D047 Rod MKP109 at the three axial locations of the samples are listed in Table 5. At each axial location, the linear burnups of time intervals (i.e., the product of interval size and LHGR) were summed for each cycle. The linear burnups per cycle were then normalized to the total burnups of the three D047 samples listed in Table 2 to produce the cumulative burnups presented in Table 6. Estimates of the cumulative burnups for samples from the other two assemblies were derived with a different procedure because no LHGR data were reported for their samples. Assembly D101 resided in the reactor during the first three of the four cycles in which D047 was present. Also, each of the axial distances to the bottom of the fuel of the D101 samples were only 3.2 to 4.1 cm less than those of the D047 samples at similar positions. Thus, the cumulative burnups of the D101 samples were estimated by assuming that the burnups experienced during a cycle at similar axial locations in both assemblies were equal fractions of the corresponding cumulative burnup over the three cycles of operations common to both assemblies. The method of estimating the sample burnup used for D101 could not be applied to BT03 because the reactor residence period of BT03 included one cycle prior to that of D047. Also, operating history data of the BT03 assembly samples were specified in terms of the cycle and cumulative burnups of the entire Rod NBD107. Therefore, the fraction of the total four-cycle burnup that was experienced in each cycle by the rod was applied to the total burnup of each sample of BT03 to produce the cycle and cumulative burnups of the samples. The final cumulative burnups of the nine samples listed in Table 6 are equal to the corresponding sample burnups in Table 2. The power histories of each of the pellet samples, also shown in Table 6, were calculated from the cycle lengths and corresponding cycle burnups.

The cycle average boron concentrations in Table 6 were derived from the data in Table 5. The first and last soluble boron concentrations for each cycle were used to estimate the rate of change in boron versus time. An initial and final boron concentration for each cycle was calculated by extrapolation from the average values in the first and last intervals, respectively, using the calculated rate of change in boron versus time. The cycle average boron concentrations in Table 6 are the average of the extrapolated initial and final concentrations. The boron concentration of cycle 1 was set equal to that of cycle 2.

The effective fuel temperature data in Table 6 was specifically for D047 Rod MKP109, but were applied to all three fuel rods since no data were available for D101 Rod MLA098 or BT03 Rod NBD107. An effective fuel temperature for each sample was derived by burnup-weighting of cycle temperatures in Table 6 for assemblies D047 and D101. Estimates of the impact of these temperature assumptions were determined. The cumulative burnup, and thus the average power, during the first three cycles of D101 Rod MLA098 was between 3 and 9.5% less than that of pellet samples from similar locations in D047 Rod MKP109. Computations for fuel temperatures with a 100 K difference, indicated a maximum uranium and plutonium isotopic change of 0.013%/K. Applying an estimate (based on Obrigheim temperature vs power data in Sect. 3.2) of 2.3 K/% change in power, the maximum isotopic error in uranium and plutonium is estimated to be 0.3% ( $9.5 \times 2.3 \times 0.013$ ). The average power of BT03 Rod NBD107 was between 6 and 18% less than the corresponding values of D047 Rod MKP109. Using the same type of estimate as applied to D101, the maximum uranium and plutonium isotopic error would be 0.5%. Although the possible bias from fuel temperature estimates are not ideal, they may be considered acceptable. Note that there were no estimates of fuel temperatures in cycle 1 to apply to assembly BT03. Thus, the effective fuel temperature for a sample in BT03 was assumed to be equal to that for a sample at the corresponding

Table 5. Power histories and boron concentrations  
Fuel Assembly D047 Rod MKP109

Cycle No. 2 (3-22-77 to 1-22-78)				
Interval days	Average soluble boron, ppm	LHGR, <sup>a</sup> kW/ft		
		13.20 cm	27.70 cm	165.22 cm
7.0	654	2.0	3.04	5.42
30.8	614	2.73	4.08	6.64
16.3	563	2.80	4.18	6.60
11.4	533	2.86	4.26	6.60
12.5	507	2.94	4.34	6.56
23.7	468	3.01	4.43	6.41
22.8	418	3.16	4.61	6.44
23.2	368	3.27	4.73	6.37
8.1	333	3.30	4.75	6.34
31.4	290	3.48	4.95	6.34
34.3	218	3.59	5.05	6.53
16.4	162	3.75	5.25	6.38
19.2	122	3.75	5.21	6.26
12.8	86	3.81	5.28	6.30
34.2	36	3.63	4.98	5.95
1.9	0	3.64	4.98	5.96
71.0	0	0	0	0
Cycle No. 3 (4-3-78 to 4-20-79)				
Interval days	Average soluble boron, ppm	LHGR, <sup>a</sup> kW/ft		
		13.20 cm	27.70 cm	165.22 cm
7.9	883	2.63	3.85	7.47
14.4	862	2.71	3.95	7.20
19.7	837	2.14	3.11	5.04
16.8	808	3.18	4.58	7.79
16.3	775	3.35	4.81	7.78
15.4	741	3.74	5.33	8.16
39.1	684	3.71	5.23	7.45
31.2	611	3.95	5.50	7.37
31.8	545	4.08	5.64	7.20
31.8	478	4.20	5.75	7.02
44.3	368	4.38	5.93	6.93
25.0	291	0	0	0
59.1	224	4.67	6.20	6.89
28.9	120	4.95	6.52	7.12
81.0	83	0	0	0

Table 5. (continued)

Cycle No. 4 (7-10-79 to 10-18-80)				
Interval days	Average soluble boron, ppm	LHGR, <sup>a</sup> kW/ft		
		13.20 cm	27.70 cm	165.22 cm
46.1	960	2.79	3.97	6.59
24.0	889	2.91	4.11	6.54
22.6	827	3.07	4.29	6.43
25.7	759	3.29	4.56	6.33
30.2	706	1.57	2.17	3.05
41.2	788	1.79	2.46	3.18
50.3	720	1.72	2.35	3.00
11.0	673	3.18	4.33	5.23
32.8	527	3.93	5.31	6.17
23.5	460	4.07	5.42	6.12
29.4	370	4.05	5.35	5.95
28.1	301	4.25	5.56	6.07
65.4	191	4.42	5.67	5.98
35.7	73	4.62	5.87	6.02
85.0 <sup>b</sup>	31	0	0	0

Cycle No. 5 <sup>c</sup> (1-11-81 to 4-17-82)				
Interval days	Average soluble boron, ppm	LHGR, <sup>a</sup> kW/ft		
		13.20 cm	27.70 cm	165.22 cm
65.0	919	1.98	2.67	4.55
5.5	911	2.15	2.91	4.80
6.6	896	2.20	2.98	4.80
28.6	854	2.36	3.15	4.79
31.2	784	2.54	3.36	4.72
27.0	715	2.66	3.52	4.73
22.7	655	2.77	3.63	4.71
27.1	603	2.46	3.22	4.05
55.2	521	2.81	3.64	4.34
20.9	434	3.17	4.08	4.75
41.9	356	3.32	4.24	4.79
21.6	281	3.38	4.30	4.80
27.6	226	3.21	4.04	4.49
19.0	173	3.57	4.49	4.87
61.2 <sup>d</sup>	79	3.05	3.79	4.00

<sup>a</sup>At indicated axial locations from bottom of fuel.

<sup>b</sup>Cooling times to dates of D101 and BT03 sample analyses (April 1987 and June 1987) were 2374 d (6.5 y) and 2447 d (6.7 y), respectively.

<sup>c</sup>Only assembly D047 was loaded in this cycle.

<sup>d</sup>Cooling time following this final irradiation interval to date of D047 sample analyses (June 1987) was 1870 d (5.1 y).

Sources: refs. 13 and 25.

Table 6. Operating data for Calvert Cliffs Assembly D047, Rod MKP109, Assembly D101, Rod MLA098, and Assembly BT03, Rod NBD107

Cycle number	1 <sup>a</sup>	2	3	4	5
Cycle length, d	816.0	306.0	381.7	466.0	461.1
Downtime after cycle, <sup>b</sup> d	81.0	71.0	81.3	85.0	–
Cumulative burnup, GWd/MTU					
Rod MKP109, 13.20 cm	–	5.28	12.69	20.63	27.35
Rod MKP109, 27.70 cm	–	7.56	17.78	28.42	37.12
Rod MKP109, 165.22 cm	–	9.52	21.93	34.14	44.34
Rod MLA098, 9.10 cm	–	4.78	11.49	18.68	–
Rod MLA098, 24.50 cm	–	7.08	16.65	26.62	–
Rod MLA098, 161.90 cm	–	9.25	21.31	33.17	–
Rod NBD107, 11.28 cm	14.59	20.31	25.29	31.40	–
Rod NBD107, 19.92 cm	17.32	24.10	30.02	37.27	–
Rod NBD107, 161.21 cm	21.59	30.05	37.42	46.46	–
Cycle average power, MW/MTU					
Rod MKP109, 13.20 cm	–	17.24	19.43	17.04	14.57
Rod MKP109, 27.70 cm	–	24.72	26.76	22.84	18.87
Rod MKP109, 165.22 cm	–	31.12	32.51	26.20	22.12
Rod MLA098, 9.10 cm	–	15.61	17.59	15.43	–
Rod MLA098, 24.50 cm	–	23.15	25.06	21.39	–
Rod MLA098, 161.90 cm	–	30.24	31.58	25.46	–
Rod NBD107, 11.28 cm	17.88	18.67	13.06	13.10	–
Rod NBD107, 19.92 cm	21.22	22.16	15.51	15.55	–
Rod NBD107, 161.21 cm	26.46	27.62	19.33	19.39	–
Cycle average boron, ppm (wt)	330.8	330.8	469.4	503.7	492.1
Effective fuel temperature, <sup>c</sup> K					
Rod MKP109, 13.20 cm	–	829	850	775	709
Rod MKP109, 27.70 cm	–	940	927	793	712
Rod MKP109, 165.22 cm	–	997	958	794	747
Rod MLA098, 9.10 cm	–	829	850	775	–
Rod MLA098, 24.50 cm	–	940	927	793	–
Rod MLA098, 161.90 cm	–	997	958	794	–

<sup>a</sup>No burnup or power specified if assembly not loaded in cycle.

<sup>b</sup>Cooling times after shutdown for discharge to time of assay analyses listed in Table 2.

<sup>c</sup>No fuel temperature data for Assembly BT03, Rod NBD107.

axial location in D047. The estimated weighted effective fuel temperatures, derived by the above procedures, are listed in Table 7.

The moderator temperatures listed in Table 7 were calculated as a function of distance from the bottom of the fuel rod. The calculation was based on an inlet temperature of 543.2°F and an outlet temperature of 593.6°F. It was assumed that the heat produced in the moderator versus fuel height was a sine function. Integrating this function yields the following formula for moderator temperature vs height:

$$T(h) = T_{IN} + \frac{T_{OUT} - T_{IN}}{2} \left( 1 - \cos \frac{\pi h}{H} \right),$$

where

$$\begin{aligned} T(h) &= \text{temperature (}^\circ\text{F) at height } h, \\ T_{IN} &= \text{inlet temperature} = 543.2^\circ\text{F}, \\ T_{OUT} &= \text{outlet temperature} = 593.6^\circ\text{F}, \\ H &= \text{total fuel height} = 347.22 \text{ cm.} \end{aligned}$$

The moderator temperatures in Table 7 are based on this formula. The moderator densities were determined by using these temperatures to interpolate on a temperature-pressure-density table at a pressure of 2247 psia. The inlet and outlet temperatures and moderator pressure were supplied by the operating utility.<sup>25</sup>

### 3.2 H. B. ROBINSON PWR SPENT FUEL DESIGN AND OPERATING DATA

The H. B. Robinson Unit 2 PWR uses Westinghouse fuel assemblies with a 15 × 15 pin lattice. Descriptions of the design characteristics of Assembly B05 and the burnable poison fixture present in the assembly during cycle 1 are presented in Table 8 (refs. 19 and 26). The assembly was loaded in H. B. Robinson during cycles 1 and 2. The location within the B05 lattice of Rod N-9, the fuel rod examined, is shown in Fig. 8.

Power histories and other operating data for Assembly B05 are listed in Table 9. Detailed operating data were condensed to that given in the table. As a modeling approximation, each reactor cycle was split into two equal irradiation time intervals to allow the placement of downtime at the cycle midpoints. The 64-day downtime was the duration of the reloading period between cycles. The specific power of each pellet sample was assumed to decrease linearly with irradiation time and was normalized to produce the final total burnup in deriving the interval burnups and corresponding average powers. The differences between the estimated and detailed power histories should not cause a significant change in the isotopic compositions calculated at the cooling times (~10 years) of the radiochemical analyses.

Moderator temperatures and densities and effective fuel temperatures are listed in Table 10. The moderator temperatures were calculated by the same method applied to the Calvert Cliffs moderator (see Sect. 3.1) using inlet and outlet temperatures of 546.5°F and 600.6°F, respectively.<sup>27</sup> The moderator densities were determined by interpolating data on a temperature-pressure-density table at a pressure of 2250 psia.<sup>27</sup> The effective fuel temperatures were determined from the fuel temperature versus rod linear power curve in Fig. 9 (from ref. 16). Although the curve was

Table 7. Moderator conditions and effective  
fuel temperatures for Calvert Cliffs 1 PWR

Test assembly	Rod ID	Axial location (cm)	Moderator temperature		Moderator density (g/cm <sup>3</sup> )	Fuel temperature (K)
			(°F)	(K)		
D047	MKP109	13.20	543.4	557	0.7575	790
		27.70	544.0	558	0.7569	841
		165.22	566.5	570	0.7332	873
D101	MLA098	9.10	543.3	557	0.7576	816
		24.50	543.8	558	0.7571	880
		161.90	565.7	570	0.7341	910
BT03	NBD107	11.28	543.3	557	0.7576	790
		19.92	543.6	557	0.7573	841
		161.21	565.6	570	0.7342	873

Table 8. Design data for H. B. Robinson Fuel Assembly B05

Parameter	Data
Assembly general data	
Designer	Westinghouse
Lattice	15 × 15
Soluble boron, cycle avg, ppm (wt)	450
Number of fuel rods	204
Number of position with only guide tubes	8
Number of burnable poison rods	12
Number of instrument tubes	1
Assembly pitch, cm (in.)	21.50 (8.466)
Assembly fuel, kg U	443.7
Fuel rod data	
Type fuel pellet	UO <sub>2</sub>
Enrichment: wt % <sup>235</sup> U	2.561
wt % <sup>234</sup> U	0.023
wt % <sup>236</sup> U	0.013
Pellet stack density, g/cm <sup>3</sup> (% TD)	9.944 (90.73)
Rod pitch, cm (in.)	1.4300 (0.563)
Rod OD, cm (in.)	1.0719 (0.422)
Rod ID, cm (in.)	0.9484 (0.3734)
Pellet diameter, cm (in.)	0.9294 (0.3659)
Active fuel length, cm (in.)	365.76 (144)
Clad temperature, K	595
Clad material	Zircaloy-4
Guide tube data	
Inner radius, cm (in.)	0.6502 (0.256)
Outer radius, cm (in.)	0.6934 (0.273)
Material	Zircaloy-4
Instrument tube data	
Inner radius, cm (in.)	0.6502 (0.256)
Outer radius, cm (in.)	0.6934 (0.273)
Material	Zircaloy-4
Burnable poison rod data	
Air OD, cm (in.)	0.5677 (0.2235)
SS304 OD, cm (in.)	0.6007 (0.2365)
Air OD, cm (in.)	0.6172 (0.2430)
Borosilicate glass OD, cm (in.)	1.0058 (0.3960)
Air OD, cm (in.)	1.0173 (0.4005)
SS304 OD, cm (in.)	1.1151 (0.4390)

Sources: refs. 19 and 26.

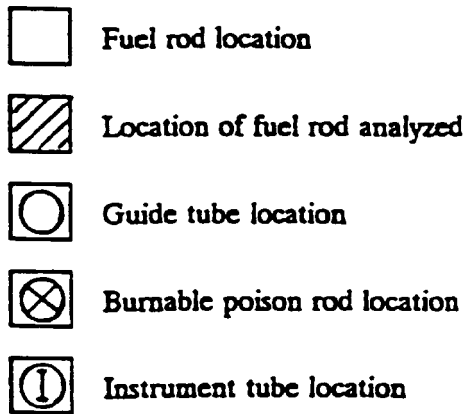
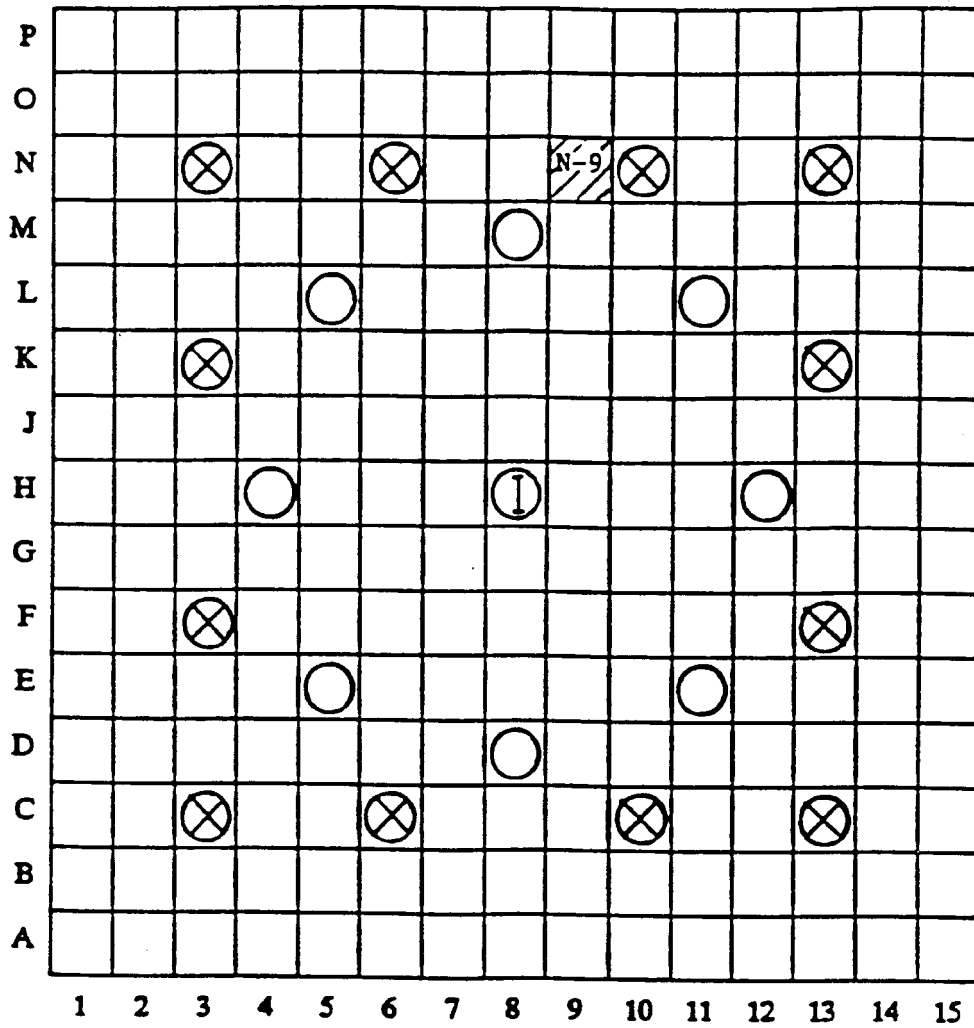


Fig. 8. Location of Fuel Rod N-9 in diagram of Assembly B05 coupled with burnable poison fixture. Sources: refs. 11 and 26.



Table 9. Operating data for H. B. Robinson Assembly B05, Rod N-9 pellet samples

Operating interval number	1	2	3	4
Cycle number including interval	1	1	2	2
Interval time, d	243.5	243.5	156.0	156.0
Downtime following interval, d	40.0	64.0	39.0	-- <sup>a</sup>
Cumulative burnup, GWd/MTU				
No. N-9B-S, 11 cm	5.08	9.99	13.04	16.02
No. N-9B-N, 26 cm	7.85	15.18	19.60	23.81
No. N-9C-J, 199 cm	9.62	18.41	23.61	28.47
No. N-9C-D, 226 cm	10.88	20.68	26.39	31.66
Interval average power, MW/MTU				
No. N-9B-S, 11 cm	20.86	20.15	19.57	18.11
No. N-9B-N, 26 cm	32.23	30.10	28.35	26.99
No. N-9C-J, 199 cm	39.50	36.11	33.33	31.16
No. N-9C-D, 226 cm	44.68	40.25	36.61	33.78
Average soluble boron, ppm (wt)	652.5	247.5	652.5	247.5
Burnable poison fixture, in/out	in	in	out	out

<sup>a</sup>Cooling times after shutdown, on May 6, 1974, for discharge to time of radiochemical analyses listed in Table 2.

Source: ref. 11.

Table 10. Moderator conditions and effective fuel temperatures for H. B. Robinson Unit 2 PWR

Pellet sample ID	Axial location (cm)	Total burnup (GWd/MTU)	Moderator temperature <sup>aa</sup>		Density of moderator <sup>b</sup> (g/cm <sup>3</sup> )	Rod linear power (W/cm)	Fuel temperature <sup>c</sup>	
			(°F)	(K)			(°C)	(K)
N-9B-S	11	16.02	546.6	559	0.7544	119.2	470	743
N-9B-N	26	23.81	547.2	559	0.7538	177.2	557	830
N-9C-J	199	28.47	577.3	576	0.7208	211.9	610	883
N-9C-D	226	31.66	583.3	579	0.7135	235.6	650	923

<sup>a</sup>Derived by method in Sect. 2.1 using 546.5°F and 600.6°F for inlet and outlet temperatures (ref. 27).

<sup>b</sup>Determined from the moderator temperature and the nominal pressure of 2250 psia (ref. 27).

<sup>c</sup>Estimated from curve of effective fuel temperature as function of linear power for reactor rod data (ref. 16) of similar dimensions and pitch (Fig. 9).

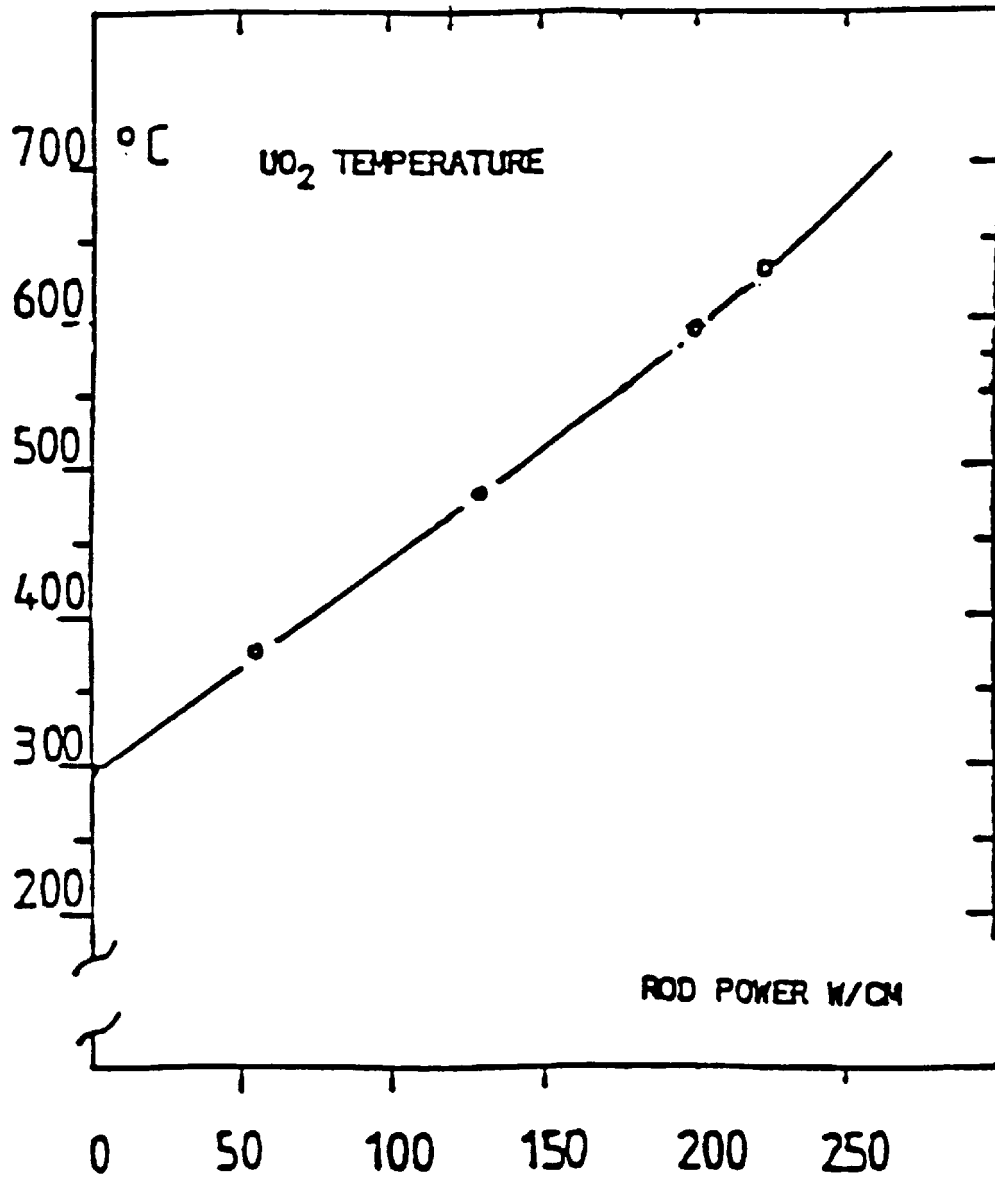


Fig. 9. Fuel temperature vs rod power for Obrigheim. Source: ref. 16.

developed for the Obrigheim PWR, the rod dimensions, rod lattice pitch, and operating conditions of the H. B. Robinson and Obrigheim fuel assemblies are similar. The temperatures were then converted from Celsius to Kelvin.

The BPRs referred to in Tables 8 and 9 and Fig. 8 contained the high-neutron absorber boron in borosilicate glass. The composition of borosilicate glass taken from ref. 28 is listed in Table 11, with the exception that the boron itself<sup>26</sup> applies to the H. B. Robinson PWR. These data, and the atomic weights and isotopic abundances from the Chart of the Nuclides<sup>29</sup> were used in calculating the atomic densities in Table 12.

### 3.3 OBRIGHEIM PWR SPENT FUEL DESIGN AND OPERATING DATA

Obrigheim is a Siemens PWR that uses a  $14 \times 14$  fuel assembly lattice. A description of the Obrigheim fuel assemblies examined is presented in Table 13. All the fuel assemblies analyzed were loaded in Obrigheim during cycles 3, 4, and 6. Power histories for these cycles are listed in Table 14. The total days of uptime and downtime for each cycle are summarized in the table.

Table 15 gives the cycle-specific operating data for the Obrigheim assemblies used to prepare the power history input. The cycle uptime and downtime is taken from Table 14. The cumulative burnups and cycle average powers are based on data<sup>16</sup> reported by the reactor operating utility. The data were normalized to the measured burnup for each assembly. The effective fuel temperatures were determined from the fuel temperature vs rod linear power curve in Fig. 9 (from ref. 16). The cycle average power was converted to the linear power of the rod in order to obtain temperatures from the curve. These temperatures were then converted from Celsius to Kelvin. A single effective fuel temperature for each assembly batch was determined by incremental burnup weighting of the cycle-dependent fuel temperatures.

### 3.4 ADDITIONAL PWR DATA USED FOR SCALE SYSTEM INPUT

The essential data for fuel depletion analyses of the problems listed in Table 2 are included in Tables 2 through 15. However, additional data (e.g., the selection of options or the generic quantities of light elements) are required as input to the SAS2H control module of SCALE-4. These data, or selections, were separately listed in this subsection because they apply more than one of the reactor types considered here.

The data presented in Tables 3 through 7 were used to prepare the SAS2H input for the isotopic calculations for the nine Calvert Cliffs spent fuel samples. Because of the large guide tubes in the CE  $14 \times 14$  fuel assembly design (refer to Fig. 4), a "path-B" model for the SAS2H calculations was set up to describe the larger unit cell as a guide tube surrounded by fuel. This was done by using input level (INPLEVEL) = 2. The path-B model is illustrated in Fig. 10. The guide tube is surrounded by a fuel zone that is equivalent in area to one-fifth of the total cross-sectional area of all fuel rods in an assembly because there are five guide tubes per assembly.

Special consideration was also needed for the H. B. Robinson "path-B" model. The path-B unit cell described in Fig. 2 accounts for the use of a different type of rod, such as a BPR or a guide tube, in addition to the fuel rods. However, it does not allow the model to explicitly simulate two different types of rods or tubes plus fuel rods. In the case of the burnable poison fixture located in Assembly B05 in the H. B. Robinson PWR, there are 12 positions with BPRs, 8 positions with only guide tubes, and a single position with an instrument tube (refer to Table 8 and Fig. 8). An effective fuel cell was derived to incorporate the BPR cell together with the

Table 11. Borosilicate glass composition<sup>a</sup>  
in BP assemblies

Compound	Weight fraction
SiO <sub>2</sub>	0.805
B <sub>2</sub> O <sub>3</sub>	0.125
Na <sub>2</sub> O	0.038
K <sub>2</sub> O	0.004
Al <sub>2</sub> O <sub>3</sub>	0.022

<sup>a</sup>Data from *The Properties of Glass*,  
by G. W. Morey (ref. 28).

Table 12. Borosilicate glass input atom densities<sup>a</sup>

Element	Isotope	Weight fraction	Density, atoms/barn-cm
O		0.5358	0.04497
Na		0.0282	0.00165
Al		0.0116	0.00058
Si		0.3763	0.01799
K		0.0033	0.00011
B		0.03882	
	<sup>10</sup> B		$9.595 \times 10^{-4}$
	<sup>11</sup> B		$3.863 \times 10^{-3}$
Total		0.99402	

<sup>a</sup>Applying weight fractions of compounds in Table 11 and 2.23 g/cm<sup>3</sup> glass density (ref. 28).

Table 13. Design data for the analyzed Obrigheim fuel assemblies

Parameter	Data
Assembly general data	
Designer	Siemens
Lattice	14 × 14
Water temperature, K	572
Water density, g/cm <sup>3</sup>	0.7283
Soluble boron, cycle avg, ppm (wt)	450
Number of fuel rods	180
Number of guide tubes	16
Assembly pitch, cm	20.12
Fuel rod data	
Type fuel pellet	UO <sub>2</sub>
Enrichment,	
wt % <sup>235</sup> U	3.13
wt % <sup>234</sup> U	0.028 <sup>a</sup>
wt % <sup>236</sup> U	0.014 <sup>a</sup>
Pellet stack density g/cm <sup>3</sup>	9.742 <sup>b</sup>
Rod pitch, cm	1.430
Rod OD, cm	1.071 <sup>b</sup>
Rod ID, cm	0.930 <sup>b</sup>
Pellet diameter, cm	0.925 <sup>b</sup>
Active fuel length, cm	295.6
Clad temperature, K	605
Clad material	Zircaloy-4
Guide tube data	
Inner radius, cm	0.6413 <sup>c</sup>
Outer radius, cm	0.6845 <sup>c</sup>
Tube material	Zircaloy-4

<sup>a</sup>Not available, calculated according to the following equations (ref. 24):

$$^{234}\text{U wt \%} = 0.0089 \times ^{235}\text{U wt \%}$$

$$^{236}\text{U wt \%} = 0.0046 \times ^{235}\text{U wt \%}$$

<sup>b</sup>Dimensions and density while hot, in operating reactor.

<sup>c</sup>Dimensions of Westinghouse 14 × 14 guide tubes assumed (ref. 23).

Sources: refs. 15 and 16.

Table 14. Power history of Obrigheim fuel assemblies 168, 170, 171, 172, and 176

Days Cycle 3	Operating condition	Days Cycle 4	Operating condition	Days Cycle 5	Operating condition	Days Cycle 6	Operating condition
4.9	FL <sup>a</sup>	124.2	FL	377	ZL <sup>c</sup>	127.8	FL
2.4	ZL <sup>b</sup>	8.5	ZL			2.4	ZL
79.1	FL	90.1	FL			54.8	FL
3.7	ZL	2.4	ZL			1.2	ZL
18.3	FL	9.7	FL			65.7	FL
1.2	ZL	1.2	ZL				
12.2	FL	13.4	FL				
37.7	ZL	4.9	ZL				
136.5	FL	1.2	FL				
6.8	ZL	2.4	ZL				
37.0	FL	70.6	FL				
29.2	ZL						
<u>Cycle length, days</u>							
369		328		377		252	
<u>Uptime days</u>							
288		309		0		248	
<u>Downtime days</u>							
81		19		377		4	

<sup>a</sup>FL = full load.

<sup>b</sup>ZL = zero load.

<sup>c</sup>The specified assemblies were not loaded in cycle 5.

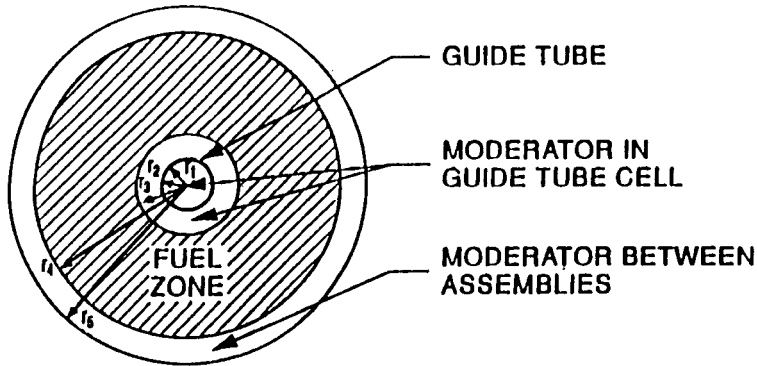
Source: ref. 16.

Table 15. Operating data for the Obrigheim fuel assemblies and dissolved fuel batches

Operating history parameter type	Assembly ID	Batch number	Cycle number				Burnup weighted fuel temp <sup>a</sup>
			3	4	5	6	
Uptime, days	all	all	288	309	–	248	
Downtime, days	all	all	81	19	377	913	
Cumulative burnup, GWd/MTU:	170	94	6.03	17.61	–	25.93	
	172	92	10.03	17.77	–	26.54	
	176	91	8.77	19.55	–	27.99	
	168	86	8.16	19.90	–	28.40	
	171	89	8.39	20.42	–	29.04	
	176	90	9.25	20.62	–	29.52	
Average power, MW/MTU:	170	94	20.929	37.468	–	33.564	
	172	92	34.833	25.035	–	35.374	
	176	91	30.457	34.894	–	34.016	
	168	86	28.336	38.005	–	34.249	
	171	89	29.124	38.952	–	34.748	
	176	90	32.121	36.801	–	35.875	
Effective fuel temperature, K:	170	94	743	896	–	851	846
	172	92	865	778	–	870	841
	176	91	825	865	–	855	849
	168	86	807	895	–	860	859
	171	89	813	905	–	865	867
	176	90	840	883	–	875	867

<sup>a</sup>Applied a constant effective fuel temperature derived from weighting the cycle temperature by cycle incremental burnup.

Source: ref. 16.



<u>Region</u>	<u>Radius (cm)</u>	<u>Description</u>	<u>Source of dimension</u>
1	1.314	Moderator inside guide tube	Guide tube inner radius
2	1.416	Guide tube	Guide tube outer radius
3	1.662	Moderator outside guide tube	Area of single unit cell
4	5.203	Fuel area per guide tube	Ratio areas by $14 \times 14$ to 20
5	5.243	Space between assemblies per guide tube	Apply assembly pitch

Fig. 10. SAS2H "path-B" model for Calvert Cliffs fuel assemblies.



guide tube cell. In the effective cell, the densities of the isotopes or elements remained unchanged from their actual densities, but rod diameters of the glass and stainless steel in the BPRs were reduced to account for their absence in the guide tube positions. The method of deriving the effective cell was such that the various material total masses were conserved. The effective cell geometry of the 21 non-fuel-rod positions is shown in Table 16, listing the effective radii from the innermost to the outside of the guide tube.

The SAS2H input data for the cases described in this report are included in Appendix A. Fuel assembly design and cycle operation data considered essential for isotopic analyses using fuel depletion codes were presented earlier in this section. These data were sufficient to prepare SAS2H input with the exception of two types of data. The first type of data was the weights of the light elements or structural materials of the specified fuel assemblies. These data were not readily available. Although large uncertainties in the light-element weights produce only small uncertainties in energy per fission, it is more complete to include the data in the SAS2H input (see input example in Sect. 2.4). A commonly applied generic set of light-element weights for PWRs,<sup>24</sup> listed in Table 17, was assumed. These data are provided both in units of kg/MTUO<sub>2</sub> and kg/MTU to allow the predictions to be compared more directly with analyses performed in units of either mass/MTUO<sub>2</sub> or mass/MTU.

The second set of SAS2H data not specified explicitly in Tables 3 through 15 are the nuclides selected as those for which cross sections should be updated during the depletion. The nuclide set to be updated is listed in Table 18. A nuclide was included in the set to be updated if any of the following criteria applied.

- The nuclide was in the set for radiochemical analyses for which results were reported.
- The nuclide was a precursor and the omission of its cross section from the calculation would cause a  $\geq 1\%$  change in the predicted concentration of a measured nuclide.
- The nuclide had a neutron absorption fraction  $\geq 0.005$  and thus could have a potential impact on the flux spectra.

Table 16. Effective parameters of the 21 nonfuel positions—  
20 guide tubes (12 with BPRs) and 1 instrument tube

Material	Density, g/cm <sup>3</sup>	Effective radius, cm
Air	$1.22 \times 10^{-3}$	0.21457
SS-304	7.92	0.22705
Air	$1.22 \times 10^{-3}$	0.23329
Glass	2.23	0.38017
Air	$1.22 \times 10^{-3}$	0.38449
SS-304	7.92	0.42145
Water	--	0.65024
Zr-4	6.44	0.69342

Table 17. Light element<sup>a</sup> mass per unit of fuel for SAS2H input

Element	<u>H. B. Robinson</u>	<u>Calvert Cliffs</u>	<u>Obrigheim</u>
	kg/MTUO <sub>2</sub>	kg/MTUO <sub>2</sub>	kg/MTU
O	119.0	119.0	135.0
Cr	5.2	5.2	5.9
Mn	0.29	0.29	0.33
Fe	11.0	11.0	13.0
Co	0.066	0.066	0.075
Ni	8.7	8.7	9.9
Zr	195.0	195.0	221.0
Nb	0.63	0.63	0.71
Sn	3.2	3.2	3.6

<sup>a</sup>Included only elements with contents exceeding  
0.5 kg/MTU plus Mn and Co.

Source: ref. 24.

Table 18. Fuel, fuel activation, fission product, and light-element nuclides for which cross sections were updated in SAS2H cases

---

Fuel nuclides and fuel activation products:

$^{234}\text{U}$	$^{237}\text{Np}$	$^{240}\text{Pu}$	$^{241}\text{Am}$
$^{235}\text{U}$	$^{238}\text{Pu}$	$^{241}\text{Pu}$	$^{243}\text{Am}$
$^{236}\text{U}$	$^{239}\text{Pu}$	$^{242}\text{Pu}$	$^{244}\text{Cm}$
$^{238}\text{U}$			

Fission products:

$^{83}\text{Kr}^a$	$^{131}\text{Xe}$	$^{144}\text{Nd}^b$	$^{150}\text{Sm}$
$^{84}\text{Kr}^a$	$^{132}\text{Xe}^a$	$^{145}\text{Nd}$	$^{151}\text{Sm}$
$^{85}\text{Kr}^a$	$^{134}\text{Xe}^a$	$^{146}\text{Nd}$	$^{152}\text{Sm}$
$^{86}\text{Kr}^a$	$^{135}\text{Xe}$	$^{147}\text{Nd}$	$^{151}\text{Eu}$
$^{94}\text{Zr}$	$^{136}\text{Xe}^a$	$^{148}\text{Nd}$	$^{153}\text{Eu}$
$^{95}\text{Nb}$	$^{133}\text{Cs}$	$^{150}\text{Nd}^b$	$^{154}\text{Eu}$
$^{94}\text{Mo}^a$	$^{134}\text{Cs}$	$^{147}\text{Pm}$	$^{155}\text{Eu}$
$^{95}\text{Mo}$	$^{135}\text{Cs}$	$^{148}\text{Pm}^b$	$^{154}\text{Gd}$
$^{99}\text{Tc}$	$^{137}\text{Cs}$	$^{149}\text{Pm}$	$^{155}\text{Gd}$
$^{106}\text{Ru}$	$^{144}\text{Ce}$	$^{147}\text{Sm}$	$^{157}\text{Gd}$
$^{103}\text{Rh}$	$^{143}\text{Pr}$	$^{148}\text{Sm}^b$	$^{158}\text{Gd}$
$^{105}\text{Rh}$	$^{143}\text{Nd}$	$^{149}\text{Sm}$	$^{160}\text{Gd}$
$^{126}\text{Sn}$			

Light-element nuclides:

---

$^1\text{H}$	$^{12}\text{C}$	$^{16}\text{O}$	$^{27}\text{Al}^c$
$^{10}\text{B}^c$	$^{14}\text{N}$	$^{23}\text{Na}^c$	$^{59}\text{Co}$
$^{11}\text{B}^c$			

---

<sup>a</sup>Included only in the Obrigheim PWR cases in order to predict fission-product ratios not analyzed in other cases.

<sup>b</sup>Included only in Assembly D047 cases in order to properly predict additional measured nuclides not analyzed in other cases.

<sup>c</sup>Updated only for BPR material of H. B. Robinson PWR cases.

## 4. PREDICTED AND MEASURED ISOTOPIC COMPOSITIONS

Comparisons of spent PWR fuel isotopic compositions predicted by SCALE-4 calculations and measured by radiochemical assay analyses are provided in this section. Percentage differences between the computed and measured values for all isotopes selected for the assay analysis are given for each sample. Also included in this section are the average percentage differences for each assembly and for each of the three reactor types. The comparisons are shown for two different SCALE cross-section libraries derived, in part, from different versions of ENDF/B data. Automated comparison outputs listing measurements, predictions, and percentage differences of all the cases are given in Appendix B.

### 4.1 CALVERT CLIFFS PWR ANALYSES

Radiochemical isotopic analyses of Calvert Cliffs PWR spent fuel were conducted by the MCC at PNL. Isotopic measurements, in units of grams per gram  $\text{UO}_2$ , of spent fuel samples from assemblies D047, D101, and BT03 are listed in Tables 19 through 21. Also, other assay data for the samples from the three assemblies measured in units of curies per gram  $\text{UO}_2$  are tabulated in Tables 22 through 24. The general description of the fuel specimens analyzed, such as the initial  $^{235}\text{U}$  enrichments and cooling times, are given in Table 2.

Spent fuel isotopic compositions predicted by SCALE-4/SAS2H for the Calvert Cliffs samples were compared with the measured data listed in Tables 19 through 24. Percentage differences between the measured and computed nuclide compositions for the three axial samples from the assemblies are given in Tables 25 and 26, applying cross-section libraries in which the actinide data were derived from ENDF/B-IV and ENDF/B-V, respectively. The average percentage difference of each assembly for the nuclides and final average of the three assembly comparisons are presented in Table 27.

### 4.2 H. B. ROBINSON PWR ANALYSES

Radiochemical analyses of H. B. Robinson spent fuel were performed by the MCC at PNL. Isotopic compositions of the samples from Assembly B05 are listed as grams per gram  $\text{UO}_2$  and curies per gram  $\text{UO}_2$  in Tables 28 and 29, respectively. Percentage differences between measured and computed nuclide compositions for the four axial samples from the assembly are listed in Tables 30 and 31 for SCALE-4/SAS2H calculations applying cross-section libraries in which the actinide data were derived from ENDF/B-IV and ENDF/B-V, respectively.

### 4.3 OBRIGHEIM PWR ANALYSES

The average isotopic measurements from Obrigheim derived from plotted data<sup>15</sup> are listed in Table 32. Also, average nuclide atomic ratio measurements (tabulated in Appendix C) are shown in Table 33. The radiochemical analyses were performed independently by the laboratories of the European Institute for Transuranic Elements, the Institute for Radiochemistry, the Karlsruhe Reprocessing Plant, and the International Atomic Energy Agency. Each fuel assembly was split lengthwise before dissolution so that two batches per assembly were available for analysis. The measured results used here were from one batch of each fuel assembly. Both the assembly ID and the batch number are used to identify samples in Tables 32 and 33. The burnups and cycle average powers in Table 15 correspond to these specific batches. Percentage differences between measured and computed nuclide compositions for the assembly samples, using cross-section libraries in which the actinide data were derived from ENDF/B-IV (27BURNULIB) and ENDF/B-V (44GROUPNDF5), are listed in Tables 34 and 35, respectively.

Table 19. Measured irradiated composition,<sup>a</sup> in g/g UO<sub>2</sub>, of Calvert Cliffs  
Assembly D047 Rod MKP109

Nuclide	Axial location, cm from bottom of fuel (Burnup, <sup>b</sup> GWd/MTU)		
	13.20 cm (27.35)	27.70 cm (37.12)	165.22 cm (44.34)
<sup>234</sup> U	$1.6 \times 10^{-4}$	$1.4 \times 10^{-4}$	$1.2 \times 10^{-4}$
<sup>235</sup> U	$8.47 \times 10^{-3}$	$5.17 \times 10^{-3}$	$3.54 \times 10^{-3}$
<sup>236</sup> U	$3.14 \times 10^{-3}$	$3.53 \times 10^{-3}$	$3.69 \times 10^{-3}$
<sup>238</sup> U	$8.425 \times 10^{-1}$	$8.327 \times 10^{-1}$	$8.2486 \times 10^{-1}$
<sup>238</sup> Pu	$1.01 \times 10^{-4}$	$1.89 \times 10^{-4}$	$2.69 \times 10^{-4}$
<sup>239</sup> Pu	$4.264 \times 10^{-3}$	$4.357 \times 10^{-3}$	$4.357 \times 10^{-3}$
<sup>240</sup> Pu	$1.719 \times 10^{-3}$	$2.239 \times 10^{-3}$	$2.543 \times 10^{-3}$
<sup>241</sup> Pu	$6.81 \times 10^{-4}$	$9.03 \times 10^{-4}$	$1.020 \times 10^{-3}$
<sup>242</sup> Pu	$2.89 \times 10^{-4}$	$5.76 \times 10^{-4}$	$8.40 \times 10^{-4}$
<sup>237</sup> Np	$2.68 \times 10^{-4}$	$3.56 \times 10^{-4}$	$4.68 \times 10^{-4}$
<sup>133</sup> Cs <sup>c</sup>	$8.5 \times 10^{-4}$	$1.09 \times 10^{-3}$	$1.24 \times 10^{-3}$
<sup>134</sup> Cs	$1.0 \times 10^{-5}$	$2.0 \times 10^{-5}$	$3.0 \times 10^{-5}$
<sup>135</sup> Cs	$3.6 \times 10^{-4}$	$4.0 \times 10^{-4}$	$4.3 \times 10^{-4}$
<sup>137</sup> Cs	$7.7 \times 10^{-4}$	$1.04 \times 10^{-3}$	$1.25 \times 10^{-3}$
<sup>143</sup> Nd <sup>d</sup>	$6.13 \times 10^{-4}$	$7.16 \times 10^{-4}$	$7.63 \times 10^{-4}$
<sup>144</sup> Nd	$9.43 \times 10^{-4}$	$1.388 \times 10^{-3}$	$1.643 \times 10^{-3}$
<sup>145</sup> Nd <sup>d</sup>	$5.10 \times 10^{-4}$	$6.53 \times 10^{-4}$	$7.44 \times 10^{-4}$
<sup>146</sup> Nd	$4.90 \times 10^{-4}$	$6.82 \times 10^{-4}$	$8.30 \times 10^{-4}$
<sup>148</sup> Nd	$2.65 \times 10^{-4}$	$3.59 \times 10^{-4}$	$4.28 \times 10^{-4}$
<sup>150</sup> Nd	$1.24 \times 10^{-4}$	$1.72 \times 10^{-4}$	$2.08 \times 10^{-4}$
<sup>147</sup> Pm + <sup>147</sup> Sm <sup>d</sup>	$2.21 \times 10^{-4}$	$2.54 \times 10^{-4}$	$2.68 \times 10^{-4}$
<sup>148</sup> Sm	$1.06 \times 10^{-4}$	$1.64 \times 10^{-4}$	$2.22 \times 10^{-4}$
<sup>149</sup> Sm <sup>d</sup>	$2.9 \times 10^{-6}$	$3.0 \times 10^{-6}$	$4.7 \times 10^{-6}$
<sup>150</sup> Sm <sup>d</sup>	$2.07 \times 10^{-4}$	$2.71 \times 10^{-4}$	$3.61 \times 10^{-4}$
<sup>151</sup> Sm + <sup>151</sup> Eu <sup>d</sup>	$9.34 \times 10^{-6}$	$9.30 \times 10^{-6}$	$9.78 \times 10^{-6}$
<sup>152</sup> Sm <sup>d</sup>	$8.7 \times 10^{-5}$	$1.04 \times 10^{-4}$	$1.21 \times 10^{-4}$
<sup>153</sup> Eu <sup>d</sup>	$7.9 \times 10^{-5}$	$1.09 \times 10^{-4}$	$1.48 \times 10^{-4}$
<sup>154</sup> Sm + <sup>154</sup> Eu + <sup>154</sup> Gd	$4.16 \times 10^{-5}$	$6.07 \times 10^{-5}$	$8.42 \times 10^{-5}$
<sup>155</sup> Eu + <sup>155</sup> Gd <sup>d</sup>	$4.74 \times 10^{-6}$	$7.10 \times 10^{-6}$	$9.82 \times 10^{-6}$

<sup>a</sup>Radiochemical analyses performed after a cooling time of 1870 days, unless different time specified.

<sup>b</sup>Burnup based on measured <sup>148</sup>Nd concentration (ASTM 1985).

<sup>c</sup>Based on <sup>137</sup>Cs/<sup>133</sup>Cs mass ratio.

<sup>d</sup>Radiochemical analyses performed after 3817 days cooling time, with reported values adjusted to 1870 days.

Sources: refs. 13, 22, and 25.

Table 20. Measured irradiated composition, in g/g UO<sub>2</sub>, of  
Calvert Cliffs Assembly D101 Rod MLA098

Nuclide	Axial location, cm from bottom of fuel (Burnup, <sup>a</sup> GWd/MTU)		
	8.90 cm (18.68)	24.30 cm (26.62)	161.70 cm (33.17)
<sup>234</sup> U	$1.400 \times 10^{-4}$	$1.210 \times 10^{-4}$	$1.200 \times 10^{-4}$
<sup>235</sup> U	$1.025 \times 10^{-2}$	$6.940 \times 10^{-3}$	$4.780 \times 10^{-3}$
<sup>236</sup> U	$2.500 \times 10^{-3}$	$2.990 \times 10^{-3}$	$3.260 \times 10^{-3}$
<sup>238</sup> U	$8.551 \times 10^{-1}$	$8.538 \times 10^{-1}$	$8.422 \times 10^{-1}$
<sup>238</sup> Pu	$4.850 \times 10^{-5}$	$9.690 \times 10^{-5}$	$1.483 \times 10^{-4}$
<sup>239</sup> Pu	$3.954 \times 10^{-3}$	$4.252 \times 10^{-3}$	$4.187 \times 10^{-3}$
<sup>240</sup> Pu	$1.243 \times 10^{-3}$	$1.766 \times 10^{-3}$	$2.111 \times 10^{-3}$
<sup>241</sup> Pu	$4.543 \times 10^{-4}$	$6.822 \times 10^{-4}$	$8.125 \times 10^{-4}$
<sup>242</sup> Pu	$1.394 \times 10^{-4}$	$3.301 \times 10^{-4}$	$5.474 \times 10^{-4}$

<sup>a</sup>Burnup based on measured <sup>148</sup>Nd concentration (ASTM 1985).

Source: ref. 12.

Table 21. Measured irradiation composition, in g/g UO<sub>2</sub>, of  
Calvert Cliffs Assembly BT03 Rod NBD107

Nuclide	Axial location, cm from bottom of fuel (Burnup, <sup>a</sup> GWd/MTU)		
	11.28 cm (31.40)	19.92 cm (37.27)	161.21 cm (46.46)
<sup>234</sup> U	$1.53 \times 10^{-4}$	$1.27 \times 10^{-4}$	$7.49 \times 10^{-5}$
<sup>235</sup> U	$3.86 \times 10^{-3}$	$2.71 \times 10^{-3}$	$1.406 \times 10^{-3}$
<sup>236</sup> U	$2.86 \times 10^{-3}$	$3.03 \times 10^{-3}$	$3.04 \times 10^{-3}$
<sup>238</sup> U	$8.446 \times 10^{-1}$	$8.438 \times 10^{-1}$	$8.272 \times 10^{-1}$
<sup>238</sup> Pu	$1.426 \times 10^{-4}$	$1.947 \times 10^{-4}$	$2.842 \times 10^{-4}$
<sup>239</sup> Pu	$3.814 \times 10^{-3}$	$3.835 \times 10^{-3}$	$3.766 \times 10^{-3}$
<sup>240</sup> Pu	$2.067 \times 10^{-3}$	$2.321 \times 10^{-3}$	$2.599 \times 10^{-3}$
<sup>241</sup> Pu	$7.260 \times 10^{-4}$	$8.130 \times 10^{-4}$	$8.862 \times 10^{-4}$
<sup>242</sup> Pu	$5.463 \times 10^{-4}$	$7.753 \times 10^{-4}$	$1.169 \times 10^{-3}$

<sup>a</sup>Burnup based on measured <sup>148</sup>Nd concentration (ASTM 1985).

Source: ref. 13.

Table 22. Measured irradiation composition, in Ci/g UO<sub>2</sub>, of Calvert Cliffs Assembly D047 Rod MKP109

Nuclide	Axial location, cm from bottom of fuel (Burnup, <sup>a</sup> GWd/MTU)		
	13.20 cm (27.35)	27.70 cm (37.12)	165.22 cm (44.34)
<sup>241</sup> Am	$8.56 \times 10^{-4}$	$1.18 \times 10^{-3}$	$1.31 \times 10^{-3}$
<sup>243</sup> Cm + <sup>244</sup> Cm	$7.34 \times 10^{-4}$	$2.93 \times 10^{-3}$	$6.40 \times 10^{-3}$
<sup>79</sup> Se	$4.55 \times 10^{-8}$	$6.036 \times 10^{-8}$	$6.49 \times 10^{-8}$
<sup>90</sup> Sr	$4.59 \times 10^{-2}$	$5.90 \times 10^{-2}$	$6.58 \times 10^{-2}$
<sup>99</sup> Tc	$9.59 \times 10^{-6}$	$1.23 \times 10^{-5}$	$1.35 \times 10^{-5}$

<sup>a</sup>Burnup based on measured <sup>148</sup>Nd concentration (ASTM 1985).

Source: ref. 13.

Table 23. Measured irradiation composition, in Ci/g UO<sub>2</sub>, of Calvert Cliffs Assembly D101 Rod MLA098

Nuclide	Axial location, cm from bottom of fuel (Burnup, <sup>a</sup> GWd/MTU)		
	8.9 cm (18.68)	24.3 cm (26.62)	161.7 cm (33.17)
<sup>237</sup> Np	$1.23 \times 10^{-7}$	$2.11 \times 10^{-7}$	$2.41 \times 10^{-7}$
<sup>241</sup> Am	$6.67 \times 10^{-4}$	$9.91 \times 10^{-4}$	$1.20 \times 10^{-3}$
<sup>243</sup> Cm + <sup>244</sup> Cm	$1.64 \times 10^{-4}$	$8.15 \times 10^{-4}$	$2.11 \times 10^{-3}$
<sup>14</sup> C	$3.91 \times 10^{-7}$	$5.03 \times 10^{-7}$	$7.69 \times 10^{-7}$
<sup>79</sup> Se	$3.43 \times 10^{-8}$	$4.59 \times 10^{-8}$	$5.54 \times 10^{-8}$
<sup>90</sup> Sr	$3.36 \times 10^{-2}$	$4.41 \times 10^{-2}$	$5.23 \times 10^{-2}$
<sup>99</sup> Tc	$7.07 \times 10^{-6}$	$9.37 \times 10^{-6}$	$1.13 \times 10^{-5}$
<sup>126</sup> Sn	$8.60 \times 10^{-8}$	$1.36 \times 10^{-7}$	$1.69 \times 10^{-7}$
<sup>129</sup> I	$1.75 \times 10^{-8}$	$2.41 \times 10^{-8}$	$3.36 \times 10^{-8}$
<sup>135</sup> Cs	$2.79 \times 10^{-7}$	$3.12 \times 10^{-7}$	$3.32 \times 10^{-7}$
<sup>137</sup> Cs	$4.59 \times 10^{-2}$	$6.53 \times 10^{-2}$	$8.06 \times 10^{-2}$

<sup>a</sup>Burnup based on measured <sup>148</sup>Nd concentration (ASTM 1985).

Source: ref. 12.

Table 24. Measured irradiation composition, in Ci/g UO<sub>2</sub>, of  
Calvert Cliffs Assembly BT03 Rod NBD107

Nuclide	Axial location, cm from bottom of fuel (Burnup, <sup>a</sup> GWd/MTU)		
	11.28 cm (31.40)	19.92 cm (37.27)	161.21 cm (46.46)
<sup>237</sup> Np	$1.84 \times 10^{-7}$	$2.26 \times 10^{-7}$	$2.66 \times 10^{-7}$
<sup>241</sup> Am	$1.18 \times 10^{-3}$	$1.46 \times 10^{-3}$	$2.18 \times 10^{-3}$
<sup>243</sup> Cm + <sup>244</sup> Cm	$1.87 \times 10^{-3}$	$4.11 \times 10^{-3}$	$9.86 \times 10^{-3}$
<sup>79</sup> Se	$4.18 \times 10^{-8}$	$5.63 \times 10^{-8}$	$5.99 \times 10^{-8}$
<sup>90</sup> Sr	$4.64 \times 10^{-2}$	$5.18 \times 10^{-2}$	$6.04 \times 10^{-2}$
<sup>99</sup> Tc	$7.70 \times 10^{-6}$	$8.96 \times 10^{-6}$	$1.09 \times 10^{-5}$
<sup>126</sup> Sn	$1.41 \times 10^{-7}$	$1.60 \times 10^{-7}$	$2.10 \times 10^{-7}$
<sup>135</sup> Cs	$4.04 \times 10^{-7}$	$4.15 \times 10^{-7}$	$4.79 \times 10^{-7}$
<sup>137</sup> Cs	$7.47 \times 10^{-2}$	$8.56 \times 10^{-2}$	$1.12 \times 10^{-1}$

<sup>a</sup>Burnup based on measured <sup>148</sup>Nd concentration (ASTM 1985).

Source: ref. 14.



Table 25. Percentage difference<sup>a</sup> between measured and computed<sup>b</sup> nuclide compositions for Calvert Cliffs PWR pellet samples (27BURNUPLIB library)

Burnup, GWd/MTU Initial wt % <sup>235</sup> U	Assembly D047			Assembly D101			Assembly BT03		
	27.35	37.12	44.34	18.68	26.62	33.17	31.40	37.27	46.46
	3.04	3.04	3.04	2.72	2.72	2.72	2.45	2.45	2.45
<b>Nuclide</b>									
<sup>234</sup> U	0.7	-0.4	4.6	14.6	17.5	7.3	-21.2	-12.6	31.4
<sup>235</sup> U	-5.5	-8.6	-9.6	-1.6	-4.4	-2.4	-0.9	-4.3	1.4
<sup>236</sup> U	3.1	2.9	1.7	-0.7	-0.4	-1.3	1.4	-0.9	-0.5
<sup>238</sup> U	-0.6	-0.3	-0.1	-1.1	-1.7	-0.9	-0.8	-1.3	-0.3
<sup>238</sup> Pu	-3.1	-0.5	0.1	-17.7	-7.1	-1.0	3.1	3.4	2.2
<sup>239</sup> Pu	0.4	1.3	4.6	-1.5	-0.8	5.6	5.8	6.5	11.8
<sup>240</sup> Pu	-6.1	-7.7	-8.6	-6.8	-7.5	-7.8	-5.6	-6.0	-5.6
<sup>241</sup> Pu	4.1	3.3	4.4	-0.9	2.2	6.4	1.8	2.3	6.6
<sup>242</sup> Pu	-4.2	-3.6	-6.5	-11.0	-7.9	-9.1	-10.5	-11.1	-14.0
<sup>237</sup> Np	17.8	28.5	19.3	10.4	2.3	17.9	36.2	33.3	39.7
<sup>241</sup> Am	0.1	-6.5	-5.6	-2.4	0.7	2.4	1.3	-9.9	-33.4
<sup>243</sup> Cm + <sup>244</sup> Cm	-18.1	-15.0	-14.7	-29.3	-19.4	-12.0	-8.9	-13.0	-11.6
<sup>14</sup> C	-	-	-	-17.3	-4.7	-20.6	-	-	-
<sup>79</sup> Se <sup>c</sup>	8.8	8.9	18.9	-0.1	4.5	6.0	32.8	15.3	32.0
<sup>90</sup> Sr	8.9	6.0	7.0	5.3	6.0	4.7	5.6	6.5	5.3
<sup>99</sup> Tc	4.8	6.0	11.1	0.4	4.1	4.2	45.0	43.5	40.1
<sup>126</sup> Sn	-	-	-	179.1	181.0	201.8	249.1	283.7	286.9
<sup>129</sup> I	-	-	-	-11.7	-6.1	-14.7	-	-	-
<sup>133</sup> Cs	1.2	1.8	2.7	-	-	-	-	-	-
<sup>134</sup> Cs	0.7	-9.5	-15.5	-	-	-	-	-	-
<sup>135</sup> Cs	9.3	7.9	7.1	9.4	9.7	10.8	14.8	17.9	11.4
<sup>137</sup> Cs	1.7	2.0	1.2	0.1	0.2	1.1	-0.6	2.9	-2.0
<sup>143</sup> Nd	1.2	1.0	1.7	-	-	-	-	-	-
<sup>144</sup> Nd	0.3	0.2	-0.3	-	-	-	-	-	-
<sup>145</sup> Nd	0.6	0.3	0.3	-	-	-	-	-	-
<sup>146</sup> Nd	0.5	0.4	0.4	-	-	-	-	-	-
<sup>148</sup> Nd	0.5	0.3	0.2	-	-	-	-	-	-
<sup>150</sup> Nd	2.3	3.3	4.1	-	-	-	-	-	-
<sup>147</sup> Pm + <sup>147</sup> Sm	-1.9	-4.6	-6.9	-	-	-	-	-	-
<sup>148</sup> Sm	-16.6	-13.7	-17.4	-	-	-	-	-	-
<sup>149</sup> Sm	-25.2	-21.0	-44.9	-	-	-	-	-	-
<sup>150</sup> Sm	-1.9	4.8	-4.5	-	-	-	-	-	-
<sup>151</sup> Sm + <sup>151</sup> Eu	13.0	28.6	36.8	-	-	-	-	-	-
<sup>152</sup> Sm	11.7	21.0	19.2	-	-	-	-	-	-
<sup>153</sup> Eu	-5.8	0.5	-9.2	-	-	-	-	-	-
<sup>154</sup> Sm + <sup>154</sup> Eu + <sup>154</sup> Gd	21.7	38.4	32.4	-	-	-	-	-	-
<sup>155</sup> Eu + <sup>155</sup> Gd	77.4	106.2	104.2	-	-	-	-	-	-

<sup>a</sup>(Calculated/measured - 1) × 100%.

<sup>b</sup>Using SAS2H/ORIGEN-S analysis sequence and 27-group cross-section library (27BURNUPLIB) of SCALE-4.

<sup>c</sup>The computed composition was converted to curies using the corrected <sup>79</sup>Se half-life of 330,000 years. The ORIGEN-S decay library contained an incorrect value (an error in the ENDF/B data) of 1000% at the time of the analysis.

Table 26. Percentage difference<sup>a</sup> between measured and computed<sup>b</sup> nuclide compositions for Calvert Cliffs PWR pellet samples (44GROUPNDF5 library)

Burnup, GWd/MTU Initial wt % <sup>235</sup> U	Assembly D047			Assembly D101			Assembly BT03		
	27.35	37.12	44.34	18.68	26.62	33.17	31.40	37.27	46.46
	3.04	3.04	3.04	2.72	2.72	2.72	2.45	2.45	2.45
<u>Nuclide</u>									
<sup>234</sup> U	-1.5	-3.1	1.4	12.6	14.9	4.5	-23.5	-15.6	26.1
<sup>235</sup> U	-4.7	-7.7	-8.7	-0.9	-3.4	-1.4	0.2	-3.1	2.5
<sup>236</sup> U	2.9	2.9	1.9	-1.0	-0.6	-1.3	1.3	-0.9	-0.3
<sup>238</sup> U	-0.6	-0.3	-0.1	-1.1	-1.7	-0.9	-0.8	-1.3	-0.3
<sup>238</sup> Pu	-8.3	-5.5	-5.0	-22.5	-12.0	-6.1	-2.6	-2.2	-3.4
<sup>239</sup> Pu	-5.3	-4.6	-1.5	-6.6	-6.4	-0.5	-0.5	0.1	5.1
<sup>240</sup> Pu	-0.6	-2.7	-3.9	-0.9	-2.0	-2.5	-0.3	-1.0	-0.8
<sup>241</sup> Pu	-1.9	-3.1	-2.4	-6.0	-3.8	-0.2	-4.3	-4.1	-0.3
<sup>242</sup> Pu	6.6	7.0	4.1	-0.5	2.4	0.9	-1.2	-1.8	-4.6
<sup>237</sup> Np	5.8	15.5	7.2	-1.7	-8.5	5.7	21.3	18.6	23.8
<sup>241</sup> Am	-4.9	-11.6	-11.0	-7.0	-4.7	-3.5	-4.1	-14.8	-37.2
<sup>243</sup> Cm + <sup>244</sup> Cm	-3.1	-1.4	-1.8	-15.1	-5.0	2.7	4.5	-1.1	-0.3
<sup>14</sup> C	-	-	-	-17.0	-4.4	-20.2	-	-	-
<sup>79</sup> Se <sup>c</sup>	8.7	8.8	18.8	-0.2	4.4	5.9	32.7	15.2	31.9
<sup>90</sup> Sr	8.7	5.9	7.0	5.0	5.8	4.6	5.6	6.4	5.4
<sup>99</sup> Tc	5.1	6.5	11.9	0.5	4.5	4.7	45.5	44.2	41.0
<sup>126</sup> Sn	-	-	-	179.8	180.9	201.3	248.5	282.7	285.7
<sup>129</sup> I	-	-	-	-11.6	-6.0	-14.7	-	-	-
<sup>133</sup> Cs	1.6	2.4	3.4	-	-	-	-	-	-
<sup>134</sup> Cs	-2.9	-12.7	-18.6	-	-	-	-	-	-
<sup>135</sup> Cs	4.6	2.7	1.7	4.8	4.5	5.2	9.6	12.2	5.8
<sup>137</sup> Cs	1.7	2.0	1.2	0.1	0.2	1.0	-0.7	2.8	-2.1
<sup>143</sup> Nd	0.6	0.1	0.5	-	-	-	-	-	-
<sup>144</sup> Nd	0.6	0.7	0.2	-	-	-	-	-	-
<sup>145</sup> Nd	0.1	-0.4	-0.6	-	-	-	-	-	-
<sup>146</sup> Nd	1.0	1.1	1.3	-	-	-	-	-	-
<sup>148</sup> Nd	0.6	0.4	0.3	-	-	-	-	-	-
<sup>150</sup> Nd	2.5	3.4	4.2	-	-	-	-	-	-
<sup>147</sup> Pm + <sup>147</sup> Sm	-0.8	-2.9	-4.8	-	-	-	-	-	-
<sup>148</sup> Sm	-17.8	-14.6	-18.2	-	-	-	-	-	-
<sup>149</sup> Sm	-31.4	-27.3	-49.1	-	-	-	-	-	-
<sup>150</sup> Sm	-2.6	3.8	-5.6	-	-	-	-	-	-
<sup>151</sup> Sm + <sup>151</sup> Eu	15.2	30.6	38.5	-	-	-	-	-	-
<sup>152</sup> Sm	14.5	23.9	22.0	-	-	-	-	-	-
<sup>153</sup> Eu	1.1	11.3	2.5	-	-	-	-	-	-
<sup>154</sup> Sm + <sup>154</sup> Eu + <sup>154</sup> Gd	-5.5	2.6	-3.4	-	-	-	-	-	-
<sup>155</sup> Eu + <sup>155</sup> Gd	-27.1	-20.7	-25.3	-	-	-	-	-	-

<sup>a</sup>(Calculated/measured - 1) × 100%.

<sup>b</sup>Using SAS2H/ORIGEN-S analysis sequence and a 44-group ENDF/B-V cross-section library with data for <sup>154</sup>Eu and <sup>155</sup>Eu taken from ENDF/B-VI.

<sup>c</sup>The computed composition was converted to curies using the corrected <sup>79</sup>Se half-life of 330,000 years. The ORIGEN-S decay library contained an incorrect value (an error in the ENDF/B data) of 1000% at the time of the analysis.

Table 27. Average percentage difference<sup>a</sup> between measured and computed nuclide compositions for each Calvert Cliffs PWR assembly, using two ENDF/B data versions

Source of cross sections	27BURNULIB			44GROUPNDF5				
Assembly ID	D047	D101	BT03	D047	D101	BT03		
Initial wt % <sup>235</sup> U	3.04	2.72	2.45	3.04	2.72	2.45		
Nuclide	% difference/assembly			Average	% difference/assembly			Average
<sup>234</sup> U	1.7	13.2	-0.8	4.7	-1.1	10.7	-4.3	-1.8
<sup>235</sup> U	-7.9	-2.8	-1.3	-4.0	-7.1	-1.9	-0.1	-3.0
<sup>236</sup> U	2.5	-0.8	<0.1	0.6	2.6	-0.9	0.1	0.6
<sup>238</sup> U	-0.4	-1.3	-0.8	-0.8	-0.4	-1.2	-0.8	-0.8
<sup>238</sup> Pu	-1.2	-8.6	2.9	-2.3	-6.3	-13.5	-2.7	-7.5
<sup>239</sup> Pu	2.1	1.1	8.0	3.8	-3.8	-4.5	1.6	-2.2
<sup>240</sup> Pu	-7.5	-7.4	-5.8	-6.9	-2.4	-1.8	-0.7	-1.6
<sup>241</sup> Pu	3.9	2.6	3.5	3.4	-2.4	-3.3	-2.9	-2.9
<sup>242</sup> Pu	-4.8	-9.3	-11.9	-8.6	5.9	0.9	-2.5	1.4
<sup>237</sup> Np	21.8	10.2	36.4	22.8	9.5	-1.5	21.2	9.7
<sup>241</sup> Am	-4.0	0.3	-14.0	-5.9	-9.2	-5.1	-18.7	-11.0
<sup>243</sup> Cm + <sup>244</sup> Cm	-15.9	-20.2	-11.2	-15.8	-2.1	-5.8	1.0	-2.3
<sup>14</sup> C	-	-14.2	-	-14.2	-	-13.8	-	-13.8
<sup>79</sup> Se	12.2	3.5	26.7	14.1	12.1	3.4	26.6	14.0
<sup>90</sup> Sr	7.3	5.3	5.8	6.1	7.2	5.1	5.8	6.0
<sup>99</sup> Tc	7.3	2.9	42.9	17.7	7.8	3.2	43.6	18.2
<sup>126</sup> Sn	-	187.3	273.3	230.3	-	187.3	272.3	229.8
<sup>129</sup> I	-	-10.8	-	-10.8	-	-10.8	-	-10.8
<sup>133</sup> Cs	1.9	-	-	1.9	2.5	-	-	2.5
<sup>134</sup> Cs	-8.1	-	-	-8.1	-11.4	-	-	-11.4
<sup>135</sup> Cs	8.1	10.0	14.7	10.9	3.0	4.8	9.2	5.7
<sup>137</sup> Cs	1.7	0.5	0.1	0.7	1.6	0.4	<0.1	0.7
<sup>143</sup> Nd	1.3	-	-	1.3	0.4	-	-	0.4
<sup>144</sup> Nd	0.1	-	-	0.1	0.5	-	-	0.5
<sup>145</sup> Nd	0.4	-	-	0.4	-0.3	-	-	-0.3
<sup>146</sup> Nd	0.4	-	-	0.4	1.1	-	-	1.1
<sup>148</sup> Nd	0.3	-	-	0.3	0.4	-	-	0.4
<sup>150</sup> Nd	3.2	-	-	3.2	3.4	-	-	3.4
<sup>147</sup> Pm + <sup>147</sup> Sm	-4.5	-	-	-4.5	-2.8	-	-	-2.8
<sup>148</sup> Sm	-15.9	-	-	-15.9	-16.9	-	-	-16.9
<sup>149</sup> Sm	-30.3	-	-	-30.3	-35.9	-	-	-35.9
<sup>150</sup> Sm	-0.5	-	-	-0.5	-1.5	-	-	-1.5
<sup>151</sup> Sm + <sup>151</sup> Eu	26.1	-	-	26.1	28.1	-	-	28.1
<sup>152</sup> Sm	17.3	-	-	17.3	20.1	-	-	20.1
<sup>153</sup> Eu	-4.8	-	-	-4.8	5.0	-	-	5.0
<sup>154</sup> Sm + <sup>154</sup> Eu + <sup>154</sup> Gd	30.8	-	-	30.8	-2.1	-	-	-2.1
<sup>155</sup> Eu + <sup>155</sup> Gd	96.0	-	-	96.0	-24.4	-	-	-24.4

<sup>a</sup>(Calculated/measured - 1) × 100%.

Table 28. Measured irradiation composition, in g/g UO<sub>2</sub>, of  
H. B. Robinson Assembly B05 Rod N-9

Nuclide	Axial location, cm from bottom of fuel (Burnup, <sup>a</sup> GWd/MTU)			
	11 cm <sup>b</sup> (16.02)	26 cm <sup>b</sup> (23.81)	199 cm <sup>c</sup> (28.47)	226 cm <sup>c</sup> (31.66)
<sup>235</sup> U	$1.07 \times 10^{-2}$	$7.21 \times 10^{-3}$	$6.18 \times 10^{-3}$	$4.86 \times 10^{-3}$
<sup>236</sup> U	$2.19 \times 10^{-3}$	$2.74 \times 10^{-3}$	$2.82 \times 10^{-3}$	$3.00 \times 10^{-3}$
<sup>238</sup> U	$8.47 \times 10^{-1}$	$8.47 \times 10^{-1}$	$8.34 \times 10^{-1}$	$8.42 \times 10^{-1}$
<sup>238</sup> Pu	$2.83 \times 10^{-5}$	$6.95 \times 10^{-5}$	$1.14 \times 10^{-4}$	$1.30 \times 10^{-4}$
<sup>239</sup> Pu	$3.64 \times 10^{-3}$	$4.02 \times 10^{-3}$	$4.39 \times 10^{-3}$	$4.20 \times 10^{-3}$
<sup>240</sup> Pu	$1.09 \times 10^{-3}$	$1.67 \times 10^{-3}$	$1.97 \times 10^{-3}$	$2.12 \times 10^{-3}$
<sup>241</sup> Pu	$3.04 \times 10^{-4}$	$5.04 \times 10^{-4}$	$6.81 \times 10^{-4}$	$6.92 \times 10^{-4}$
<sup>237</sup> Np	$1.55 \times 10^{-4}$	$2.60 \times 10^{-4}$	$3.04 \times 10^{-4}$	$3.33 \times 10^{-4}$

<sup>a</sup>Burnup based on measured <sup>148</sup>Nd concentration (ASTM 1985).

<sup>b</sup>Sample radiochemical analyses in April 1984.

<sup>c</sup>Sample radiochemical analyses in February 1985.

Source: ref. 11.

Table 29. Measured irradiation composition, in Ci/g UO<sub>2</sub>, of  
H. B. Robinson Assembly B05 Rod N-9

Nuclide	Axial location, cm from bottom of fuel (Burnup, <sup>a</sup> GWd/MTU)			
	11 cm <sup>b</sup> (16.02)	26 cm <sup>b</sup> (23.81)	199 cm <sup>c</sup> (28.47)	226 cm <sup>c</sup> (31.66)
<sup>99</sup> Tc	$5.44 \times 10^{-6}$	$8.09 \times 10^{-6}$	$8.95 \times 10^{-6}$	$1.01 \times 10^{-5}$
<sup>137</sup> Cs	$3.59 \times 10^{-2}$	$5.39 \times 10^{-2}$	$6.27 \times 10^{-2}$	$7.13 \times 10^{-2}$

<sup>a</sup>Burnup based on measured <sup>148</sup>Nd concentration (ASTM 1985).

<sup>b</sup>Sample radiochemical analyses in April 1984.

<sup>c</sup>Sample radiochemical analyses in February 1985.

Source: ref. 11.

Table 30. Percentage difference<sup>a</sup> between measured and computed<sup>b</sup> nuclide compositions for H. B. Robinson PWR pellet samples and average from Assembly B05 Rod N-9 (27BURNUPLIB library)

Sample number	N-9B-S	N-9B-N	N-9C-J	N-9C-D	
Pellet height, cm	11	26	199	226	
Burnup, GWd/MTU	16.02	23.81	28.47	31.66	
Initial wt % <sup>235</sup> U	2.561	2.561	2.561	2.561	
Nuclide					Average
<sup>235</sup> U	0.6	1.4	-4.9	3.3	0.1
<sup>236</sup> U	-1.5	-2.2	2.2	-0.4	-0.5
<sup>238</sup> U	0.1	-0.6	0.5	-0.8	-0.2
<sup>238</sup> Pu	1.5	0.9	-6.5	2.6	-0.4
<sup>239</sup> Pu	7.0	7.7	5.3	12.8	8.2
<sup>240</sup> Pu	-1.5	-4.2	-4.9	-4.1	-3.7
<sup>241</sup> Pu	5.9	6.0	0.5	9.1	5.4
<sup>237</sup> Np	6.0	5.5	14.3	18.4	11.1
<sup>99</sup> Tc	12.4	8.6	14.6	11.2	11.7
<sup>137</sup> Cs	0.2	-0.8	3.9	1.5	1.2

<sup>a</sup>(Calculated/measured – 1) × 100%.

<sup>b</sup>Using SAS2H/ORIGEN-S analysis sequence and 27-group cross-section library (27BURNUPLIB) of SCALE-4.

Table 31. Percentage difference<sup>a</sup> between measured and computed<sup>b</sup> nuclide compositions for H. B. Robinson PWR pellet samples and average from Assembly B05 Rod N-9 (44GROUPNDF5 library)

Sample number	N-9B-S	N-9B-N	N-9C-J	N-9C-D	
Pellet height, cm	11	26	199	226	
Burnup, GWd/MTU	16.02	23.81	28.47	31.66	
Initial wt % <sup>235</sup> U	2.561	2.561	2.561	2.561	
Nuclide					Average
<sup>235</sup> U	1.3	2.4	-3.9	4.5	1.0
<sup>236</sup> U	-1.8	-2.4	2.1	-0.4	-0.6
<sup>238</sup> U	0.1	-0.6	0.5	-0.8	-0.2
<sup>238</sup> Pu	-5.3	-5.1	-11.9	-3.4	-6.4
<sup>239</sup> Pu	1.6	1.8	-0.5	6.5	2.3
<sup>240</sup> Pu	4.5	1.3	0.2	0.9	1.7
<sup>241</sup> Pu	0.6	<0.1	-5.4	2.5	-0.6
<sup>237</sup> Np	-6.4	-5.9	2.2	6.0	-1.0
<sup>99</sup> Tc	12.5	8.9	15.1	11.8	12.1
<sup>137</sup> Cs	0.1	-0.9	3.8	1.5	1.1

<sup>a</sup>(Calculated/measured – 1) × 100%.

<sup>b</sup>Using SAS2H/ORIGEN-S analysis sequence and a 44-group ENDF/B-V cross-section library.

Table 32. Obrigheim average measured nuclide composition relative to time of unloading, in g/MTU

Batch	94	92	91	86	89	90
Reactor assembly	170	172	176	168	171	176
Burnup, GWd/MTU	25.93	26.54	27.99	28.40	29.04	29.52
<u>Nuclide</u>						
<sup>235</sup> U	10950	10580	9850	9680	9580	9180
<sup>236</sup> U	3590	3620	3700	3730	3750	3810
<sup>238</sup> Pu <sup>a</sup>	80.1	88.9	94.8	105.4	101.3	107.1
<sup>239</sup> Pu	4805	4713	4925	5013	4957	4943
<sup>240</sup> Pu	1800	1830	1920	2020	2000	2040
<sup>241</sup> Pu	978	978	1058	1103	1107	1128
<sup>242</sup> Pu	312	328	372	407	405	438
<sup>242</sup> Cm	17.1	19.4	18.5	20.1	20.8	21.8
<sup>244</sup> Cm	10.3	11.6	14.1	15.8	16.9	19.2

<sup>a</sup>Based on correction for the measured discharged component from <sup>242</sup>Cm, as analyzed by only the European Institute for Transuranic Elements (TUI).

Source: ref. 15.

Table 33. Obrigheim average measured isotopic atomic ratios adjusted to time of unloading

Batch	94	92	91	86	89	90
Reactor assembly	170	172	176	168	171	176
Burnup, GWd/MTU	25.93	26.54	27.99	28.40	29.04	29.52
<u>Nuclide</u>						
<sup>83</sup> Kr/ <sup>86</sup> Kr	0.252	0.245	0.231	0.248	0.238	0.241
<sup>84</sup> Kr/ <sup>86</sup> Kr	0.64	0.64	0.63	0.65	0.63	0.66
<sup>131</sup> Xe/ <sup>134</sup> Xe	0.308	0.304	0.297	0.306	0.286	0.292
<sup>132</sup> Xe/ <sup>134</sup> Xe	0.706	0.710	0.714	0.745	0.705	0.720
<sup>136</sup> Xe/ <sup>134</sup> Xe	1.483	1.490	1.505	1.470	1.540	1.520
<sup>134</sup> Cs/ <sup>137</sup> Cs	0.0733	0.0726	0.0782	0.0760	0.0770	0.0794
<sup>143</sup> Nd/ <sup>148</sup> Nd	2.45	2.45	2.35	2.35	2.35	2.34
<sup>145</sup> Nd/ <sup>148</sup> Nd	1.938	1.950	1.915	1.910	1.920	1.920
<sup>146</sup> Nd/ <sup>148</sup> Nd	1.857	1.876	1.851	1.850	1.873	1.865

Table 34. Percentage difference<sup>a</sup> between measured and computed<sup>b</sup> nuclide compositions and atomic ratios for Obrigheim PWR assembly samples (using 27BURNUPLIB cross sections)

Batch <sup>c</sup>	94	92	91	86	89	90	
Reactor assembly	170	172	176	168	171	176	
Burnup, GWd/MTU	25.93	26.54	27.99	28.40	29.04	29.52	
Nuclide							Average
<sup>235</sup> U	-3.3	-2.8	-2.6	-2.7	-4.7	-2.9	-3.2
<sup>236</sup> U	1.0	1.4	1.8	1.7	2.1	1.3	1.6
<sup>238</sup> Pu <sup>d</sup>	6.3	2.8	8.4	0.5	10.0	8.2	6.1
<sup>239</sup> Pu	6.1	8.7	5.0	3.5	5.1	5.7	5.7
<sup>240</sup> Pu	-5.3	-4.1	-4.4	-8.1	-5.4	-5.8	-5.5
<sup>241</sup> Pu	7.5	9.7	7.4	4.8	7.0	6.7	7.2
<sup>242</sup> Pu	-11.9	-12.0	-11.3	-15.9	-10.8	-14.5	-12.8
<sup>242</sup> Cm	-22.4	-23.6	-13.4	-18.5	-17.5	-16.7	-18.7
<sup>244</sup> Cm	-24.7	-23.7	-19.8	-23.5	-20.5	-24.1	-22.7
Atomic ratio							Average
<sup>83</sup> Kr/ <sup>86</sup> Kr	-4.9	-2.6	2.2	-5.0	-1.5	-3.1	-2.5
<sup>84</sup> Kr/ <sup>86</sup> Kr	-3.6	-3.3	-1.1	-4.0	-0.6	-5.0	-2.9
<sup>131</sup> Xe/ <sup>134</sup> Xe	1.4	2.1	3.4	0.1	6.5	3.8	2.9
<sup>132</sup> Xe/ <sup>134</sup> Xe	-3.2	-3.3	-2.9	-6.7	-1.0	-2.8	-3.3
<sup>136</sup> Xe/ <sup>134</sup> Xe	-1.5	-1.8	-2.0	0.6	-3.6	-2.1	-1.7
<sup>134</sup> Cs/ <sup>137</sup> Cs	-2.9	-0.2	-4.0	0.3	0.9	-0.4	-1.1
<sup>143</sup> Nd/ <sup>148</sup> Nd	-1.3	-2.2	0.2	0.5	-1.2	-1.5	-0.9
<sup>145</sup> Nd/ <sup>148</sup> Nd	1.9	0.9	1.9	1.9	1.0	0.7	1.4
<sup>146</sup> Nd/ <sup>148</sup> Nd	<0.1	-0.8	0.9	1.0	-0.1	0.5	0.3

<sup>a</sup>(Calculated/measured - 1) × 100%.

<sup>b</sup>Using SAS2H/ORIGEN-S analysis of SCALE-4.2 with 27-group cross-section library (27BURNUPLIB).

<sup>c</sup>Assembly cut in half lengthwise and separately dissolved.

<sup>d</sup>Corrected for the measured discharge component from <sup>242</sup>Cm, which was measured only by European Institute of Transuranic Elements.

Table 35. Percentage difference<sup>a</sup> between measured and computed<sup>b</sup> nuclide compositions and atomic ratios for Obrigheim PWR assembly samples (using 44GROUPNDF5 cross sections)

Batch	94	92	91	86	89	90	
Reactor assembly <sup>c</sup>	170	172	176	168	171	176	
Burnup, GWd/MTU	25.93	26.54	27.99	28.40	29.04	29.52	
Nuclide							Average
<sup>235</sup> U	-2.5	-2.0	-1.7	-1.9	-3.8	-2.0	-2.3
<sup>236</sup> U	0.9	1.3	1.7	1.5	2.0	1.2	1.4
<sup>238</sup> Pu <sup>d</sup>	1.1	-2.3	3.1	-4.4	4.7	3.0	0.8
<sup>239</sup> Pu	0.5	2.9	-0.7	-2.1	-0.6	<0.1	<0.1
<sup>240</sup> Pu	0.6	1.7	1.4	-2.5	0.3	-0.1	0.2
<sup>241</sup> Pu	1.5	3.6	1.2	-1.2	0.7	0.5	1.0
<sup>242</sup> Pu	-1.6	-1.7	-1.1	-6.2	-0.6	-4.7	-2.6
<sup>242</sup> Cm	-28.5	-29.4	-20.2	-24.9	-23.9	-23.1	-25.0
<sup>244</sup> Cm	-9.0	-8.1	-3.7	-8.2	-4.7	-9.1	-7.1
Atomic ratio							Average
<sup>83</sup> Kr/ <sup>86</sup> Kr	-4.9	-2.6	2.2	-5.0	-1.5	-3.1	-2.5
<sup>84</sup> Kr/ <sup>86</sup> Kr	-3.5	-3.2	-1.0	-3.9	-0.6	-4.9	-2.9
<sup>131</sup> Xe/ <sup>134</sup> Xe	-1.2	-0.6	0.5	-2.8	3.3	0.7	<0.1
<sup>132</sup> Xe/ <sup>134</sup> Xe	-1.9	-2.0	-1.6	-5.4	0.4	-1.4	-2.0
<sup>136</sup> Xe/ <sup>134</sup> Xe	-0.7	-0.9	-1.1	1.5	-2.8	-1.3	-0.9
<sup>134</sup> Cs/ <sup>137</sup> Cs	-6.3	-3.7	-7.3	-3.3	-2.7	-4.0	-4.6
<sup>143</sup> Nd/ <sup>148</sup> Nd	-1.9	-2.8	-0.4	-0.1	-1.9	-2.2	-1.6
<sup>145</sup> Nd/ <sup>148</sup> Nd	1.4	0.4	1.4	1.4	0.4	0.2	0.9
<sup>146</sup> Nd/ <sup>148</sup> Nd	0.4	-0.4	1.3	1.5	0.4	1.0	0.7

<sup>a</sup>(Calculated/measured - 1) × 100%.

<sup>b</sup>Using SAS2H/ORIGEN-S analysis of SCALE-4.2 with 44-group ENDF/B-V data (44GROUPNDF5).

<sup>c</sup>Assembly cut in half lengthwise and separately dissolved.

<sup>d</sup>Corrected for the measured discharge component from <sup>242</sup>Cm, which was measured only by European Institute of Transuranic Elements.



## 5. SUMMARY AND DISCUSSION OF RESULTS

The percentage differences between measured and calculated nuclide compositions were provided in Sects. 4.1 through 4.3. A statistical data analysis of these differences is given in Appendix D. The purpose of this section is to summarize and discuss the measured/calculated comparisons. The most significant differences or inconsistencies in the comparisons are discussed in this summary. Reasonable explanations for many of the differences or apparent inconsistencies also are discussed in Appendix E.

### 5.1 SUMMARY OF THE RESULTS

The percentage differences between calculated and measured compositions as presented in Sects. 4.1 through 4.3 represent data for 19 spent nuclear fuel samples taken from nine spent fuel assemblies representing three different PWRs. Assembly-averaged results were obtained for H. B. Robinson and Calvert Cliffs by averaging data for pellet samples within the same assembly. The six Obrigheim samples (two from the same assembly) were taken from dissolutions of half-assemblies, split lengthwise, and effectively represent average-assembly results. Individual percentage differences in measured and computed compositions by nuclide for results using the 27BURNUPLIB data are shown in Figs. 11 and 12. Figure 11 shows the data using all 19 cases, and Fig. 12 shows the data using assembly averages as compiled in Table 36. The same types of plots are shown in Figs. 13 and 14 for results using 44GROUPNDF5 cross sections. The assembly-averaged data using 44GROUPNDF5 is summarized in Table 37. The right-hand columns in Tables 36 and 37 provide a global average of all the assembly data.

There are numerous means by which one could evaluate the results of Sects. 4.1 through 4.3. Table 38 provides a summary of average percentage differences and the spread (maximum and minimum) in the percentage differences for all the nuclide results, by case (i.e., sample) and by assembly average. The average percentage differences of Table 38 could be interpreted as representing an estimate of the constant bias in the calculation of the nuclide composition. The uncertainty (or error) in the bias can be represented qualitatively by the maximum-minimum pair of percentage differences. Table 39 shows the average percentage difference for each element based on the absolute values of average percentage differences between measured and computed compositions for the isotopes of the element. This table, which lists the average element percentage differences based on the absolute averages of Tables 36 and 37 data, is a concise means for summarizing the quantitative bias and/or validation comparisons of the SCALE-4.2 (SAS2/ORIGEN-S) fuel depletion analysis sequence.

### 5.2 BASIS FOR DISCUSSION

The purpose of the SAS2H fuel depletion sequence in SCALE is to predict the set of fuel volume-averaged nuclide densities of a specified LWR spent fuel assembly. In general, the fuel assembly is the smallest unit of fuel moved or loaded into the reactor core, placed into storage, or transported by a shipping cask. Associated with each fuel assembly are its burnup, initial enrichment, design, power history, and other operating conditions. Specific space-dependent nuclide densities are not explicitly computed, because final densities are derived from cross sections integrated over space- and energy-dependent flux. However, if nuclide densities vary from one fuel rod to another for equal burnups, this variation would be reflected as a fraction of the difference between the measured and computed values of a fuel pellet at a specified location.

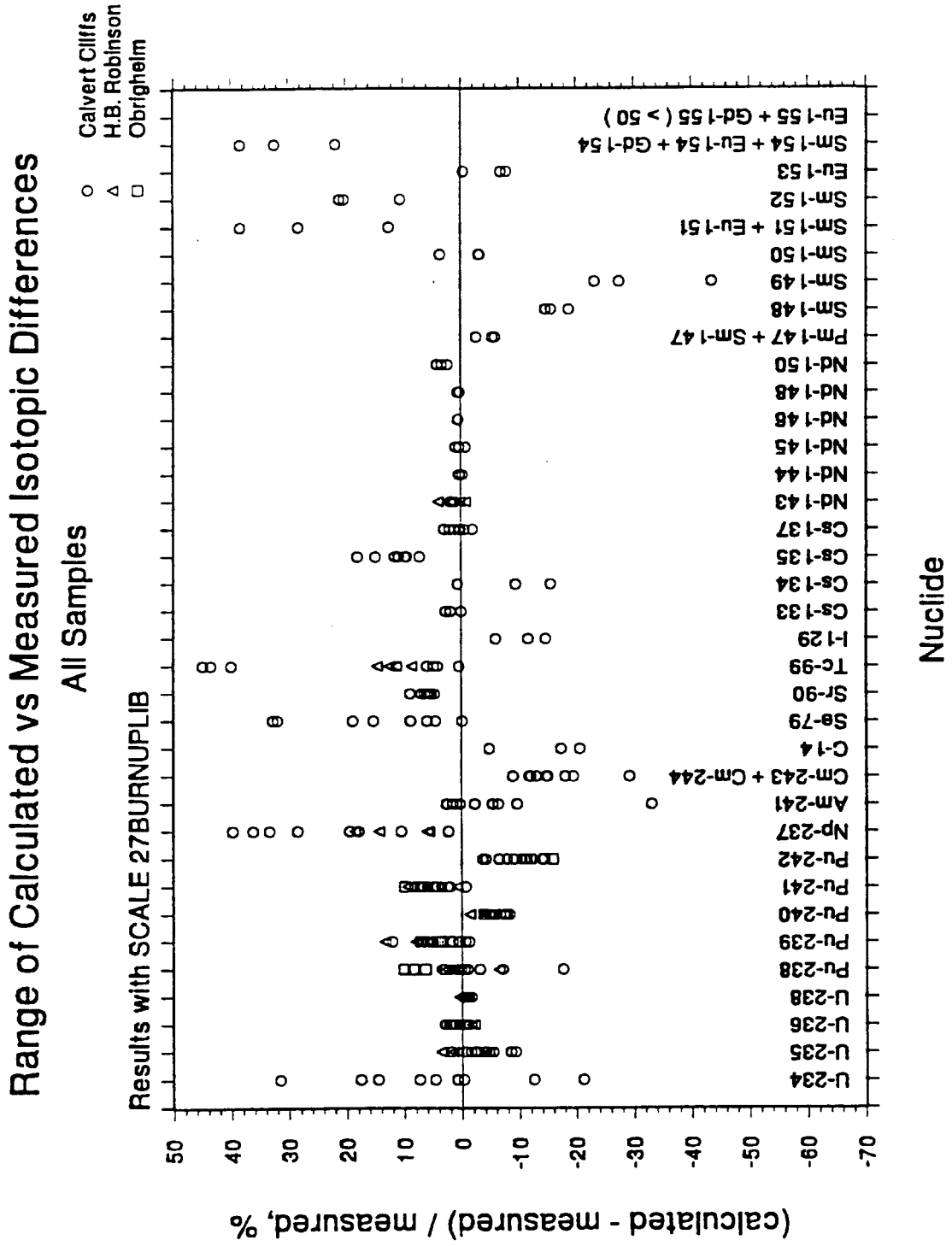


Fig. 11. Range in calculated vs measured isotopic differences for 19 cases (27BURNUPLIB cross-section data).

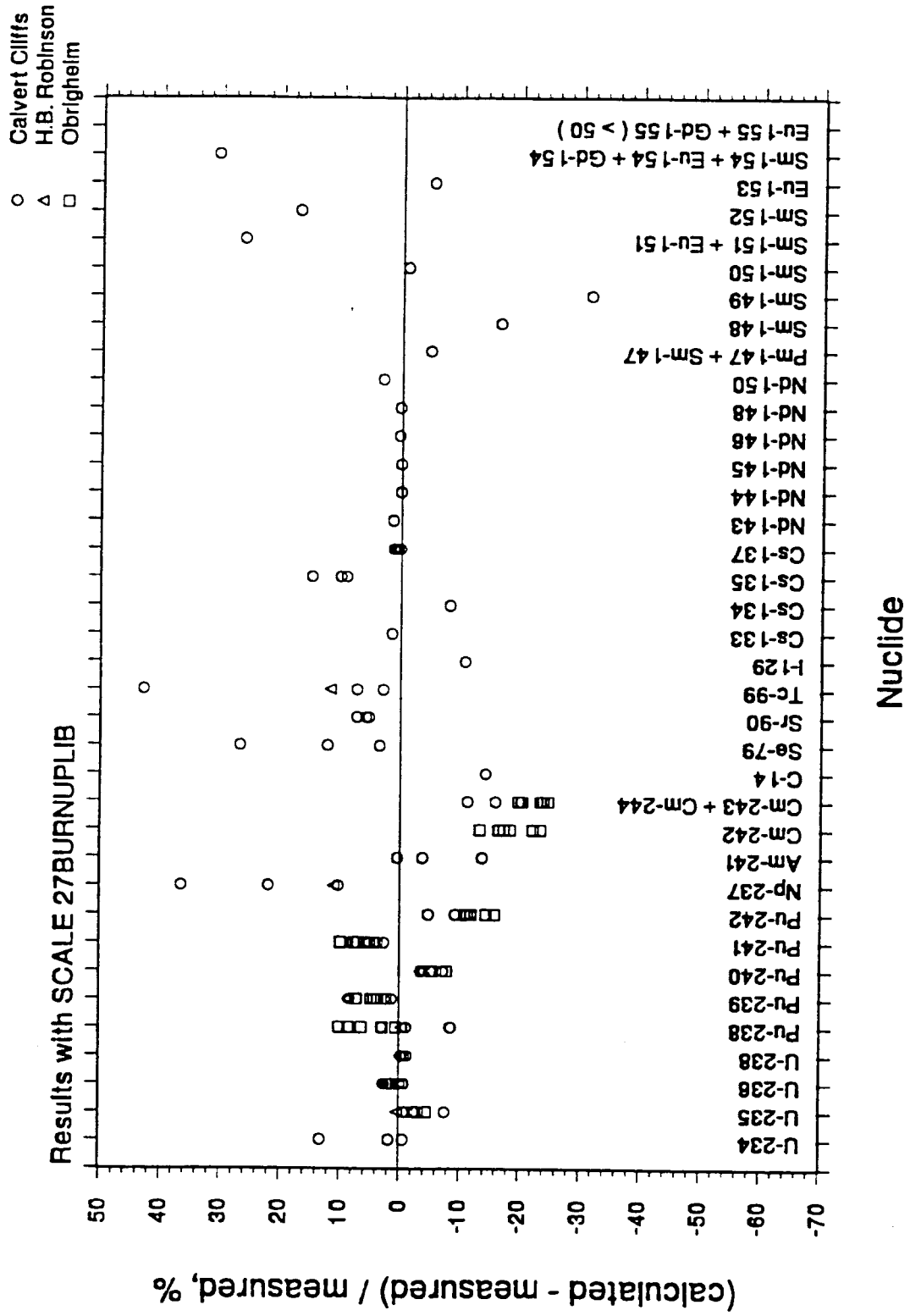


Fig. 12. Range in calculated vs measured isotopic differences for 10 assembly averages (27BURNUPLIB cross-section data).



Table 36. (continued)

PWR analyzed	Calvert Cliffs			H. B. Robinson	Obrigheim						Average
Assembly ID	D047	D101	BT03	B05	170	172	176	168	171	176	
Batch	–	–	–	–	94	92	91	86	89	90	
Initial wt % <sup>235</sup> U	3.04	2.72	2.45	2.561	3.13	3.13	3.13	3.13	3.13	3.13	
Nuclide or ratio											
<sup>145</sup> Nd	0.4	–	–	–	–	–	–	–	–	–	0.4
<sup>146</sup> Nd	0.4	–	–	–	–	–	–	–	–	–	0.4
<sup>148</sup> Nd	0.3	–	–	–	–	–	–	–	–	–	0.3
<sup>150</sup> Nd	3.2	–	–	–	–	–	–	–	–	–	3.2
<sup>147</sup> Pm + <sup>147</sup> Sm	-4.5	–	–	–	–	–	–	–	–	–	-4.5
<sup>148</sup> Sm	-15.9	–	–	–	–	–	–	–	–	–	-15.9
<sup>149</sup> Sm	-30.3	–	–	–	–	–	–	–	–	–	-30.3
<sup>150</sup> Sm	-0.5	–	–	–	–	–	–	–	–	–	-0.5
<sup>151</sup> Sm + <sup>151</sup> Eu	26.1	–	–	–	–	–	–	–	–	–	26.1
<sup>152</sup> Sm	17.3	–	–	–	–	–	–	–	–	–	17.3
<sup>153</sup> Eu	-4.8	–	–	–	–	–	–	–	–	–	-4.8
<sup>154</sup> Sm + <sup>154</sup> Eu + <sup>154</sup> Gd	30.8	–	–	–	–	–	–	–	–	–	30.8
<sup>155</sup> Eu + <sup>155</sup> Gd	96.0	–	–	–	–	–	–	–	–	–	96.0
<sup>83</sup> Kr/ <sup>86</sup> Kr	–	–	–	–	-4.9	-2.6	2.2	-5.0	-1.5	-3.1	-2.5
<sup>85</sup> Kr/ <sup>86</sup> Kr	–	–	–	–	-3.6	-3.3	-1.1	-4.0	-0.6	-5.0	-2.9
<sup>131</sup> Xe/ <sup>134</sup> Xe	–	–	–	–	1.4	2.1	3.4	0.1	6.5	3.8	2.9
<sup>132</sup> Xe/ <sup>134</sup> Xe	–	–	–	–	-3.2	-3.3	-2.9	-6.7	-1.0	-2.8	-3.3
<sup>136</sup> Xe/ <sup>134</sup> Xe	–	–	–	–	-1.5	-1.8	-2.0	0.6	-3.6	-2.1	-1.7
<sup>134</sup> Cs/ <sup>137</sup> Cs	–	–	–	–	-2.9	-0.2	-4.0	0.3	0.9	-0.4	-1.1
<sup>143</sup> Nd/ <sup>148</sup> Nd	–	–	–	–	-1.3	-2.2	0.2	0.5	-1.2	-1.5	-0.9
<sup>145</sup> Nd/ <sup>148</sup> Nd	–	–	–	–	1.9	0.8	1.9	1.9	1.0	0.7	1.4
<sup>146</sup> Nd/ <sup>148</sup> Nd	–	–	–	–	<0.1	-0.8	0.9	1.0	-0.1	0.5	0.3

<sup>a</sup>(Calculated/measured – 1) × 100%.

<sup>b</sup>Using SAS2H/ORIGEN-S analysis of SCALE-4.2 with 27-group cross-section library (27BURNUPLIB).

<sup>c</sup>Used the averages of rod data for Calvert Cliffs and H. B. Robinson PWRs and batches for Obrigheim PWR.

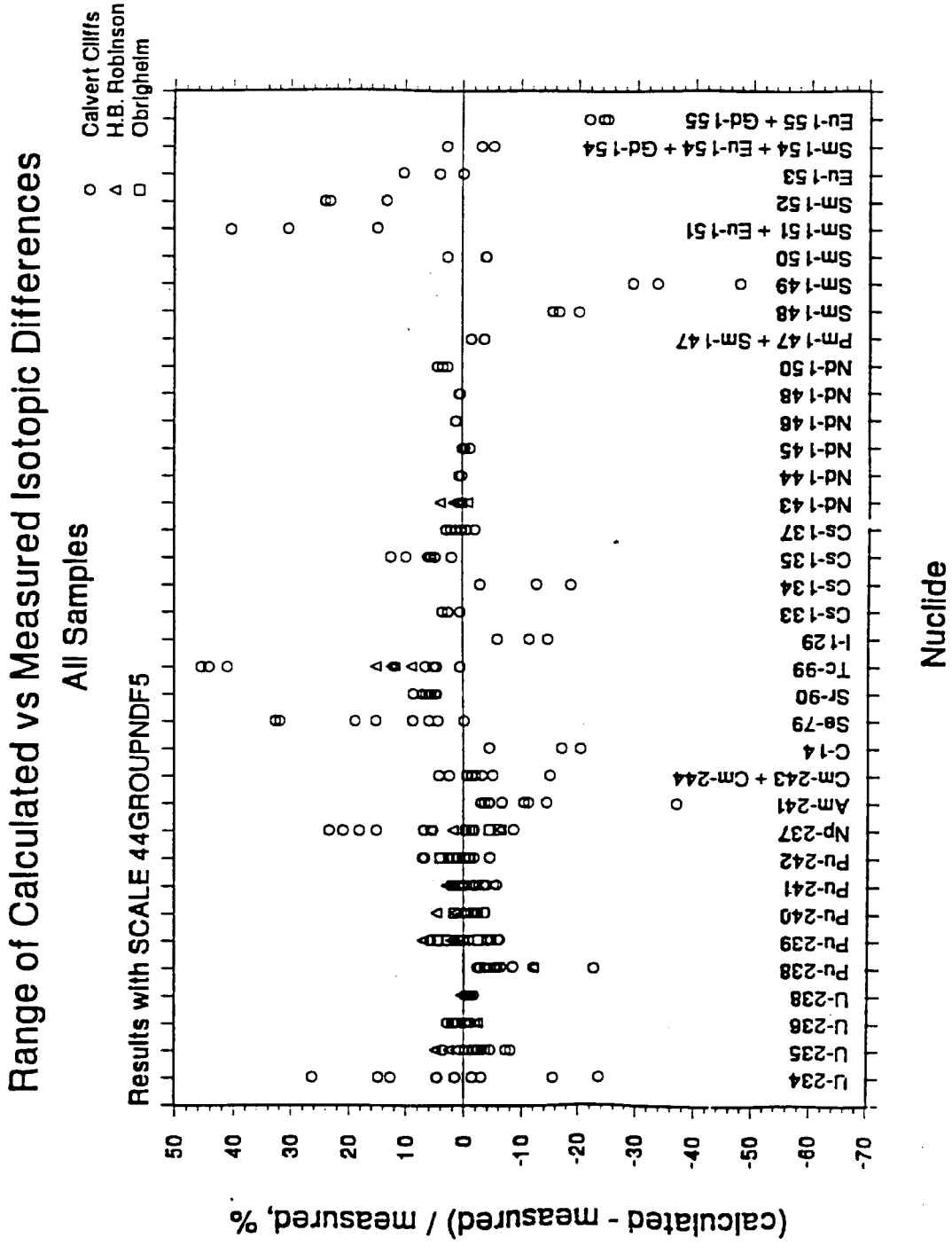


Fig. 13. Range in calculated vs measured isotopic differences for 19 cases (44GROUPNDF5 cross-section data).

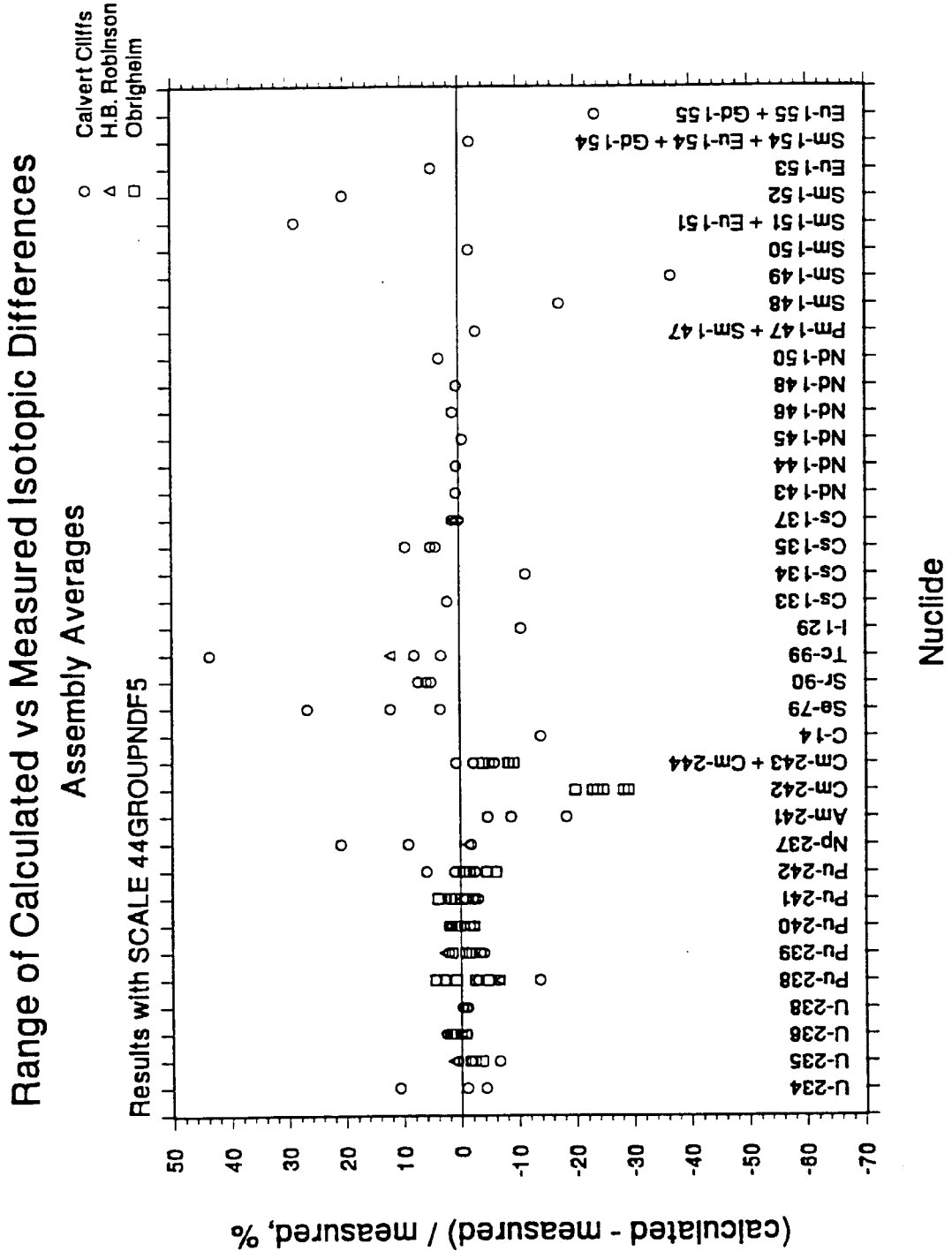


Fig. 14. Range in calculated-vs-measured isotopic differences for 10 assembly averages (44GROUPNDF5 cross-section data).





Table 37 (continued)

PWR analyzed	Calvert Cliffs			H. B. Robinson	Obrigheim						Average
Assembly ID	D047	D101	BT03	B05	170	172	176	168	171	176	
Batch	–	–	–	–	94	92	91	86	89	90	
Initial wt % <sup>235</sup> U	3.04	2.72	2.45	2.561	3.13	3.13	3.13	3.13	3.13	3.13	
Nuclide or ratio											
<sup>145</sup> Nd	-0.3	–	–	–	–	–	–	–	–	–	-0.3
<sup>146</sup> Nd	1.1	–	–	–	–	–	–	–	–	–	1.1
<sup>148</sup> Nd	0.4	–	–	–	–	–	–	–	–	–	0.4
<sup>150</sup> Nd	3.4	–	–	–	–	–	–	–	–	–	3.4
<sup>147</sup> Pm + <sup>147</sup> Sm	-2.8	–	–	–	–	–	–	–	–	–	-2.8
<sup>148</sup> Sm	-16.9	–	–	–	–	–	–	–	–	–	-16.9
<sup>149</sup> Sm	-35.9	–	–	–	–	–	–	–	–	–	-35.9
<sup>150</sup> Sm	-1.5	–	–	–	–	–	–	–	–	–	-1.5
<sup>151</sup> Sm + <sup>151</sup> Eu	28.1	–	–	–	–	–	–	–	–	–	28.1
<sup>152</sup> Sm	20.2	–	–	–	–	–	–	–	–	–	20.2
<sup>153</sup> Eu	5.0	–	–	–	–	–	–	–	–	–	5.0
<sup>154</sup> Sm + <sup>154</sup> Eu + <sup>154</sup> Gd	-2.1	–	–	–	–	–	–	–	–	–	-2.1
<sup>155</sup> Eu + <sup>155</sup> Gd	-24.4	–	–	–	–	–	–	–	–	–	-24.4
<sup>83</sup> Kr/ <sup>86</sup> Kr	–	–	–	–	-4.9	-2.6	2.2	-5.0	-1.5	-3.1	-2.5
<sup>85</sup> Kr/ <sup>86</sup> Kr	–	–	–	–	-3.5	-3.2	-1.0	-3.9	-0.6	-4.9	-2.9
<sup>131</sup> Xe/ <sup>134</sup> Xe	–	–	–	–	-1.2	-0.6	0.5	-2.8	3.3	0.7	<0.1
<sup>132</sup> Xe/ <sup>134</sup> Xe	–	–	–	–	-1.9	-2.0	-1.6	-5.4	0.4	-1.4	-2.0
<sup>136</sup> Xe/ <sup>134</sup> Xe	–	–	–	–	-0.7	-0.9	-1.1	1.5	-2.8	-1.3	-0.9
<sup>134</sup> Cs/ <sup>137</sup> Cs	–	–	–	–	-6.3	-3.7	-7.3	-3.3	-2.7	-4.0	-4.6
<sup>143</sup> Nd/ <sup>148</sup> Nd	–	–	–	–	-1.9	-2.8	-0.4	-0.1	-1.9	-2.2	-1.6
<sup>145</sup> Nd/ <sup>148</sup> Nd	–	–	–	–	1.4	0.4	1.4	1.4	0.4	0.2	0.9
<sup>146</sup> Nd/ <sup>148</sup> Nd	–	–	–	–	0.4	-0.4	1.3	1.5	0.4	1.0	0.7

<sup>a</sup>(Calculated/measured – 1) × 100%.

<sup>b</sup>Using SAS2H/ORIGEN-S analysis of SCALE-4.2 with 44-group ENDF/B-V data (44GROUPNDF5).

<sup>c</sup>Used ten averages of rods for Calvert Cliffs and H. B. Robinson PWRs and batches for Obrigheim PWR.

Table 38. Summary of percentage difference<sup>a</sup> averages and spreads

Nuclide or ratio	27BURNUPLIB data						44GROUPNDF5 data					
	Average		Spread in data				Average		Spread in data			
	Case <sup>b</sup>	Assembly <sup>c</sup>	Case		Assembly		Case	Assembly	Case		Assembly	
			Max	Min	Max	Min			Max	Min	Max	Min
<sup>234</sup> U	4.7	4.7	31.4	-21.2	13.2	-0.8	1.8	1.8	26.1	-23.5	10.7	-4.3
<sup>235</sup> U	-2.9	-3.1	3.3	-9.6	0.1	-7.9	-1.9	-2.2	4.5	-8.7	1.0	-7.1
<sup>236</sup> U	0.7	1.1	3.1	-2.2	2.5	-0.8	0.6	1.0	2.9	-2.4	2.6	-0.9
<sup>238</sup> U	-0.6	-0.7	0.5	-1.7	-0.2	-1.3	-0.6	-0.7	0.5	-1.7	-0.2	-1.2
<sup>238</sup> Pu	0.7	2.9	10.0	-17.7	10.0	-8.6	-4.6	-2.4	4.7	-22.5	4.7	-13.5
<sup>239</sup> Pu	5.3	5.4	12.8	-1.5	8.7	1.1	-0.6	-0.4	6.5	-6.6	2.9	-4.5
<sup>240</sup> Pu	-5.8	-5.7	-1.5	-8.6	-3.7	-8.1	-0.3	-0.2	4.5	-3.9	1.7	-2.5
<sup>241</sup> Pu	5.0	5.9	9.7	-0.9	9.7	2.6	-1.2	-0.3	3.6	-6.0	3.6	-3.3
<sup>242</sup> Pu	-10.3	-11.4	-3.6	-15.9	-4.8	-15.9	-0.2	-1.3	7.0	-6.2	5.9	-6.2
<sup>237</sup> Np	19.2	19.9	39.7	2.3	36.4	10.2	6.4	7.0	23.8	-8.5	21.2	-1.5
<sup>241</sup> Am	-5.9	-5.9	2.4	-33.4	0.3	-14.0	-11.0	-11.0	-3.5	-37.2	-5.1	-18.7
<sup>242</sup> Cm	-18.7	-18.7	-13.4	-23.6	-13.4	-23.6	-25.0	-25.0	-20.2	-29.4	-20.2	-29.4
<sup>243</sup> Cm + <sup>244</sup> Cm or <sup>244</sup> Cm	-18.6	-20.4	-8.9	-29.3	-11.2	-24.7	-4.2	-5.5	4.5	-15.1	1.0	-9.1
<sup>14</sup> C	-14.2	-14.2	-4.7	-20.6	-14.2	-14.2	-13.8	-13.8	-4.4	-20.2	-13.8	-13.8
<sup>79</sup> Se	14.1	14.1	32.8	-0.1	26.7	3.5	14.0	14.0	32.7	-0.2	26.6	3.4
<sup>90</sup> Sr	6.1	6.1	8.9	4.7	7.3	5.3	6.0	6.0	8.7	4.6	7.2	5.1
<sup>99</sup> Tc	15.8	16.2	45.0	0.4	42.9	2.9	16.3	16.7	45.5	0.5	43.6	3.2
<sup>126</sup> Sn	230.3	230.3	286.9	179.1	273.3	187.3	229.8	229.8	285.7	179.8	272.3	187.3
<sup>129</sup> I	-10.8	-10.8	-6.1	-14.7	-10.8	-10.8	-10.8	-10.8	-6.0	-14.7	-10.8	-10.8
<sup>133</sup> Cs	1.9	1.9	2.7	1.2	1.9	1.9	2.5	2.5	3.4	1.6	2.5	2.5
<sup>134</sup> Cs	-8.1	-8.1	0.7	-15.5	-8.1	-8.1	-11.4	-11.4	-2.9	-18.6	-11.4	-11.4
<sup>135</sup> Cs	10.9	10.9	17.9	7.1	14.7	8.1	5.7	5.7	12.2	1.7	9.2	3.0
<sup>137</sup> Cs	0.9	0.8	3.9	-2.0	1.7	0.1	0.8	0.8	3.8	-2.1	1.6	0.0
<sup>143</sup> Nd	1.3	1.3	1.7	1.0	1.3	1.3	0.4	0.4	0.6	0.1	0.4	0.4
<sup>144</sup> Nd	0.1	0.1	0.3	-0.3	0.1	0.1	0.5	0.5	0.7	0.2	0.5	0.5

Table 38 (continued)

Nuclide or ratio	27BURNUPLIB data						44GROUPNDF5 data					
	Average		Spread in data				Average		Spread in data			
	Case <sup>b</sup>	Assembly <sup>c</sup>	Case		Assembly		Case	Assembly	Case		Assembly	
			Max	Min	Max	Min			Max	Min	Max	Min
<sup>145</sup> Nd	0.4	0.4	0.6	0.3	0.4	0.4	-0.3	-0.3	0.1	-0.6	-0.3	-0.3
<sup>146</sup> Nd	0.4	0.4	0.5	0.4	0.4	0.4	1.1	1.1	1.3	1.0	1.1	1.1
<sup>148</sup> Nd	0.3	0.3	0.5	0.2	0.3	0.3	0.4	0.4	0.6	0.3	0.4	0.4
<sup>150</sup> Nd	3.2	3.2	4.1	2.3	3.2	3.2	3.4	3.4	4.2	2.5	3.4	3.4
<sup>147</sup> Pm + <sup>147</sup> Sm	-4.5	-4.5	-1.9	-6.9	-4.5	-4.5	-2.8	-2.8	-0.8	-4.8	-2.8	-2.8
<sup>148</sup> Sm	-15.9	-15.9	-13.7	-17.4	-15.9	-15.9	-16.9	-16.9	-14.6	-18.2	-16.9	-16.9
<sup>149</sup> Sm	-30.3	-30.3	-21.0	-44.9	-30.3	-30.3	-35.9	-35.9	-27.3	-49.1	-35.9	-35.9
<sup>150</sup> Sm	-0.5	-0.5	4.8	-4.5	-0.5	-0.5	-1.5	-1.5	3.8	-5.6	-1.5	-1.5
<sup>151</sup> Sm + <sup>151</sup> Eu	26.1	26.1	36.8	13.0	26.1	26.1	28.1	28.1	38.5	15.2	28.1	28.1
<sup>152</sup> Sm	17.3	17.3	21.0	11.7	17.3	17.3	20.2	20.2	23.9	14.5	20.2	20.2
<sup>153</sup> Eu	-4.8	-4.8	0.5	-9.2	-4.8	-4.8	5.0	5.0	11.3	1.1	5.0	5.0
<sup>154</sup> Sm + <sup>154</sup> Eu + <sup>154</sup> Gd	30.8	30.8	38.4	21.7	30.8	30.8	-2.1	-2.1	2.6	-5.5	-2.1	-2.1
<sup>155</sup> Eu + <sup>155</sup> Gd	96.0	96.0	106.	77.4	96.0	96.0	-24.4	-24.4	-20.7	-27.1	-24.4	-24.4
<sup>83</sup> Kr/ <sup>86</sup> Kr	-2.5	-2.5	2	-5.0	2.2	-5.0	-2.4	-2.4	2.2	-5.0	2.2	-5.0
<sup>85</sup> Kr/ <sup>86</sup> Kr	-2.9	-2.9	2.2	-5.0	-0.6	-5.0	-2.9	-2.9	-0.6	-4.9	-0.6	-4.9
<sup>131</sup> Xe/ <sup>134</sup> Xe	2.9	2.9	-0.6	0.1	6.5	0.1	<0.1	<0.1	3.3	-2.8	3.3	-2.8
<sup>132</sup> Xe/ <sup>134</sup> Xe	-3.3	-3.3	6.5	-6.7	-1.0	-6.7	-2.0	-2.0	0.4	-5.4	0.4	-5.4
<sup>136</sup> Xe/ <sup>134</sup> Xe	-1.7	-1.7	-1.0	-3.6	0.6	-3.6	-0.9	-0.9	1.5	-2.8	1.5	-2.8
<sup>134</sup> Cs/ <sup>137</sup> Cs	-1.1	-1.1	0.6	-4.0	0.9	-4.0	-4.7	-4.7	-2.7	-7.3	-2.7	-7.3
<sup>143</sup> Nd/ <sup>148</sup> Nd	-0.9	-0.9	0.9	-2.2	0.5	-2.2	-1.5	-1.5	-0.1	-2.8	-0.1	-2.8
<sup>145</sup> Nd/ <sup>148</sup> Nd	1.4	1.4	0.5	0.7	1.9	0.7	0.9	0.9	1.4	0.2	1.4	0.2
<sup>146</sup> Nd/ <sup>148</sup> Nd	0.3	0.3	1.9	-0.8	1.0	-0.8	0.7	0.7	1.5	-0.4	1.5	-0.4
			1.0									

<sup>a</sup>(Calculated/measured - 1) × 100%.

<sup>b</sup>Data listed under "Case" pertains to either the average or spread of the data applying the values of each of the 19 cases.

<sup>c</sup>Data listed under "Assembly" pertains to either the average or spread of the data applying the averages of each of the 10 assemblies or batches.

Table 39. Percentage differences for each element averaged<sup>a</sup> over the absolute values of percentage differences of all isotopes of the element

Element (single isotopes given)	No. of isotopes	Cross-section source	
		27BURNUPLIB	44GROUPNDF5
U	4	2.4	1.4
Pu	5	6.3	0.9
Np ( <sup>237</sup> Np)	1	19.9	7.0
Am ( <sup>241</sup> Am)	1	5.9	11.0
Cm	2	19.6	15.3
C ( <sup>14</sup> C)	1	14.2	13.8
Se ( <sup>79</sup> Se)	1	14.1	14.0
Sr ( <sup>90</sup> Sr)	1	6.1	6.0
Tc ( <sup>99</sup> Tc)	1	16.2	16.7
Sn ( <sup>126</sup> Sn)	1	230.3	229.8
I ( <sup>129</sup> I)	1	10.8	10.8
Cs	4	5.4	5.1
Nd	6	1.0	1.0
Pm ( <sup>147</sup> Pm)	1	4.5	2.8
Sm	7	17.9	15.4
Eu	4	39.4	14.9
Gd	2	63.4	13.3
Kr ratios	2	2.7	2.7
Xe ratios	3	2.6	1.0
Cs ratio ( <sup>134</sup> Cs/ <sup>137</sup> Cs)	1	1.1	4.6
Nd ratios	3	0.9	1.1

<sup>a</sup>Average percentage difference for each element based on the absolute values of average percentage differences between measured and computed composition or atom ratio for the isotopes of the element using the data of Tables 36 and 37.

Similarly, in the axial direction even if the spatial variation in power density is well-known, the characterization of axially dependent isotopes has shortcomings due to the space-independent nature of the calculational models. These effects, as well as others, are investigated in detail in Appendix E. The remainder of this section discusses and summarizes the trends seen for assembly-averaged predicted as compared with assembly data and appropriately averaged pellet data.

The average of the assembly data and the data spread shown in Table 38 provide the basis for much of the discussion that follows. The average of the assembly data is used as an estimate of the probable bias in the calculated individual nuclide contents and, as such, is used to predict general effects on global variables such as decay heat rates, effective neutron multiplication factors ( $k_{\text{eff}}$ ), and radiation source spectra.

### 5.3 ACTINIDE NUCLIDE RESULTS

This project provides data for a comparison of the differences between the results computed by applying actinide cross sections from ENDF/B-IV data (27BURNUPLIB) and the corresponding results using ENDF/B-V data (44GROUPNDF5). Table 38 contains the averages of assembly-averaged and sample-specific differences between computed and measured isotopic compositions using both versions of cross-section data. The averages of absolute values of assembly-averaged percentage differences for all actinide nuclides in Table 38 are 8.1 and 4.5% using 27BURNUPLIB and 44GROUPNDF5, respectively. More noteworthy are the average absolute values of the differences for uranium and plutonium shown in Table 39. These averages are reduced from 2.4 to 1.4% for uranium and from 6.3 to 0.9% for plutonium in changing from 27BURNUPLIB to 44GROUPNDF5, respectively. In particular, the average differences in plutonium isotopes when using the ENDF/B-IV-based library are 5.4% for  $^{239}\text{Pu}$ , -5.7% for  $^{240}\text{Pu}$ , 5.9% for  $^{241}\text{Pu}$ , and -11.4% for  $^{242}\text{Pu}$ , whereas when using the ENDF/B-V-based library the differences reduce to -0.4% for  $^{239}\text{Pu}$ , -0.2% for  $^{240}\text{Pu}$ , -0.3% for  $^{241}\text{Pu}$ , and -1.3% for  $^{242}\text{Pu}$ . Further discussions of the reasons for this improved agreement are given later in this section.

Several of the actinide isotopes are more significant than others in computing useful variables such as  $k_{\text{eff}}$ , neutron and photon sources and decay heat. Three major fissionable isotopes,  $^{235}\text{U}$ ,  $^{239}\text{Pu}$ , and  $^{241}\text{Pu}$ , have both positive and negative differences in cases using the 27BURNUPLIB data. Thus, there would be some cancellation of errors in determining the bias of a final computed  $k_{\text{eff}}$ . However, in cases using the 44GROUPNDF5 data, the three fissionable isotopes listed above have near-zero or negative differences, resulting in a small nonconservative bias in the computed  $k_{\text{eff}}$ .

The isotopic percentage differences (in Table 38) for  $^{238}\text{Pu}$ ,  $^{240}\text{Pu}$ ,  $^{241}\text{Am}$ ,  $^{242}\text{Cm}$ , and  $^{244}\text{Cm}$ , that are significant as  $\alpha$ -n or spontaneous-fission neutron sources, are 2.9, -5.7, -5.9, -18.7, and -20.4%, respectively, using the 27BURNUPLIB data. The corresponding differences for 44GROUPNDF5 cases are -2.4, -0.2, -11.0, -25.0, and -5.5%. Within a few years after shutdown (the cooling period when most spent fuel shipments would be made),  $^{244}\text{Cm}$  dominates the neutron source sufficiently that a more correct neutron source would be produced (from the indicated 15% reduction in the  $^{244}\text{Cm}$  difference) by the use of the 44GROUPNDF5 data. For computations of actinide decay heat rates, it is indefinite which source of cross-section data would produce the better results because the decay heat distribution among the actinides changes with time (most is distributed among  $^{238}\text{Pu}$ ,  $^{241}\text{Am}$ ,  $^{242}\text{Cm}$ , and  $^{244}\text{Cm}$  for <100 years cooling time). Actinide photon source spectra are not significant compared with those from fission products in the 0.5- to 2.0-MeV gamma energy range (typically about 4 to 5 orders of magnitude lower). This range represents the source interval primarily responsible for the dose from shipping casks. The following observations were noted in the spread of percentage differences in actinide data of Table 38 and Figs. 11 through 14. The data spreads, or maximum-minimum ranges, can be useful in developing conservative error bounds in global variables derived from computed spent fuel compositions. The three largest actinide spreads in Table 38 for cases using the actinide ENDF/B-IV data are 53% [31.4% -(-21.2%)] for  $^{234}\text{U}$ , 28% [10.0 - (-17.7)] for  $^{238}\text{Pu}$ , and 37% (39.7% - 2.3%) for  $^{237}\text{Np}$ . The reasons for these large spreads are not known. The initial  $^{234}\text{U}$  content was not given and could possibly have varied from that assumed. All three of these nuclides are produced from multilink chains and to some extent by more than one chain path. However, the smaller spreads of 12.9% for  $^{235}\text{U}$  and 14.3% for  $^{239}\text{Pu}$  are more significant because they are the two most important nuclides in computing  $k_{\text{eff}}$ , and are of much greater significance than  $^{234}\text{U}$ ,  $^{238}\text{Pu}$ , or  $^{237}\text{Np}$ . Reasons for the large scatter in the  $^{235}\text{U}$  and  $^{239}\text{Pu}$  data are discussed in Sect. 5.5.

A detailed study of the differences in the cross-section values produced from ENDF/B-IV and ENDF/B-V actinide data was not intended in this project. However, the distinct improvement in the Pu isotopic densities (in particular,  $^{239}\text{Pu}$ ) prompted a brief comparison of cross-section data examples relative to Pu production. Reaction rate comparisons are more meaningful if related to the fission cross section of  $^{235}\text{U}$  (see Appendix E). Thus, cross-section tabulations for starting and ending cycle libraries computed in two example cases are given in Table 40. The types of data listed are the  $(n,\gamma)$  cross sections for  $^{238}\text{U}$ , the absorption cross sections for  $^{239}\text{Pu}$  and the fission cross sections for  $^{235}\text{U}$  and  $^{239}\text{Pu}$ . Also, the ratios taken with respect to the fission cross section of  $^{235}\text{U}$  are listed. Note that although there are essentially no changes in the  $\sigma(n,\gamma)_{\text{U}238}/\sigma(n,f)_{\text{U}235}$  ratios, the other two ratios for  $^{239}\text{Pu}$  absorption and fission cross sections are from 5.4 to 7.5% larger by using actinide data from ENDF/B-V relative to that derived by using data from ENDF/B-IV. These larger cross sections could be due to either changes in the underlying data or group structure/flux-weighting effects, or both. Only the  $^{239}\text{Pu}$  production was examined in this example, partly because it was easier to evaluate. Also,  $^{239}\text{Pu}$  density computations have indirect effects on other isotopes such as  $^{235}\text{U}$  and the other Pu nuclides and heavier actinides. Finally, the chief motivation for investigating the reasons for the  $^{239}\text{Pu}$  density change was the large magnitude in the reduction of the difference between the computed and measured densities (from 4.6 to  $-1.0\%$  for averages by assembly) in changing versions of ENDF data.

#### 5.4 FISSION-PRODUCT RESULTS

Sample densities were measured for 27 different fission-product isotopes or isobars. Six of these analyses included 6 to 13 pellet samples taken from 2 to 4 fuel assemblies. The other 21 fission products were analyses of only three different samples from Assembly D047 Rod MKP109 of Calvert Cliffs Unit 1 PWR. Although the set of fission-product nuclides in the radiochemical analyses is not nearly as complete as that of the actinide nuclides, it encompasses the largest set of significant spent fuel fission products (with respect to  $k_{\text{eff}}$  or decay heat) in assay measurements conducted and documented to date.

A review of the differences in the two cross-section libraries applied may be helpful in the understanding of the comparisons in fission-product results. One of the libraries in the "27BURNULIB" SCALE system library (Vol. III, Sect. M4.2.8 of ref. 1). This library has actinide and light-element data derived (via the 218-group SCALE library) from ENDF/B-IV files and fission-product data processed from ENDF/B-V files. The other library is a 44-energy-group library<sup>17</sup> (denoted as 44GROUPNDF5) derived from the 238-group library processed from ENDF/B-V files for all of the nuclides with the exception of  $^{16}\text{O}$ ,  $^{154}\text{Eu}$ , and  $^{155}\text{Eu}$ , which have cross sections derived from ENDF/B-VI files. Note that although the ENDF/B-V files were the same source for some of the data in both libraries, somewhat different group collapse procedures were used (e.g., the weighting function) for each, and the resultant data representations would be somewhat different. Highly significant differences between the  $^{155}\text{Eu}$  cross sections derived from ENDF/B-V and ENDF/B-VI are shown in the  $(n,\gamma)$  cross-section plots over two energy ranges,  $1 \times 10^{-5} - 1$  eV and  $1 - 100$  eV, in Figs. 15 and 16, respectively.

The results in Table 38 again may be observed for comparisons in the fission-product results between using the two versions of cross-section data. The difference seen in Table 38 for isobar 155 (or  $^{155}\text{Eu} + ^{155}\text{Gd}$ ) is 96.0% applying the ENDF/B-V Eu data and  $-24.4\%$  using the ENDF/B-VI Eu data. This unusually large change in the isobar 155 results is due to the large  $^{155}\text{Eu}$  resonance at approximately 0.5 eV in the ENDF/B-VI data (Fig. 15) compared with the absence of resonances in ENDF/B-V data (increased resonance absorption results in greater depletion of  $^{155}\text{Eu}$  during operation). The percentage difference for isobar 154 ( $^{154}\text{Sm} + ^{154}\text{Eu} + ^{154}\text{Gd}$ ) is 30.8% using ENDF/B-V Eu data

Table 40. Examples of differences between SCALE derived actinide cross sections processed from ENDF/B-IV and ENDF/B-V data

Burnup, GWd/MTU	Cycle	ENDF version	Cross section (barns) <sup>a</sup>				Ratio in $\sigma$		
			$\sigma(n,f)_{U235}$	$\sigma(n,\gamma)_{U238}$	$\sigma(n,f)_{Pu239}$	$\sigma(abs)_{Pu239}$	$\frac{\sigma(n,\gamma)_{U238}}{\sigma(n,f)_{U235}}$	$\frac{\sigma(n,f)_{Pu239}}{\sigma(n,f)_{U235}}$	$\frac{\sigma(abs)_{Pu239}}{\sigma(n,f)_{U235}}$
27.35	1	B-IV	326.7	5.65	782	1,219	0.0173	2.394	3.73
27.35	1	B-V	306.7	5.32	785	1,231	0.0173	2.560	4.01
Differences <sup>bb</sup>							0.0%	6.9%	7.5%
27.35	4	B-IV	336.9	6.12	754	1,167	0.0182	2.238	3.46
27.35	4	B-V	318.3	5.78	753	1,173	0.0182	2.366	3.68
Differences							0.0%	5.7%	6.4%
44.34	1	B-IV	327.6	5.95	782	1,217	0.0182	2.387	3.71
44.34	1	B-V	309.6	5.61	783	1,228	0.0181	2.529	3.97
Differences							0.6%	5.9%	7.0%
44.34	4	B-IV	342.3	6.33	755	1,165	0.0185	2.206	3.40
44.34	4	B-V	323.5	5.98	752	1,170	0.0185	2.325	3.62
Differences							0.0%	5.4%	6.5%

<sup>a</sup>Cross sections are normalized to the thermal flux.

<sup>b</sup>Percentage differences in the cross-section ratios determined by  $(\text{ENDF/B-V ratio}/\text{ENDF/B-IV ratio} - 1) \times 100\%$ .

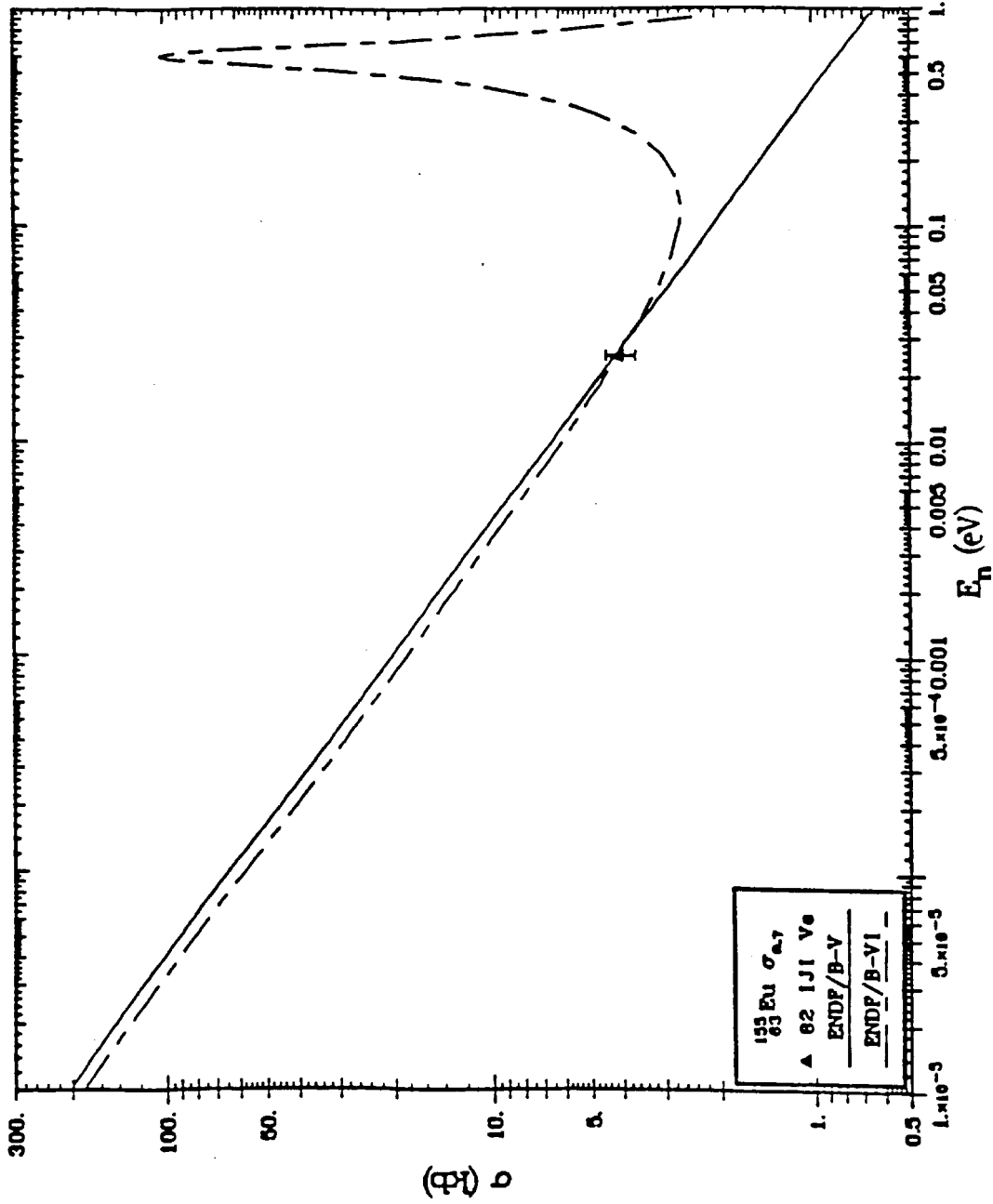


Fig. 15. ENDF/B Versions V and VI (n,  $\gamma$ ) cross sections of  $^{155}\text{Eu}$  at low neutron energies.



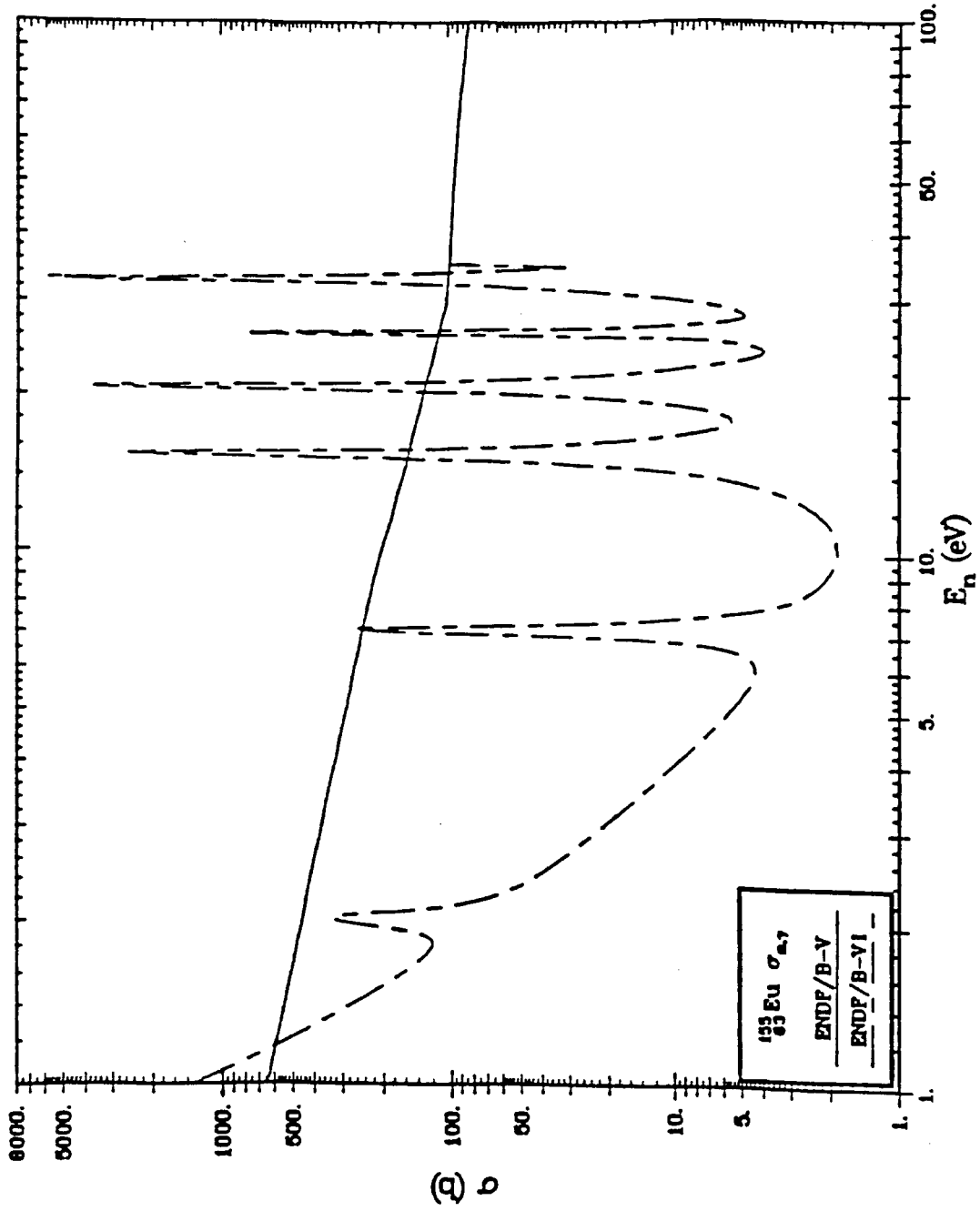


Fig. 16. ENDF/B Versions V and VI ( $\sigma$ ) cross sections of  $^{155}\text{Eu}$  in a significant part of resonance region.

and  $-2.1\%$  using ENDF/B-VI Eu data. The change is due to comparable structural variations in the  $^{154}\text{Eu}$  data in the two libraries. The changes for other fission products using the two different cross-section libraries are far less than the changes in isobars 154 and 155. Of all nuclides for which the differences between the computed and measured contents exceed  $5\%$ , there are only two nuclides for which the average differences changed more than  $20\%$  between the results for the two libraries. The percentage differences for  $^{134}\text{Cs}$  are  $-8.1$  and  $-11.4\%$  and for  $^{135}\text{Cs}$  are  $10.9$  and  $5.7\%$ , applying data from 27BURNUPLIB and 44GROUPNDF5, respectively. The  $^{134}\text{Cs}$  and  $^{135}\text{Cs}$  contents are highly dependent on  $(n,\gamma)$  cross sections of  $^{133}\text{Cs}$  and  $^{135}\text{Xe}$ , respectively. Thus, the differences for either of the  $^{134}\text{Cs}$  and  $^{135}\text{Cs}$  results could be caused by spectral shifts in the neutron flux, resulting from the changes in actinide cross sections between ENDF/B-IV and ENDF/B-V data. Also, the smaller differences between results from using data of the two ENDF versions observed in Table 38 for all other fission products could result from the flux changes to a lesser degree.

In addition to the nuclides already discussed, there are five fission products ( $^{79}\text{Se}$ ,  $^{99}\text{Tc}$ ,  $^{126}\text{Sn}$ ,  $^{149}\text{Sm}$ , and isobar 151) that have either large differences in the comparisons or excessive spreads in the results of all cases, irrespective of the cross-section library applied. The cause of the large differences or data spreads may result from inadequate cross sections, half-lives, power histories, pellet sample locations, radiochemical measurements, computational methodology or a combination of any or all of these possibilities. The differences for  $^{149}\text{Sm}$  and isobar 151 are in the ranges  $-21.0$  to  $-49.1\%$  and  $13.0$  to  $38.5\%$ , respectively. A study<sup>30</sup> was conducted on the effect of power histories on both  $k_{\text{eff}}$  and isotopes significant to the computed value of  $k_{\text{eff}}$ . It was determined that  $^{149}\text{Sm}$  was sensitive to the operating history, in particular to the power at shutdown for discharge. The  $^{149}\text{Sm}$  is increased as the final internal power is increased. Also, it was determined that  $^{151}\text{Sm}$  was slightly sensitive in the opposite direction to late-cycle changes in the operating power. The use of the actual power history of assembly D047 from data in ref. 13 and values in the study of ref. 30 would account for approximately one-third of the difference for  $^{149}\text{Sm}$  for the cases in this project, for which a constant cycle power was used to reduce computing time. A similar estimate for isobar 151 gave a correction in the correct direction but was estimated to account for  $<1\%$ . The difference in  $^{99}\text{Tc}$ , for the cases using 27BURNUPLIB data, changed from an average of  $7.3\%$  for assemblies D047, D101, and B05 to  $42.9\%$  for assembly BT03. This may provide a reason to discard the BT03  $^{99}\text{Tc}$  result as an "outlier" case. An analysis of the uncertainties in half-lives for isotopes affecting results for  $^{99}\text{Tc}$ ,  $^{149}\text{Sm}$ , and isobar 151 proved that source of error to be a small or insignificant fraction of the differences. The reasons for the significant differences for the fission products not accounted for in the above discussion (i.e.,  $^{79}\text{Se}$  and  $^{126}\text{Sn}$ ) are unknown. Although  $^{99}\text{Tc}$ ,  $^{149}\text{Sm}$ , and  $^{151}\text{Sm}$  rank among the most significant fission products in computing  $k_{\text{eff}}$ , the total contribution to uncertainty in  $k_{\text{eff}}$  from actinide nuclides is several times greater than the contribution from these three isotopes.

The sample activities of the long-lived isotopes  $^{79}\text{Se}$  and  $^{126}\text{Sn}$  were measured and reported in units of curies. The calculations in units of mass were converted to curies for the reported comparisons. The conversion factor for mass-to-curies is inversely proportional to half-life, and, thus, a percentage error in the half-life contributes an equal percentage error to the result as curies. At the start of this project, it was found that the computed  $^{79}\text{Se}$  curies were approximately ten times the measured values. In examining the document<sup>31</sup> in which the  $^{79}\text{Se}$  half-life measurement was reported, it was found that the conversion of sample activity to half-life was too small by a factor of 10. This

"measured" half-life was then reported<sup>31</sup> as an upper limit. The ENDF/B-VI value, used initially from the ORIGEN-S library, was obtained by an average of the measured upper limit and a lower limit that was a theoretical calculated minimum. A similar procedure was used with the corrected upper limit, changing the final half-life from 33,000 years to 330,000 years. The ORIGEN-S library used in SCALE was modified to the new value for use in this project. The average percentage differences in Table 38 for <sup>79</sup>Se of approximately 14% could be primarily due to the final uncertainty in the half-life. The spread of -0.1 to 32.8% between cases could be partly due to effects from the pellet locations (discussed for actinides in Sect. 5.5).

The average difference in Table 38 for <sup>126</sup>Sn is about 230%. A detailed analysis of the data and equations applied in computing the mass of <sup>126</sup>Sn in the cases under consideration indicated that the cross-section data, the fission-product yields, and the computational model would not likely have caused an error of 230%. The initial source<sup>32</sup> that reported the half-life, along with photon energy measurements, stated "the half-life of <sup>126</sup>Sn is estimated to be ~10<sup>5</sup> years" and noted that the work should be continued. Thus, the 230% difference would not be unexpected when only an "order of magnitude" value is used for the half-life.

Several specific nuclides significant to decay-heat generation from fission products were examined. These included <sup>85</sup>Kr, <sup>90</sup>Sr, <sup>134</sup>Cs, <sup>137</sup>Cs, <sup>147</sup>Pm, and <sup>154</sup>Eu (which may be inferred from isobar 154). Also, the contribution of two other nuclides that are dominant contributors to decay heat (<sup>90</sup>Y and <sup>137m</sup>Ba) may be partially inferred because they are in secular equilibrium with <sup>90</sup>Sr and <sup>137</sup>Cs, respectively. The differences in the above decay heat nuclides as listed in Table 38 vary from -8.1% for <sup>134</sup>Cs to 6.1% for <sup>90</sup>Sr and 30.8% for <sup>154</sup>Eu. The smallest difference was the 0.8% value for <sup>137</sup>Cs. A problem-dependent set of fission-product contents would be required to accurately determine the propagated bias in the total fission-product decay heat rate, but the <sup>90</sup>Sr and <sup>137</sup>Cs data indicate that the heat rates at cooling times where these nuclides and their daughters make a dominant contribution (<100 years) would have a propagated bias that is not likely to exceed a few percent. This estimate agrees with the average difference of 1.5 ± 1.3% between measured and SCALE-computed heat rates of 10 PWR fuel assemblies.<sup>21</sup> The fission products significant to heat rates at the very long cooling times important in repository waste storage analyses include <sup>79</sup>Se, <sup>99</sup>Tc, and <sup>126</sup>Sn. These nuclides are somewhat less well characterized with maximum differences of 14.1% for <sup>79</sup>Se, 16.7% for <sup>99</sup>Tc, and 230% for <sup>126</sup>Sn.

The photon source production predictions important in shielding studies for spent nuclear fuel are dependent upon accurate characterizations of <sup>144</sup>Pr, <sup>60</sup>Co, <sup>134</sup>Cs, <sup>154</sup>Eu, <sup>106</sup>Rh, <sup>90</sup>Y, and <sup>137m</sup>Ba for cooling times less than 100 years. With the exception of <sup>60</sup>Co (an impurity material) and <sup>106</sup>Rh, direct or indirect estimates of the accuracy of predicted concentrations of these isotopes are available. The maximum differences seen are 0.5% for <sup>144</sup>Pr (indirectly from <sup>144</sup>Nb), -11.4% for <sup>134</sup>Cs, 30.8% for <sup>154</sup>Eu (from the 154 isobar), 6.1% for <sup>90</sup>Y (from <sup>90</sup>Sr), and 0.9% for <sup>137m</sup>Be (from <sup>137</sup>Cs). Thus, there are considerable variations in the quality of predictions for individual fission products that should produce differing impacts upon the specific areas of application.

## 5.5 COMPARISON OF MEASURED VS PREDICTED DIFFERENCES WITH EXPERIMENTAL UNCERTAINTIES

Thus far in this report, only measured vs predicted differences have been discussed. Of primary importance are the magnitude of these differences relative to the experimental uncertainties.

Comparisons are shown in Table 41 between the differences in the measured and computed values and the uncertainties (1 standard deviation) of the radiochemical analyses. The quoted uncertainties<sup>12-16,22</sup> apply to the measured nuclide composition derived for each Calvert Cliffs or Obrigheim PWR case (i.e., each pellet or dissolved sample). These uncertainties relate only to the experimental measurements and do not include any of the variations discussed in subsections 5.5.1-5.5.3 and Appendix E that arise from flux or other neutronic changes at different pellet locations.

Note that the standard deviation of a single case measurement is not directly comparable with an average percentage difference, but it does permit at least a qualitative comparison. It is seen in Table 41 that for the use of ENDF/B-IV data the actinide results compare reasonably well for the more significant isotopes of U and Pu. However, the percentage differences for most of the isotopes sufficiently exceed the experimental uncertainties to indicate computational bias. These differences in the Calvert Cliffs cases for U and Pu vary from  $0.4\sigma$  for  $^{236}\text{U}$  to  $5.4\sigma$  for  $^{242}\text{Pu}$  (where  $\sigma$  is 1 standard deviation), with an average of  $2.4\sigma$  for the nine isotopes measured. Correspondingly, for the Obrigheim cases, the variation is  $0.8\sigma$  for  $^{238}\text{Pu}$  to  $7.5\sigma$  for  $^{242}\text{Pu}$ , with an average of  $4.6\sigma$  for the seven isotopes listed. Note that most of the measurement uncertainties in U and Pu isotopes for Obrigheim cases are lower than those uncertainties for the Calvert Cliffs cases, causing most of the increase from  $2.4\sigma$  to  $4.6\sigma$  in the above average values. Although the  $^{241}\text{Am}$  difference is only slightly more than 1 standard deviation,  $^{237}\text{Np}$  and  $^{243}\text{Cm} + ^{244}\text{Cm}$  exceed the uncertainties by excessive quantities ( $12\sigma$  and  $4\sigma$ , respectively). The comparisons of the differences for  $^{242}\text{Cm}$  and  $^{244}\text{Cm}$  for the assembly-averaged measurements of the Obrigheim fuel are well within the measurement uncertainties.

Comparisons in Table 41 for the use of ENDF/B-V data show that the predictions for the actinide isotopes agree well with measurements for most nuclides. The percentage differences of the Calvert Cliffs cases for U and Pu vary from  $0.4\sigma$  for  $^{236}\text{Pu}$  to  $4.7\sigma$  for  $^{238}\text{Pu}$ , with an average of  $1.5\sigma$  for the nine isotopes. Also, for the Obrigheim cases, the variation is  $<0.1\sigma$  for  $^{239}\text{Pu}$  to  $4.6\sigma$  for  $^{235}\text{U}$ , with an average of  $1.5\sigma$  for the seven U and Pu isotopes compared. The percentage differences for  $^{237}\text{Np}$  and  $^{241}\text{Am}$  of 9.7 and -11.0% exceed the measurement standard deviations of 1.9 and 4.9%, respectively.

With the two exceptions, isobar 154 and isobar 155, there are essentially no differences between fission products (plus  $^{14}\text{C}$ ) applying cross-section data from either of the two ENDF libraries. Most of the fission-product isotopes in Table 41, for which there are uncertainties given, have differences several times the corresponding experimental error. The half-life is mostly likely in error for  $^{126}\text{Sn}$ . Either half-life or cross-section error (and some model discrepancies) are likely to contribute to the computed differences. Observing the differences listed by isotopes in Tables 36 and 37, there are seven fission product nuclides or isobars that exceed 15%:  $^{99}\text{Tc}$ ,  $^{148}\text{Sm}$ ,  $^{149}\text{Sm}$ ,  $^{151}\text{Sm} + ^{151}\text{Eu}$ ,  $^{152}\text{Sm}$ , isobar 154, and isobar 155. Most of these isotopes or their significant precursors have large cross sections. It can be shown that for very large absorption cross sections (e.g., that of  $^{149}\text{Sm}$ ), the sensitivity of the final nuclide density to changes in cross section may significantly exceed unity; thus, producing a greater fractional standard deviation in the density than that of the cross section. Also, it was noted in Sect. 5.4 that the change in  $^{154}\text{Eu}$  and  $^{155}\text{Eu}$  cross sections from ENDF/B-V to ENDF/B-VI data improved the difference from 96.0 to -24.4%. Although the major contribution to the uncertainty of  $k_{\text{eff}}$  is from isotopes of U and Pu, some of these seven fission-product isotopes, having less accurate predictions (e.g.,  $^{155}\text{Gd}$  and  $^{149}\text{Sm}$ ) also significantly contribute to the uncertainty.

Table 41. Summary of experimental uncertainties compared with average percentage differences<sup>a</sup> in measured and computed compositions

Nuclide or element	Radiochemical measurement, % uncertainty		Average % differences between measured and computed composition					
			27BURNUPLIB library			44GROUPNDF5 library		
	Calvert Cliffs <sup>b</sup>	Obrigheim <sup>c</sup>	Calvert Cliffs	Obrigheim	Ave. of absolute values <sup>d</sup>	Calvert Cliffs	Obrigheim	Ave. of absolute values
U	1.6				2.4			1.4
<sup>234</sup> U	1.6		4.7			-1.8		
<sup>235</sup> U	1.6	0.5	-4.0	-3.2		-3.0	-2.3	
<sup>236</sup> U	1.6	0.4	0.6	1.6		0.6	1.4	
<sup>238</sup> U	1.6		-0.8			-0.8		
Pu	1.6				6.3			0.9
<sup>238</sup> Pu	1.6	7.7	-2.3	6.1		-7.5	0.8	
<sup>239</sup> Pu	1.6	1.3	3.8	5.7		-2.2	<0.1	
<sup>240</sup> Pu	1.6	1.4	-6.9	-5.5		-1.6	0.2	
<sup>241</sup> Pu	1.6	1.3	3.4	7.2		-2.9	1.0	
<sup>242</sup> Pu	1.6	1.7	-8.6	-12.8		1.4	-2.6	
<sup>237</sup> Np	1.9		22.8			9.7		
<sup>241</sup> Am	4.9		-5.9			-11.0		
<sup>242</sup> Cm		30-90 <sup>e</sup>		-18.7			-25.0	
<sup>244</sup> Cm		20-30		-22.7			-7.1	
<sup>243</sup> Cm + <sup>244</sup> Cm	4.1		-15.8			-2.3		
<sup>14</sup> C	5.6		-14.2			-13.8		
<sup>79</sup> Se	4.9		14.1			14.0		
<sup>90</sup> Sr	5.7		6.1			6.0		
<sup>99</sup> Tc	3.5		17.7			18.2		
<sup>126</sup> Sn	10.2		230.3			229.8		
<sup>129</sup> I	2.2		-10.8			-10.8		
<sup>135</sup> Cs	14.0		11.2			6.0		
<sup>137</sup> Cs	3.5		0.6			0.6		
Cs	9.0 <sup>f</sup>				5.4			5.1
Nd	1.0 <sup>g</sup>				1.0			1.0
Pm	4.0 <sup>g</sup>				4.5			2.8
Sm	7.0 <sup>g</sup>				17.9			15.4
Eu	13.0 <sup>g</sup>				39.4			14.9
Gd	18.0 <sup>g</sup>				63.4			13.3

<sup>a</sup> (Calculated/measured - 1) × 100%.

<sup>b</sup> Uncertainty as the standard deviation of measurements conducted by the MCC at PNL.

<sup>c</sup> Uncertainty as the standard deviation in the estimate of the average of the measurements conducted by TUI, IAEA, WAK, and IRCH.

<sup>d</sup> Average percentage difference of the element based on the absolute values of the average differences for the isotopes of the element.

<sup>e</sup> Uncertainty based on KORIGEN calculations 30% lower than the measurements and repeated  $\alpha$ -spectrometer analyses showing differences of up to 90%.

<sup>f</sup> Based on average of <sup>135</sup>Cs and <sup>137</sup>Cs only.

<sup>g</sup> Averages of isotopic standard deviations of the individual measurements.<sup>22</sup>

## 6. GENERAL SUMMARY

The purpose of this project is to perform, report, and evaluate computations applying the SCALE modular code system for isotopic compositions of irradiated fuel from pressurized-water power plants. This summary includes both a brief synopsis of the body of the report and a few concluding remarks.

### 6.1 SUMMARY OF THE BENCHMARK COMPARISONS

Reactor fuel depletion calculations are performed by the SCALE control module SAS2H. This module applies the neutronics analyses of the well-known XSDRNPM-S, NITAWL-II, and BONAMI-S functional modules and the depletion and decay evaluations of the COUPLE and ORIGEN-S codes. Although the 2-D effects from the guide-tube water holes or BPRs are included in the model, the method is intended to compute the average isotopic compositions of the spent fuel assembly. An extensive description of the SAS2H model and the basic applications performed by XSDRNPM-S and ORIGEN-S, in particular, are included in Sect. 2 of this report.

Nineteen different PWR fuel benchmark problems are analyzed in this study. Data on PWR fuel design and operating conditions for the 19 cases, sufficient for input to a SCALE computation, are presented in Sect. 3. Fuel assemblies were analyzed from Calvert Cliffs Unit 1, H. B. Robinson Unit 2, and Obrigheim power plants. The basic parameters (i.e., burnup and  $^{235}\text{U}$  enrichment) are summarized in Table 2.

Comparisons of predicted and measured isotopic compositions of each of the 19 benchmark cases are given in Sects. 4.1 through 4.3. Data for each reactor are listed as radiochemical assay measurements and followed by listings of the percentage differences between measured and computed nuclide compositions. All problems were calculated using two different libraries. One is the 27-energy-group SCALE-4 library, which has actinide and light-element data derived from ENDF/B-IV and fission-product data processes from ENDF/B-V. The second library applied here is a 44-energy-group library derived entirely from ENDF/B-V files with the exceptions that data for  $^{16}\text{O}$ ,  $^{154}\text{Eu}$ , and  $^{155}\text{Eu}$  were taken from ENDF/B-VI. The comparative differences included tables listing the results from both of the cross-section libraries. The ranges or data spreads in the nuclide density differences, along with the corresponding averages, are given in Table 38 of Sect. 5.1. Plots of the ranges in data spreads are also shown. In general, results based on the 44-group ENDF/B-V library are better than those obtained using the 27-group ENDF/B-IV and ENDF/B-V libraries. While some of the improvement is due to the group structure and collapsing spectrum used in creating the 44-group library (especially for plutonium), most of the improved agreement results from better data in the ENDF/B-V (plus some ENDF/B-VI) cross sections.

The average differences between the computed and measured compositions for each assembly or batch (for Obrigheim cases) in addition to the overall averages are summarized in Tables 36 and 37 for application of the two cross-section libraries. A final concise summary of average element differences based on the absolute values of average differences for the isotopes of the element are given in Table 39. The final averages in Tables 36 through 39 discussed in Sects. 5.1 through 5.5 are indicative of the overall bias in the SCALE model calculations. The final average differences for nuclides  $^{235}\text{U}$  and  $^{239}\text{Pu}$  and elements U and Pu are  $-3.1$ ,  $5.4$ ,  $2.4$ , and  $6.3\%$ , respectively, applying actinide cross-section data from ENDF/B-IV. Positive differences for nuclides denote that the computed value is higher than that measured. Note that these differences for the elements are always positive because they are the average of the absolute values of percentage differences of all isotopes of

the element. The corresponding averages for  $^{235}\text{U}$ ,  $^{239}\text{Pu}$ , U, and Pu for cases applying ENDF/B-V data are  $-2.2$ ,  $-0.4$ ,  $1.4$ , and  $0.9\%$ , respectively. These results indicate a substantial improvement in major actinide compositions by applying actinide cross sections derived from ENDF/B-V compared with that from ENDF/B-IV. The reasons for the major differences in the computations using the two different cross-section libraries were examined, as discussed in Sect. 5.3. Also, note that these average comparisons indicate the magnitude of overall bias in the computed (or measured) densities and do not show individual case fluctuations or random errors.

The discussions in Sect. 5.5 and Appendix E deal with evaluations of some of the inconsistencies, and, in part, the fluctuations in the percentage difference between the measured and computed density of a specific nuclide in the various samples. The samples analyzed in most of the benchmark cases were taken from individual fuel pellets. Several pellets were examined at different axial heights within a fuel rod. The radial location of a fuel rod analyzed was taken at different distances from the nearest guide tube. The advantage to examining pellets of different heights and various assemblies was to produce cases having a wide range of burnup and other conditions. The selection of fuel rods of different proximities to guide tubes succeeded in covering the possible variations in conditions that may prevail within an assembly. These differences may be essential in evaluating axial and/or radial effects in 3-D computations of  $k_{\text{eff}}$ . Although such pellet analyses are necessary in fully characterizing the fuel densities, the possibility that a significant part of the spread in comparisons for a nuclide depends on spatial effects within an assembly was motivation for making a limited study of these effects. It was determined that the radial and axial variation in differences of measured and computed  $^{239}\text{Pu}$  was affected by changes in the spatially dependent flux spectrum. Also, secondary effects of variation of  $^{239}\text{Pu}$  differences on  $^{235}\text{U}$  were observed, although with less consistency than in the evaluations of spatial effect.

Other significant differences in comparisons were reviewed in Sect. 5.5. Table 41 presents a summary of known experimental uncertainties compared with average percentage differences in measured and computed compositions. The magnitudes of the measured/computed differences for many isotopes correspond to similar quantities in the uncertainty of the measurement. However, seven of the heavier fission-product isotopes had somewhat excessive differences exceeding 15%:  $^{99}\text{Tc}$ ,  $^{148}\text{Sm}$ ,  $^{149}\text{Sm}$ ,  $^{151}\text{Sm} + ^{151}\text{Eu}$ ,  $^{152}\text{Sm}$ ,  $^{154}\text{Sm} + ^{154}\text{Eu} + ^{154}\text{Gd}$ , and  $^{155}\text{Eu} + ^{155}\text{Gd}$ .

## 6.2 CONCLUSIONS

The validation process of a computational model has a twofold purpose. One purpose is to determine if the code or method under review calculates the required quantities with a reasonable degree of accuracy, in comparisons with corresponding measurements. A "reasonable accuracy" can depend on the ultimate application. For example, the accuracy of the  $^{244}\text{Cm}$  content may be very significant in determining total decay heat rate or neutron source but it may be insignificant in the calculation of  $k_{\text{eff}}$ . The other purpose of validation is the determination of uncertainties, or some other representation of error, in the quantity being computed. This purpose of validation, in a broader meaning of the process, tends to override the former purpose (i.e., accuracy) because it provides a method for establishing the safety factor to be applied to the computed quantity.

The fuel depletion analyses computed in this project agree with measurements sufficiently well to apply the SCALE code system as a basic tool for predicting isotopic compositions of spent fuel from PWR power plants. However, a method to define and determine the bias and uncertainties of the SCALE approach relative to the measured data must be established before this approach may be applied in criticality safety analyses of spent fuel.



## REFERENCES

1. *SCALE: A Modular Code System for Performing Standardized Computer Analyses for Licensing Evaluation*, NUREG/CR-0200, Rev. 4 (ORNL/NUREG/CSD-2/R4), Vols. I, II, and III (draft November 1993). Available from Radiation Shielding Information Center, Oak Ridge National Laboratory, as CCC-545.
2. T. L. Sanders and R. M. Westfall, "Feasibility and Incentives for Burnup Credit in Spent Fuel Transport Casks," *Nucl. Sci. Eng.* 104 (1990).
3. M. C. Brady and T. L. Sanders, "A Validated Methodology for Evaluating Burnup Credit in Spent Fuel Casks," *Proc. International Conference on Nuclear Criticality Safety*, Christ Church, Oxford, United Kingdom, September 9-13, 1991.
4. M. C. Brady, T. L. Sanders, K. D. Seager, and W. H. Lake, "Burnup Credit Issues in Transportation and Storage," *Proc. Tenth International Symposium on the Packaging and Transportation of Radioactive Materials*, September 13-18, 1992, Yokohama City, Japan.
5. S. M. Bowman, O. W. Hermann, and M. C. Brady, "Burnup Credit Validation of SCALE-4 Using Light-Water Reactor Criticals," *Trans. Am. Nucl. Soc.* 68(A), 243-245 (1993).
6. M. C. Brady, C. V. Parks, and C. R. Marotta, "End Effects in the Criticality Analysis of Burnup Credit Casks," *Trans. Am. Nucl. Soc.* 62, 317 (1990).
7. "American National Standard for Nuclear Criticality Safety in Operations with Fissionable Materials Outside Reactors," ANSI/ANS-8.1-1983, American Nuclear Society, 1983.
8. S. M. Bowman and O. W. Hermann, *Reference Problem Set to Benchmark Analysis Methods for Burnup Credit Applications*, ORNL/TM-12295 (to be published).
9. C. V. Parks, O. W. Hermann, and B. L. Broadhead, "The SCALE Analysis Sequence for LWR Fuel Depletion," *Proc. ANS/ENS International Topical Meeting*, Pittsburgh, Pa., April 28-May 1, 1991.
10. O. W. Hermann and C. V. Parks, "SAS2H: The SCALE-4 Analysis Sequence for LWR Fuel Depletion," *Proc. Seminar on SCALE-4 and Related Modular Systems for the Evaluation of Nuclear Fuel Facilities and Package Design Featuring Criticality, Shielding, and Heat Transfer Capabilities*, September 17-19, 1991, OECD NEA Data Bank, Saclay.
11. J. O. Barner, *Characterization of LWR Spent Fuel MCC-Approved Testing Material - ATM-101*, PNL-5109, Rev. 1, Pacific Northwest Laboratory, 1985.
12. R. J. Guenther et al., *Characterization of Spent Fuel Approved Testing Material - ATM-103*, PNL-5109-103, Pacific Northwest Laboratory, 1988.
13. R. J. Guenther et al., *Characterization of Spent Fuel Approved Testing Material - ATM-104*, PNL-5109-104, Pacific Northwest Laboratory, 1991.

14. R. J. Guenther et al., *Characterization of Spent Fuel Approved Testing Material - ATM-106*, PNL-5109-106, Pacific Northwest Laboratory, 1988.
15. U. Fischer and H. W. Wiese, *Improved and Consistent Determination of the Nuclear Inventory of Spent PWR Fuel on the Basis of Cell Burnup Methods Using KORIGEN* (ORNL-TR-5043), KFK 3014, Karlsruhe Nuclear Research Center, January 1983; available from Radiation Shielding Information Center, Oak Ridge National Laboratory, as CCC-457.
16. U. Hesse, *Verification of the OREST (HAMMER-ORIGEN) Depletion Program System Using Post-Irradiation Analyses of Fuel Assemblies 168, 170, 171, and 176 from the Obrigheim Reactor* (ORNL-TR-88/20), GRS-A-962, Gesellschaft für Reaktorsicherheit (GRS) mbH, 1984.
17. M. D. DeHart and S. M. Bowman, *Validation of the SCALE Broad Structure 44-Group ENDF/B-V Cross-Section Library for Use in Criticality Safety Analyses*, NUREG/CR-6102 ORNL/TM-12460, Martin Marietta Energy Systems, Inc., Oak Ridge Natl. Lab., 1994.
18. R. Q. Wright, "Fission Product Evaluations for ENDF/B-VI," *Trans. Am. Nucl. Soc.* 61, 398-399 (1990).
19. J. C. Ryman et al., *Fuel Inventory and Afterheat Power Studies of Uranium-Fueled Pressurized Water Reactor Fuel Assemblies Using the SAS2 and ORIGEN-S Modules of SCALE with an ENDF/B-V Updated Cross Section Library*, NUREG/CR-2397 (ORNL/CSD-90), Union Carbide Corp., Nucl. Div., Oak Ridge Natl. Lab., September 1982.
20. N. M. Greene et al., *AMPX: A Modular Code System for Generating Coupled Multigroup Neutron-Gamma Libraries from ENDF/B*, ORNL/TM-3706, Union Carbide Corp., Nucl. Div., Oak Ridge Natl. Lab., March 1976.
21. O. W. Hermann, C. V. Parks, and J. P. Renier, "A Proposed Regulatory Guide Basis for Spent Fuel Decay Heat," *Proc. Second Annual International Conference on High Level Radioactive Waste Management*, Vol. 2, Las Vegas, Nevada, April 28-May 3, 1991; also see O. W. Hermann, C. V. Parks, and J. P. Renier, *Technical Support for a Proposed Decay Heat Guide Using SAS2H/ORIGEN-S Data*, NUREG/CR-5625, ORNL-6698, Martin Marietta Energy Systems, Inc., Oak Ridge Natl. Lab. (1994).
22. S. R. Bierman, *Benchmark Data for Validating Irradiated Fuel Compositions Used in Criticality Calculations*, SAND 94-0860 (TIC-1044), Pacific Northwest Laboratory (draft June 1994).
23. J. W. Roddy et al., *Physical and Decay Characteristics of Commercial LWR Spent Fuel*, ORNL/TM-9591, Martin Marietta Energy Systems, Inc., Oak Ridge Natl. Lab., October 1985.
24. S. M. Bowman et al., "Validation of SCALE-4 for LWR Fuel in Transportation and Storage Cask Conditions," *Trans. Am. Nucl. Soc.* 62, 338-340 (1990).

25. S. R. Bierman, "Spent Reactor Fuel Benchmark Composition Data for Code Validation," *Proc. of International Conference on Nuclear Criticality Safety*, Oxford, United Kingdom, September 1991.
26. Letter, O. Ozer of Electric Power Research Institute to W. B. Lowenstein and B. A. Zolotar, "EPRI-CELL Test Calculations of Isotopes as a Function of Burnup," April 1976.
27. "Robinson 2," Section in *Nuclear Power Experience, Plant Descriptions, and Histories*, Vol. PWR-1, p. 5, August 1981.
28. G. W. Morey, *The Properties of Glass*, 2nd Ed., Reinhold, New York, 1954.
29. F. W. Walker, J. R. Parrington, and F. Feiner (revisors of edition), *Nuclides and Isotopes*, 14th Ed., General Electric Co., San Jose, California, 1989.
30. M. C. Brady, *Task Monthly Report, February 1992*, BCAV-PGR-048, 1992.
31. G. W. Parker et al., "Radiations and Half-Life of Long-Lived Fission Selenium," in *Chemistry Division Quarterly Progress Report for Period Ending September 30, 1949*, ORNL-499, 1949.
32. C. J. Orth and B. J. Dropesky, "Decay of Long-Lived  $^{126}\text{Sn}$ ," *Bull. Am. Phys. Soc.* 3, 207 (1958).



**APPENDIX A**

**SAS2H INPUT FILES FOR CALVERT CLIFFS, H. B. ROBINSON,  
AND OBRIGHEIM FUEL ASSEMBLIES**

Table A.1. Calvert Cliffs Assembly D047 Rod MKP109, 27.35 GWd/MTU, ENDF/B-IV

```

=sas2      parm='halt04,skipshipdata'
calvert cliffs 1 pwr, d047, rod mkp109, 13.200 cm, 27.35/mtu b4 aug-94
  cooled 1870 d
-----
.
.
.
mixtures of fuel-pin-unit-cell:
.
27burnuplib latticecell
uo2 1 den=10.045 1 790
  92234 0.027 92235 3.038 92236 0.014 92238 96.921 end
c 1 den=1.8-4 1 790 end
n 1 den=2.3-4 1 790 end
co-59 3 0 1-20 557 end
zr-94 1 0 1-20 790 end
mo-94 1 0 1-20 790 end
nb-95 1 0 1-20 790 end
mo-95 1 0 1-20 790 end
tc-99 1 0 1-20 790 end
rh-103 1 0 1-20 790 end
rh-105 1 0 1-20 790 end
ru-106 1 0 1-20 790 end
sn-126 1 0 1-20 790 end
xe-131 1 0 1-20 790 end
cs-134 1 0 1-20 790 end
cs-135 1 0 1-20 790 end
cs-137 1 0 1-20 790 end
pr-143 1 0 1-20 790 end
nd-143 1 0 1-20 790 end
ce-144 1 0 1-20 790 end
nd-144 1 0 1-20 790 end
nd-145 1 0 1-20 790 end
nd-146 1 0 1-20 790 end
nd-147 1 0 1-20 790 end
pm-147 1 0 1-20 790 end
sm-147 1 0 1-20 790 end
nd-148 1 0 1-20 790 end
pm-148 1 0 1-20 790 end
sm-148 1 0 1-20 790 end
pm-149 1 0 1-20 790 end
sm-149 1 0 1-20 790 end
nd-150 1 0 1-20 790 end
sm-150 1 0 1-20 790 end
sm-151 1 0 1-20 790 end
eu-151 1 0 1-20 790 end
sm-152 1 0 1-20 790 end
eu-153 1 0 1-20 790 end
eu-154 1 0 1-20 790 end
gd-154 1 0 1-20 790 end
eu-155 1 0 1-20 790 end
gd-155 1 0 1-20 790 end
gd-157 1 0 1-20 790 end
gd-158 1 0 1-20 790 end
gd-160 1 0 1-20 790 end
zircalloy 2 1 620 end
h2o 3 den=0.7575 1 557 end
arbm-bormod 0.7575 1 1 0 0 5000 100 3 330.8e-6 557 end
.
.
  331 ppm boron (wt) in moderator
-----
end comp
.
.
fuel-pin-cell geometry:
squarepitch 1.4732 0.9563 1 3 1.1176 2 0.9855 0 end
.
.
assembly and cycle parameters:
npin/assm=176 fuelnght=787.52 ncycles=4 nlib/cyc=1
printlevel=4 lightel=9 inplevel=2 numztot=5 end
3 1.314 2 1.416 3 1.662 500 5.203 3 5.243
power=15.197 burn=306.0 down=71 end
power=17.124 burn=381.7 down=81.3 bfrac=1.419 end
power=15.018 burn=466.0 down=85 bfrac=1.523 end
power=12.843 burn=461.1 down=1870 bfrac=1.488 end
o 119 cr 5.2 mn 0.29
fe 11. co 0.066 ni 8.7
zr 195 nb 0.63 sn 3.2
.
.
-----
end

```

Table A.2. Calvert Cliffs Assembly D047 Rod MKP109, 37.12 GWd/MTU, ENDF/B-IV

```

=sas2      parm='halt04,skipshipdata'
calvert cliffs 1 pwr, d047, rod mkp109, 27.700 cm, 37.12/mtu b4 aug-94
  cooled 1870 d
-----
.
.
.
mixtures of fuel-pin-unit-cell:
.
27burnuplib latticecell
uo2 1 den=10.045 1 841
  92234 0.027 92235 3.038 92236 0.014 92238 96.921 end
c 1 den=1.8-4 1 841 end
n 1 den=2.3-4 1 841 end
co-59 3 0 1-20 558 end
zr-94 1 0 1-20 841 end
.
.
  *fission product nuclide set same as table a.1 with new temperatures*
.
gd-160 1 0 1-20 841 end
zircalloy 2 1 620 end
h2o 3 den=0.7569 1 558 end
arbm-bormod 0.7569 1 1 0 0 5000 100 3 330.8e-6 558 end
.
.
  331 ppm boron (wt) in moderator
-----
end comp
.
.
fuel-pin-cell geometry:
squarepitch 1.4732 0.9563 1 3 1.1176 2 0.9855 0 end
.
.
assembly and cycle parameters:
npin/assm=176 fuelnght=787.52 ncycles=4 nlib/cyc=1
printlevel=4 lightel=9 inplevel=2 numztot=5 end
3 1.314 2 1.416 3 1.662 500 5.203 3 5.243
power=21.789 burn=306.0 down=71 end
power=23.583 burn=381.7 down=81.3 bfrac=1.419 end
power=20.133 burn=466.0 down=85 bfrac=1.523 end
power=16.630 burn=461.1 down=1870 bfrac=1.488 end
o 119 cr 5.2 mn 0.29
fe 11. co 0.066 ni 8.7
zr 195 nb 0.63 sn 3.2
.
.
-----
end

```

Table A.3. Calvert Cliffs Assembly D047 Rod  
MKP109, 44.34 GWd/MTU, ENDF/B-IV

```
=sas2      parm='halt04,skipshipdata'
calvert cliffs 1 pwr, d047, rod mkp109, 165.22 cm, 44.34/mtu b4 aug-94
' 1870 d cooling time
'
'-----
'
' mixtures of fuel-pin-unit-cell:
'
27burnuplib latticecell
uo2 1 den=10.045 1 873
    92234 0.027 92235 3.038 92236 0.014 92238 96.921 end
c 1 den=1.8-4 1 873 end
n 1 den=2.3-4 1 873 end
co-59 3 0 1-20 570 end
zr-94 1 0 1-20 873 end
|
*fission product nuclide set same as table a.1 with new temperatures*
|
gd-160 1 0 1-20 873 end
' need the following to use endf/b5 library:
' from st5: (2nd line same as def. of zircalloy in sect. m8, scale-4.1)
' arbmzirc 6.5 4 0 0 1 40000 97.91 26000 0.5 50118 0.64 50120 0.95 2
1 end
' arbmzirc 6.44 4 0 0 1 40000 97.91 26000 0.5 50118 0.64 50120 0.95 2 1 620
end
zircalloy 2 1 620 end
h2o 3 den=0.7332 1 570 end
arbm-bormod 0.7332 1 1 0 0 5000 100 3 330.8e-6 570 end
'
' 331 ppm boron (wt) in moderator
'
end comp
'
'-----
'
' fuel-pin-cell geometry:
'
squarepitch 1.4732 0.9563 1 3 1.1176 2 0.9855 0 end
'
'-----
'
' assembly and cycle parameters:
'
npin/assm=176 fuelnght=787.52 ncycles=4 nlib/cyc=1
printlevel=4 lightel=9 implevel=2 numztotal=5 end
3 1.314 2 1.416 3 1.662 500 5.203 3 5.243
power=27.432 burn=306.0 down=71 end
power=28.654 burn=381.7 down=81.3 bfrac=1.419 end
power=23.094 burn=466.0 down=85 bfrac=1.523 end
power=19.499 burn=461.1 down=1870 bfrac=1.488 end
o 119 cr 5.2 mn 0.29
fe 11. co 0.066 ni 8.7
zr 195 nb 0.63 sn 3.2
'
'-----
'
end
```

Table A.4. Calvert Cliffs Assembly D101 Rod  
MLA098, 18.68 GWd/MTU, ENDF/B-IV

```
=sas2      parm='halt03,skipshipdata'
calvert cliffs 1 pwr, d101, rod mla098, atm-103 18.68gwd/mtu aug 1994
' 8.90 cm sample pellet -- assy #2
'
'-----
'
' mixtures of fuel-pin-unit-cell:
'
27burnuplib latticecell
uo2 1 den=10.045 1 816
    92234 0.024 92235 2.72 92236 0.016 92238 97.24 end
c 1 den=1.2-4 1 816 end
n 1 den=2.4-4 1 816 end
co-59 3 0 1-20 557 end
zr-94 1 0 1-20 816 end
mo-94 1 0 1-20 816 end
nb-95 1 0 1-20 816 end
mo-95 1 0 1-20 816 end
tc-99 1 0 1-20 816 end
rh-103 1 0 1-20 816 end
rh-105 1 0 1-20 816 end
ru-106 1 0 1-20 816 end
xe-131 1 0 1-20 816 end
cs-134 1 0 1-20 816 end
cs-135 1 0 1-20 816 end
cs-137 1 0 1-20 816 end
pr-143 1 0 1-20 816 end
nd-143 1 0 1-20 816 end
ce-144 1 0 1-20 816 end
nd-145 1 0 1-20 816 end
nd-146 1 0 1-20 816 end
nd-147 1 0 1-20 816 end
pm-147 1 0 1-20 816 end
sm-147 1 0 1-20 816 end
nd-148 1 0 1-20 816 end
pm-149 1 0 1-20 816 end
sm-149 1 0 1-20 816 end
sm-150 1 0 1-20 816 end
sm-151 1 0 1-20 816 end
eu-151 1 0 1-20 816 end
sm-152 1 0 1-20 816 end
eu-153 1 0 1-20 816 end
eu-154 1 0 1-20 816 end
gd-154 1 0 1-20 816 end
eu-155 1 0 1-20 816 end
gd-155 1 0 1-20 816 end
gd-157 1 0 1-20 816 end
gd-158 1 0 1-20 816 end
gd-160 1 0 1-20 816 end
zircalloy 2 1 620 end
h2o 3 den=0.7576 1 557 end
arbm-bormod 0.7576 1 1 0 0 5000 100 3 330.8e-6 557 end
'
'
' 331 ppm boron (wt) in moderator
'
'-----
'
end comp
'
'-----
'
' fuel-pin-cell geometry:
'
squarepitch 1.4732 0.9563 1 3 1.1176 2 0.9855 0 end
'
'-----
'
' assembly and cycle parameters:
'
npin/assm=176 fuelnght=787.52 ncycles=3 nlib/cyc=1
printlevel=4 lightel=9 implevel=2 numztotal=5 end
3 1.314 2 1.416 3 1.662 500 5.203 3 5.243
power=13.760 burn=306.0 down=71 end
power=15.504 burn=381.7 down=81.3 bfrac=1.419 end
power=13.598 burn=466.0 down=2374 bfrac=1.523 end
o 119 cr 5.2 mn 0.29
fe 11. co 0.066 ni 8.7
zr 195 nb 0.63 sn 3.2
'
'-----
'
end
```

Table A.5. Calvert Cliffs Assembly D101 Rod  
MLA098, 26.62 GWd/MTU, ENDF/B-IV

```
=sas2      parm='halt03,skipshipdata'
calvert cliffs 1 pwr, d101, rod mla098, atm-103 26.62gwd/mtu aug 1994
'
' 24.300 cm sample pellet -- assy #2
'
'-----
'
' mixtures of fuel-pin-unit-cell:
'
27burnuplib latticecell
uo2 1 den=10.045 1 880
' 92234 0.024 92235 2.72 92236 0.016 92238 97.24 end
c 1 den=1.2-4 1 880 end
n 1 den=2.4-4 1 880 end
co-59 3 0 1-20 558 end
zr-94 1 0 1-20 880 end
'
' fission product nuclide set same as table a.4 with new temperatures*
'
gd-160 1 0 1-20 880 end
zircalloy 2 1 620 end
h2o 3 den=0.7571 1 558 end
arbm-bormod 0.7571 1 1 0 0 5000 100 3 330.8e-6 558 end
'
' 331 ppm boron (wt) in moderator
'
'-----
end comp
'
'-----
' fuel-pin-cell geometry:
'
squarepitch 1.4732 0.9563 1 3 1.1176 2 0.9855 0 end
'
'-----
' assembly and cycle parameters:
'
npin/assm=176 fuelnght=787.52 ncycles=3 nlib/cyc=1
printlevel=4 lightel=9 inplevel=2 numztot=5 end
3 1.314 2 1.416 3 1.662 500 5.203 3 5.243
power=20.408 burn=306.0 down=71 end
power=22.089 burn=381.7 down=81.3 bfrac=1.419 end
power=18.857 burn=466.0 down=2374 bfrac=1.523 end
o 119 cr 5.2 mn 0.29
fe 11. co 0.066 ni 8.7
zr 195 nb 0.63 sn 3.2
'
'-----
end
```

Table A.6. Calvert Cliffs Assembly D101 Rod  
MLA098, 33.17 GWd/MTU, ENDF/B-IV

```
=sas2      parm='halt03,skipshipdata'
calvert cliffs 1 pwr, d101, rod mla098, atm-103 33.17gwd/mtu aug 1994
'
' 161.70 cm sample pellet -- assy #2
'
'-----
'
' mixtures of fuel-pin-unit-cell:
'
27burnuplib latticecell
uo2 1 den=10.045 1 910
' 92234 0.024 92235 2.72 92236 0.016 92238 97.24 end
c 1 den=1.2-4 1 910 end
n 1 den=2.4-4 1 910 end
co-59 3 0 1-20 570 end
zr-94 1 0 1-20 910 end
'
' fission product nuclide set same as table a.4 with new temperatures*
'
gd-160 1 0 1-20 910 end
zircalloy 2 1 620 end
h2o 3 den=0.7341 1 570 end
arbm-bormod 0.7341 1 1 0 0 5000 100 3 330.8e-6 570 end
'
' 331 ppm boron (wt) in moderator
'
'-----
end comp
'
'-----
' fuel-pin-cell geometry:
'
squarepitch 1.4732 0.9563 1 3 1.1176 2 0.9855 0 end
'
'-----
' assembly and cycle parameters:
'
npin/assm=176 fuelnght=787.52 ncycles=3 nlib/cyc=1
printlevel=4 lightel=9 inplevel=2 numztot=5 end
3 1.314 2 1.416 3 1.662 500 5.203 3 5.243
power=26.652 burn=306.0 down=71 end
power=27.839 burn=381.7 down=81.3 bfrac=1.419 end
power=22.437 burn=466.0 down=2374 bfrac=1.523 end
o 119 cr 5.2 mn 0.29
fe 11. co 0.066 ni 8.7
zr 195 nb 0.63 sn 3.2
'
'-----
end
```



Table A.7. Calvert Cliffs Assembly BT03 Rod  
NBD107, 31.40 GWd/MTU, ENDF/B-IV

```
=sas2      parm='halt04,skipshipdata'
calvert cliffs 1 pwr, bt03, rod nbd107, atm-106, 31.40gwd, b4 aug-1994
' decay time 6.7 years (or 2447 days) for measurement of
' pml-5109-106, page 4.64, table 4.17
'
'-----
' mixtures of fuel-pin-unit-cell:
'
27burnuplib latticecell
uo2 1 den=10.036 1 790
  92234 0.022 92235 2.453 92236 0.011 92238 97.514 end
c 1 den=1.95-4 1 790 end
n 1 den=4.42-4 1 790 end
co-59 3 0 1-20 557 end
zr-94 1 0 1-20 790 end
'
|
*fission product nuclide set same as table a.4 with new temperatures*
|
gd-160 1 0 1-20 790 end
zirralloy 2 1 620 end
h2o 3 den=0.7576 1 557 end
arbm-bormod 0.7576 1 1 0 0 5000 100 3 330.8e-6 557 end
'
|
331 ppm boron (wt) in moderator
'-----
end comp
'
' fuel-pin-cell geometry:
'
squarepitch 1.4732 0.9639 1 3 1.1176 2 0.9855 0 end
'
'-----
' assembly and cycle parameters:
'
npin/assm=172 fuelngth=793.88 ncycles=4 nlib/cyc=1
printlevel=5 lightel=9 inplevel=2 numztot=5 end
3 1.314 2 1.416 3 1.662 500 5.156 3 5.243
power=15.765 burn=816.0 down=81 end
power=16.457 burn=306.0 down=71 end
power=11.514 burn=381.7 down=81.3 bfrac=1.419 end
power=11.550 burn=466.0 down=2447 bfrac=1.532 end
o 119 cr 5.2 mn 0.29
fe 11. co 0.066 ni 8.7
zr 195 nb 0.63 sn 3.2
'
'-----
end
```

Table A.8. Calvert Cliffs Assembly BT03 Rod  
NBD107, 37.27 GWd/MTU, ENDF/B-IV

```
=sas2      parm='halt04,skipshipdata'
calvert cliffs 1 pwr, bt03, rod nbd107, atm-106, 37.27gwd, b4 aug-1994
' decay time 6.7 years (or 2447 days) for measurement of
' pml-5109-106, page 4.64, table 4.17
'
'-----
' mixtures of fuel-pin-unit-cell:
'
27burnuplib latticecell
uo2 1 den=10.036 1 841
  92234 0.022 92235 2.453 92236 0.011 92238 97.514 end
c 1 den=1.95-4 1 841 end
n 1 den=4.42-4 1 841 end
co-59 3 0 1-20 557 end
zr-94 1 0 1-20 841 end
'
|
*fission product nuclide set same as table a.4 with new temperatures*
|
gd-160 1 0 1-20 841 end
zirralloy 2 1 620 end
h2o 3 den=0.7573 1 557 end
arbm-bormod 0.7573 1 1 0 0 5000 100 3 330.8e-6 557 end
'
|
331 ppm boron (wt) in moderator
'-----
end comp
'
' fuel-pin-cell geometry:
'
squarepitch 1.4732 0.9639 1 3 1.1176 2 0.9855 0 end
'
'-----
' assembly and cycle parameters:
'
npin/assm=172 fuelngth=793.88 ncycles=4 nlib/cyc=1
printlevel=5 lightel=9 inplevel=2 numztot=5 end
3 1.314 2 1.416 3 1.662 500 5.156 3 5.243
power=18.712 burn=816.0 down=81 end
power=19.533 burn=306.0 down=71 end
power=13.666 burn=381.7 down=81.3 bfrac=1.419 end
power=13.709 burn=466.0 down=2447 bfrac=1.532 end
o 119 cr 5.2 mn 0.29
fe 11. co 0.066 ni 8.7
zr 195 nb 0.63 sn 3.2
'
'-----
end
```

Table A.9. Calvert Cliffs Assembly BT03 Rod  
NBD107, 46.46 GWd/MTU, ENDF/B-IV

```
=sas2      parm='halt04,skipshipdata'
calvert cliffs 1 pwr, bt03, rod nbd107, atm-106, 46.46gwd, b4 aug-1994
' decay time 6.7 years (or 2447 days) for measurement of
'   pnl-5109-106, page 4.64, table 4.17
'
' -----
'   mixtures of fuel-pin-unit-cell:
'
27burnuplib latticecell
uo2 1 den=10.036 1 873
   92234 0.022 92235 2.453 92236 0.011 92238 97.514 end
c 1 den=1.95-4 1 873 end
n 1 den=4.42-4 1 873 end
co-59 3 0 1-20 570 end
zr-94 1 0 1-20 873 end
|
*fission product nuclide set same as table a.4 with new temperatures*
|
gd-160 1 0 1-20 873 end
zirccalloy 2 1 620 end
h2o 3 den=0.7342 1 570 end
arbm-bormod 0.7342 1 1 0 0 5000 100 3 330.8e-6 570 end
'
' 331 ppm boron (wt) in moderator
' -----
end comp
'
' -----
'   fuel-pin-cell geometry:
'
squarepitch 1.4732 0.9639 1 3 1.1176 2 0.9855 0 end
'
' -----
'   assembly and cycle parameters:
'
npin/assm=172 fuelngth=793.88 ncycles=4 nlib/cyc=1
printlevel=5 lightel=9 inplevel=2 numztot=5 end
3 1.314 2 1.416 3 1.662 500 5.155 3 5.243
power=23.326 burn=816.0 down=81 end
power=24.350 burn=306.0 down=71 end
power=17.036 burn=381.7 down=81.3 bfrac=1.419 end
power=17.090 burn=466.0 down=2447 bfrac=1.532 end
o 119 cr 5.2 mn 0.29
fe 11. co 0.066 ni 8.7
zr 195 nb 0.63 sn 3.2
'
' -----
end
```

Table A.10. H. B. Robinson Assembly B05 Rod  
N-9, 16.02 GWd/MTU, ENDF/B-IV

```
=sas2h      parm='halt04,skipshipdata'
h.b. robinson 1 pwr case 1-s: b0-5, rod n-9, 11 cm, 16.02 gwd/mtu b4
aug-94
'
' -----
'   for burnup credit project (see exper-data of feb. 85 in atm-101)
'
' -----
'   mixtures of fuel-pin-unit-cell:
'
27burnuplib latticecell
uo2 1 den=9.944 1 743
   92234 0.023 92235 2.561 92236 0.013 92238 97.403 end
co-59 3 0 1-20 559 end
zr-94 1 0 1-20 743 end
mo-94 1 0 1-20 743 end
nb-95 1 0 1-20 743 end
mo-95 1 0 1-20 743 end
tc-99 1 0 1-20 743 end
rh-103 1 0 1-20 743 end
rh-105 1 0 1-20 743 end
ru-106 1 0 1-20 743 end
xe-131 1 0 1-20 743 end
cs-134 1 0 1-20 743 end
cs-135 1 0 1-20 743 end
cs-137 1 0 1-20 743 end
pr-143 1 0 1-20 743 end
nd-143 1 0 1-20 743 end
ce-144 1 0 1-20 743 end
nd-145 1 0 1-20 743 end
nd-146 1 0 1-20 743 end
```

Table A.10 (continued)

```
nd-147 1 0 1-20 743 end
pm-147 1 0 1-20 743 end
sm-147 1 0 1-20 743 end
nd-148 1 0 1-20 743 end
pm-149 1 0 1-20 743 end
sm-149 1 0 1-20 743 end
sm-150 1 0 1-20 743 end
sm-151 1 0 1-20 743 end
eu-151 1 0 1-20 743 end
sm-152 1 0 1-20 743 end
eu-153 1 0 1-20 743 end
eu-154 1 0 1-20 743 end
gd-154 1 0 1-20 743 end
eu-155 1 0 1-20 743 end
gd-155 1 0 1-20 743 end
gd-157 1 0 1-20 743 end
gd-158 1 0 1-20 743 end
gd-160 1 0 1-20 743 end
'
' need the following to use endf/b5 library:
'   from st5: (2nd line same as def. of zirccalloy in sect. m8,
'   scale-4.1)
'   arbmzirc 6.5 4 0 0 1 40000 97.91 26000 0.5 50118 0.64 50120 0.95
'   2 1 end
'   arbmzirc 6.44 4 0 0 1 40000 97.91 26000 0.5 50118 0.64 50120 0.95 2 1
'   595 end
zirccalloy 2 1 595 end
h2o 3 den=0.7544 1 559 end
arbm-bormod 0.7544 1 1 0 0 5000 100 3 652.5e-6 559 end
'
' 652.5 ppm boron (wt) in moderator
' -----
'   input materials for the burnable poison coupled assembly:
'
ss304 5 1 559 end
o 6 0 0.04497 559 end
na 6 0 0.00165 559 end
al 6 0 0.00058 559 end
si 6 0 0.01799 559 end
k 6 0 0.00011 559 end
b-10 6 0 9.595-4 559 end
b-11 6 0 3.863-3 559 end
n 4 0 5-5 559 end
end comp
'
' -----
'   fuel-pin-cell geometry:
'
squarepitch 1.4300 0.9294 1 3 1.0719 2 0.9484 0 end
'
' -----
'   assembly and cycle parameters:
'
npin/assm=204 fuelngth=726.63 ncycles=4 nlib/cyc=1
printlevel=5 lightel=9 inplevel=2 numztot=10 mxrepeats=0 end
' the 10 larger unit cell zones follow for 2 passes bp, 2 passes h2o
'
4 0.21457 5 0.22705 4 0.23329 6 0.38017 4 0.38449 5 0.42145
3 0.65024 2 0.69342 3 0.80680 500 2.64088
4 0.21457 5 0.22705 4 0.23329 6 0.38017 4 0.38449 5 0.42145
3 0.65024 2 0.69342 3 0.80680 500 2.64088
3 0.21457 3 0.22705 3 0.23329 3 0.38017 3 0.38449 3 0.42145
3 0.65024 2 0.69342 3 0.80680 500 2.64088
3 0.21457 3 0.22705 3 0.23329 3 0.38017 3 0.38449 3 0.42145
3 0.65024 2 0.69342 3 0.80680 500 2.64088
'
power=18.389 burn=243.5 down=40 end
power=17.762 burn=243.5 down=64 bfrac=0.379 end
power=17.247 burn=156 down=39 bfrac=1.0 end
power=16.846 burn=156 down=3936 bfrac=0.379 end
o 119 cr 5.2 mn 0.29
fe 11. co 0.066 ni 8.7
zr 195 nb 0.63 sn 3.2
'
' the above light elements converted to kg per mtuo2...
'
' -----
end
```

Table A.11. H. B. Robinson Assembly B05 Rod N-9, 23.81 GWd/MTU, ENDF/B-IV

```

=sas2h parm='halt04,skipshipdata'
h.b. robinson 1 pwr case 1-n: b0-5, rod n-9, 26 cm, 23.81 gwd/mtu b4 augt-94
'
'-----
' for burnup credit project (see exper-data of feb. 85 in atm-101)
'-----
'
' mixtures of fuel-pin-unit-cell:
'
27burnuplib latticecell
uo2 1 den=9.944 1 830
      92234 0.023 92235 2.561 92236 0.013 92238 97.403 end
co-59 3 0 1-20 559 end
zr-94 1 0 1-20 830 end
'
' fission product nuclide set same as table a.10 with new temperatures*
'
gd-160 1 0 1-20 830 end
' need the following to use endf/b5 library:
' from st5: (2nd line same as def. of zircalloy in sect. m8, scale-4.1)
' arbmzirc 6.5 4 0 0 1 40000 97.91 26000 0.5 50118 0.64 50120 0.95 2 1 end
' arbmzirc 6.44 4 0 0 1 40000 97.91 26000 0.5 50118 0.64 50120 0.95 2 1 595 end
zircalloy 2 1 595 end
h2o 3 den=0.7538 1 559 end
arbm-bormod 0.7538 1 1 0 0 5000 100 3 652.5e-6 559 end
'
' 652.5 ppm boron (wt) in moderator
'-----
' input materials for the burnable poison coupled assembly:
'
ss304 5 1 559 end
o 6 0 0.04497 559 end
na 6 0 0.00165 559 end
al 6 0 0.00058 559 end
si 6 0 0.01799 559 end
k 6 0 0.00011 559 end
b-10 6 0 9.595-4 559 end
b-11 6 0 3.863-3 559 end
n 4 0 5-5 559 end
'
end comp
'
'-----
' fuel-pin-cell geometry:
'
squarepitch 1.4300 0.9294 1 3 1.0719 2 0.9484 0 end
'
'-----
' assembly and cycle parameters:
'
npin/assm=204 fuelnght=726.63 ncycles=4 nlib/cyc=1
printlevel=5 lightel=9 inplevel=2 numztotal=10 mxrepeats=0 end
' the 10 larger unit cell zones follow for 2 passes bp, 2 passes h2o :
4 0.21457 5 0.22705 4 0.23329 6 0.38017 4 0.38449 5 0.42145
3 0.65024 2 0.69342 3 0.80680 500 2.64088
4 0.21457 5 0.22705 4 0.23329 6 0.38017 4 0.38449 5 0.42145
3 0.65024 2 0.69342 3 0.80680 500 2.64088
3 0.21457 3 0.22705 3 0.23329 3 0.38017 3 0.38449 3 0.42145
3 0.65024 2 0.69342 3 0.80680 500 2.64088
3 0.21457 3 0.22705 3 0.23329 3 0.38017 3 0.38449 3 0.42145
3 0.65024 2 0.69342 3 0.80680 500 2.64088
'
power=28.410 burn=243.5 down=40 end
power=26.532 burn=243.5 down=64 bfrac=0.379 end
power=24.991 burn=156 down=39 bfrac=1.0 end
'
power=23.788 burn=156 down=3936 bfrac=0.379 end
o 119 cr 5.2 mn 0.29
'
fe 11. co 0.066 ni 8.7
'
zr 195 nb 0.63 sn 3.2
'
' the above light elements converted to kg per mtuo2...
'
'-----
end

```

Table A.12. H. B. Robinson Assembly B05 Rod N-9, 28.47 GWd/MTU, ENDF/B-IV

```

=sas2h parm='halt04,skipshipdata'
h.b. robinson 1 pwr case 1-j: b0-5, rod n-9, 199 cm, 28.47gwd/mtu b4
augt-94
'
'-----
' for burnup credit project (see exper-data of april 84 in atm-101)
'-----
'
' mixtures of fuel-pin-unit-cell:
'
27burnuplib latticecell
uo2 1 den=9.944 1 883
      92234 0.023 92235 2.561 92236 0.013 92238 97.403 end
co-59 3 0 1-20 576 end
zr-94 1 0 1-20 883 end
'
' fission product nuclide set same as table a.10 with new temperatures*
'
gd-160 1 0 1-20 883 end
' need the following to use endf/b5 library:
' from st5: (2nd line same as def. of zircalloy in sect. m8, scale-4.1)
' arbmzirc 6.5 4 0 0 1 40000 97.91 26000 0.5 50118 0.64 50120 0.95 2 1 end
' arbmzirc 6.44 4 0 0 1 40000 97.91 26000 0.5 50118 0.64 50120 0.95 2 1 595 end
zircalloy 2 1 595 end
h2o 3 den=0.7208 1 576 end
arbm-bormod 0.7208 1 1 0 0 5000 100 3 652.5e-6 576 end
'
' 652.5 ppm boron (wt) in moderator
'-----
' input materials for the burnable poison coupled assembly:
'
ss304 5 1 576 end
o 6 0 0.04497 576 end
na 6 0 0.00165 576 end
al 6 0 0.00058 576 end
si 6 0 0.01799 576 end
k 6 0 0.00011 576 end
b-10 6 0 9.595-4 576 end
b-11 6 0 3.863-3 576 end
n 4 0 5-5 576 end
'
end comp
'
'-----
' fuel-pin-cell geometry:
'
squarepitch 1.4300 0.9294 1 3 1.0719 2 0.9484 0 end
'
'-----
' assembly and cycle parameters:
'
npin/assm=204 fuelnght=726.63 ncycles=4 nlib/cyc=1
printlevel=5 lightel=9 inplevel=2 numztotal=10 mxrepeats=0 end
' the 10 larger unit cell zones follow for 2 passes bp, 2 passes h2o :
4 0.21457 5 0.22705 4 0.23329 6 0.38017 4 0.38449 5 0.42145
3 0.65024 2 0.69342 3 0.80680 500 2.64088
4 0.21457 5 0.22705 4 0.23329 6 0.38017 4 0.38449 5 0.42145
3 0.65024 2 0.69342 3 0.80680 500 2.64088
3 0.21457 3 0.22705 3 0.23329 3 0.38017 3 0.38449 3 0.42145
3 0.65024 2 0.69342 3 0.80680 500 2.64088
3 0.21457 3 0.22705 3 0.23329 3 0.38017 3 0.38449 3 0.42145
3 0.65024 2 0.69342 3 0.80680 500 2.64088
'
power=34.817 burn=243.5 down=40 end
power=31.829 burn=243.5 down=64 bfrac=0.379 end
power=29.378 burn=156 down=39 bfrac=1.0 end
power=27.464 burn=156 down=3631 bfrac=0.379 end
o 119 cr 5.2 mn 0.29
fe 11. co 0.066 ni 8.7
zr 195 nb 0.63 sn 3.2
'
' the above light elements converted to kg per mtuo2...
'
'-----
end

```

Table A.13. H. B. Robinson Assembly B05  
Rod N-9, 31.66 GWd/MTU, ENDF/B-IV

```
=sas2h      parm='halt04,skipshipdata'
h.b. robinson 1 pwr case 1-d: b0-5, rod n-9, 226 cm, 31.66gwd/mtu b4 augt-94
'
'-----
' for burnup credit project (see exper-data of april 84 in atm-101)
'-----
'
' mixtures of fuel-pin-unit-cell:
'
27burnuplib latticecell
uo2 1 den=9.944 1 923
      92234 0.023 92235 2.561 92236 0.013 92238 97.403 end
co-59 3 0 1-20 579 end
zr-94 1 0 1-20 923 end
'
' *fission product nuclide set same as table a.10 with new temperatures*
'
gd-160 1 0 1-20 923 end
' need the following to use endf/b5 library:
' from st5: (2nd line same as def. of zircalloy in sect. m8, scale=4.1)
' arbmzirc 6.5 4 0 0 1 40000 97.91 26000 0.5 50118 0.64 50120 0.95 2 1 end
' arbmzirc 6.44 4 0 0 1 40000 97.91 26000 0.5 50118 0.64 50120 0.95 2 1 595 end
zircalloy 2 1 595 end
h2o 3 den=0.7135 1 579 end
arbm-bormod 0.7135 1 1 0 0 5000 100 3 652.5e-6 579 end
'
' 652.5 ppm boron (wt) in moderator
'-----
' input materials for the burnable poison coupled assembly:
'
ss304 5 1 579 end
o 6 0 0.04497 579 end
na 6 0 0.00165 579 end
al 6 0 0.00058 579 end
si 6 0 0.01799 579 end
k 6 0 0.00011 579 end
b-10 6 0 9.595-4 579 end
b-11 6 0 3.863-3 579 end
n 4 0 5-5 579 end
'
end comp
'
'-----
' fuel-pin-cell geometry:
'
squarepitch 1.4300 0.9294 1 3 1.0719 2 0.9484 0 end
'
'-----
' assembly and cycle parameters:
'
npin/assm=204 fuelnght=726.63 ncycles=4 nlib/cyc=1
printlevel=5 lightel=9 inplevel=2 numztotal=10 mxrepeats=0 end
' the 10 larger unit cell zones follow for 2 passes bp, 2 passes h2o :
4 0.21457 5 0.22705 4 0.23329 6 0.38017 4 0.38449 5 0.42145
3 0.65024 2 0.69342 3 0.80680 500 2.64088
4 0.21457 5 0.22705 4 0.23329 6 0.38017 4 0.38449 5 0.42145
3 0.65024 2 0.69342 3 0.80680 500 2.64088
3 0.21457 3 0.22705 3 0.23329 3 0.38017 3 0.38449 3 0.42145
3 0.65024 2 0.69342 3 0.80680 500 2.64088
3 0.21457 3 0.22705 3 0.23329 3 0.38017 3 0.38449 3 0.42145
3 0.65024 2 0.69342 3 0.80680 500 2.64088
'
power=39.382 burn=243.5 down=40 end
power=35.477 burn=243.5 down=64 bfrac=0.379 end
power=32.274 burn=156 down=39 bfrac=1.0 end
'
power=29.772 burn=156 down=3631 bfrac=0.379 end
o 119 cr 5.2 mn 0.29
fe 11. co 0.066 ni 8.7
zr 195 nb 0.63 sn 3.2
'
' the above light elements converted to kg per mtuo2...
'-----
end
```

Table A.14. Obrigheim (KWO) Assembly 170  
Batch 94, 25.93 GWd/MTU, ENDF/B-IV

```
=sas2      parm='halt03,skipshipdata'
obrigheim (kwo) pwr, assm 170, batch 94, 25.93 gwd/mtu 3-cyc endf/b4
aug-94
'
'-----
' .....used 180 fuel rode, 16 guide tubes....
'-----
'
' mixtures of fuel-pin-unit-cell:
'
27burnuplib latticecell
uo2 1 den=9.742 1 846
      92234 0.028 92235 3.13 92236 0.014 92238 96.828 end
co-59 3 0 1-20 572 end
kr-83 1 0 1-20 846 end
kr-84 1 0 1-20 846 end
kr-85 1 0 1-20 846 end
kr-86 1 0 1-20 846 end
zr-94 1 0 1-20 846 end
mo-94 1 0 1-20 846 end
nb-95 1 0 1-20 846 end
mo-95 1 0 1-20 846 end
tc-99 1 0 1-20 846 end
rh-103 1 0 1-20 846 end
rh-105 1 0 1-20 846 end
ru-106 1 0 1-20 846 end
sn-126 1 0 1-20 846 end
xe-131 1 0 1-20 846 end
xe-132 1 0 1-20 846 end
xe-134 1 0 1-20 846 end
cs-134 1 0 1-20 846 end
cs-135 1 0 1-20 846 end
xe-136 1 0 1-20 846 end
cs-137 1 0 1-20 846 end
pr-143 1 0 1-20 846 end
nd-143 1 0 1-20 846 end
ce-144 1 0 1-20 846 end
nd-145 1 0 1-20 846 end
nd-146 1 0 1-20 846 end
nd-147 1 0 1-20 846 end
pm-147 1 0 1-20 846 end
sm-147 1 0 1-20 846 end
nd-148 1 0 1-20 846 end
pm-149 1 0 1-20 846 end
sm-149 1 0 1-20 846 end
sm-150 1 0 1-20 846 end
sm-151 1 0 1-20 846 end
eu-151 1 0 1-20 846 end
sm-152 1 0 1-20 846 end
eu-153 1 0 1-20 846 end
eu-154 1 0 1-20 846 end
gd-154 1 0 1-20 846 end
eu-155 1 0 1-20 846 end
gd-155 1 0 1-20 846 end
gd-157 1 0 1-20 846 end
gd-158 1 0 1-20 846 end
gd-160 1 0 1-20 846 end
zircalloy 2 1 605 end
h2o 3 den=0.7283 1 572 end
arbm-bormod 0.7283 1 1 0 0 5000 100 3 450.0e-6 572 end
'
' 450 ppm boron (wt) in moderator
'-----
end comp
'
'-----
' fuel-pin-cell geometry:
'
squarepitch 1.43 0.925 1 3 1.071 2 0.930 0 end
'
'-----
' assembly and cycle parameters:
'
npin/assm=180 fuelnght=962.75 ncycles=3 nlib/cyc=1
printlevel=4 lightel=9 inplevel=1 asmpitch=20.12 numins=0
ortube=0.6845 srtube=0.6413 end
power=20.929 burn=288.0 down=81 end
power=37.468 burn=309.0 down=396 end
power=33.564 burn=248.0 down=913.1 end
o 135 cr 5.9 mn 0.33
fe 13 co 0.075 ni 9.9
zr 221 nb 0.71 sn 3.6
'
'-----
end
```

Table A.15. Obrigheim (KWO) Assembly 172  
Batch 92, 26.54 GWd/MTU, ENDF/B-IV

```
=sas2      parm='halt03,skipshipdata'

obrigheim (kwo) pwr, assm 172, batch 92, 26.54 gwd/mtu 3-cyc endf/b4 aug-94
'
'   ....used 180 fuel rode, 16 guide tubes....
'
'-----
'
'   mixtures of fuel-pin-unit-cell:
'
27burnuplib  latticecell
uo2 1 den=9.742 1 841
    92234 0.028 92235 3.13 92236 0.014 92238 96.828  end
co-59 3 0 1-20 572  end
kr-83 1 0 1-20 841  end
'
'   *fission product nuclide set same as table a.14 with new temperatures*
'
gd-160 1 0 1-20 841  end
zircalloy 2 1 605  end
h2o 3 den=0.7283 1 572  end
arbm-bormod 0.7283 1 1 0 0 5000 100 3 450.0e-6 572  end
'
'   450 ppm boron (wt) in moderator
'
'-----
end comp
'
'-----
'
'   fuel-pin-cell geometry:
'
squarepitch 1.43 0.925 1 3 1.071 2 0.930 0 end
'
'-----
'
'   assembly and cycle parameters:
'
npin/assm=180 fuelnght=962.75 ncycles=3 nlib/cyc=1
printlevel=4 lightel=9 inplevel=1 asmpitch=20.12 numins=0
ortube=0.6845 srtube=0.6413  end
power=34.833 burn=288.0 down=81  end
power=25.035 burn=309.0 down=396  end
power=35.374 burn=248.0 down=913.1  end
  o 135 cr 5.9 mn 0.33
  fe 13 co 0.075 ni 9.9
  zr 221 nb 0.71 sn 3.6
'
'-----
end
```

Table A.16. Obrigheim (KWO) Assembly 176  
Batch 91, 27.99 GWd/MTU, ENDF/B-IV

```
=sas2      parm='halt03,skipshipdata'

obrigheim (kwo) pwr, assm 176, batch 91, 27.99 gwd/mtu 3-cyc endf/b4
aug-94
'
'   ....used 180 fuel rode, 16 guide tubes....
'
'-----
'
'   mixtures of fuel-pin-unit-cell:
'
27burnuplib  latticecell
uo2 1 den=9.742 1 849
    92234 0.028 92235 3.13 92236 0.014 92238 96.828  end
co-59 3 0 1-20 572  end
kr-83 1 0 1-20 849  end
'
'   *fission product nuclide set same as table a.14 with new temperatures*
'
gd-160 1 0 1-20 846  end
zircalloy 2 1 605  end
h2o 3 den=0.7283 1 572  end
arbm-bormod 0.7283 1 1 0 0 5000 100 3 450.0e-6 572  end
'
'   450 ppm boron (wt) in moderator
'
'-----
end comp
'
'-----
'
'   fuel-pin-cell geometry:
'
squarepitch 1.43 0.925 1 3 1.071 2 0.930 0 end
'
'-----
'
'   assembly and cycle parameters:
'
npin/assm=180 fuelnght=962.75 ncycles=3 nlib/cyc=1
printlevel=4 lightel=9 inplevel=1 asmpitch=20.12 numins=0
ortube=0.6845 srtube=0.6413  end
power=30.457 burn=288.0 down=81  end
power=34.894 burn=309.0 down=396  end
power=34.016 burn=248.0 down=913.1  end
  o 135 cr 5.9 mn 0.33
  fe 13 co 0.075 ni 9.9
  zr 221 nb 0.71 sn 3.6
'
'-----
end
```

Table A.17. Obrigheim (KWO) Assembly 168  
Batch 86, 28.40 GWd/MTU, ENDF/B-IV

```
=sas2      parm='halt03,skipshipdata'
obrigheim (kwo) pwr, assm 168, batch 86, 28.40 gwd/mtu 3-cyc endf/b4 aug-94
'      ....used 180 fuel rode, 16 guide tubes...., t-fuel=859k
'
'-----
'      mixtures of fuel-pin-unit-cell:
'
27burnuplib latticecell
uo2 1 den=9.742 1 859
    92234 0.028 92235 3.13 92236 0.014 92238 96.828 end
co-59 3 0 1-20 572 end
kr-83 1 0 1-20 859 end
'
'      *fission product nuclide set same as table a.14 with new temperatures*
'
gd-160 1 0 1-20 859 end
zircalloy 2 1 605 end
h2o 3 den=0.7283 1 572 end
arbm-bormod 0.7283 1 1 0 0 5000 100 3 450.0e-6 572 end
'
'      450 ppm boron (wt) in moderator
'-----
end comp
'
'-----
'      fuel-pin-cell geometry:
'
squarepitch 1.43 0.925 1 3 1.071 2 0.930 0 end
'
'-----
'      assembly and cycle parameters:
'
npin/assm=180 fuelnght=962.75 ncycles=3 nlib/cyc=1
printlevel=4 lightel=9 inplevel=1 asmpitch=20.12 numins=0
ortube=0.6845 srtube=0.6413 end
power=28.336 burn=288.0 down=81 end
power=38.005 burn=309.0 down=396 end
power=34.249 burn=248.0 down=913.1 end
o 135 cr 5.9 mn 0.33
fe 13 co 0.075 ni 9.9
zr 221 nb 0.71 sn 3.6
'
'-----
end
```

Table A.18. Obrigheim (KWO) Assembly 171  
Batch 89, 29.04 GWd/MTU, ENDF/B-IV

```
=sas2      parm='halt03,skipshipdata'
obrigheim (kwo) pwr, assm 171, batch 89, 29.04 gwd/mtu 3-cyc endf/b4
aug-94
'      ....used 180 fuel rode, 16 guide tubes....
'
'-----
'      mixtures of fuel-pin-unit-cell:
'
27burnuplib latticecell
uo2 1 den=9.742 1 867
    92234 0.028 92235 3.13 92236 0.014 92238 96.828 end
co-59 3 0 1-20 572 end
kr-83 1 0 1-20 867 end
'
'      *fission product nuclide set same as table a.14 with new temperatures*
'
gd-160 1 0 1-20 867 end
zircalloy 2 1 605 end
h2o 3 den=0.7283 1 572 end
arbm-bormod 0.7283 1 1 0 0 5000 100 3 450.0e-6 572 end
'
'      450 ppm boron (wt) in moderator
'-----
end comp
'
'-----
'      fuel-pin-cell geometry:
'
squarepitch 1.43 0.925 1 3 1.071 2 0.930 0 end
'
'-----
'      assembly and cycle parameters:
'
npin/assm=180 fuelnght=962.75 ncycles=3 nlib/cyc=1
printlevel=4 lightel=9 inplevel=1 asmpitch=20.12 numins=0
ortube=0.6845 srtube=0.6413 end
power=29.124 burn=288.0 down=81 end
power=38.952 burn=309.0 down=396 end
power=34.748 burn=248.0 down=913.1 end
o 135 cr 5.9 mn 0.33
fe 13 co 0.075 ni 9.9
zr 221 nb 0.71 sn 3.6
'
'-----
end
```

Table A.19. Obrigheim (KWO) Assembly 176  
Batch 90, 29.52 GWd/MTU, ENDF/B-IV

```
=sas2      parm='halt03,skipshipdata'
obrigheim (kwo) pwr, assm 176, batch 90, 29.52 gwd/mtu 3-cyc endf/b4 aug-94
'
' .....used 180 fuel rode, 16 guide tubes....
'
' -----
'
'   mixtures of fuel-pin-unit-cell:
'
27burnuplib latticecell
uo2 1 den=9.742 1 867
    92234 0.028 92235 3.13 92236 0.014 92238 96.828 end
co-59 3 0 1-20 572 end
kr-83 1 0 1-20 867 end
'
' *fission product nuclide set same as table a.14 with new temperatures*
'
gd-160 1 0 1-20 867 end
zircalloy 2 1 605 end
h2o 3 den=0.7283 1 572 end
arbm-bormod 0.7283 1 1 0 0 5000 100 3 450.0e-6 572 end
'
'   450 ppm boron (wt) in moderator
'
' -----
'
end comp
'
' -----
'
'   fuel-pin-cell geometry:
'
squarepitch 1.43 0.925 1 3 1.071 2 0.930 0 end
'
' -----
'
'   assembly and cycle parameters:
'
npin/assm=180 fuelnght=962.75 ncycles=3 nlib/cyc=1
printlevel=4 lightel=9 inplevel=1 asmpitch=20.12 numins=0
ortube=0.6845 srtube=0.6413 end
power=32.121 burn=288.0 down=81 end
power=36.801 burn=309.0 down=396 end
power=35.875 burn=248.0 down=913.1 end
o 135 cr 5.9 mn 0.33
fe 13 co 0.075 ni 9.9
zr 221 nb 0.71 sn 3.6
'
' -----
'
end
```

Table A.20. Calvert Cliffs Assembly D047  
Rod MKP109, 27.35 GWd/MTU, ENDF/B-V

```
=sas2      parm='halt04,skipshipdata'
calvert cliffs 1 pwr, d047, rod mkp109, atm-104, 27.35gwd/mtu eu6 aug-94
'
' cooled 1870 d
'
' -----
'
'   mixtures of fuel-pin-unit-cell:
'
27burnuplib latticecell
uo2 1 den=10.045 1 790
    92234 0.027 92235 3.038 92236 0.014 92238 96.921 end
c 1 den=1.8-4 1 790 end
n 1 den=2.3-4 1 790 end
co-59 3 0 1-20 557 end
zr-94 1 0 1-20 790 end
mo-94 1 0 1-20 790 end
nb-95 1 0 1-20 790 end
mo-95 1 0 1-20 790 end
tc-99 1 0 1-20 790 end
rh-103 1 0 1-20 790 end
rh-105 1 0 1-20 790 end
ru-106 1 0 1-20 790 end
sn-126 1 0 1-20 790 end
xe-131 1 0 1-20 790 end
cs-134 1 0 1-20 790 end
cs-135 1 0 1-20 790 end
cs-137 1 0 1-20 790 end
pr-143 1 0 1-20 790 end
nd-143 1 0 1-20 790 end
ce-144 1 0 1-20 790 end
nd-144 1 0 1-20 790 end
nd-145 1 0 1-20 790 end
nd-146 1 0 1-20 790 end
nd-147 1 0 1-20 790 end
pm-147 1 0 1-20 790 end
sm-147 1 0 1-20 790 end
nd-148 1 0 1-20 790 end
pm-148 1 0 1-20 790 end
sm-148 1 0 1-20 790 end
pm-149 1 0 1-20 790 end
sm-149 1 0 1-20 790 end
nd-150 1 0 1-20 790 end
sm-150 1 0 1-20 790 end
sm-151 1 0 1-20 790 end
eu-151 1 0 1-20 790 end
sm-152 1 0 1-20 790 end
eu-153 1 0 1-20 790 end
eu-154 1 0 1-20 790 end
gd-154 1 0 1-20 790 end
eu-155 1 0 1-20 790 end
gd-155 1 0 1-20 790 end
gd-157 1 0 1-20 790 end
gd-158 1 0 1-20 790 end
gd-160 1 0 1-20 790 end
'
' need the following to use endf/b5 library:
arbmzirc 6.44 4 0 0 1 40000 97.91 26000 0.5 50116 0.86 50120 0.73 2 1 620
end
h2o 3 den=0.7575 1 557 end
arbm-bormod 0.7575 1 1 0 0 5000 100 3 330.8e-6 557 end
'
'   331 ppm boron (wt) in moderator
'
' -----
'
end comp
'
' -----
'
'   fuel-pin-cell geometry:
'
squarepitch 1.4732 0.9563 1 3 1.1176 2 0.9855 0 end
'
' -----
'
'   assembly and cycle parameters:
'
npin/assm=176 fuelnght=787.52 ncycles=4 nlib/cyc=1
printlevel=4 lightel=9 inplevel=2 numtotal=5 end
3 1.314 2 1.416 3 1.662 500 5.203 3 5.243
power=15.197 burn=306.0 down=71 end
power=17.124 burn=381.7 down=81.3 bfrac=1.419 end
power=15.018 burn=466.0 down=85 bfrac=1.523 end
power=12.843 burn=461.1 down=1870 bfrac=1.488 end
o 119 cr 5.2 mn 0.29
fe 11. co 0.066 ni 8.7
zr 195 nb 0.63 sn 3.2
'
' -----
'
end
```

Table A.21. Calvert Cliffs Assembly D047  
Rod MKP109, 37.12 GWd/MTU, ENDF/B-V

```
=sas2      parm='halt04,skipshipdata'
calvert cliffs 1 pwr, d047, rod mkp109, atm-104, 37.12gwd/mtu eu6 aug-94
' cooled 1870 d
'
' -----
'
' mixtures of fuel-pin-unit-cell:
'
27burnuplib latticecell
uo2 1 den=10.045 1 841
   92234 0.027 92235 3.038 92236 0.014 92238 96.921 end
c 1 den=1.8-4 1 841 end
n 1 den=2.3-4 1 841 end
co-59 3 0 1-20 558 end
zr-94 1 0 1-20 841 end
'
' |
' *fission product nuclide set same as table a.20 with new temperatures*
'
gd-160 1 0 1-20 841 end
' need the following to use endf/b5 library:
arbmzirc 6.44 4 0 0 1 40000 97.91 26000 0.5 50116 0.86 50120 0.73 2 1 620 end
h2o 3 den=0.7569 1 558 end
arbm-bormod 0.7569 1 1 0 0 5000 100 3 330.8e-6 558 end
'
' |
' 331 ppm boron (wt) in moderator
'
' -----
'
end comp
'
' -----
'
' fuel-pin-cell geometry:
'
squarepitch 1.4732 0.9563 1 3 1.1176 2 0.9855 0 end
'
' -----
'
' assembly and cycle parameters:
'
npin/assm=176 fuelnght=787.52 ncycles=4 nlib/cyc=1
printlevel=4 lightel=9 inplevel=2 numztot=5 end
3 1.314 2 1.416 3 1.662 500 5.203 3 5.243
power=21.789 burn=306.0 down=71 end
power=23.583 burn=381.7 down=81.3 bfrac=1.419 end
power=20.133 burn=466.0 down=85 bfrac=1.523 end
power=16.630 burn=461.1 down=1870 bfrac=1.488 end
o 119 cr 5.2 mn 0.29
fe 11. co 0.066 ni 8.7
zr 195 nb 0.63 sn 3.2
'
' -----
'
end
```

Table A.22. Calvert Cliffs Assembly D047  
Rod MKP109, 44.34 GWd/MTU, ENDF/B-V

```
=sas2      parm='halt04,skipshipdata'
calvert cliffs 1 pwr, d047, rod mkp109, atm-104, 44.34gwd/mtu eu6 aug-94
' cooled 1870 d
'
' -----
'
' mixtures of fuel-pin-unit-cell:
'
27burnuplib latticecell
uo2 1 den=10.045 1 873
   92234 0.027 92235 3.038 92236 0.014 92238 96.921 end
c 1 den=1.8-4 1 873 end
n 1 den=2.3-4 1 873 end
co-59 3 0 1-20 570 end
zr-94 1 0 1-20 873 end
'
' |
' *fission product nuclide set same as table a.20 with new temperatures*
'
gd-160 1 0 1-20 873 end
' need the following to use endf/b5 library:
arbmzirc 6.44 4 0 0 1 40000 97.91 26000 0.5 50116 0.86 50120 0.73 2 1 620 end
h2o 3 den=0.7332 1 570 end
arbm-bormod 0.7332 1 1 0 0 5000 100 3 330.8e-6 570 end
'
' |
' 331 ppm boron (wt) in moderator
'
' -----
'
end comp
'
' -----
'
' fuel-pin-cell geometry:
'
squarepitch 1.4732 0.9563 1 3 1.1176 2 0.9855 0 end
'
' -----
'
' assembly and cycle parameters:
'
npin/assm=176 fuelnght=787.52 ncycles=4 nlib/cyc=1
printlevel=4 lightel=9 inplevel=2 numztot=5 end
3 1.314 2 1.416 3 1.662 500 5.203 3 5.243
power=27.432 burn=306.0 down=71 end
power=28.654 burn=381.7 down=81.3 bfrac=1.419 end
power=23.094 burn=466.0 down=85 bfrac=1.523 end
power=19.499 burn=461.1 down=1870 bfrac=1.488 end
o 119 cr 5.2 mn 0.29
fe 11. co 0.066 ni 8.7
zr 195 nb 0.63 sn 3.2
'
' -----
'
end
```



Table A.23. Calvert Cliffs Assembly D101  
Rod MLA098, 18.68 GWd/MTU, ENDF/B-V

```
=sas2      parm='halt03,skipshipdata'
calvert cliffs 1 pwr, d101, rod mla098, atm-103 18.68gwd/mtu eu6 aug-94
'
'      8.90 cm sample pellet -- assy #2
'
'-----
'
'      mixtures of fuel-pin-unit-cell:
'
27burnuplib latticecell
uo2 1 den=10.045 1 816
'      92234 0.024 92235 2.72 92236 0.016 92238 97.24 end
c 1 den=1.2-4 1 816 end
n 1 den=2.4-4 1 816 end
co-59 3 0 1-20 557 end
zr-94 1 0 1-20 816 end
mo-94 1 0 1-20 816 end
nb-95 1 0 1-20 816 end
mo-95 1 0 1-20 816 end
tc-99 1 0 1-20 816 end
rh-103 1 0 1-20 816 end
rh-105 1 0 1-20 816 end
ru-106 1 0 1-20 816 end
sn-126 1 0 1-20 816 end
xe-131 1 0 1-20 816 end
cs-134 1 0 1-20 816 end
cs-135 1 0 1-20 816 end
cs-137 1 0 1-20 816 end
pr-143 1 0 1-20 816 end
nd-143 1 0 1-20 816 end
ce-144 1 0 1-20 816 end
nd-145 1 0 1-20 816 end
nd-146 1 0 1-20 816 end
nd-147 1 0 1-20 816 end
pm-147 1 0 1-20 816 end
sm-147 1 0 1-20 816 end
nd-148 1 0 1-20 816 end
pm-149 1 0 1-20 816 end
sm-149 1 0 1-20 816 end
sm-150 1 0 1-20 816 end
sm-151 1 0 1-20 816 end
eu-151 1 0 1-20 816 end
sm-152 1 0 1-20 816 end
eu-153 1 0 1-20 816 end
eu-154 1 0 1-20 816 end
gd-154 1 0 1-20 816 end
eu-155 1 0 1-20 816 end
gd-155 1 0 1-20 816 end
gd-157 1 0 1-20 816 end
gd-158 1 0 1-20 816 end
gd-160 1 0 1-20 816 end
'      need the following to use endf/b5 library:
arbmzirc 6.44 4 0 0 1 40000 97.91 26000 0.5 50116 0.86 50120 0.73 2 1 620 end
h2o 3 den=0.7576 1 557 end
arbm-bormod 0.7576 1 1 0 0 5000 100 3 330.8e-6 557 end
'
'      331 ppm boron (wt) in moderator
'
'-----
end comp
'
'-----
'
'      fuel-pin-cell geometry:
'
squarepitch 1.4732 0.9563 1 3 1.1176 2 0.9855 0 end
'
'-----
'
'      assembly and cycle parameters:
'
npin/assm=176 fuelnght=787.52 ncycles=3 nlib/cyc=1
printlevel=4 lightel=9 inplevel=2 numztot=5 end
3 1.314 2 1.416 3 1.662 500 5.203 3 5.243
power=13.760 burn=306.0 down=71 end
power=15.504 burn=381.7 down=81.3 bfrac=1.419 end
power=13.598 burn=466.0 down=2374 bfrac=1.523 end
o 119 cr 5.2 mn 0.29
fe 11. co 0.066 ni 8.7
zr 195 nb 0.63 sn 3.2
'
'-----
end
```

Table A.24. Calvert Cliffs Assembly D101  
Rod MLA098, 26.62 GWd/MTU, ENDF/B-V

```
=sas2      parm='halt03,skipshipdata'
calvert cliffs 1 pwr, d101, rod mla098, atm-103 26.62gwd/mtu eu6 aug-94
'
'      24.300 cm sample pellet -- assy #2
'
'-----
'
'      mixtures of fuel-pin-unit-cell:
'
27burnuplib latticecell
uo2 1 den=10.045 1 880
'      92234 0.024 92235 2.72 92236 0.016 92238 97.24 end
c 1 den=1.2-4 1 880 end
n 1 den=2.4-4 1 880 end
co-59 3 0 1-20 558 end
zr-94 1 0 1-20 880 end
'
'      *fission product nuclide set same as table a.23 with new temperatures*
'
gd-160 1 0 1-20 880 end
'      need the following to use endf/b5 library:
arbmzirc 6.44 4 0 0 1 40000 97.91 26000 0.5 50116 0.86 50120 0.73 2 1 620
end
h2o 3 den=0.7571 1 558 end
arbm-bormod 0.7571 1 1 0 0 5000 100 3 330.8e-6 558 end
'
'      331 ppm boron (wt) in moderator
'
'-----
end comp
'
'-----
'
'      fuel-pin-cell geometry:
'
squarepitch 1.4732 0.9563 1 3 1.1176 2 0.9855 0 end
'
'-----
'
'      assembly and cycle parameters:
'
npin/assm=176 fuelnght=787.52 ncycles=3 nlib/cyc=1
printlevel=4 lightel=9 inplevel=2 numztot=5 end
3 1.314 2 1.416 3 1.662 500 5.203 3 5.243
power=20.408 burn=306.0 down=71 end
power=22.089 burn=381.7 down=81.3 bfrac=1.419 end
power=18.857 burn=466.0 down=2374 bfrac=1.523 end
o 119 cr 5.2 mn 0.29
fe 11. co 0.066 ni 8.7
zr 195 nb 0.63 sn 3.2
'
'-----
end
```

Table A.25. Calvert Cliffs Assembly D101  
Rod MLA098, 33.17 GWd/MTU, ENDF/B-V

```
=sas2      parm='halt03,skipshipdata'
calvert cliffs 1 pwr, d101, rod mla098, atm-103 33.17gwd/mtu eu6 aug-94
'
' 161.70 cm sample pellet -- assy #2
'
' -----
'
' mixtures of fuel-pin-unit-cell:
'
27burnuplib latticecell
uo2 1 den=10.045 1 910
' 92234 0.024 92235 2.72 92236 0.016 92238 97.24 end
c 1 den=1.2-4 1 910 end
n 1 den=2.4-4 1 910 end
co-59 3 0 1-20 570 end
zr-94 1 0 1-20 910 end
'
' *fission product nuclide set same as table a.23 with new temperatures*
'
gd-160 1 0 1-20 910 end
' need the following to use endf/b5 library:
arbmzirc 6.44 4 0 0 1 40000 97.91 26000 0.5 50116 0.86 50120 0.73 2 1 620 end
h2o 3 den=0.7341 1 570 end
arbm-bormod 0.7341 1 1 0 0 5000 100 3 330.8e-6 570 end
'
' 331 ppm boron (wt) in moderator
'
' -----
'
' fuel-pin-cell geometry:
'
squarepitch 1.4732 0.9563 1 3 1.1176 2 0.9855 0 end
'
' -----
'
' assembly and cycle parameters:
'
npin/assm=176 fuelnght=787.52 ncycles=3 nlib/cyc=1
printlevel=4 lightel=9 inplevel=2 numztotal=5 end
3 1.314 2 1.416 3 1.662 500 5.203 3 5.243
power=26.652 burn=306.0 down=71 end
power=27.839 burn=381.7 down=81.3 bfrac=1.419 end
power=22.437 burn=466.0 down=2374 bfrac=1.523 end
o 119 cr 5.2 mn 0.29
fe 11. co 0.066 ni 8.7
zr 195 nb 0.63 sn 3.2
'
' -----
'
end
```

Table A.26. Calvert Cliffs Assembly BT03  
Rod NBD107, 31.40 GWd/MTU, ENDF/B-V

```
=sas2      parm='halt04,skipshipdata'
calvert cliffs 1 pwr, bt03, rod nbd107, atm-106, 31.40gwd/mtu, eu6 aug-94
'
' decay time 6.7 years (or 2447 days) for measurement of
' pnl-5109-106, page 4.64, table 4.17
'
' -----
'
' mixtures of fuel-pin-unit-cell:
'
27burnuplib latticecell
uo2 1 den=10.036 1 790
' 92234 0.022 92235 2.453 92236 0.011 92238 97.514 end
c 1 den=1.95-4 1 790 end
n 1 den=4.42-4 1 790 end
co-59 3 0 1-20 557 end
zr-94 1 0 1-20 790 end
'
' *fission product nuclide set same as table a.23 with new temperatures*
'
gd-160 1 0 1-20 790 end
' need the following to use endf/b5 library:
arbmzirc 6.44 4 0 0 1 40000 97.91 26000 0.5 50116 0.86 50120 0.73 2 1 620 end
h2o 3 den=0.7576 1 557 end
arbm-bormod 0.7576 1 1 0 0 5000 100 3 330.8e-6 557 end
'
' 331 ppm boron (wt) in moderator
'
' -----
'
' fuel-pin-cell geometry:
'
squarepitch 1.4732 0.9639 1 3 1.1176 2 0.9855 0 end
'
' -----
'
' assembly and cycle parameters:
'
npin/assm=172 fuelnght=793.88 ncycles=4 nlib/cyc=1
printlevel=5 lightel=9 inplevel=2 numztotal=5 end
3 1.314 2 1.416 3 1.662 500 5.156 3 5.243
power=15.765 burn=816.0 down=81 end
power=16.457 burn=306.0 down=71 end
power=11.514 burn=381.7 down=81.3 bfrac=1.419 end
power=11.550 burn=466.0 down=2447 bfrac=1.532 end
o 119 cr 5.2 mn 0.29
fe 11. co 0.066 ni 8.7
zr 195 nb 0.63 sn 3.2
'
' -----
'
end
```

Table A.27. Calvert Cliffs Assembly BT03  
Rod NBD107, 37.27 GWd/MTU, ENDF/B-V

```
=sas2      parm='halt04,skipshipdata'
calvert cliffs 1 pwr, bt03, rod nbd107, atm-106, 37.27gwd/mtu, eu6 aug-94
' decay time 6.7 years (or 2447 days) for measurement of
'   pnl-5109-106, page 4.64, table 4.17
' -----
' mixtures of fuel-pin-unit-cell:
'
27burnuplib latticecell
uo2 1 den=10.036 1 841
   92234 0.022 92235 2.453 92236 0.011 92238 97.514 end
c 1 den=1.95-4 1 841 end
n 1 den=4.42-4 1 841 end
co-59 3 0 1-20 557 end
zr-94 1 0 1-20 841 end

|
*fission product nuclide set same as table a.23 with new temperatures*
|
gd-160 1 0 1-20 841 end
' need the following to use endf/b5 library:
arbmzirc 6.44 4 0 0 1 40000 97.91 26000 0.5 50116 0.86 50120 0.73 2 1 620 end
h2o 3 den=0.7573 1 557 end
arbm-bormod 0.7573 1 1 0 0 5000 100 3 330.8e-6 557 end
'
' 331 ppm boron (wt) in moderator
' -----
end comp
'
' fuel-pin-cell geometry:
'
squarepitch 1.4732 0.9639 1 3 1.1176 2 0.9855 0 end
'
' -----
' assembly and cycle parameters:
'
npin/assm=172 fuelngth=793.88 ncycles=4 nlib/cyc=1
printlevel=5 lightel=9 inplevel=2 numztotal=5 end
3 1.314 2 1.416 3 1.662 500 5.156 3 5.243
power=18.712 burn=816.0 down=81 end
power=19.533 burn=306.0 down=71 end
power=13.666 burn=381.7 down=81.3 bfrac=1.419 end
power=13.709 burn=466.0 down=2447 bfrac=1.532 end
o 119 cr 5.2 mn 0.29
fe 11. co 0.066 ni 8.7
zr 195 nb 0.63 sn 3.2
'
' -----
end
```

Table A.28. Calvert Cliffs Assembly BT03  
Rod NBD107, 46.46 GWd/MTU, ENDF/B-V

```
=sas2      parm='halt04,skipshipdata'
calvert cliffs 1 pwr, bt03, rod nbd107, atm-106, 46.46gwd/mtu, eu6 aug-94
' decay time 6.7 years (or 2447 days) for measurement of
'   pnl-5109-106, page 4.64, table 4.17
' -----
' mixtures of fuel-pin-unit-cell:
'
27burnuplib latticecell
uo2 1 den=10.036 1 873
   92234 0.022 92235 2.453 92236 0.011 92238 97.514 end
c 1 den=1.95-4 1 873 end
n 1 den=4.42-4 1 873 end
co-59 3 0 1-20 570 end
zr-94 1 0 1-20 873 end

|
*fission product nuclide set same as table a.23 with new temperatures*
|
gd-160 1 0 1-20 873 end
' need the following to use endf/b5 library:
arbmzirc 6.44 4 0 0 1 40000 97.91 26000 0.5 50116 0.86 50120 0.73 2 1 620 end
h2o 3 den=0.7342 1 570 end
arbm-bormod 0.7342 1 1 0 0 5000 100 3 330.8e-6 570 end
'
' 331 ppm boron (wt) in moderator
' -----
end comp
'
' fuel-pin-cell geometry:
'
squarepitch 1.4732 0.9639 1 3 1.1176 2 0.9855 0 end
'
' -----
' assembly and cycle parameters:
'
npin/assm=172 fuelngth=793.88 ncycles=4 nlib/cyc=1
printlevel=5 lightel=9 inplevel=2 numztotal=5 end
3 1.314 2 1.416 3 1.662 500 5.155 3 5.243
power=23.326 burn=816.0 down=81 end
power=24.350 burn=306.0 down=71 end
power=17.036 burn=381.7 down=81.3 bfrac=1.419 end
power=17.090 burn=466.0 down=2447 bfrac=1.532 end
o 119 cr 5.2 mn 0.29
fe 11. co 0.066 ni 8.7
zr 195 nb 0.63 sn 3.2
'
' -----
end
```

Table A.29. H. B. Robinson Assembly B05  
Rod N-9, 16.02 GWd/MTU, ENDF/B-V

```

=sas2h      parm='halt04,skipshipdata'
h.b. robinson 1 pwr case 1-s: b0-5, rod n-9, 11 cm, 16.02 gwd/mtu b5 augt-94
'
' *****endf/b-v*****
'
' for burnup credit project (see exper-data of feb. 85 in atm-101)
'
'
' mixtures of fuel-pin-unit-cell:
'
27burnuplib latticecell
uo2 1 den=9.944 1 743
'
' 92234 0.023 92235 2.561 92236 0.013 92238 97.403 end
co-59 3 0 1-20 559 end
zr-94 1 0 1-20 743 end
mo-94 1 0 1-20 743 end
nb-95 1 0 1-20 743 end
mo-95 1 0 1-20 743 end
tc-99 1 0 1-20 743 end
rh-103 1 0 1-20 743 end
rh-105 1 0 1-20 743 end
ru-106 1 0 1-20 743 end
xe-131 1 0 1-20 743 end
cs-134 1 0 1-20 743 end
cs-135 1 0 1-20 743 end
cs-137 1 0 1-20 743 end
pr-143 1 0 1-20 743 end
nd-143 1 0 1-20 743 end
ce-144 1 0 1-20 743 end
nd-145 1 0 1-20 743 end
nd-146 1 0 1-20 743 end
nd-147 1 0 1-20 743 end
pm-147 1 0 1-20 743 end
sm-147 1 0 1-20 743 end
nd-148 1 0 1-20 743 end
pm-149 1 0 1-20 743 end
sm-149 1 0 1-20 743 end
sm-150 1 0 1-20 743 end
sm-151 1 0 1-20 743 end
eu-151 1 0 1-20 743 end
sm-152 1 0 1-20 743 end
eu-153 1 0 1-20 743 end
eu-154 1 0 1-20 743 end
gd-154 1 0 1-20 743 end
eu-155 1 0 1-20 743 end
gd-155 1 0 1-20 743 end
gd-157 1 0 1-20 743 end
gd-158 1 0 1-20 743 end
gd-160 1 0 1-20 743 end
'
' need the following to use endf/b5 library:
'
' from st5: (2nd line same as def. of zircalloy in sect. m8, scale-4.1)
' arbmzirc 6.5 4 0 0 1 40000 97.91 26000 0.5 50118 0.64 50120 0.95 2 1 end
' arbmzirc 6.44 4 0 0 1 40000 97.91 26000 0.5 50118 0.64 50120 0.95 2 1 595 end
' old b4 std-comp: zircalloy 2 1 595 end
h2o 3 den=0.75444 1 559 end
' arbm-bormod 0.7538 1 1 0 0 5000 100 3 652.5e-6 559 end
'
' 652.5 ppm boron (wt) in moderator
'
' input materials for the burnable poison coupled assembly:
'
ss304 5 1 559 end
o 6 0 0.04497 559 end
na 6 0 0.00165 559 end
al 6 0 0.00058 559 end
si 6 0 0.01799 559 end
k 6 0 0.00011 559 end
b-10 6 0 9.595-4 559 end
b-11 6 0 3.863-3 559 end
n 4 0 5-5 559 end
'
end comp
'
'
' fuel-pin-cell geometry:
'
squarepitch 1.4300 0.9294 1 3 1.0719 2 0.9484 0 end
'
'
' assembly and cycle parameters:
'
npin/assm=204 fuelnght=726.63 ncycles=4 nlib/cyc=1
printlevel=5 lightel=9 inplevel=2 numztotal=10 mxrepeats=0 end
' the 10 larger unit cell zones follow for 2 passes bp, 2 passes h2o :
4 0.21457 5 0.22705 4 0.23329 6 0.38017 4 0.38449 5 0.42145
3 0.65024 2 0.69342 3 0.80680 500 2.64088
4 0.21457 5 0.22705 4 0.23329 6 0.38017 4 0.38449 5 0.42145
3 0.65024 2 0.69342 3 0.80680 500 2.64088
3 0.21457 3 0.22705 3 0.23329 3 0.38017 3 0.38449 3 0.42145
3 0.65024 2 0.69342 3 0.80680 500 2.64088
3 0.21457 3 0.22705 3 0.23329 3 0.38017 3 0.38449 3 0.42145
3 0.65024 2 0.69342 3 0.80680 500 2.64088
'
power=18.389 burn=243.5 down=40 end
power=17.762 burn=243.5 down=64 bfrac=0.379 end
power=17.247 burn=156 down=39 bfrac=1.0 end
power=16.846 burn=156 down=3936 bfrac=0.379 end
'
o 119 cr 5.2 mn 0.29
'
fe 11. co 0.066 ni 8.7
'
zr 195 nb 0.63 sn 3.2
'
'
' the above light elements converted to kg per mtuo2...
'
'
'
end

```

Table A.30. H. B. Robinson Assembly B05  
Rod N-9, 23.81 GWd/MTU, ENDF/B-V

```

=sas2h      parm='halt04,skipshipdata'
h.b. robinson 1 pwr case 1-n: b0-5, rod n-9, 26 cm, 23.81 gwd/mtu b5
augt-94
'
' *****endf/b-v*****
'
' for burnup credit project (see exper-data of feb. 85 in atm-101)
'
'
' mixtures of fuel-pin-unit-cell:
'
27burnuplib latticecell
uo2 1 den=9.944 1 830
'
' 92234 0.023 92235 2.561 92236 0.013 92238 97.403 end
co-59 3 0 1-20 559 end
zr-94 1 0 1-20 830 end
'
'
' *fission product nuclide set same as table a.29 with new temperatures*
'
gd-160 1 0 1-20 830 end
'
' need the following to use endf/b5 library:
'
' from st5: (2nd line same as def. of zircalloy in sect. m8, scale-4.1)
' arbmzirc 6.5 4 0 0 1 40000 97.91 26000 0.5 50118 0.64 50120 0.95 2 1
end
' arbmzirc 6.44 4 0 0 1 40000 97.91 26000 0.5 50118 0.64 50120 0.95 2 1 595
end
'
' old b4 std-comp: zircalloy 2 1 595 end
h2o 3 den=0.7538 1 559 end
' arbm-bormod 0.7538 1 1 0 0 5000 100 3 652.5e-6 559 end
'
' 652.5 ppm boron (wt) in moderator
'
' input materials for the burnable poison coupled assembly:
'
ss304 5 1 559 end
o 6 0 0.04497 559 end
na 6 0 0.00165 559 end
al 6 0 0.00058 559 end
si 6 0 0.01799 559 end
k 6 0 0.00011 559 end
b-10 6 0 9.595-4 559 end
b-11 6 0 3.863-3 559 end
n 4 0 5-5 559 end
'
end comp
'
'
' fuel-pin-cell geometry:
'
squarepitch 1.4300 0.9294 1 3 1.0719 2 0.9484 0 end
'
'
' assembly and cycle parameters:
'
npin/assm=204 fuelnght=726.63 ncycles=4 nlib/cyc=1
printlevel=5 lightel=9 inplevel=2 numztotal=10 mxrepeats=0 end
' the 10 larger unit cell zones follow for 2 passes bp, 2 passes h2o :
4 0.21457 5 0.22705 4 0.23329 6 0.38017 4 0.38449 5 0.42145
3 0.65024 2 0.69342 3 0.80680 500 2.64088
4 0.21457 5 0.22705 4 0.23329 6 0.38017 4 0.38449 5 0.42145
3 0.65024 2 0.69342 3 0.80680 500 2.64088
3 0.21457 3 0.22705 3 0.23329 3 0.38017 3 0.38449 3 0.42145
3 0.65024 2 0.69342 3 0.80680 500 2.64088
3 0.21457 3 0.22705 3 0.23329 3 0.38017 3 0.38449 3 0.42145
3 0.65024 2 0.69342 3 0.80680 500 2.64088
'
power=28.410 burn=243.5 down=40 end
power=26.532 burn=243.5 down=64 bfrac=0.379 end
power=24.991 burn=156 down=39 bfrac=1.0 end
power=23.788 burn=156 down=3936 bfrac=0.379 end
'
o 119 cr 5.2 mn 0.29
'
fe 11. co 0.066 ni 8.7
'
zr 195 nb 0.63 sn 3.2
'
'
' the above light elements converted to kg per mtuo2...
'
'
'
end

```

Table A.31. H. B. Robinson Assembly B05  
Rod N-9, 28.47 GWd/MTU, ENDF/B-V

```

=sas2h   parm='halt04,skipshipdata'
h.b. robinson 1 pwr case 1-j: b0-5, rod n-9, 199 cm, 28.47gdw/mtu b5 augt-94
'
' *****endf/b-v*****
'
' -----
' for burnup credit project (see exper-data of april 84 in atm-101)
'
' -----
'
' mixtures of fuel-pin-unit-cell:
'
27burnuplib  latticecell
uo2 1 den=9.944 1 883
      92234 0.023 92235 2.561 92236 0.013 92238 97.403  end
co-59 3 0 1-20 576  end
zr-94 1 0 1-20 883  end
'
' *fission product nuclide set same as table a.29 with new temperatures*
'
gd-160 1 0 1-20 883  end
' need the following to use endf/b5 library:
' from st5: (2nd line same as def. of zircalloy in sect. m8, scale-4.1)
' arbmzirc 6.5 4 0 0 1 40000 97.91 26000 0.5 50118 0.64 50120 0.95 2 1  end
' arbmzirc 6.44 4 0 0 1 40000 97.91 26000 0.5 50118 0.64 50120 0.95 2 1 595  end
' old b4 std-comp: zircalloy 2 1 595  end
h2o 3 den=0.7208 1 576  end
arbm-bormod 0.7208 1 1 0 0 5000 100 3 652.5e-6 576  end
'
' 652.5 ppm boron (wt) in moderator
'
' -----
' input materials for the burnable poison coupled assembly:
'
ss304 5 1 576  end
o 6 0 0.04497 576  end
na 6 0 0.00165 576  end
al 6 0 0.00058 576  end
si 6 0 0.01799 576  end
k 6 0 0.00011 576  end
b-10 6 0 9.595-4 576  end
b-11 6 0 3.863-3 576  end
n 4 0 5-5 576  end
'
end comp
'
' -----
' fuel-pin-cell geometry:
'
squarepitch 1.4300 0.9294 1 3 1.0719 2 0.9484 0  end
'
' -----
' assembly and cycle parameters:
'
npin/assm=204 fuelnght=726.63 ncycles=4 nlib/cyc=1
printlevel=5 lightel=9 inplevel=2 numztotal=10 mxrepeats=0  end
' the 10 larger unit cell zones follow for 2 passes bp, 2 passes h2o :
4 0.21457 5 0.22705 4 0.23329 6 0.38017 4 0.38449 5 0.42145
3 0.65024 2 0.69342 3 0.80680 500 2.64088
4 0.21457 5 0.22705 4 0.23329 6 0.38017 4 0.38449 5 0.42145
3 0.65024 2 0.69342 3 0.80680 500 2.64088
3 0.21457 3 0.22705 3 0.23329 3 0.38017 3 0.38449 3 0.42145
3 0.65024 2 0.69342 3 0.80680 500 2.64088
3 0.21457 3 0.22705 3 0.23329 3 0.38017 3 0.38449 3 0.42145
3 0.65024 2 0.69342 3 0.80680 500 2.64088
'
power=34.817 burn=243.5 down=40  end
power=31.829 burn=243.5 down=64 bfrac=0.379  end
power=29.378 burn=156 down=39 bfrac=1.0  end
power=27.464 burn=156 down=3631 bfrac=0.379  end
o 119 cr 5.2 mn 0.29
'
fe 11. co 0.066 ni 8.7
'
zr 195 nb 0.63 sn 3.2
'
' the above light elements converted to kg per mtuo2...
'
' -----
end

```

Table A.32. H. B. Robinson Assembly B05  
Rod N-9, 31.66 GWd/MTU, ENDF/B-V

```

=sas2h   parm='halt04,skipshipdata'
h.b. robinson 1 pwr case 1-d: b0-5, rod n-9, 226 cm, 31.66gdw/mtu b5
augt-94
'
' *****endf/b-v*****
'
' -----
' for burnup credit project (see exper-data of april 84 in atm-101)
'
' -----
'
' mixtures of fuel-pin-unit-cell:
'
27burnuplib  latticecell
uo2 1 den=9.944 1 923
      92234 0.023 92235 2.561 92236 0.013 92238 97.403  end
co-59 3 0 1-20 579  end
zr-94 1 0 1-20 923  end
'
' *fission product nuclide set same as table a.29 with new temperatures*
'
gd-160 1 0 1-20 923  end
' need the following to use endf/b5 library:
' from st5: (2nd line same as def. of zircalloy in sect. m8, scale-4.1)
' arbmzirc 6.5 4 0 0 1 40000 97.91 26000 0.5 50118 0.64 50120 0.95 2 1  end
' arbmzirc 6.44 4 0 0 1 40000 97.91 26000 0.5 50118 0.64 50120 0.95 2 1 595  end
' old b4 std-comp: zircalloy 2 1 595  end
h2o 3 den=0.7135 1 579  end
arbm-bormod 0.7135 1 1 0 0 5000 100 3 652.5e-6 579  end
'
' 652.5 ppm boron (wt) in moderator
'
' -----
' input materials for the burnable poison coupled assembly:
'
ss304 5 1 579  end
o 6 0 0.04497 579  end
na 6 0 0.00165 579  end
al 6 0 0.00058 579  end
si 6 0 0.01799 579  end
k 6 0 0.00011 579  end
b-10 6 0 9.595-4 579  end
b-11 6 0 3.863-3 579  end
n 4 0 5-5 579  end
'
end comp
'
' -----
' fuel-pin-cell geometry:
'
squarepitch 1.4300 0.9294 1 3 1.0719 2 0.9484 0  end
'
' -----
' assembly and cycle parameters:
'
npin/assm=204 fuelnght=726.63 ncycles=4 nlib/cyc=1
printlevel=5 lightel=9 inplevel=2 numztotal=10 mxrepeats=0  end
' the 10 larger unit cell zones follow for 2 passes bp, 2 passes h2o :
4 0.21457 5 0.22705 4 0.23329 6 0.38017 4 0.38449 5 0.42145
3 0.65024 2 0.69342 3 0.80680 500 2.64088
4 0.21457 5 0.22705 4 0.23329 6 0.38017 4 0.38449 5 0.42145
3 0.65024 2 0.69342 3 0.80680 500 2.64088
3 0.21457 3 0.22705 3 0.23329 3 0.38017 3 0.38449 3 0.42145
3 0.65024 2 0.69342 3 0.80680 500 2.64088
3 0.21457 3 0.22705 3 0.23329 3 0.38017 3 0.38449 3 0.42145
3 0.65024 2 0.69342 3 0.80680 500 2.64088
'
power=39.382 burn=243.5 down=40  end
power=35.477 burn=243.5 down=64 bfrac=0.379  end
power=32.274 burn=156 down=39 bfrac=1.0  end
power=29.772 burn=156 down=3631 bfrac=0.379  end
o 119 cr 5.2 mn 0.29
'
fe 11. co 0.066 ni 8.7
'
zr 195 nb 0.63 sn 3.2
'
' the above light elements converted to kg per mtuo2...
'
' -----
end

```

Table A.33. Obrigheim (KWO) Assembly 170  
Batch 94, 25.93 GWd/MTU, ENDF/B-V

```
=sas2      parm='halt03,skipshipdata'
obrigheim (kwo) pwr, assm 170, batch 94, 25.93 gwd/mtu 3-cyc endf/b5 aug-94
'
'   ....used 180 fuel rode, 16 guide tubes....
'
' -----
'   mixtures of fuel-pin-unit-cell:
'
27burnuplib  latticecell
uo2 1 den=9.742 1 846
    92234 0.028 92235 3.13 92236 0.014 92238 96.828  end
co-59 3 0 1-20 572  end
kr-83 1 0 1-20 846  end
kr-84 1 0 1-20 846  end
kr-85 1 0 1-20 846  end
kr-86 1 0 1-20 846  end
zr-94 1 0 1-20 846  end
mo-94 1 0 1-20 846  end
nb-95 1 0 1-20 846  end
mo-95 1 0 1-20 846  end
tc-99 1 0 1-20 846  end
rh-103 1 0 1-20 846  end
rh-105 1 0 1-20 846  end
ru-106 1 0 1-20 846  end
sn-126 1 0 1-20 846  end
xe-131 1 0 1-20 846  end
xe-132 1 0 1-20 846  end
xe-134 1 0 1-20 846  end
cs-134 1 0 1-20 846  end
cs-135 1 0 1-20 846  end
xe-136 1 0 1-20 846  end
cs-137 1 0 1-20 846  end
pr-143 1 0 1-20 846  end
nd-143 1 0 1-20 846  end
ce-144 1 0 1-20 846  end
nd-145 1 0 1-20 846  end
nd-146 1 0 1-20 846  end
nd-147 1 0 1-20 846  end
pm-147 1 0 1-20 846  end
sm-147 1 0 1-20 846  end
nd-148 1 0 1-20 846  end
pm-149 1 0 1-20 846  end
sm-149 1 0 1-20 846  end
sm-150 1 0 1-20 846  end
sm-151 1 0 1-20 846  end
eu-151 1 0 1-20 846  end
sm-152 1 0 1-20 846  end
eu-153 1 0 1-20 846  end
eu-154 1 0 1-20 846  end
gd-154 1 0 1-20 846  end
eu-155 1 0 1-20 846  end
gd-155 1 0 1-20 846  end
gd-157 1 0 1-20 846  end
gd-158 1 0 1-20 846  end
gd-160 1 0 1-20 846  end
'
'   need the following to use endf/b5 library:
arbmzirc 6.44 4 0 0 1 40000 97.91 26000 0.5 50116 0.86 50120 0.73 2 1 605  end
h2o 3 den=0.7283 1 572  end
arbm-bormod 0.7283 1 1 0 0 5000 100 3 450.0e-6 572  end
'
'   450 ppm boron (wt) in moderator
'
' -----
```

Table A.33 (continued)

```
end comp
'
' -----
'   fuel-pin-cell geometry:
'
squarepitch 1.43 0.925 1 3 1.071 2 0.930 0  end
'
' -----
'   assembly and cycle parameters:
'
npin/assm=180 fuelnght=962.75 ncycles=3 nlib/cyc=1
printlevel=4 lightel=9 inplevel=1 asmpitch=20.12 numins=0
ortube=0.6845 srtube=0.6413  end
power=20.929 burn=288.0  down=81  end
power=37.468 burn=309.0  down=396  end
power=33.564 burn=248.0  down=913.1  end
  o 135  cr 5.9  mn 0.33
  fe 13  co 0.075 ni 9.9
  zr 221 nb 0.71 sn 3.6
'
' -----
end
```

Table A.34. Obrigheim (KWO) Assembly 172  
Batch 92, 26.54 GWd/MTU, ENDF/B-V

```
=sas2      parm='halt03,skipshipdata'
obrigheim (kwo) pwr, assm 172, batch 92, 26.54 gwd/mtu 3-cyc endf/b5 aug-94
'
' .....used 180 fuel rode, 16 guide tubes....
'
' -----
'
' mixtures of fuel-pin-unit-cell:
'
'
27burnuplib latticecell
uo2 1 den=9.742 1 841
    92234 0.028 92235 3.13 92236 0.014 92238 96.828 end
co-59 3 0 1-20 572 end
kr-83 1 0 1-20 841 end

*fission product nuclide set same as table a.33 with new temperatures*
gd-160 1 0 1-20 841 end
' need the following to use endf/b5 library:
arbmzirc 6.44 4 0 0 1 40000 97.91 26000 0.5 50116 0.86 50120 0.73 2 1 605 end
h2o 3 den=0.7283 1 572 end
arbm-bormod 0.7283 1 1 0 0 5000 100 3 450.0e-6 572 end
'
' 450 ppm boron (wt) in moderator
'
' -----
end comp
'
' -----
'
' fuel-pin-cell geometry:
'
squarepitch 1.43 0.925 1 3 1.071 2 0.930 0 end
'
' -----
'
' assembly and cycle parameters:
'
npin/assm=180 fuelnght=962.75 ncycles=3 nlib/cyc=1
printlevel=4 lightel=9 inplevel=1 asmpitch=20.12 numins=0
ortube=0.6845 strtube=0.6413 end
power=34.833 burn=288.0 down=81 end
power=25.035 burn=309.0 down=396 end
power=35.374 burn=248.0 down=913.1 end
  o 135 cr 5.9 mn 0.33
  fe 13 co 0.075 ni 9.9
  zr 221 nb 0.71 sn 3.6
'
' -----
end
```

Table A.35. Obrigheim (KWO) Assembly 176  
Batch 91, 27.99 GWd/MTU, ENDF/B-V

```
=sas2      parm='halt03,skipshipdata'
obrigheim (kwo) pwr, assm 176, batch 91, 27.99 gwd/mtu 3-cyc endf/b5
aug-94
'
' .....used 180 fuel rode, 16 guide tubes....
'
' -----
'
' mixtures of fuel-pin-unit-cell:
'
'
27burnuplib latticecell
uo2 1 den=9.742 1 849
    92234 0.028 92235 3.13 92236 0.014 92238 96.828 end
co-59 3 0 1-20 572 end
kr-83 1 0 1-20 849 end

*fission product nuclide set same as table a.33 with new temperatures*
gd-160 1 0 1-20 846 end
' need the following to use endf/b5 library:
arbmzirc 6.44 4 0 0 1 40000 97.91 26000 0.5 50116 0.86 50120 0.73 2 1 605
end
h2o 3 den=0.7283 1 572 end
arbm-bormod 0.7283 1 1 0 0 5000 100 3 450.0e-6 572 end
'
' 450 ppm boron (wt) in moderator
'
' -----
end comp
'
' -----
'
' fuel-pin-cell geometry:
'
squarepitch 1.43 0.925 1 3 1.071 2 0.930 0 end
'
' -----
'
' assembly and cycle parameters:
'
npin/assm=180 fuelnght=962.75 ncycles=3 nlib/cyc=1
printlevel=4 lightel=9 inplevel=1 asmpitch=20.12 numins=0
ortube=0.6845 strtube=0.6413 end
power=30.457 burn=288.0 down=81 end
power=34.894 burn=309.0 down=396 end
power=34.016 burn=248.0 down=913.1 end
  o 135 cr 5.9 mn 0.33
  fe 13 co 0.075 ni 9.9
  zr 221 nb 0.71 sn 3.6
'
' -----
end
```

Table A.36. Obrigheim (KWO) Assembly 168  
Batch 86, 28.40 GWd/MTU, ENDF/B-V

```
=sas2      parm='halt03,skipshipdata'
obrigheim (kwo) pwr, assm 168, batch 86, 28.40 gwd/mtu 3-cyc endf/b5 aug-94
'      ....used 180 fuel rode, 16 guide tubes...., t-fuel = 859k
'
' -----
'      mixtures of fuel-pin-unit-cell:
'
27burnuplib  latticecell
uo2  1 den=9.742  1  859
      92234 0.028 92235 3.13 92236 0.014 92238 96.828  end
co-59  3 0 1-20 572  end
kr-83  1 0 1-20 859  end

*fission product nuclide set same as table a.33 with new temperatures*
gd-160 1 0 1-20 859  end
'      need the following to use endf/b5 library:
arbmzirc 6.44 4 0 0 1 40000 97.91 26000 0.5 50116 0.86 50120 0.73 2 1 605  end
h2o  3 den=0.7283 1  572  end
arbm-bormod  0.7283 1 1 0 0 5000 100 3 450.0e-6  572  end
'
'      450 ppm boron (wt) in moderator
' -----
end comp
'
' -----
'      fuel-pin-cell geometry:
'
squarepitch  1.43 0.925 1 3 1.071 2 0.930  0  end
'
' -----
'      assembly and cycle parameters:
'
npin/assm=180 fuelnght=962.75 ncycles=3  nlib/cyc=1
printlevel=4 lightel=9  inplevel=1  asmpitch=20.12  numins=0
ortube=0.6845  srtube=0.6413  end
power=28.336  burn=288.0  down=81  end
power=38.005  burn=309.0  down=396  end
power=34.249  burn=248.0  down=913.1  end
  o 135  cr  5.9  mn  0.33
  fe 13  co 0.075 ni  9.9
  zr 221 nb  0.71 sn  3.6
'
' -----
end
```

Table A.37. Obrigheim (KWO) Assembly 171  
Batch 89, 29.04 GWd/MTU, ENDF/B-V

```
=sas2      parm='halt03,skipshipdata'
obrigheim (kwo) pwr, assm 171, batch 89, 29.04 gwd/mtu 3-cyc endf/b5
aug-94
'      ....used 180 fuel rode, 16 guide tubes....
'
' -----
'      mixtures of fuel-pin-unit-cell:
'
27burnuplib  latticecell
uo2  1 den=9.742  1  867
      92234 0.028 92235 3.13 92236 0.014 92238 96.828  end
co-59  3 0 1-20 572  end
kr-83  1 0 1-20 867  end

*fission product nuclide set same as table a.33 with new temperatures*
gd-160 1 0 1-20 867  end
'      need the following to use endf/b5 library:
arbmzirc 6.44 4 0 0 1 40000 97.91 26000 0.5 50116 0.86 50120 0.73 2 1 605  end
h2o  3 den=0.7283 1  572  end
arbm-bormod  0.7283 1 1 0 0 5000 100 3 450.0e-6  572  end
'
'      450 ppm boron (wt) in moderator
' -----
end comp
'
' -----
'      fuel-pin-cell geometry:
'
squarepitch  1.43 0.925 1 3 1.071 2 0.930  0  end
'
' -----
'      assembly and cycle parameters:
'
npin/assm=180 fuelnght=962.75 ncycles=3  nlib/cyc=1
printlevel=4 lightel=9  inplevel=1  asmpitch=20.12  numins=0
ortube=0.6845  srtube=0.6413  end
power=29.124  burn=288.0  down=81  end
power=38.952  burn=309.0  down=396  end
power=34.748  burn=248.0  down=913.1  end
  o 135  cr  5.9  mn  0.33
  fe 13  co 0.075 ni  9.9
  zr 221 nb  0.71 sn  3.6
'
' -----
end
```



Table A.38. Obrigheim (KWO) Assembly 176  
Batch 90, 29.52 GWd/MTU, ENDF/B-V

```

=sas2      parm='halt03,skipshipdata'
obrigheim (kwo) pwr, assm 176, batch 90, 29.52 gwd/mtu 3-cyc endf/b5 aug-94
'
'...used 180 fuel rode, 16 guide tubes....
'
'-----
'
' mixtures of fuel-pin-unit-cell:
'
27burnuplib latticecell
uo2 1 den=9.742 1 867
' 92234 0.028 92235 3.13 92236 0.014 92238 96.828 end
co-59 3 0 1-20 572 end
kr-83 1 0 1-20 867 end
'
' fission product nuclide set same as table a.33 with new temperatures*
'
gd-160 1 0 1-20 867 end
' need the following to use endf/b5 library:
arbmzirc 6.44 4 0 0 1 40000 97.91 26000 0.5 50116 0.86 50120 0.73 2 1 605 end
h2o 3 den=0.7283 1 572 end
arbm-bormod 0.7283 1 1 0 0 5000 100 3 450.0e-6 572 end
'
' 450 ppm boron (wt) in moderator
'-----
end comp
'
'-----
'
' fuel-pin-cell geometry:
'
squarepitch 1.43 0.925 1 3 1.071 2 0.930 0 end
'
'-----
'
' assembly and cycle parameters:
'
npin/assm=180 fuelnght=962.75 ncycles=3 nlib/cyc=1
printlevel=4 lightel=9 inplevel=1 asmpitch=20.12 numins=0
ortube=0.6845 srtube=0.6413 end
power=32.121 burn=288.0 down=81 end
power=36.801 burn=309.0 down=396 end
power=35.875 burn=248.0 down=913.1 end
' o 135 cr 5.9 mn 0.33
' fe 13 co 0.075 ni 9.9
' zr 221 nb 0.71 sn 3.6
'
'-----
'
end

```



**APPENDIX B**  
**COMPARISONS OF MEASURED ISOTOPIC**  
**DATA TO SAS2H CALCULATIONS**

Table B.1. Calvert Cliffs Assembly D047 Rod MKP109, 27.35 GWd/MTU

---

```

calvert cliffs unit 1 pwr
measured and computed irradiated fuel composition, mg/g fuel (uo2)
atm-104, fuel assembly d047, rod mkp109 at 13.20 cm, 27.35 gwd/mtu
run sept. 1994
...measured and calculated at 1870 day cooling time...
..compares cases using endf/b-iv and endf/b-v(eu)* libraries..
nuclide, z & name      measured  endf/b-iv  %diff  endf/b-ve*  %diff
92  u234      1.600E-01  1.612E-01 ( 0.7%)  1.577E-01 (-1.5%)
92  u235      8.470E+00  8.002E+00 (-5.5%)  8.071E+00 (-4.7%)
92  u236      3.140E+00  3.237E+00 ( 3.1%)  3.233E+00 ( 2.9%)
92  u238      8.425E+02  8.372E+02 (-0.6%)  8.373E+02 (-0.6%)
94  pu238      1.010E-01  9.789E-02 (-3.1%)  9.257E-02 (-8.3%)
94  pu239      4.264E+00  4.280E+00 ( 0.4%)  4.040E+00 (-5.3%)
94  pu240      1.719E+00  1.614E+00 (-6.1%)  1.709E+00 (-0.6%)
94  pu241      6.810E-01  7.087E-01 ( 4.1%)  6.681E-01 (-1.9%)
94  pu242      2.890E-01  2.769E-01 (-4.2%)  3.082E-01 ( 6.6%)
93  np237      2.680E-01  3.156E-01 (17.8%)  2.835E-01 ( 5.8%)
55  cs133      8.500E-01  8.601E-01 ( 1.2%)  8.634E-01 ( 1.6%)
55  cs134      1.000E-02  1.007E-02 ( 0.7%)  9.711E-03 (-2.9%)
55  cs135      3.600E-01  3.935E-01 ( 9.3%)  3.766E-01 ( 4.6%)
55  cs137      7.700E-01  7.832E-01 ( 1.7%)  7.830E-01 ( 1.7%)
60  nd143      6.130E-01  6.206E-01 ( 1.2%)  6.166E-01 ( 0.6%)
60  nd144      9.430E-01  9.462E-01 ( 0.3%)  9.490E-01 ( 0.6%)
60  nd145      5.100E-01  5.131E-01 ( 0.6%)  5.105E-01 ( 0.1%)
60  nd146      4.900E-01  4.925E-01 ( 0.5%)  4.949E-01 ( 1.0%)
60  nd148      2.650E-01  2.664E-01 ( 0.5%)  2.665E-01 ( 0.6%)
60  nd150      1.240E-01  1.268E-01 ( 2.3%)  1.271E-01 ( 2.5%)
61  pm147      3.085E-02  3.135E-02  1.880E-01
62  sm147      1.859E-01  2.193E-01 (17.1%)  2.193E-01 (17.1%)
62  pm147..sm147  2.210E-01  2.167E-01 (-1.9%)  2.193E-01 (-0.8%)
62  sm148      1.060E-01  8.842E-02 (-16.6%)  8.717E-02 (-17.8%)
62  sm149      2.900E-03  2.169E-03 (-25.2%)  1.988E-03 (-31.4%)
62  sm150      2.070E-01  2.030E-01 (-1.9%)  2.016E-01 (-2.6%)
62  sm151      1.012E-02  4.320E-04  1.032E-02
63  eu151      4.320E-04  1.055E-02 (13.0%)  1.076E-02 (15.2%)
63  sm151..eu151  9.340E-03  9.721E-02 (11.7%)  9.964E-02 (14.5%)
62  sm152      8.700E-02  7.443E-02 (-5.8%)  7.986E-02 (1.1%)
63  eu153      7.900E-02  2.465E-02  2.469E-02
63  sm154      1.519E-02  8.500E-03  8.500E-03
64  gd154      1.079E-02  6.123E-03  6.123E-03
64  sm154..gd154  4.160E-02  5.062E-02 (21.7%)  3.931E-02 (-5.5%)
63  eu155      3.885E-03  1.596E-03  1.596E-03
64  gd155      4.524E-03  1.861E-03  1.861E-03
64  eu155..gd155  4.740E-03  8.410E-03 (77.4%)  3.457E-03 (-27.1%)

units changed: curies/ gram uo2
95  am241      8.560E-04  8.572E-04 ( 0.1%)  8.145E-04 (-4.9%)
96  cm243      1.125E-05  8.130E-06  8.130E-06
96  cm244      5.902E-04  7.029E-04  7.029E-04
96  cm243..cm244  7.340E-04  6.014E-04 (-18.1%)  7.110E-04 (-3.1%)
34  se 79      4.550E-08  4.952E-08 ( 8.8%)  4.948E-08 ( 8.7%)
38  sr 90      4.590E-02  4.998E-02 ( 8.9%)  4.989E-02 ( 8.7%)
43  tc 99      9.590E-06  1.005E-05 ( 4.8%)  1.008E-05 ( 5.1%)
endf/b-iv  %diff  for: sas2 27-group endf/b4 library, 4-cycle case, 27.35 gwd/mtu
endf/b-ve* %diff  for: *sas2 44-group endf/b5 (with b6: eu-154, 155) lib., 4-cyc case, 27.35 gwd/mtu

```

---

Table B.2. Calvert Cliffs Assembly D047 Rod MKP109, 37.12 Gwd/MTU

---

calvert cliffs unit 1 pwr

measured and computed irradiated fuel composition, mg/g fuel (uo2)

atm-104, fuel assembly d047, rod mkp109 at 27.70 cm, 37.12 gwd/mtu

run sept. 1994

...measured and calculated at 1870 day cooling time....

..compares cases using endf/b-iv and endf/b-v(eu)\* libraries..

nuclide, z & name	measured	endf/b-iv	%diff	endf/b-ve*	%diff
92 u234	1.400E-01	1.395E-01	( -0.4%)	1.356E-01	( -3.1%)
92 u235	5.170E+00	4.723E+00	( -8.6%)	4.771E+00	( -7.7%)
92 u236	3.530E+00	3.631E+00	( 2.9%)	3.633E+00	( 2.9%)
92 u238	8.327E+02	8.298E+02	( -0.4%)	8.299E+02	( -0.3%)
94 pu238	1.890E-01	1.881E-01	( -0.5%)	1.786E-01	( -5.5%)
94 pu239	4.357E+00	4.415E+00	( 1.3%)	4.157E+00	( -4.6%)
94 pu240	2.239E+00	2.066E+00	( -7.7%)	2.178E+00	( -2.7%)
94 pu241	9.030E-01	9.332E-01	( 3.3%)	8.750E-01	( -3.1%)
94 pu242	5.760E-01	5.551E-01	( -3.6%)	6.163E-01	( 7.0%)
93 np237	3.560E-01	4.573E-01	( 28.5%)	4.112E-01	( 15.5%)
55 cs133	1.090E+00	1.110E+00	( 1.8%)	1.116E+00	( 2.4%)
55 cs134	2.000E-02	1.811E-02	( -9.5%)	1.746E-02	( -12.7%)
55 cs135	4.000E-01	4.317E-01	( 7.9%)	4.109E-01	( 2.7%)
55 cs137	1.040E+00	1.061E+00	( 2.0%)	1.061E+00	( 2.0%)
60 nd143	7.160E-01	7.234E-01	( 1.0%)	7.166E-01	( 0.1%)
60 nd144	1.338E+00	1.341E+00	( 0.2%)	1.347E+00	( 0.7%)
60 nd145	6.530E-01	6.547E-01	( 0.3%)	6.501E-01	( -0.4%)
60 nd146	6.820E-01	6.847E-01	( 0.4%)	6.895E-01	( 1.1%)
60 nd148	3.590E-01	3.601E-01	( 0.3%)	3.603E-01	( 0.4%)
60 nd150	1.720E-01	1.776E-01	( 3.3%)	1.779E-01	( 3.4%)
61 pm147		3.455E-02		3.537E-02	
62 sm147		2.078E-01		2.112E-01	
62 pm147..sm147	2.540E-01	2.423E-01	( -4.6%)	2.466E-01	( -2.9%)
62 sm148	1.640E-01	1.416E-01	( -13.7%)	1.400E-01	( -14.6%)
62 sm149	3.000E-03	2.371E-03	( -21.0%)	2.182E-03	( -27.3%)
62 sm150	2.710E-01	2.840E-01	( 4.8%)	2.812E-01	( 3.8%)
62 sm151		1.148E-02		1.165E-02	
63 eu151		4.811E-04		4.882E-04	
63 sm151..eu151	9.300E-03	1.196E-02	( 28.6%)	1.214E-02	( 30.6%)
62 sm152	1.040E-01	1.258E-01	( 21.0%)	1.289E-01	( 23.9%)
63 eu153	1.090E-01	1.095E-01	( 0.5%)	1.214E-01	( 11.3%)
62 sm154		3.749E-02		3.748E-02	
63 eu154		2.707E-02		1.435E-02	
64 gd154		1.947E-02		1.047E-02	
64 sm154..gd154	6.070E-02	8.403E-02	( 38.4%)	6.230E-02	( 2.6%)
63 eu155		6.790E-03		2.608E-03	
64 gd155		7.854E-03		3.020E-03	
64 eu155..gd155	7.100E-03	1.464E-02	( 106.2%)	5.628E-03	( -20.7%)

units changed: curies/ gram uo2

95 am241	1.180E-03	1.103E-03	( -6.5%)	1.043E-03	( -11.6%)
96 cm243		2.544E-05		1.932E-05	
96 cm244		2.464E-03		2.871E-03	
96 cm243..cm244	2.930E-03	2.490E-03	( -15.0%)	2.890E-03	( -1.4%)
34 se 79	6.036E-08	6.571E-08	( 8.9%)	6.565E-08	( 8.8%)
38 sr 90	5.900E-02	6.255E-02	( 6.0%)	6.251E-02	( 5.9%)
43 tc 99	1.230E-05	1.303E-05	( 6.0%)	1.310E-05	( 6.5%)

endf/b-iv %diff for: sas2 27-group endf/b4 library, 4-cycle case, 37.12 gwd/mtu

endf/b-ve\* %diff for: \*sas2 44-group endf/b5 (with b6: eu-154, 155) lib., 4-cyc case, 37.12 gwd/mtu

---

Table B.3. Calvert Cliffs Assembly D047 Rod MKP109, 44.34 GWd/MTU

---

calvert cliffs unit 1 pwr

measured and computed irradiated fuel composition, mg/g fuel (uo2)

atm-104, fuel assembly d047, rod mkp109 at 165.22 cm, 44.34 gwd/mtu

run sept. 1994

...measured and calculated at 1870 day cooling time....

..compares cases using endf/b-iv and endf/b-v(eu)\* libraries..

nuclide, z & name	measured	endf/b-iv	%diff	endf/b-ve*	%diff
92 u234	1.200E-01	1.255E-01 ( 4.6%)		1.217E-01 ( 1.4%)	
92 u235	3.540E+00	3.199E+00 (-9.6%)		3.231E+00 (-8.7%)	
92 u236	3.690E+00	3.753E+00 ( 1.7%)		3.759E+00 ( 1.9%)	
92 u238	8.249E+02	8.236E+02 (-0.1%)		8.238E+02 (-0.1%)	
94 pu238	2.690E-01	2.693E-01 ( 0.1%)		2.555E-01 (-5.0%)	
94 pu239	4.357E+00	4.559E+00 ( 4.6%)		4.292E+00 (-1.5%)	
94 pu240	2.543E+00	2.324E+00 (-8.6%)		2.444E+00 (-3.9%)	
94 pu241	1.020E+00	1.065E+00 ( 4.4%)		9.959E-01 (-2.4%)	
94 pu242	8.400E-01	7.858E-01 (-6.5%)		8.741E-01 ( 4.1%)	
93 np237	4.680E-01	5.584E-01 (19.3%)		5.015E-01 ( 7.2%)	
55 cs133	1.240E+00	1.273E+00 ( 2.7%)		1.282E+00 ( 3.4%)	
55 cs134	3.000E-02	2.535E-02 (-15.5%)		2.443E-02 (-18.6%)	
55 cs135	4.300E-01	4.605E-01 ( 7.1%)		4.372E-01 ( 1.7%)	
55 cs137	1.250E+00	1.265E+00 ( 1.2%)		1.265E+00 ( 1.2%)	
60 nd143	7.630E-01	7.757E-01 ( 1.7%)		7.667E-01 ( 0.5%)	
60 nd144	1.643E+00	1.639E+00 (-0.3%)		1.647E+00 ( 0.2%)	
60 nd145	7.440E-01	7.463E-01 ( 0.3%)		7.396E-01 (-0.6%)	
60 nd146	8.300E-01	8.333E-01 ( 0.4%)		8.404E-01 ( 1.3%)	
60 nd148	4.280E-01	4.289E-01 ( 0.2%)		4.291E-01 ( 0.3%)	
60 nd150	2.080E-01	2.166E-01 ( 4.1%)		2.168E-01 ( 4.2%)	
61 pm147		3.586E-02		3.691E-02	
62 sm147		2.137E-01		2.181E-01	
62 pm147..sm147	2.680E-01	2.496E-01 (-6.9%)		2.550E-01 (-4.8%)	
62 sm148	2.220E-01	1.833E-01 (-17.4%)		1.816E-01 (-18.2%)	
62 sm149	4.700E-03	2.592E-03 (-44.9%)		2.391E-03 (-49.1%)	
62 sm150	3.610E-01	3.449E-01 (-4.5%)		3.409E-01 (-5.6%)	
62 sm151		1.285E-02		1.300E-02	
63 eu151		5.345E-04		5.407E-04	
63 sm151..eu151	9.780E-03	1.338E-02 (36.8%)		1.354E-02 (38.5%)	
62 sm152	1.210E-01	1.443E-01 (19.2%)		1.476E-01 (22.0%)	
63 eu153	1.480E-01	1.344E-01 (-9.2%)		1.517E-01 ( 2.5%)	
62 sm154		4.814E-02		4.809E-02	
63 eu154		3.667E-02		1.916E-02	
64 gd154		2.664E-02		1.411E-02	
64 sm154..gd154	8.420E-02	1.114E-01 (32.4%)		8.136E-02 (-3.4%)	
63 eu155		9.311E-03		3.405E-03	
64 gd155		1.074E-02		3.935E-03	
64 eu155..gd155	9.820E-03	2.005E-02 (104.2%)		7.340E-03 (-25.3%)	

units changed: curies/ gram uo2

95 am241	1.310E-03	1.236E-03 (-5.6%)		1.166E-03 (-11.0%)	
96 cm243		3.825E-05		3.002E-05	
96 cm244		5.424E-03		6.256E-03	
96 cm243..cm244	6.400E-03	5.462E-03 (-14.7%)		6.286E-03 (-1.8%)	
34 se 79	6.490E-08	7.715E-08 (18.9%)		7.709E-08 (18.8%)	
38 sr 90	6.580E-02	7.043E-02 (7.0%)		7.041E-02 (7.0%)	
43 tc 99	1.350E-05	1.500E-05 (11.1%)		1.511E-05 (11.9%)	

endf/b-iv %diff for: sas2 27-group endf/b4 library, 4-cycle case, 44.34 gwd/mtu  
endf/b-ve\* %diff for: \*sas2 44-group endf/b5 (with b6: eu-154, 155) lib., 4-cyc case, 44.34 gwd/mtu

---

Table B.4. Calvert Cliffs Assembly D101 Rod MLA098, 18.68 GWd/MTU

---

calvert cliffs unit 1 pwr

measured and computed irradiated fuel composition, mg/g fuel (uo2)

atm-103, fuel assembly d101, rod mla098 at 8.9 cm, 18.68 gwd/mtu

run sept. 1994

\*\* case using new sas2h model \*\*

..compares cases using endf/b-iv and endf/b-v(eu)\* libraries..

nuclide, z & name	measured	endf/b-iv	%diff	endf/b-ve*	%diff
92 u234	1.400E-01	1.604E-01	( 14.6%)	1.577E-01	( 12.6%)
92 u235	1.025E+01	1.008E+01	( -1.6%)	1.016E+01	( -0.9%)
92 u236	2.500E+00	2.482E+00	( -0.7%)	2.476E+00	( -1.0%)
92 u238	8.551E+02	8.453E+02	( -1.1%)	8.454E+02	( -1.1%)
94 pu238	4.850E-02	3.990E-02	(-17.7%)	3.758E-02	(-22.5%)
94 pu239	3.945E+00	3.885E+00	( -1.5%)	3.684E+00	( -6.6%)
94 pu240	1.243E+00	1.159E+00	( -6.8%)	1.232E+00	( -0.9%)
94 pu241	4.542E-01	4.503E-01	( -0.9%)	4.271E-01	( -6.0%)
94 pu242	1.394E-01	1.241E-01	(-11.0%)	1.387E-01	( -0.5%)
units changed: curies/ gram uo2					
93 np237	1.230E-07	1.358E-07	( 10.4%)	1.209E-07	( -1.7%)
95 am241	6.670E-04	6.511E-04	( -2.4%)	6.201E-04	( -7.0%)
96 cm243		3.425E-06		2.400E-06	
96 cm244		1.125E-04		1.369E-04	
96 cm243..cm244	1.640E-04	1.159E-04	(-29.3%)	1.393E-04	(-15.1%)
6 c 14	3.910E-07	3.234E-07	(-17.3%)	3.246E-07	(-17.0%)
34 se 79	3.430E-08	3.428E-08	( -0.1%)	3.425E-08	( -0.2%)
38 sr 90	3.360E-02	3.537E-02	( 5.3%)	3.527E-02	( 5.0%)
43 tc 99	7.070E-06	7.095E-06	( 0.4%)	7.108E-06	( 0.5%)
50 sn126	8.600E-08	2.400E-07	(179.1%)	2.406E-07	(179.8%)
53 i129	1.750E-08	1.546E-08	(-11.7%)	1.548E-08	(-11.6%)
55 cs135	2.790E-07	3.053E-07	( 9.4%)	2.924E-07	( 4.8%)
55 cs137	4.590E-02	4.595E-02	( 0.1%)	4.594E-02	( 0.1%)

endf/b-iv %diff for: sas2 27-group endf/b4 library, 4-cycle case, 18.68 gwd/mtu

endf/b-ve\* %diff for: \*sas2 44-group endf/b5 (with b6: eu-154, 155) lib., 4-cyc case, 18.68 gwd/mtu

---

Table B.5. Calvert Cliffs Assembly D101 Rod MLA098, 26.62 GWd/MTU

---

calvert cliffs unit 1 pwr

measured and computed irradiated fuel composition, mg/g fuel (uo2)

atm-103, fuel assembly d101, rod mla098 at 24.3 cm, 26.62 gwd/mtu

run sept. 1994

\*\* case using new sas2h model \*\*

..compares cases using endf/b-iv and endf/b-v(eu)\* libraries..

nuclide, z & name	measured	endf/b-iv	%diff	endf/b-ve*	%diff
92 u234	1.210E-01	1.422E-01	( 17.5%)	1.390E-01	( 14.9%)
92 u235	6.940E+00	6.638E+00	( -4.4%)	6.704E+00	( -3.4%)
92 u236	2.990E+00	2.977E+00	( -0.4%)	2.973E+00	( -0.6%)
92 u238	8.538E+02	8.395E+02	( -1.7%)	8.397E+02	( -1.7%)
94 pu238	9.690E-02	9.006E-02	( -7.1%)	8.530E-02	( -12.0%)
94 pu239	4.252E+00	4.218E+00	( -0.8%)	3.981E+00	( -6.4%)
94 pu240	1.766E+00	1.634E+00	( -7.5%)	1.731E+00	( -2.0%)
94 pu241	6.822E-01	6.972E-01	( 2.2%)	6.564E-01	( -3.8%)
94 pu242	3.301E-01	3.042E-01	( -7.9%)	3.381E-01	( 2.4%)
units changed: curies/ gram uo2					
93 np237	2.110E-07	2.158E-07	( 2.3%)	1.931E-07	( -8.5%)
95 am241	9.910E-04	9.981E-04	( 0.7%)	9.442E-04	( -4.7%)
96 cm243		1.079E-05		7.867E-06	
96 cm244		6.460E-04		7.668E-04	
96 cm243..cm244	8.150E-04	6.568E-04	(-19.4%)	7.746E-04	( -5.0%)
6 c 14	5.030E-07	4.792E-07	( -4.7%)	4.811E-07	( -4.4%)
34 se 79	4.590E-08	4.795E-08	( 4.5%)	4.790E-08	( 4.4%)
38 sr 90	4.410E-02	4.673E-02	( 6.0%)	4.665E-02	( 5.8%)
43 tc 99	9.370E-06	9.758E-06	( 4.1%)	9.789E-06	( 4.5%)
50 sn126	1.360E-07	3.822E-07	(181.0%)	3.820E-07	(180.9%)
53 i129	2.410E-08	2.264E-08	( -6.1%)	2.265E-08	( -6.0%)
55 cs135	3.120E-07	3.424E-07	( 9.7%)	3.259E-07	( 4.5%)
55 cs137	6.530E-02	6.545E-02	( 0.2%)	6.543E-02	( 0.2%)

endf/b-iv %diff for: sas2 27-group endf/b4 library, 4-cycle case, 26.62 gwd/mtu

endf/b-ve\* %diff for: \*sas2 44-group endf/b5 (with b6: eu-154, 155) lib., 4-cyc case, 26.62 gwd/mtu

---



Table B.6. Calvert Cliffs Assembly D101 Rod MLA098, 33.17 GWd/MTU

---

calvert cliffs unit 1 pwr

measured and computed irradiated fuel composition, mg/g fuel (uo2)

atm-103, fuel assembly d101, rod mla098 at 161.7 cm, 33.17 gwd/mtu

run sept. 1994

\*\* case using new sas2h model \*\*

..compares cases using endf/b-iv and endf/b-v(eu)\* libraries..

nuclide, z & name	measured	endf/b-iv	%diff	endf/b-ve*	%diff
92 u234	1.200E-01	1.288E-01 ( 7.3%)		1.254E-01 ( 4.5%)	
92 u235	4.780E+00	4.663E+00 (-2.4%)		4.715E+00 (-1.4%)	
92 u236	3.260E+00	3.219E+00 (-1.3%)		3.219E+00 (-1.3%)	
92 u238	8.422E+02	8.342E+02 (-0.9%)		8.344E+02 (-0.9%)	
94 pu238	1.483E-01	1.468E-01 (-1.0%)		1.392E-01 (-6.1%)	
94 pu239	4.187E+00	4.423E+00 ( 5.6%)		4.168E+00 (-0.5%)	
94 pu240	2.111E+00	1.946E+00 (-7.8%)		2.058E+00 (-2.5%)	
94 pu241	8.125E-01	8.647E-01 ( 6.4%)		8.106E-01 (-0.2%)	
94 pu242	5.474E-01	4.976E-01 (-9.1%)		5.526E-01 ( 0.9%)	
units changed: curies/ gram uo2					
93 np237	2.410E-07	2.842E-07 ( 17.9%)		2.546E-07 ( 5.7%)	
95 am241	1.200E-03	1.229E-03 ( 2.4%)		1.158E-03 (-3.5%)	
96 cm243		2.005E-05		1.507E-05	
96 cm244		1.836E-03		2.151E-03	
96 cm243..cm244	2.110E-03	1.857E-03 (-12.0%)		2.166E-03 ( 2.7%)	
6 c 14	7.690E-07	6.109E-07 (-20.6%)		6.138E-07 (-20.2%)	
34 se 79	5.540E-08	5.874E-08 ( 6.0%)		5.869E-08 ( 5.9%)	
38 sr 90	5.230E-02	5.475E-02 ( 4.7%)		5.469E-02 ( 4.6%)	
43 tc 99	1.130E-05	1.177E-05 ( 4.2%)		1.183E-05 ( 4.7%)	
50 sn126	1.690E-07	5.101E-07 (201.8%)		5.092E-07 (201.3%)	
53 i129	3.360E-08	2.866E-08 (-14.7%)		2.865E-08 (-14.7%)	
55 cs135	3.320E-07	3.680E-07 ( 10.8%)		3.492E-07 ( 5.2%)	
55 cs137	8.060E-02	8.146E-02 ( 1.1%)		8.142E-02 ( 1.0%)	

endf/b-iv %diff for: sas2 27-group endf/b4 library, 4-cycle case, 33.17 gwd/mtu

endf/b-ve\* %diff for: \*sas2 44-group endf/b5 (with b6: eu-154, 155) lib., 4-cyc case, 33.17 gwd/mtu

---

Table B.7. Calvert Cliffs Assembly BT03 Rod NBD107, 31.40 Gwd/MTU

---

```

calvert cliffs unit 1 pwr
measured and computed irradiated fuel composition, mg/g fuel (uo2)
atm-106, fuel assembly bt03, rod nbd107 at 11.28 cm, 31.40 gwd/mtu
run sept. 1994
** case using new sas2h model **
..compares cases using endf/b-iv and endf/b-v(eu)* libraries..
nuclide, z & name      measured      endf/b-iv    %diff      endf/b-ve*   %diff
92  u234                1.530E-01    1.206E-01   (-21.2%)    1.170E-01   (-23.5%)
92  u235                3.860E+00    3.823E+00   (-0.9%)     3.869E+00   ( 0.2%)
92  u236                2.860E+00    2.899E+00   ( 1.4%)     2.898E+00   ( 1.3%)
92  u238                8.446E+02    8.376E+02   (-0.8%)     8.377E+02   (-0.8%)
94  pu238                1.426E-01    1.471E-01   ( 3.1%)     1.389E-01   (-2.6%)
94  pu239                3.814E+00    4.037E+00   ( 5.8%)     3.796E+00   (-0.5%)
94  pu240                2.067E+00    1.951E+00   (-5.6%)     2.060E+00   (-0.3%)
94  pu241                7.260E-01    7.393E-01   ( 1.8%)     6.947E-01   (-4.3%)
94  pu242                5.463E-01    4.890E-01  (-10.5%)    5.399E-01   (-1.2%)

units changed: curies/ gram uo2
93  np237                1.840E-07    2.506E-07   (36.2%)     2.232E-07   (21.3%)
95  am241                1.180E-03    1.196E-03   ( 1.3%)     1.132E-03   (-4.1%)
96  cm243                1.986E-05    1.986E-05   ( 0.0%)     1.499E-05   (-24.5%)
96  cm244                1.683E-03    1.683E-03   ( 0.0%)     1.938E-03   (14.6%)
96  cm243..cm244        1.870E-03    1.703E-03   (-8.9%)     1.953E-03   ( 4.5%)
34  se 79                4.180E-08    5.553E-08   (32.8%)     5.548E-08   ( 32.7%)
38  sr 90                4.640E-02    4.902E-02   ( 5.6%)     4.898E-02   ( 5.6%)
43  tc 99                7.700E-06    1.116E-05   (45.0%)     1.120E-05   (45.5%)
50  sn126                1.410E-07    4.923E-07  (249.1%)    4.913E-07  (248.5%)
55  cs135                4.040E-07    4.637E-07   (14.8%)     4.428E-07   ( 9.6%)
55  cs137                7.470E-02    7.423E-02   (-0.6%)     7.420E-02   (-0.7%)

endf/b-iv  %diff  for: sas2 27-group endf/b4 library, 4-cycle case, 31.40 gwd/mtu
endf/b-ve* %diff  for: *sas2 44-group endf/b5 (with b6: eu-154, 155) lib., 4-cyc case, 31.40 gwd/mtu

```

---

Table B.8. Calvert Cliffs Assembly BT03 Rod NBD107, 37.27 GWd/MTU

---

```

calvert cliffs unit 1 pwr
measured and computed irradiated fuel composition, mg/g fuel (uo2)
atm-106, fuel assembly bt03, rod nbd107 at 19.92 cm, 37.27 gwd/mtu
run sept. 1994
** case using new sas2h model **
..compares cases using endf/b-iv and endf/b-v(eu)* libraries..
nuclide, z & name      measured      endf/b-iv      %diff      endf/b-ve*      %diff
92  u234      1.270E-01      1.110E-01      (-12.6%)      1.072E-01      (-15.6%)
92  u235      2.710E+00      2.593E+00      (-4.3%)      2.625E+00      (-3.1%)
92  u236      3.030E+00      3.002E+00      (-0.9%)      3.004E+00      (-0.9%)
92  u238      8.438E+02      8.327E+02      (-1.3%)      8.328E+02      (-1.3%)
94  pu238      1.947E-01      2.013E-01      ( 3.4%)      1.905E-01      (-2.2%)
94  pu239      3.835E+00      4.083E+00      ( 6.5%)      3.839E+00      ( 0.1%)
94  pu240      2.321E+00      2.181E+00      (-6.0%)      2.297E+00      (-1.0%)
94  pu241      8.130E-01      8.313E-01      ( 2.3%)      7.800E-01      (-4.1%)
94  pu242      7.753E-01      6.891E-01      (-11.1%)      7.614E-01      (-1.8%)

units changed: curies/ gram uo2
93  np237      2.260E-07      3.012E-07      ( 33.3%)      2.679E-07      ( 18.6%)
95  am241      1.460E-03      1.316E-03      (-9.9%)      1.243E-03      (-14.8%)
96  cm243      2.885E-05      2.885E-05      ( 0.0%)      2.238E-05      (-22.4%)
96  cm244      3.546E-03      3.546E-03      ( 0.0%)      4.044E-03      (14.3%)
96  cm243..cm244 4.110E-03      3.575E-03      (-13.0%)      4.066E-03      (-1.1%)
34  se 79      5.630E-08      6.489E-08      (15.3%)      6.484E-08      (-0.1%)
38  sr 90      5.180E-02      5.515E-02      ( 6.5%)      5.513E-02      ( 6.4%)
43  tc 99      8.960E-06      1.286E-05      (43.5%)      1.292E-05      ( 0.1%)
50  sn126      1.600E-07      6.140E-07      (283.7%)      6.123E-07      (-0.3%)
55  cs135      4.150E-07      4.892E-07      (17.9%)      4.658E-07      (12.2%)
55  cs137      8.560E-02      8.808E-02      ( 2.9%)      8.804E-02      ( 0.0%)

endf/b-iv  %diff  for: sas2 27-group endf/b4 library, 4-cycle case, 37.27 gwd/mtu
endf/b-ve* %diff  for: *sas2 44-group endf/b5 (with b6: eu-154, 155) lib., 4-cyc case, 37.27 gwd/mtu

```

---

Table B.9. Calvert Cliffs Assembly BT03 Rod NBD107, 46.46 GWd/MTU

---

```

calvert cliffs unit 1 pwr
measured and computed irradiated fuel composition, mg/g fuel (uo2)
atm-106, fuel assembly bt03, rod nbd107 at 161.21 cm, 46.46 gwd/mtu
run sept. 1994
** case using new sas2h model **
..compares cases using endf/b-iv and endf/b-v(eu)* libraries..
nuclide, z & name      measured      endf/b-iv      %diff      endf/b-ve*      %diff
92  u234              7.490E-02     9.845E-02 ( 31.4%)  9.447E-02 ( 26.1%)
92  u235              1.406E+00     1.426E+00 (  1.4%)  1.441E+00 (  2.5%)
92  u236              3.040E+00     3.024E+00 (  -0.5%)  3.030E+00 (  -0.3%)
92  u238              8.272E+02     8.244E+02 (  -0.3%)  8.245E+02 (  -0.3%)
94  pu238              2.842E-01     2.903E-01 (  2.2%)  2.745E-01 ( -3.4%)
94  pu239              3.766E+00     4.210E+00 ( 11.8%)  3.959E+00 (  5.1%)
94  pu240              2.599E+00     2.453E+00 (  -5.6%)  2.579E+00 (  -0.8%)
94  pu241              8.862E-01     9.443E-01 (  6.6%)  8.838E-01 (  -0.3%)
94  pu242              1.169E+00     1.005E+00 (-14.0%)  1.116E+00 ( -4.6%)

units changed:  curies/ gram uo2
93  np237              2.660E-07     3.715E-07 ( 39.7%)  3.292E-07 ( 23.8%)
95  am241              2.180E-03     1.452E-03 (-33.4%)  1.368E-03 (-37.2%)
96  cm243              4.240E-05     4.240E-05
96  cm244              8.670E-03     8.670E-03
96  cm243..cm244      9.860E-03     8.713E-03 (-11.6%)  9.827E-03 (  -0.3%)
34  se 79              5.990E-08     7.908E-08 ( 32.0%)  7.901E-08 ( 31.9%)
38  sr 90              6.040E-02     6.363E-02 (  5.4%)  6.365E-02 (  5.4%)
43  tc 99              1.090E-05     1.527E-05 ( 40.1%)  1.537E-05 ( 41.0%)
50  sn126              2.100E-07     8.126E-07 (286.9%)  8.099E-07 (285.7%)
55  cs135              4.790E-07     5.334E-07 ( 11.4%)  5.066E-07 (  5.8%)
55  cs137              1.120E-01     1.097E-01 (  -2.0%)  1.097E-01 (  -2.1%)

endf/b-iv  %diff  for:  sas2 27-group endf/b4 library, 4-cycle case, 46.46 gwd/mtu
endf/b-ve* %diff  for:  *sas2 44-group endf/b5 (with b6: eu-154, 155) lib., 4-cyc case, 46.46 gwd/mtu

```

---

Table B.10. H. B. Robinson Assembly B05 Rod N-9, 16.02 GWd/MTU

---

h. b. robinson unit 2 pwr

measured and computed irradiated fuel composition, mg/g fuel (uo2)

atm-101, fuel assembly b0-5, rod n-9 at 11.00 cm, 16.02 gwd/mtu

run sept. 1994

\*\* case using sas2h model \*\*

nuclide, z & name	measured	endf/b-iv	%diff	endf/b-ve*	%diff
92 u235	1.070E+01	1.076E+01	( .6%)	1.084E+01	( 1.3%)
92 u236	2.190E+00	2.156E+00	( -1.5%)	2.150E+00	( -1.8%)
92 u238	8.470E+02	8.477E+02	( .1%)	8.478E+02	( .1%)
94 pu238	2.830E-02	2.871E-02	( 1.5%)	2.679E-02	( -5.3%)
94 pu239	3.640E+00	3.894E+00	( 7.0%)	3.699E+00	( 1.6%)
94 pu240	1.090E+00	1.073E+00	( -1.5%)	1.139E+00	( 4.5%)
94 pu241	3.040E-01	3.219E-01	( 5.9%)	3.059E-01	( .6%)
93 np237	1.550E-01	1.643E-01	( 6.0%)	1.451E-01	( -6.4%)

units changed: curies/ gram uo2

43 tc 99	5.440E-06	6.114E-06	( 12.4%)	6.122E-06	( 12.5%)
55 cs137	3.590E-02	3.595E-02	( .2%)	3.595E-02	( .1%)

endf/b-iv %diff for: sas2 27-group endf/b4 library, 4-cycle case, 16.02 gwd/mtu  
endf/b-ve\* %diff for: \*sas2 44-group endf/b5 (with b6: eu-154, 155) lib., 4-cyc case, 16.02 gwd/mtu

---

Table B.11. H. B. Robinson Assembly B05 Rod N-9, 23.81 GWd/MTU

---

h. b. robinson unit 2 pwr

measured and computed irradiated fuel composition, mg/g fuel (uo2)

atm-101, fuel assembly b0-5, rod n-9 at 26.0 cm, 23.81gwd/mtu

run sept. 1994

\*\* case using sas2h model \*\*

nuclide, z & name	measured	endf/b-iv	%diff	endf/b-ve*	%diff
92 u235	7.210E+00	7.312E+00	( 1.4%)	7.380E+00	( 2.4%)
92 u236	2.740E+00	2.680E+00	( -2.2%)	2.675E+00	( -2.4%)
92 u238	8.470E+02	8.419E+02	( -.6%)	8.420E+02	( -.6%)
94 pu238	6.950E-02	7.012E-02	( .9%)	6.595E-02	( -5.1%)
94 pu239	4.020E+00	4.331E+00	( 7.7%)	4.092E+00	( 1.8%)
94 pu240	1.670E+00	1.601E+00	( -4.2%)	1.691E+00	( 1.3%)
94 pu241	5.040E-01	5.340E-01	( 6.0%)	5.040E-01	( .0%)
93 np237	2.600E-01	2.744E-01	( 5.5%)	2.446E-01	( -5.9%)

units changed: curies/ gram uo2

43 tc 99	8.090E-06	8.782E-06	( 8.6%)	8.806E-06	( 8.9%)
55 cs137	5.390E-02	5.345E-02	( -.8%)	5.344E-02	( -.9%)

endf/b-iv %diff for: sas2 27-group endf/b4 library, 4-cycle case, 23.81 gwd/mtu  
endf/b-ve\* %diff for: \*sas2 44-group endf/b5 (with b6: eu-154, 155) lib., 4-cyc case, 23.81 gwd/mtu

---

Table B.12. H. B. Robinson Assembly B05 Rod N-9, 28.47 GWd/MTU

---

h. b. robinson unit 2 pwr

measured and computed irradiated fuel composition, mg/g fuel (uo2)

atm-101, fuel assembly b0-5, rod n-9 at 199.0 cm, 28.47gwd/mtu

run sept. 1994

\*\* case using sas2h model \*\*

nuclide, z & name	measured	endf/b-iv	%diff	endf/b-ve*	%diff
92 u235	6.180E+00	5.880E+00	( -4.9%)	5.940E+00	( -3.9%)
92 u236	2.820E+00	2.883E+00	( 2.2%)	2.880E+00	( 2.1%)
92 u238	8.340E+02	8.379E+02	( .5%)	8.380E+02	( .5%)
94 pu238	1.140E-01	1.066E-01	( -6.5%)	1.004E-01	(-11.9%)
94 pu239	4.390E+00	4.625E+00	( 5.3%)	4.366E+00	( -.5%)
94 pu240	1.970E+00	1.873E+00	(-4.9%)	1.974E+00	( .2%)
94 pu241	6.810E-01	6.844E-01	( .5%)	6.442E-01	(-5.4%)
93 np237	3.040E-01	3.474E-01	( 14.3%)	3.107E-01	( 2.2%)

units changed: curies/ gram uo2

43 tc 99	8.950E-06	1.026E-05	( 14.6%)	1.030E-05	( 15.1%)
55 cs137	6.270E-02	6.512E-02	( 3.9%)	6.510E-02	( 3.8%)

endf/b-iv %diff for: sas2 27-group endf/b4 library, 4-cycle case, 28.47 gwd/mtu  
endf/b-ve\* %diff for: \*sas2 44-group endf/b5 (with b6: eu-154, 155) lib., 4-cyc case, 28.47 gwd/mtu

---

Table B.13. H. B. Robinson Assembly B05 Rod N-9, 31.66 GWd/MTU

---

h. b. robinson unit 2 pwr

measured and computed irradiated fuel composition, mg/g fuel (uo2)

atm-101, fuel assembly b0-5, rod n-9 at 226.0 cm, 31.66gwd/mtu

run sept. 1994

\*\* case using sas2h model \*\*

nuclide, z & name	measured	endf/b-iv	%diff	endf/b-ve*	%diff
92 u235	4.860E+00	5.022E+00	( 3.3%)	5.077E+00	( 4.5%)
92 u236	3.000E+00	2.988E+00	( -.4%)	2.986E+00	( -.5%)
92 u238	8.420E+02	8.352E+02	( -.8%)	8.353E+02	( -.8%)
94 pu238	1.300E-01	1.333E-01	( 2.6%)	1.256E-01	(-3.4%)
94 pu239	4.200E+00	4.739E+00	( 12.8%)	4.472E+00	( 6.5%)
94 pu240	2.120E+00	2.032E+00	(-4.1%)	2.139E+00	( .9%)
94 pu241	6.920E-01	7.551E-01	( 9.1%)	7.094E-01	( 2.5%)
93 np237	3.330E-01	3.944E-01	( 18.4%)	3.531E-01	( 6.0%)

units changed: curies/ gram uo2

43 tc 99	1.010E-05	1.124E-05	( 11.2%)	1.129E-05	( 11.8%)
55 cs137	7.130E-02	7.240E-02	( 1.5%)	7.237E-02	( 1.5%)

endf/b-iv %diff for: sas2 27-group endf/b4 library, 4-cycle case, 31.66 gwd/mtu  
endf/b-ve\* %diff for: \*sas2 44-group endf/b5 (with b6: eu-154, 155) lib., 4-cyc case, 31.66 gwd/mtu

---

Table B.14. Obrigheim (KWO) Assembly 170 Batch 94, 25.93 GWd/MTU

---

obrigheim (kwo) pwr (germany)

measured and computed irradiated fuel composition, mg/g fuel (u)

fuel assembly 170, batch 94, 25.93 gwd/mtu

(run sept. 1994)

..compares cases using endf/b-iv and endf/b-v(eu)\* libraries..

nuclide, z & name	measured	endf/b-iv	%diff	endf/b-ve*	%diff
92 u235	1.095E+01	1.059E+01	( -3.3%)	1.068E+01	( -2.5%)
92 u236	3.590E+00	3.628E+00	( 1.0%)	3.621E+00	( -.9%)
94 pu238	8.010E-02*	8.518E-02	( 6.3%)	8.095E-02	( 1.1%)
94 pu239	4.805E+00	5.098E+00	( 6.1%)	4.828E+00	( .5%)
94 pu240	1.800E+00	1.705E+00	( -5.3%)	1.811E+00	( .6%)
94 pu241	9.780E-01	1.051E+00	( 7.5%)	9.924E-01	( 1.5%)
94 pu242	3.120E-01	2.749E-01	(-11.9%)	3.071E-01	( -1.6%)
96 cm242	1.710E-02	1.327E-02	(-22.4%)	1.222E-02	(-28.5%)
96 cm244	1.030E-02	7.756E-03	(-24.7%)	9.373E-03	( -9.0%)
units changed: atomic ratio					
36 kr 83/kr 86	2.520E-01	2.397E-01	( -4.9%)	2.397E-01	( -4.9%)
36 kr 84/kr 86	6.400E-01	6.171E-01	( -3.6%)	6.177E-01	( -3.5%)
54 xe131/xe134	3.080E-01	3.123E-01	( 1.4%)	3.042E-01	( -1.2%)
54 xe132/xe134	7.060E-01	6.837E-01	(-3.2%)	6.928E-01	(-1.9%)
54 xe136/xe134	1.483E+00	1.460E+00	( -1.5%)	1.473E+00	( -.7%)
55 cs134/cs137	7.330E-02	7.119E-02	( -2.9%)	6.870E-02	( -6.3%)
60 nd143/nd148	2.450E+00	2.419E+00	( -1.3%)	2.404E+00	( -1.9%)
60 nd145/nd148	1.938E+00	1.974E+00	( 1.9%)	1.964E+00	( 1.4%)
60 nd146/nd148	1.857E+00	1.857E+00	( .0%)	1.864E+00	( .4%)

\* corrected for the measured discharged component from cm-242, which was measured only by european institute for transuranic elements.

endf/b-iv %diff for: sas2 27-group endf/b4 lib, 3-cycle case, 25.93 gwd/mtu  
endf/b-ve\* %diff for: \*sas2 44-group endf/b5 (with b6: eu-154, 155) lib., 3-cyc case, 25.93 gwd/mtu

---

Table B.15. Obrigheim (KWO) Assembly 172 Batch 92, 26.54 GWd/MTU

---

```

      obligheim (kwo) pwr (germany)
measured and computed irradiated fuel composition, mg/g fuel (u)
      fuel assembly 172, batch 92, 26.54 gwd/mtu
      (run sept. 1994)
      ..compares cases using endf/b-iv and endf/b-v(eu)* libraries..
nuclide, z & name      measured      endf/b-iv      %diff      endf/b-ve*      %diff
92  u235      1.058E+01      1.029E+01      (-2.8%)      1.037E+01      (-2.0%)
92  u236      3.620E+00      3.672E+00      ( 1.4%)      3.666E+00      ( 1.3%)
94  pu238      8.890E-02*      9.142E-02      ( 2.8%)      8.686E-02      (-2.3%)
94  pu239      4.713E+00      5.122E+00      ( 8.7%)      4.849E+00      ( 2.9%)
94  pu240      1.830E+00      1.755E+00      (-4.1%)      1.862E+00      ( 1.7%)
94  pu241      9.780E-01      1.073E+00      ( 9.7%)      1.013E+00      ( 3.6%)
94  pu242      3.280E-01      2.886E-01     (-12.0%)      3.223E-01      (-1.7%)
96  cm242      1.940E-02      1.482E-02     (-23.6%)      1.370E-02     (-29.4%)
96  cm244      1.160E-02      8.854E-03     (-23.7%)      1.067E-02      (-8.1%)

units changed: atomic ratio
36  kr 83/kr 86  2.450E-01      2.387E-01      (-2.6%)      2.386E-01      (-2.6%)
36  kr 84/kr 86  6.400E-01      6.189E-01      (-3.3%)      6.194E-01      (-3.2%)
54  xe131/xe134  3.040E-01      3.104E-01      ( 2.1%)      3.021E-01      (-.6%)
54  xe132/xe134  7.100E-01      6.865E-01      (-3.3%)      6.957E-01      (-2.0%)
54  xe136/xe134  1.490E+00      1.464E+00      (-1.8%)      1.477E+00      (-.9%)
55  cs134/cs137  7.260E-02      7.246E-02      (-.2%)      6.993E-02      (-3.7%)
60  nd143/nd148  2.450E+00      2.396E+00      (-2.2%)      2.381E+00      (-2.8%)
60  nd145/nd148  1.950E+00      1.968E+00      (  .9%)      1.958E+00      (  .4%)
60  nd146/nd148  1.876E+00      1.860E+00      (-.8%)      1.868E+00      (-.4%)

* corrected for the measured discharged component from cm-242, which was
  measured only by european institute for transuranic elements.

endf/b-iv  %diff for: sas2 27-group endf/b4 lib, 3-cycle case, 26.54 gwd/mtu
endf/b-ve* %diff for: *sas2 44-group endf/b5 (with b6: eu-154, 155) lib., 3-cyc case, 26.54 gwd/mtu

```

---



Table B.16. Obrigheim (KWO) Assembly 176 Batch 91, 27.99 Gwd/MTU

---

```

      obrigheim (kwo) pwr (germany)
measured and computed irradiated fuel composition, mg/g fuel (u)
      fuel assembly 176, batch 91, 27.99 gwd/mtu
      (run sept. 1994)
      ..compares cases using endf/b-iv and endf/b-v(eu)* libraries..
nuclide, z & name      measured      endf/b-iv      %diff      endf/b-ve*      %diff
92  u235      9.850E+00      9.598E+00      (-2.6%)      9.684E+00      (-1.7%)
92  u236      3.700E+00      3.767E+00      ( 1.8%)      3.762E+00      ( 1.7%)
94  pu238      9.480E-02*     1.028E-01      ( 8.4%)      9.776E-02      ( 3.1%)
94  pu239      4.925E+00      5.171E+00      ( 5.0%)      4.893E+00      (-.7%)
94  pu240      1.920E+00      1.835E+00      (-4.4%)      1.947E+00      ( 1.4%)
94  pu241      1.058E+00      1.136E+00      ( 7.4%)      1.071E+00      ( 1.2%)
94  pu242      3.720E-01      3.298E-01     (-11.3%)      3.679E-01      (-1.1%)
96  cm242      1.850E-02      1.602E-02     (-13.4%)      1.477E-02     (-20.2%)
96  cm244      1.410E-02      1.131E-02     (-19.8%)      1.358E-02      (-3.7%)

units changed: atomic ratio
36  kr 83/kr 86  2.310E-01      2.362E-01      ( 2.2%)      2.362E-01      ( 2.2%)
36  kr 84/kr 86  6.300E-01      6.230E-01      (-1.1%)      6.235E-01      (-1.0%)
54  xe131/xe134  2.970E-01      3.072E-01      ( 3.4%)      2.985E-01      (  .5%)
54  xe132/xe134  7.140E-01      6.932E-01      (-2.9%)      7.029E-01      (-1.6%)
54  xe136/xe134  1.505E+00      1.475E+00      (-2.0%)      1.488E+00      (-1.1%)
55  cs134/cs137  7.820E-02      7.511E-02      (-4.0%)      7.246E-02      (-7.3%)
60  nd143/nd148  2.350E+00      2.355E+00      (  .2%)      2.340E+00      (-.4%)
60  nd145/nd148  1.915E+00      1.952E+00      ( 1.9%)      1.941E+00      ( 1.4%)
60  nd146/nd148  1.851E+00      1.867E+00      (  .9%)      1.875E+00      ( 1.3%)

* corrected for the measured discharged component from cm-242, which was
  measured only by european institute for transuranic elements.

endf/b-iv  %diff for: sas2 27-group endf/b4 lib, 3-cycle case, 27.99 gwd/mtu
endf/b-ve* %diff for: *sas2 44-group endf/b5 (with b6: eu-154, 155) lib., 3-cyc case, 27.99 gwd/mtu

```

---

Table B.17. Obrigheim (KWO) Assembly 168 Batch 86, 28.40 GWd/MTU

---

```

    obrigheim (kwo) pwr (germany)
measured and computed irradiated fuel composition, mg/g fuel (u)
    fuel assembly 168, batch 86, 28.40 gwd/mtu
        (run sept. 1994)
    ..compares cases using endf/b-iv and endf/b-v(eu)* libraries..
nuclide, z & name      measured  endf/b-iv  %diff  endf/b-ve*  %diff
 92  u235              9.680E+00  9.415E+00 (-2.7%)  9.501E+00 (-1.9%)
 92  u236              3.730E+00  3.792E+00 ( 1.7%)  3.787E+00 ( 1.5%)
 94  pu238             1.054E-01* 1.059E-01 (  .5%)  1.007E-01 (-4.4%)
 94  pu239             5.013E+00  5.188E+00 ( 3.5%)  4.909E+00 (-2.1%)
 94  pu240             2.020E+00  1.856E+00 (-8.1%)  1.969E+00 (-2.5%)
 94  pu241             1.103E+00  1.156E+00 ( 4.8%)  1.090E+00 (-1.2%)
 94  pu242             4.070E-01  3.422E-01 (-15.9%)  3.817E-01 (-6.2%)
 96  cm242             2.010E-02  1.638E-02 (-18.5%)  1.509E-02 (-24.9%)
 96  cm244             1.580E-02  1.208E-02 (-23.5%)  1.450E-02 (-8.2%)

units changed: atomic ratio
 36  kr 83/kr 86      2.480E-01  2.355E-01 (-5.0%)  2.355E-01 (-5.0%)
 36  kr 84/kr 86      6.500E-01  6.241E-01 (-4.0%)  6.247E-01 (-3.9%)
 54  xe131/xe134      3.060E-01  3.062E-01 (  .1%)  2.974E-01 (-2.8%)
 54  xe132/xe134      7.450E-01  6.950E-01 (-6.7%)  7.047E-01 (-5.4%)
 54  xe136/xe134      1.470E+00  1.479E+00 (  .6%)  1.492E+00 ( 1.5%)
 55  cs134/cs137      7.600E-02  7.620E-02 (  .3%)  7.350E-02 (-3.3%)
 60  nd143/nd148      2.330E+00  2.342E+00 (  .5%)  2.327E+00 (-.1%)
 60  nd145/nd148      1.910E+00  1.947E+00 ( 1.9%)  1.936E+00 ( 1.4%)
 60  nd146/nd148      1.850E+00  1.869E+00 ( 1.0%)  1.877E+00 ( 1.5%)

* corrected for the measured discharged component from cm-242, which was
measured only by european institute for transuranic elements.

endf/b-iv  %diff for: sas2 27-group endf/b4 lib, 3-cycle case, 28.40 gwd/mtu
endf/b-ve* %diff for: *sas2 44-group endf/b5 (with b6: eu-154, 155) lib., 3-cyc case, 28.40 gwd/mtu

```

---

Table B.18. Obrigheim (KWO) Assembly 171 Batch 89, 29.04 GWd/MTU

---

```

      obligheim (kwo) pwr (germany)
measured and computed irradiated fuel composition, mg/g fuel (u)
      fuel assembly 171, batch 89, 29.04 gwd/mtu
      (run sept. 1994)
      ..compares cases using endf/b-iv and endf/b-v(eu)* libraries..
nuclide, z & name      measured      endf/b-iv      %diff      endf/b-ve*      %diff
92  u235      9.580E+00      9.129E+00      (-4.7%)      9.213E+00      (-3.8%)
92  u236      3.750E+00      3.830E+00      ( 2.1%)      3.826E+00      ( 2.0%)
94  pu238      1.013E-01*     1.114E-01      (10.0%)      1.060E-01      ( 4.7%)
94  pu239      4.957E+00      5.210E+00      ( 5.1%)      4.929E+00      (-.6%)
94  pu240      2.000E+00      1.892E+00      (-5.4%)      2.007E+00      (.3%)
94  pu241      1.107E+00      1.184E+00      ( 7.0%)      1.115E+00      (.7%)
94  pu242      4.050E-01      3.611E-01     (-10.8%)      4.026E-01      (-.6%)
96  cm242      2.080E-02      1.716E-02     (-17.5%)      1.582E-02     (-23.9%)
96  cm244      1.690E-02      1.344E-02     (-20.5%)      1.611E-02      (-4.7%)

units changed: atomic ratio
36  kr 83/kr 86  2.380E-01      2.344E-01      (-1.5%)      2.344E-01      (-1.5%)
36  kr 84/kr 86  6.300E-01      6.259E-01      (-.6%)      6.265E-01      (-.6%)
54  xe131/xe134  2.860E-01      3.045E-01      ( 6.5%)      2.956E-01      ( 3.3%)
54  xe132/xe134  7.050E-01      6.978E-01      (-1.0%)      7.078E-01      (.4%)
54  xe136/xe134  1.540E+00      1.484E+00      (-3.6%)      1.497E+00      (-2.8%)
55  cs134/cs137  7.700E-02      7.771E-02      (.9%)      7.494E-02      (-2.7%)
60  nd143/nd148  2.350E+00      2.322E+00      (-1.2%)      2.306E+00      (-1.9%)
60  nd145/nd148  1.920E+00      1.939E+00      ( 1.0%)      1.928E+00      (.4%)
60  nd146/nd148  1.873E+00      1.871E+00      (-.1%)      1.880E+00      (.4%)

* corrected for the measured discharged component from cm-242, which was
  measured only by european institute for transuranic elements.

endf/b-iv      %diff for: sas2 27-group endf/b4 lib, 3-cycle case, 29.04 gwd/mtu
endf/b-ve*     %diff for: *sas2 44-group endf/b5 (with b6: eu-154, 155) lib., 3-cyc case, 29.04 gwd/mtu

```

---

Table B.19. Obrigheim (KWO) Assembly 176 Batch 90, 29.52 GWd/MTU

---

```

      obrigheim (kwo) pwr (germany)
measured and computed irradiated fuel composition, mg/g fuel (u)
      fuel assembly 176, batch 90, 29.52 gwd/mtu
      (run sept. 1994)
      ..compares cases using endf/b-iv and endf/b-v(eu)* libraries..
nuclide, z & name      measured      endf/b-iv      %diff      endf/b-ve*      %diff
 92  u235              9.180E+00      8.917E+00      (-2.9%)      9.000E+00      (-2.0%)
 92  u236              3.810E+00      3.859E+00      ( 1.3%)      3.854E+00      ( 1.2%)
 94  pu238             1.071E-01*     1.159E-01      ( 8.2%)      1.103E-01      ( 3.0%)
 94  pu239             4.943E+00      5.224E+00      ( 5.7%)      4.941E+00      (  .0%)
 94  pu240             2.040E+00      1.921E+00      (-5.8%)      2.037E+00      (-.1%)
 94  pu241             1.128E+00      1.204E+00      ( 6.7%)      1.133E+00      (  .5%)
 94  pu242             4.380E-01      3.745E-01     (-14.5%)      4.175E-01      (-4.7%)
 96  cm242             2.150E-02      1.791E-02     (-16.7%)      1.654E-02     (-23.1%)
 96  cm244             1.920E-02      1.458E-02     (-24.1%)      1.745E-02      (-9.1%)

units changed:  atomic ratio
 36  kr 83/kr 86      2.410E-01      2.336E-01      (-3.1%)      2.335E-01      (-3.1%)
 36  kr 84/kr 86      6.600E-01      6.273E-01      (-5.0%)      6.279E-01      (-4.9%)
 54  xe131/xe134      2.920E-01      3.031E-01      ( 3.8%)      2.940E-01      (  .7%)
 54  xe132/xe134      7.200E-01      6.999E-01      (-2.8%)      7.099E-01      (-1.4%)
 54  xe136/xe134      1.520E+00      1.488E+00      (-2.1%)      1.500E+00      (-1.3%)
 55  cs134/cs137      7.940E-02      7.908E-02      (-.4%)      7.626E-02      (-4.0%)
 60  nd143/nd148      2.340E+00      2.305E+00      (-1.5%)      2.289E+00      (-2.2%)
 60  nd145/nd148      1.920E+00      1.934E+00      (  .7%)      1.923E+00      (  .2%)
 60  nd146/nd148      1.865E+00      1.874E+00      (  .5%)      1.883E+00      ( 1.0%)

* corrected for the measured discharged component from cm-242, which was
  measured only by european institute for transuranic elements.

endf/b-iv  %diff for: sas2 27-group endf/b4 lib, 3-cycle case, 29.52 gwd/mtu
endf/b-ve* %diff for: *sas2 44-group endf/b5 (with b6: eu-154, 155) lib., 3-cyc case, 29.52 gwd/mtu

```

---

## APPENDIX C

### INDIVIDUAL LABORATORY OBRIGHEIM FUEL ISOTOPIC MEASUREMENTS, AVERAGES, AND $1\sigma$ IN ESTIMATE OF AVERAGES

The Obrigheim PWR spent fuel compositions, as read by the author from the plots given in ref. 16, are tabulated in Tables C.1, C.2, and C.4 through C.7, inclusive. The density data were converted by the laboratories from values at the analysis date to values at the discharge or unloading date, with one exception. Two of the three laboratories reporting  $^{238}\text{Pu}$  data did not measure  $^{242}\text{Cm}$ , which is required in the adjustment of  $^{238}\text{Pu}$  density to the unloading date density. However, the necessary adjustment was made by the author, applying the single set of  $^{242}\text{Cm}$  data available before tabulating the  $^{238}\text{Pu}$  data for the other two laboratories in Table C.3.

The acronyms listed in the tables for the names of the laboratories conducting the analyses are: TUI, European Institute for Transuranic Elements; IAEA, International Atomic Energy Agency; WAK, Karlsruhe Reprocessing Plant; and IRCH, Institute of Radiochemistry.

Averages from this appendix are listed in Table 32. Data for  $^{242}\text{Cm}$  and  $^{244}\text{Cm}$  and fission-product ratios (Tables 32 and 33) are not listed in this appendix because the isotopic analyses were performed only at TUI. The data for  $^{241}\text{Am}$  and  $^{243}\text{Am}$  were not used because there was significant interference from the alpha spectrum of  $^{238}\text{Pu}$  in determining  $^{241}\text{Am}$  data and the ratio of  $^{243}\text{Am}/^{241}\text{Am}$  was used in deriving  $^{243}\text{Am}$  data.<sup>16</sup>

Table C.1. Obrigheim fuel composition measurements, their averages, and  $1\sigma$  in the averages for  $^{235}\text{U}$  (milligrams/gram U)

isotope: u235							
Assembly number	170	172	176	168	171	176	
Batch number	94	92	91	86	89	90	
Laboratory							average
TUI	11.30	10.70	9.80	9.60	9.60	9.10	
IAEA	10.80	10.60	9.80	9.70	9.50	9.20	
WAK	10.90	10.40	9.90	9.70	9.60	9.20	
IRCH	10.80	10.60	9.90	9.70	9.60	9.20	
Average	10.950	10.575	9.850	9.675	9.575	9.175	
Sigma (in avg.)	0.119	0.063	0.029	0.025	0.025	0.025	0.048
Sigma, %	1.1	0.6	0.3	0.3	0.3	0.3	0.5

Table C.2. Obrigheim fuel composition measurements, their averages, and  $1\sigma$  in the averages for  $^{236}\text{U}$

isotope: u236							
Assembly number	170	172	176	168	171	176	
Batch number	94	92	91	86	89	90	
Laboratory							average
TUI	3.61	3.69	3.70	3.72	3.74	3.83	
IAEA	3.57	3.60	3.68	3.73	3.76	3.78	
WAK	3.57	3.56	3.66	3.75	3.75	3.75	
IRCH	3.62	3.64	3.74	--	3.76	3.86	
Average	3.592	3.623	3.695	3.733	3.753	3.805	
Sigma (in avg.)	0.013	0.028	0.017	0.009	0.005	0.025	0.016
Sigma, %	0.4	0.8	0.5	0.2	0.1	0.6	0.4

Table C.3. Obrigheim fuel composition measurements, their averages, and 1  $\sigma$  in the averages for  $^{238}\text{Pu}$  (milligrams/gram U)

isotope: pu238							
Assembly number	170	172	176	168	171	176	
Batch number	94	92	91	86	89	90	
Laboratory							average
TUI	0.0820	0.0840	0.0970	0.1190	0.1060	0.1150	
IAEA	0.0861	0.0938	0.1067	0.1111	0.1144	0.1187	
WAK	0.0721	--	0.0807	0.0861	0.0834	0.0877	
Average	0.0801	0.0889	0.0948	0.1054	0.1013	0.1071	
Sigma (in avg)	0.0042	0.0049	0.0076	0.0099	0.0093	0.0098	0.0076
Sigma, %	5.2	5.5	8.0	9.4	9.1	9.1	7.7

Table C.4. Obrigheim fuel composition measurements, their averages, and 1  $\sigma$  in the averages for  $^{239}\text{Pu}$  (milligrams/gram U)

isotope: pu239							
Assembly number	170	172	176	168	171	176	
Batch number	94	92	91	86	89	90	
Laboratory							average
TUI	4.91	4.76	4.96	5.06	5.00	5.00	
IAEA	4.83	4.78	4.87	5.08	5.04	4.91	
WAK	4.58	4.49	4.83	4.90	4.83	4.80	
IRCH	4.90	4.82	5.04	--	--	5.06	
Average	4.805	4.713	4.925	5.013	4.957	4.943	
Sigma (in avg.)	0.077	0.075	0.047	0.057	0.064	0.057	0.063
Sigma, %	1.6	1.6	1.0	1.1	1.3	1.1	1.3

Table C.5. Obrigheim fuel composition measurements, their averages, and 1  $\sigma$  in the averages for  $^{240}\text{Pu}$  (milligrams/gram U)

isotope: pu240							
Assembly number	170	172	176	168	171	176	
Batch number	94	92	91	86	89	90	
Laboratory							average
TUI	1.83	1.91	1.93	2.08	2.01	2.05	
IAEA	1.80	1.84	1.90	2.03	2.03	2.03	
WAK	1.72	1.73	1.88	1.96	1.95	1.99	
IRCH	1.84	1.85	1.97	--	--	2.07	
Average	1.798	1.832	1.920	2.023	1.997	2.035	
Sigma (in avg)	0.027	0.037	0.020	0.035	0.024	0.017	0.027
Sigma, %	1.5	2.0	1.0	1.7	1.2	0.8	1.4

Table C.6. Obrigheim fuel composition measurements, their averages, and 1  $\sigma$  in the averages for  $^{241}\text{Pu}$  (milligrams/gram U)

isotope: pu241							
Assembly number	170	172	176	168	171	176	
Batch number	94	92	91	86	89	90	
Laboratory							average
TUI	1.000	0.970	1.060	1.130	1.120	1.140	
IAEA	0.970	0.990	1.050	1.110	1.130	1.120	
WAK	0.950	0.940	1.040	1.070	1.070	1.100	
IRCH	0.990	1.010	1.080	--	--	1.150	
Average	0.9775	0.9775	1.0575	1.1033	1.1067	1.1275	
Sigma (in avg.)	0.0111	0.0149	0.0085	0.0176	0.0186	0.0111	0.0136
Sigma, %	1.1	1.5	0.8	1.6	1.7	1.0	1.3



Table C.7. Obrigheim fuel composition measurements, their averages, and 1  $\sigma$  in the averages for  $^{242}\text{Pu}$  (milligrams/gram U)

isotope: pu242							
Assembly number	170	172	176	168	171	176	
Batch number	94	92	91	86	89	90	
Laboratory							average
TUI	0.320	0.325	0.376	0.397	0.412	0.435	
IAEA	0.310	0.330	0.362	0.390	0.408	0.420	
WAK	0.303	0.320	0.370	0.435	0.390	0.465	
IRCH	0.315	0.335	0.378	--	0.410	0.430	
Average	0.3120	0.3275	0.3715	0.4073	0.4050	0.4375	
Sigma (in avg.)	0.0036	0.0032	0.0036	0.0140	0.0051	0.0097	0.0065
Sigma, %	1.2	1.0	1.0	3.4	1.3	2.2	1.7



## APPENDIX D

### STATISTICAL DATA ANALYSIS OF SAS2H PREDICTIONS VS MEASUREMENTS

SCALE fuel depletion isotopic predictions were compared with radiochemical analyses as percentage differences of the computed minus the measured results. These comparisons for each benchmark case are listed in detail in the body of the report. The individual percentage differences of all cases, or samples, provided data for the statistical analyses shown in Tables D.1 and D.2. Densities of isotopes or isobars were analyzed by both radiochemistry and SCALE/SAS2H calculations for 3 to 19 cases, depending on the component. The statistical analysis determined the standard deviation in the estimate of the average and the standard deviation in the population of the individual values. Results are listed for each nuclide or isobar as the average and  $1\sigma$  values for cases computed with actinide cross sections processed from ENDF/B Versions IV and V in Tables D.1 and D.2, respectively.

The formula used for the standard deviation in the estimate of the average  $X_{ave}$  of the N data points  $X_i$  is

$$\sigma(X_{ave}) = \left[ \frac{\sum_{i=1}^N (X_i - X_{ave})^2}{N(N-1)} \right]^{\frac{1}{2}}, \quad (D.1)$$

where

$$X_{ave} = \frac{\sum_{i=1}^N X_i}{N}. \quad (D.2)$$

Also, the equation used for the standard deviation in the individual  $X_i$  taken from the population of N data points is

$$\sigma(X_i) = \left[ \frac{\sum_{i=1}^N (X_i - X_{ave})^2}{N-1} \right]^{\frac{1}{2}}. \quad (D.3)$$

Table D.1. Statistics for SAS2H vs measurements, actinide data from ENDF/B-IV

		For 3 to 19 irradiation cases Cross-section source: SCALE 27-group ENDF/B-IV			
		Percentage difference			
Nuclide or isobar	Cases	Average	1 $\sigma$ of estimate of average	1 $\sigma$ of individual data points	
1	C14	3	-14.2	4.8	8.4
2	Se79	9	14.1	3.9	11.8
3	Sr90	9	6.1	0.4	1.2
4	Tc99	13	15.8	4.4	15.9
5	Sn126	6	230.3	20.2	49.6
6	I129	3	-10.8	2.5	4.4
7	Cs133	3	1.9	0.4	0.7
8	Cs134	3	-8.1	4.7	8.2
9	Cs135	9	10.9	1.1	3.4
10	Cs137	13	0.9	0.4	1.6
11	Nd143	3	1.3	0.2	0.3
12	Nd144	3	0.1	0.2	0.3
13	Nd145	3	0.4	0.1	0.2
14	Nd146	3	0.4	0.0	0.1
15	Nd148	3	0.3	0.1	0.2
16	Nd150	3	3.2	0.5	0.9
17	Pm147..Sm147	3	-4.5	1.4	2.5
18	Sm148	3	-15.9	1.1	2.0
19	Sm149	3	-30.3	7.4	12.7
20	Sm150	3	-0.5	2.8	4.8
21	Sm152	3	17.3	2.8	4.9
22	Sm151..Eu151	3	26.1	7.0	12.1
23	Eu153	3	-4.8	2.8	4.9
24	Sm154..Gd154	3	30.8	4.9	8.5
25	Eu155..Gd155	3	96.0	9.3	16.1
26	U234	9	4.7	5.3	15.8
27	U235	19	-2.9	0.7	3.3
28	U236	19	0.7	0.4	1.6
29	U238	13	-0.6	0.2	0.6
30	Np237	13	19.2	3.3	12.1
31	Pu238	19	0.7	1.5	6.4
32	Pu239	19	5.3	0.9	3.7
33	Pu240	19	-5.8	0.4	1.7
34	Pu241	19	5.0	0.7	2.9
35	Pu242	15	-10.3	0.9	3.5
36	Am241	9	-5.9	3.7	11.1
37	Cm242	6	-18.7	1.5	3.8
38	Cm243..Cm244	15	-18.6	1.5	5.9

Table D.2. Statistics for SAS2H vs measurements, actinide data from ENDF/B-V

For 3 to 19 irradiation cases					
Cross-section source: special 44-group, ENDF/B-V					
(with Eu-154 and Eu-155 from ENDF/B-VI)					
		Percentage difference			
Nuclide or isobar	Cases	Average	1 $\sigma$ of estimate of average	1 $\sigma$ of individual data points	
1	C14	3	-13.8	4.8	8.4
2	Se79	9	14.0	3.9	11.8
3	Sr90	9	6.0	0.4	1.2
4	Tc99	13	16.3	4.5	16.1
5	Sn126	6	229.8	20.0	48.9
6	I129	3	-10.8	2.5	4.4
7	Cs133	3	2.5	0.5	0.9
8	Cs134	3	-11.4	4.6	7.9
9	Cs135	9	5.7	1.1	3.3
10	Cs137	13	0.8	0.4	1.6
11	Nd143	3	0.4	0.2	0.3
12	Nd144	3	0.5	0.1	0.2
13	Nd145	3	-0.3	0.2	0.4
14	Nd146	3	1.1	0.1	0.1
15	Nd148	3	0.4	0.1	0.1
16	Nd150	3	3.4	0.5	0.9
17	Pm147..Sm14	3	-2.8	1.2	2.0
18	Sm148	3	-16.9	1.1	1.9
19	Sm149	3	-35.9	6.7	11.6
20	Sm150	3	-1.5	2.8	4.8
21	Sm152	3	20.2	2.9	5.0
22	Sm151..Eu151	3	28.1	6.8	11.8
23	Eu153	3	5.0	3.2	5.5
24	Sm154..Gd154	3	-2.1	2.4	4.2
25	Eu155..Gd155	3	-24.4	1.9	3.3
26	U234	9	1.8	5.1	15.3
27	U235	19	-1.9	0.8	3.3
28	U236	19	0.6	0.4	1.6
29	U238	13	-0.6	0.2	0.6
30	Np237	13	6.4	3.0	10.7
31	Pu238	19	-4.6	1.4	6.2
32	Pu239	19	-0.6	0.8	3.5
33	Pu240	19	-0.3	0.4	1.9
34	Pu241	19	-1.2	0.6	2.7
35	Pu242	15	-0.2	1.0	3.9
36	Am241	9	-11.0	3.5	10.6
37	Cm242	6	-25.0	1.4	3.5
38	Cm243..Cm244	15	-4.2	1.3	5.1



## APPENDIX E

### MISCELLANEOUS SPATIAL FACTORS AFFECTING ASSEMBLY AVERAGED RESULTS

Final assembly densities of the SCALE depletion sequence are derived from cross sections integrated over space- and energy-dependent flux. Thus, space-dependent densities are not explicitly computed. Note that if nuclide densities vary from one rod to another for equal burnups (i.e., the fissions within a fuel pellet as determined by  $^{148}\text{Nd}$  analysis), the variation would also be reflected in differences between computed average values and measured values of a fuel pellet at a specified location. Similarly, it is also important to note systematic variations in the computed vs measured comparisons with axial location. These effects arise due to the lack of an assumed uniform axial distribution of nuclides and the resulting spectral variations.

Random errors in the computational model, the specified reactor parameter input (e.g., material densities, temperatures, power histories, and burnup) and the radiochemical analysis contribute to fluctuations in the differences between the measured and calculated values of a nuclide composition. However, for completeness, this appendix seeks to evaluate the significance of other conditions that are not taken into account in the SCALE calculational model which might cause the variations encountered.

Conditions related to the following topics will be discussed:

1. radial variation in  $^{239}\text{Pu}$ ,
2. axial variation in  $^{239}\text{Pu}$ ,
3. secondary effects of variation in  $^{239}\text{Pu}$  on  $^{235}\text{U}$ , and
4. other significant differences in comparisons.

#### E.1 RADIAL VARIATION IN $^{239}\text{Pu}$

The objective of this investigation is to determine whether the production rate of  $^{239}\text{Pu}$  changes significantly with the fuel rod distance from the nearest guide tube for equivalent burnups within a given assembly. It will be assumed that burnup and isotopic densities remain constant in the radial direction (i.e., between rods at equal heights). Although it will be shown that this constant density assumption is not true, once a first-order calculation of the production rate correction of  $^{239}\text{Pu}$  is estimated, the objective is accomplished.

The production rate of  $^{239}\text{Pu}$  is assumed to be proportional to the  $(n,\gamma)$  reaction rate of  $^{238}\text{U}$  because the  $^{239}\text{U}$  and  $^{239}\text{Np}$  in the decay chain producing  $^{239}\text{Pu}$  have short half-lives. To obtain the same burnup requires that the specific powers be equal over the same time interval. The constant power, P (MW/unit of fuel), can be converted to flux for the fissionable nuclides of weight  $X_i$ (gram-atoms) and fission cross section  $\sigma_{f,i}$  (see Sect. F7.2.5, ref. 1) by

$$\phi = \frac{3.125 \times 10^{16} P}{\sum_i X_i \sigma_{f,i}} = \frac{K}{N_{\text{U}235} \sigma(n,f)_{\text{U}235}}, \quad (\text{E.1})$$

where  $K$  is a constant because cycle power is kept constant. Note that in the example, all the fissioning is assumed to be produced by  $^{235}\text{U}$ ; this simplification is believed to have no effect on the basic conclusion. Also, consider only the example in which all rods within the assembly have the same composition ( $^{235}\text{U}$  enrichment). The  $^{238}\text{U}$  ( $n,\gamma$ ) reaction rate,  $R$ , which essentially equals the  $^{239}\text{Pu}$  production rate, by definition is

$$R = N_{\text{U}238} \sigma(n,\gamma)_{\text{U}238} \phi . \quad (\text{E.2})$$

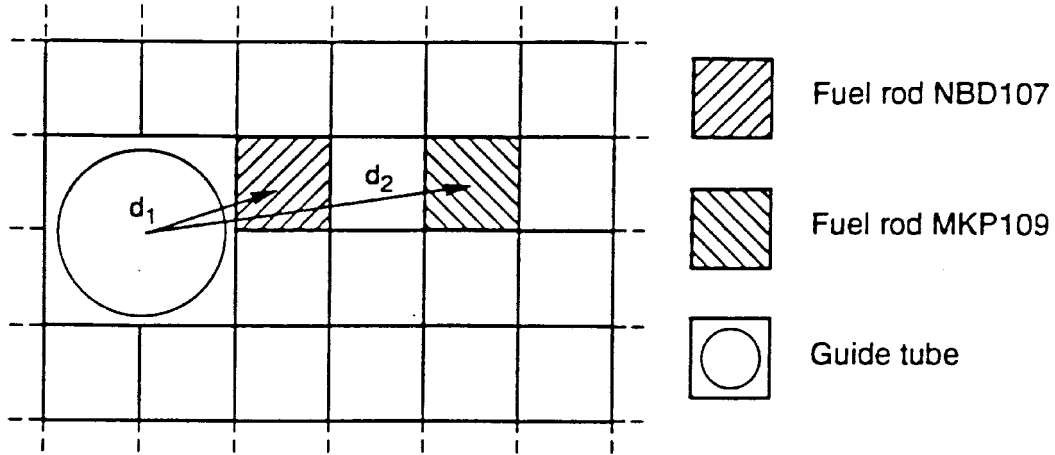
Substituting  $\phi$  from Eq. (E.1) for constant power into Eq. (E.2) to derive the formula for  $^{239}\text{Pu}$  production rate normalized to the  $^{235}\text{U}$  fission rate (or equivalent burnups):

$$\begin{aligned} R &= K \frac{N_{\text{U}238} \sigma(n,\gamma)_{\text{U}238}}{N_{\text{U}235} \sigma(n,f)_{\text{U}235}} \\ &= C \frac{\sigma(n,\gamma)_{\text{U}238}}{\sigma(n,f)_{\text{U}235}} , \end{aligned} \quad (\text{E.3})$$

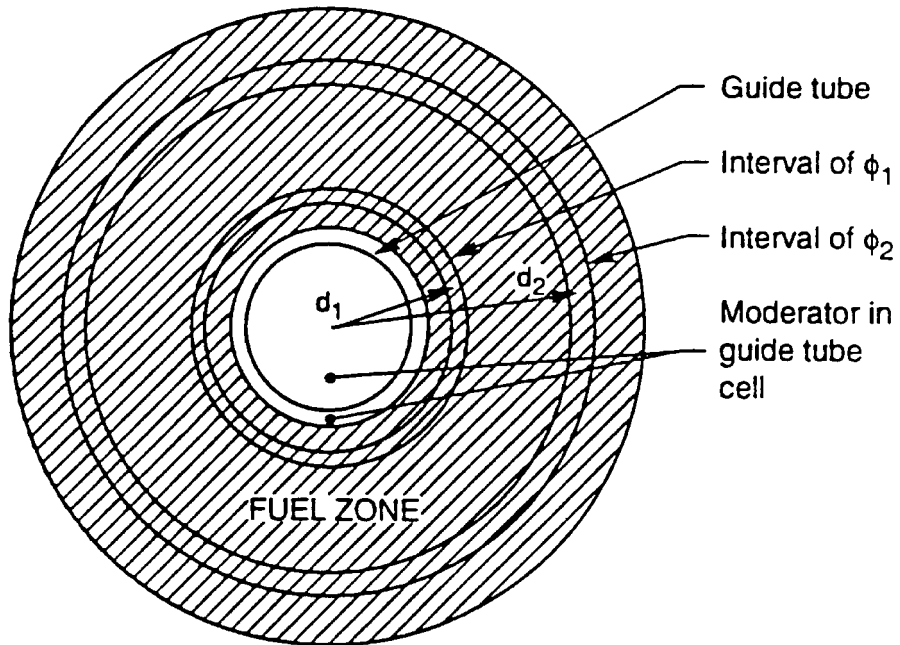
where the atomic density ratio  $N_{\text{U}238}/N_{\text{U}235}$  is assumed constant in all fuel rods during the irradiation, and thus  $C$  is a constant. The  $^{239}\text{Pu}$  production rate may be derived as a function of  $C$  at two different locations. Then the value of the ratio of the two production rates may be calculated because  $C$  is contained in both the numerator and denominator of the ratio and may be eliminated.

Energy-dependent flux is computed at different mesh intervals of a unit cell by the XSDRNPM code in SCALE. The relative locations of the fuel rod positions in Figs. 5 and 7 are shown in Fig. E.1. Then, in the method described in Sect. 2 and shown in Fig. 2, the path-B unit cell is developed. The center-to-center distances,  $d_1$  and  $d_2$ , between the guide tube and the two fuel rods are similar to the distances in Fig. E.1 between the center of the cell, or guide tube, and the two intervals in the fuel zone at which the code computes flux,  $\phi_1$  and  $\phi_2$ , respectively.





(a) Relative locations of fuel rods NBD107 and MKP109 at distances  $d_1$  and  $d_2$  from guide tube.



(b) Larger unit cell of path B in SAS2 with intervals of XSDRNPM case shown at  $d_1$  and  $d_2$ .

Fig. E.1. Method of simulating the actual rod locations (a) in unit cell (b) to obtain  $\phi_1$  and  $\phi_2$ .

The XSDRNPM code was used to obtain the 27-group flux spectrum by mesh intervals within the zones of the path-B cell, including the fuel zone intervals at  $d_1$  and  $d_2$ . The AMPX system ALE code was used to edit the working cross-section library input to XSDRNPM, determining the 27-group values for  $\sigma(n,f)_{U235}$  and  $\sigma(n,\gamma)_{U238}$ . Data at the end of the first cycle calculation of the 37.12-GWd/MTU case for Assembly D047, Rod MKP109, were used in this example. Table E.1 shows the two sets of group cross sections and the interval flux  $\phi_1$  and  $\phi_2$  at  $d_1$  and  $d_2$  of Fig. E.1. The group products  $\sigma_i\phi_{1,i}$  and  $\sigma_i\phi_{2,i}$  and sums of these products for the above nuclides are also listed. The one-group or effective cross sections are then computed by

$$\sigma_{\text{eff}} = \frac{\sum_{i=1}^{27} \sigma_i \phi_i}{\sum_{j=1}^{27} \phi_j} . \quad (\text{E.4})$$

The  $\sigma_{\text{eff}}$  values computed from Eq. (E.4) for  $\sigma(n,\gamma)_{U238}$  are 0.902 and 0.942 and for  $\sigma(n,f)_{U235}$  are 48.04 and 54.82 at  $d_2$  and  $d_1$ , respectively. The ratios of  $\sigma(n,\gamma)_{U238}/\sigma(n,f)_{U235}$  are 0.01878 and 0.01718 at  $d_2$  and  $d_1$ , respectively. Dividing the first ratio by the second equals 1.093, indicating an increase in the  $^{239}\text{Pu}$  production rate at  $d_2$  (or in the simulated fuel rod MKP109 of Assembly D047) of 9.3% over the  $^{239}\text{Pu}$  production rate at  $d_1$  (or in fuel rod NBD107 of Assembly BT03). Thus, this example tends to show that the different neutron spectra significantly affect  $^{239}\text{Pu}$  production rates at different fuel locations.

Table E.1 shows individual energy-group data for flux, cross sections and their products, in addition to the integrated data and  $\sigma_{\text{eff}}$ . Significant differences are found in the reaction rates starting with group 22. The largest differences are in  $\sigma(n,f)_{U235,i} \phi_i$  because  $\sigma(n,f)_{U235}$  increases more at thermal energies (higher groups) than the corresponding increases in  $\sigma(n,\gamma)_{U238}$ .

All the fissions in the above method are assumed to be produced by  $^{235}\text{U}$ . Although the method has the benefits of showing group data, it is not as complete as applying the total fission cross section as indicated in Eq. (E.1). The XSDRNPM code has an option for printing requested activities by unit cell radial interval. Table E.2 displays a list of these activities at  $\phi_1$  and  $\phi_2$  during cycles 2 and 4 of the same case used in the above example. Activities associated with the cross sections for  $\Sigma(n,\gamma)_{U238}$ ,  $\Sigma(n,f)_{U235}$ ,  $\Sigma(n,f)_{U238}$ ,  $\Sigma(n,f)_{\text{Pu}239}$ , and  $\Sigma(n,f)_{\text{Pu}241}$  are listed. Thus, a more complete derivation of the  $^{239}\text{Pu}$  production rate for the interval activities is computed. The ratio of these production rates of the two intervals is 1.0785 during cycle 2 and 1.0775 during cycle 4, or an average of 1.078. Thus, the more complete method of computing the example indicates an increase in  $^{239}\text{Pu}$  production rate at  $\phi_2$  of 7.8% more than the rate at  $\phi_1$ .

Note that the preceding example does not provide a method for computing the actual changes in nuclide compositions at different rod locations. That type of calculation would require multidimensional tracking of the nuclide densities over the complete irradiation history. This example was simply a "snapshot" case, which assumed no density variation between rods. However, the example does illustrate that the variation in flux spectra as a function of distance from the extra moderator at the guide tubes can cause a significant change in isotopic reaction rates. Also, the variation in reaction rates at different rod locations should affect final nuclide concentrations of the spent fuel pellet samples. This variation may partially explain the first set of  $^{239}\text{Pu}$  data in Table 38 listing the assembly average as 5.4% and a spread in data from all 10 assemblies, or batches of 1.1 to 8.7%. Also, in Table 27 it is seen that the  $^{239}\text{Pu}$  percentage differences are 2.1, 1.1, and 8.0% for assemblies D047, D101, and BT03, respectively, but

Table E.1. Example of effective cross sections,  $\sigma(n,\gamma)_{U238}$  and  $\sigma(n,f)_{U235}$ , derived from group values and flux  $\phi_1$  and  $\phi_2$  at unit cell locations  $d_1$  and  $d_2$ 

Energy group	$\phi_1$	$\phi_2$	$\sigma(n,\gamma)_{U238}$	$\sigma(n,\gamma)_{U238}\phi_1$	$\sigma(n,\gamma)_{U238}\phi_2$	$\sigma(n,f)_{U235}$	$\sigma(n,f)_{U235}\phi_1$	$\sigma(n,f)_{U235}\phi_2$
1	0.40	0.40	0.01	0.0	0.0	2	1	1
2	2.81	2.83	0.01	0.0	0.0	1	3	3
3	3.27	3.46	0.04	0.0	0.0	1	3	3
4	1.99	2.11	0.07	0.1	0.1	1	2	2
5	2.92	3.12	0.11	0.3	0.3	1	3	3
6	5.23	5.62	0.12	0.6	0.6	1	5	6
7	5.13	5.42	0.13	0.7	0.7	1	5	5
8	3.85	3.97	0.37	1.4	1.5	2	8	8
9	3.05	3.08	0.82	2.5	2.5	4	12	12
10	2.82	2.83	1.29	3.7	3.7	8	23	23
11	2.66	2.65	2.06	5.5	5.5	18	48	48
12	1.72	1.70	3.30	5.7	5.6	38	65	65
13	1.50	1.47	3.11	4.7	4.6	42	63	62
14	1.42	1.38	6.01	8.5	8.3	34	48	47
15	0.83	0.80	0.50	0.4	0.4	14	12	11
16	0.46	0.45	0.48	0.2	0.2	16	7	7
17	0.20	0.19	0.48	0.1	0.1	56	11	11
18	0.13	0.13	0.41	0.1	0.1	73	9	9
19	0.30	0.29	0.49	0.1	0.1	57	17	17
20	1.04	1.00	0.62	0.6	0.6	75	78	75
21	0.32	0.31	0.71	0.2	0.2	132	42	41
22	0.70	0.63	0.76	0.5	0.5	166	116	105
23	2.76	2.39	1.09	3.0	2.6	194	535	464
24	2.29	1.94	1.53	3.5	3.0	298	682	578
25	1.01	0.85	1.97	2.0	1.7	412	416	350
26	0.68	0.57	2.65	1.8	1.5	584	397	333
27	0.11	0.10	4.31	0.5	0.4	983	108	98
Totals	49.60	49.69		46.7	44.8		2719	2387
$\frac{\sum_i \sigma_i \phi_i}{\sum_j \phi_j}$				0.942	0.902		54.82	48.04

Table E.2. Fuel-rod-dependent  $^{239}\text{Pu}$  production rate ratio from XSDRNPM computed activities  $\Sigma(n,\gamma)_{\text{U}238} \phi$  and  $\Sigma(n,f)_{\text{Total}} \phi$

	Activities by input cycle and space interval			
	2	2	4	4
Cycle, $c$	2	2	4	4
Interval, $k$	1	2	1	2
Distance, $d_k$	$d_1$	$d_2$	$d_1$	$d_2$
$\Sigma(n,\gamma)_{\text{U}238,c,k} \phi_{c,k}$	$3.3592 \times 10^{-3}$	$3.2171 \times 10^{-3}$	$3.3491 \times 10^{-3}$	$3.2055 \times 10^{-3}$
$\Sigma(n,f)_{\text{U}235,c,k} \phi_{c,k}$	$3.7084 \times 10^{-3}$	$3.2554 \times 10^{-3}$	$1.4528 \times 10^{-3}$	$1.2750 \times 10^{-3}$
$\Sigma(n,f)_{\text{U}238,c,k} \phi_{c,k}$	$3.499 \times 10^{-4}$	$3.529 \times 10^{-4}$	$3.504 \times 10^{-4}$	$3.535 \times 10^{-4}$
$\Sigma(n,f)_{\text{Pu}239,c,k} \phi_{c,k}$	$1.6644 \times 10^{-3}$	$1.4749 \times 10^{-3}$	$2.2690 \times 10^{-3}$	$2.0039 \times 10^{-3}$
$\Sigma(n,f)_{\text{Pu}241,c,k} \phi_{c,k}$	$2.014 \times 10^{-4}$	$1.771 \times 10^{-4}$	$6.579 \times 10^{-4}$	$5.777 \times 10^{-4}$
$\Sigma(n,f)_{\text{Total},c,k} \phi_{c,k}$	$5.924 \times 10^{-3}$	$5.260 \times 10^{-3}$	$4.730 \times 10^{-3}$	$4.209 \times 10^{-3}$
$R_{c,k} = \frac{(n,\gamma)_{\text{U}238,c,k}}{(n,f)_{\text{Total},c,k}}$	0.5670 K <sup>a</sup>	0.6116 K	0.7080 K	0.7615 K
$(R_2/R_1)_c = R_{c,2}/R_{c,1}$	1.0785		1.0775	
$R_{\text{av}} = (R_2/R_1)_{\text{average}}$	1.0780			
$R_{\text{ap}} = (R_2/R_1)_{\text{applied}}$	1.0000 <sup>b</sup>			
$\text{Diff} = \left( \frac{R_{\text{av}} - R_{\text{ap}}}{R_{\text{ap}}} \right) 100\%$	7.8%			
$^{239}\text{Pu}$ -%-diff: D047-BT03	5.9%			
$^{239}\text{Pu}$ -%-diff: D101-BT03	7.0%			

<sup>a</sup>Constant K in relationship for  $R_{c,k}$ , Eq. (E.3).

<sup>b</sup>Assumption applied in comparing compositions at  $d_1$  and  $d_2$  assembly average values.

the average of the three Calvert Cliffs assemblies for  $^{239}\text{Pu}$  is 4.0%. Although the average percentage difference of 4.0% for assemblies in which the analyzed rod locations were both near and far from the guide tubes was close to the 5.4% average of all 10 assemblies, the spread of 5.9% in the D047 and BT03 assembly data and the spread of 6.9% in the D101 and BT03 data tend to support the 7.8% difference in the radial variation of nuclide contents of the above example. In both cases, it was shown that the  $^{239}\text{Pu}$  of a rod adjacent to the guide tube would tend to be overpredicted by an assembly average calculation. At least part of the variation in percentage differences in pellet sample comparison are from the choice of sampled fuel rods, in addition to the numerous reasons for random fluctuations in computing or measuring nuclide compositions.

## E.2 AXIAL VARIATION IN $^{239}\text{Pu}$

It was estimated by calculations in the preceding discussion that the  $^{239}\text{Pu}$  production rate can be dependent on the change in the flux spectrum resulting from the proximity to the extra moderation within a guide tube. It was concluded that the accuracy of the SCALE calculation of assembly average isotopic composition is significantly reduced when applied to various individual rods. Thus, there are significant radial spatial effects in a fuel assembly that are found to account for part of the differences in measured and computed compositions. This, in turn, leads to the question of whether spatial effects in the axial dimension may also be significant. The axial burnups listed in Table 2 show burnup ratios in the range 1.5 to 2.0 in pellet samples taken from the same fuel rod for Calvert Cliffs and H. B. Robinson reactors. A summary of the differences between measured and computed  $^{239}\text{Pu}$  contents for the lowest and highest burnups along the fuel rods is shown in Table E.3. Included in the table are the pellet heights above the bottom of the fuel, the burnups, the initial  $^{235}\text{U}$  enrichments, and the differences and their ranges. The percentage difference at the higher burnup was always larger than that at the lower burnup by a minimum of 4.2% or by an average of 5.8%. Although this variation was not analyzed in great detail for this project, some of the reasons for this condition are given consideration in the following discussion.

Typical initial  $^{235}\text{U}$  enrichments associated with various fuel burnups, supplied by reactor facilities for a project to determine decay heat rates,<sup>21</sup> are listed in Table E.4. In order to operate for longer fuel cycles, the initial enrichment of the fuel must be increased. A freshly loaded assembly is usually given enough excess reactivity to balance the deficiency in the fissionable nuclide content of adjacent assemblies during the last portion of their residence time. This reactivity balance takes place when the net transfer of neutrons between assemblies is such that the fresher fuel is supplying neutrons to the older fuel. More generally, the net transfer of neutrons takes place from one fuel volume of higher reactivity to another of lower reactivity. At burnups much larger than normal for a given enrichment, there would be substantially more neutrons in the net transfer. Although the initial  $^{235}\text{U}$  enrichment was constant in the fuel within an assembly for all cases in this study, there was some variation during irradiation in the density of a fissionable nuclide of the different fuel pellets. Table E.5 shows data for the three analyzed pellets in Assembly D047 Rod MKP109 from Calvert Cliffs Unit 1 PWR. The measured burnups and compositions of the dominant fissionable nuclides  $^{235}\text{U}$ ,  $^{239}\text{Pu}$ , and  $^{241}\text{Pu}$  are listed. There is a large decrease in the density of  $^{235}\text{U}$  or the total of the three fissile nuclides as the burnup is increased. Thus, there would tend to be a significant decrease in reactivity, or infinite neutron multiplication constant  $k_{\infty}$ , with an increase in burnup. This effect was verified by values equivalent to  $k_{\infty}$ , computed in the neutronics treatment by XSDRNPM at the middle of the last cycle. The  $k_{\infty}$  values are listed in Table E.5 also. The decrease in  $k_{\infty}$  from 0.983 to 0.876 is not inconsistent with the 13.415 to 8.917 mg/g  $\text{UO}_2$  decrease in the total density of  $^{235}\text{U}$ ,  $^{239}\text{Pu}$ , and  $^{241}\text{Pu}$  of the pellet at the lowest height compared with the more central pellet.

Table E.3. Differences between measured and computed  $^{239}\text{Pu}$  contents<sup>a</sup> over the range in burnup along the fuel rods

Assembly (rod)	Lowest burnup	Highest burnup	% (high) - % (low)
D047 (MKP109):			
Sample pellet height, cm	13.20	165.22	
Burnup, GWd/MTU	27.35	44.34	
Initial enrichment, wt % $^{235}\text{U}$	3.04	3.04	
$^{239}\text{Pu}$ percentage difference <sup>b</sup>	0.4	4.6	4.2
D101 (MLA098):			
Sample pellet height, cm	9.10	161.90	
Burnup, GWd/MTU	18.68	33.17	
Initial enrichment, wt % $^{235}\text{U}$	2.72	2.72	
$^{239}\text{Pu}$ percentage difference <sup>b</sup>	-1.5	5.6	7.1
BT03 (NBD107):			
Sample pellet height, cm	11.28	161.21	
Burnup, GWd/MTU	31.40	46.46	
Initial enrichment, wt % $^{235}\text{U}$	2.45	2.45	
$^{239}\text{Pu}$ percentage difference <sup>b</sup>	5.8	11.8	6.0
B05 (N-9)			
Sample pellet height, cm	11.0	226.0	
Burnup, GWd/MTU	16.02	31.60	
Initial enrichment, wt % $^{235}\text{U}$	2.56	2.56	
$^{239}\text{Pu}$ percentage difference <sup>b</sup>	7.0	12.8	5.8

<sup>a</sup>Computed by applying 27BURNUPLIB library.

<sup>b</sup>(Calculated/measured - 1)  $\times$  100%.

Table E.4. PWR  $^{235}\text{U}$  enrichments for different burnups

Fuel burnup, GWd/MTU	Initial enrichment, wt % $^{235}\text{U}$
25	2.4
30	2.8
35	3.2
40	3.6
45	3.9
50	4.2

Table E.5. Measured fissionable nuclide contents and computed neutron multiplication constant ( $k_{\infty}$ ) of Assembly D047 Rod MKP109

Pellet location, cm height	13.20	27.70	165.22
Burnup, GWd/MTU	27.35	37.12	44.43
Percentage increase in burnup	0	22	33
Initial enrichment, wt % $^{235}\text{U}$	3.04	3.04	3.04
<b>Nuclide</b>			
$^{235}\text{U}$ , mg/g $\text{UO}_2$	8.470	5.170	3.540
$^{239}\text{U}$ , mg/g $\text{UO}_2$	4.264	4.357	4.357
$^{241}\text{U}$ , mg/g $\text{UO}_2$	0.681	0.903	1.020
Total, mg/g $\text{UO}_2$	13.415	10.430	8.917
Computed $k_{\infty}$ <sup>a</sup>	0.983	0.915	0.876

<sup>a</sup>At midpoint of the final cycle that assembly was loaded in the reactor.

The difference between the calculational model assumptions and the prevailing conditions of the fuel should be considered. The model assumes that fuel composition, burnup, and reactivity remain constant axially. However, as seen in Table E.5 and discussed above, differences in the neutronics characteristics produce a net flow of neutrons into the axial segment that includes the more central pellet. Some of these neutrons are absorbed and cause the production of a fission reaction. The SCALE model, in contrast to the actual neutron transfer, simply increases the flux sufficiently to produce the required burnup or fission reactions. Note the differences in the actual case and the model. The combined net flow of neutrons by energy group is similar to a source of neutrons having traversed a finite (and significant) path distance. Conversely, the model requires that this source of neutrons be replaced by additional fission neutrons which at birth have traversed a path distance of zero. Thus, the average neutron absorbed in the central rod pellet in the real case is better moderated (having more scattering collisions in the longer path) than those of the calculation. Alternatively, there would be a harder flux spectrum, more significantly in the latter part of the burnup, in applying the uniform axial reactivity in the SCALE model. This harder flux spectrum, as in the radial variation case discussed earlier, produces an increased  $^{239}\text{Pu}$  reaction rate per fission and leads to the overprediction of  $^{239}\text{Pu}$  at the rod center relative to that closer to the bottom of the rod.

### E.3 SECONDARY EFFECTS OF VARIATION IN $^{239}\text{Pu}$ ON $^{235}\text{U}$

Assuming the burnup and isotopic energies per fission to be accurate, any error in the number of fissions by one of the fissile nuclides must be compensated by changes in the number of fissions of other fissile isotopes. The two major fissile nuclides are  $^{235}\text{U}$  and  $^{239}\text{Pu}$ . A higher computed production rate in  $^{239}\text{Pu}$  would produce an excess or positive difference for  $^{239}\text{Pu}$ . Thus, an excess  $^{239}\text{Pu}$  content prediction should tend to reduce the number of  $^{235}\text{U}$  fissions and cause an excess in the  $^{235}\text{U}$  prediction, provided that relative changes in cross sections of  $^{235}\text{U}$  and  $^{239}\text{Pu}$  are not significant. In brief, this states (1) that the differences in contents for  $^{235}\text{U}$  and  $^{239}\text{Pu}$  should have the same sign and (2) that the contents for  $^{235}\text{U}$  and  $^{239}\text{Pu}$  should change similarly (in terms of change in recoverable fission energy) from case to case.

Limited testing of this effect showed it was not true in all cases. For example, if cases are chosen along the Rod MKP109 of Assembly D047, the positive increases in the differences in  $^{239}\text{Pu}$  as heights increase are accompanied by decreases in the differences in  $^{235}\text{U}$ . Possibly the changes in burnup and other axial-dependent conditions cause complexities in the neutronics and depletion calculations sufficient to introduce other more dominant effects. Note that one of the conditions stated at the outset of the above discussion on the effects of variation of  $^{239}\text{Pu}$  on  $^{235}\text{U}$  was that relative changes in the cross sections of  $^{235}\text{U}$  and  $^{239}\text{Pu}$  were assumed to be insignificant. The possibility does exist that although there was a calculated increase in content of  $^{239}\text{Pu}$ , the number of fissions from  $^{239}\text{Pu}$  would decrease due to a relatively lower fission cross section. However, the correlations between  $^{235}\text{U}$  and  $^{239}\text{Pu}$  contents for cases of similar heights in different rods were very significant because the radial variations in flux are computed in XSDRNPM whereas the axial flux is held constant in the 1-D radial model applied by the calculation.



**INTERNAL DISTRIBUTION**

- |                     |                                                               |
|---------------------|---------------------------------------------------------------|
| 1. C. W. Alexander  | 23-27. C. V. Parks                                            |
| 2. S. M. Bowman     | 28. L. M. Petrie                                              |
| 3. B. L. Broadhead  | 29. R. T. Primm                                               |
| 4. J. A. Bucholz    | 30. J.-P. Renier                                              |
| 5. R. D. Dabbs      | 31. J. W. Roddy                                               |
| 6. M. D. DeHart     | 32. R. W. Roussin                                             |
| 7. M. B. Emmett     | 33. J. C. Ryman                                               |
| 8. N. M. Greene     | 34. C. H. Shappert                                            |
| 9-10. O. W. Hermann | 35. R. M. Westfall                                            |
| 11. M. Kuliasha     | 36. B. A. Worley                                              |
| 12. L. C. Leal      | 37. R. Q. Wright                                              |
| 13. S. B. Ludwig    | 38-39. Laboratory Records Dept.                               |
| 14. S. K. Martin    | 40. Laboratory Records, ORNL-RC<br>Document Reference Section |
| 15. G. E. Michaels  | 41. ORNL Y-12 Research Library                                |
| 16. B. D. Murphy    | 42. Central Research Library                                  |
| 17-21. L. F. Norris | 43. ORNL Patent Section                                       |
| 22. J. V. Pace      |                                                               |

**EXTERNAL DISTRIBUTION**

44. R. Anderson, General Nuclear Systems, Inc., 220 Stoneridge Dr., Columbia, SC 29210
45. M. G. Bailey, Office of Nuclear Material Safety & Safeguards, U.S. Nuclear Regulatory Commission, MS TWFN 8F5, Washington, DC 20555
46. L. Barrett, Office of Civilian Radioactive Waste Management, RW-232 20545, U.S. Department of Energy, Washington, DC 20545
47. P. Baylor, Office of Civilian Radioactive Waste Management, RW-36, U.S. Department of Energy, Washington, DC 20545
48. C. J. Benson, Bettis Atomic Power Laboratory, P.O. Box 79, West Mifflin, PA 15122
49. J. Bickel, U.S. Department of Energy, Albuquerque Operations Office, P.O. Box 5400, Albuquerque, NM 87115
50. J. Boshoven, GA Technologies, Inc., P.O. Box 85608, 10955 John J. Hopkins Dr., San Diego, CA 92121
51. M. C. Brady, Sandia National Laboratories, 101 Convention Center Drive, Suite 880, Las Vegas, NV 89109
52. P. Bunton, U.S. Department of Energy, RW-1, Washington, DC 20545
53. R. J. Cacciapouti, Yankee Atomic Electric Co., 1617 Worcester Rd., Framington, MA 01701
54. R. Carlson, Lawrence Livermore National Laboratory, P.O. Box 808, Livermore, CA 94550
55. C. R. Chappell, U.S. Nuclear Regulatory Commission, Office of Nuclear Material Safety and Safeguards, TWFN 8F5, Washington, DC 20555
56. J. S. Choi, Lawrence Livermore National Laboratory, P.O. Box 808, Livermore, CA 94550

57. J. Clark, 2650 Park Tower Drive, Suite 800, Vienna, VA 22180
58. J. Conde, Consejo de Seguridad Nuclear, Justo Dorado, 11, 28040 Madrid, Spain
59. D. R. Conners, Bettis Atomic Power Laboratory, P.O. Box 79, West Mifflin, PA 15122
60. M. Conroy, U.S. Department of Energy, M-261 Quince Orchard, Washington, DC 20585-0002
61. P. J. Cooper, Sandia National Laboratories, P.O. Box 5800, Albuquerque, NM 87185-0716
62. W. Davidson, Los Alamos National Laboratory, Group A4, MSF-611, Los Alamos, NM 87845
- 63-65. F. J. Davis, Sandia National Laboratories, P.O. Box 5800, Div. 6302, MS 1333, Albuquerque, NM 87185-0716
66. D. Dawson, Transnuclear, Inc., 2 Skyline Dr., Hawthorne, NY 10532-2120
67. T. W. Doering, TESS, B&W Fuel Co., MS 423, Suite 527, P.O. Box 98608, 101 Convention Center Drive, Las Vegas, NV 89109
68. R. Doman, Nuclear Packaging, Inc., 1010 S. 336th St., Suite 220, Federal Way, WA 98003
69. E. Easton, U.S. Nuclear Regulatory Commission, Office of Nuclear Materials Safety and Safeguards, Washington, DC 20555
70. R. C. Ewing, Sandia National Laboratories, P.O. Box 5800, Div. 6643, MS 0716, Albuquerque, NM 87185-0716
71. C. Garcia, U.S. Department of Energy, Albuquerque Operations Office, P.O. Box 5400, Albuquerque, NM 87115
72. I. Gauld, Whiteshell Laboratories, AECL Research, Pinawa Manitoba R0E1L0 Canada
73. G. Gualdrini, ENEA-TIB/FICS, C.R.E. "E. Clementel," Via Mazzini, 2, I-40139 Bologna, Italy
74. H. Geiser, Wissenschaftlich-Technische Ingenieurberatung GmbH, Mozartstrasse 13, 5177 Titz-Rodingen, Federal Republic of Germany
75. S. Hanauer, U.S. Department of Energy, RW-22, Washington, DC 20545
76. C. Haughney, U.S. Nuclear Regulatory Commission, Office of Nuclear Materials Safety and Safeguards, TWFN 8F5, Washington, DC 20555
77. L. Hassler, Babcock & Wilcox, P.O. Box 10935, Lynchburg, VA 24506-0935
78. U. Jenquin, Battelle Pacific Northwest Laboratory, P.O. Box 999, Richland, WA 99352
79. E. Johnson, E. R. Johnson Associates, Inc., 9302 Lee Hwy, Suite 200, Fairfax, VA 22031
80. R. Kelleher, International Atomic Energy Agency, Division of Publications, Wagramerstrasse 5, P.O. Box 100, Vienna, Austria A-1400
81. R. Kidman, Los Alamos National Laboratory, Group A4, MSF-611, Los Alamos, NM 87845
82. G. Kirchner, University of Bremen, FB 1 Postfach 330440, D-W-2800 Bremen 33, Federal Republic of Germany
83. C. Kouts, Office of Civilian Radioactive Waste Management, RW-36, U.S. Department of Energy, Washington, DC 20545
84. S. Kraft, Nuclear Energy Institute, 1776 I Street, Suite 400, Washington, DC 20086
85. P. Krishna, TRW Environmental Safety Systems, 600 Maryland Ave. S.W., Suite 695, Washington, DC 20024
86. A. Kubo, 2650 Park Tower Drive, Suite 800, Vienna, VA 22180
87. W. H. Lake, Office of Civilian Radioactive Waste Management, U.S. Department of Energy, RW-46, Washington, DC 20585
88. R. Lambert, Electric Power Research Institute, 3412 Hillview Ave., Palo Alto, CA 94304
- 89-91. D. Lancaster, 2650 Park Tower Drive, Suite 800, Vienna, VA 22180
92. D. Langstaff, U.S. Department of Energy, Richland Operations Office, P.O. Box 550, Richland, WA 99352
93. D. Lillian, U.S. Department of Energy, M-261 Quince Orchard, Washington, DC 20585-0002
94. C. Marotta, 1504 Columbia Ave., Rockville, MD 20850

95. M. Mason, Transnuclear, Two Skyline Drive, Hawthorne, NY 10532-2120
96. J. Massey, Sierra Nuclear Corporation, 5619 Scotts Valley Drive, Number 240, Scotts Valley, CA 95066
97. W. Mings, U.S. Department of Energy, Idaho Operations Office, 550 2nd St., Idaho Falls, ID 83401
98. A. Mobashevan, Roy F. Weston, Inc., 955 L'Enfant Plaza, SW, 8th Floor, Washington, DC 20024
99. R. Morgan, 2650 Park Tower Drive, Suite 800, Vienna, VA 22180
100. M. Mount, LLNL/FESSP Washington Operations, 20201 Century Blvd., 2nd floor, Germantown, MD 20874
101. P. K. Nair, Manager, Engineered Barrier System, Center for Nuclear Waste Regulatory Analyses, Southwest Research Institute, 6220 Culebra Road, San Antonio, TX 78238-5166
102. D. Napolitano, Nuclear Assurance Corp., 5720 Peachtree Parkway, Norcross, GA 30092
103. C. W. Nilsen, Office of Nuclear Material Safety and Safeguards, U.S. Nuclear Regulatory Commission, MS TWFN-9F29, Washington, DC 20555
104. D. J. Nolan, 2650 Park Tower Drive, Suite 800, Vienna, VA 22180
- 105-106. Office of Scientific and Technical Information, U.S. Department of Energy, P.O. Box 62, Oak Ridge, TN 37831
107. Office of the Assistant Manager for Energy Research and Development, Department of Energy Oak Ridge Operations (DOE-ORO), P.O. Box 2008, Oak Ridge, TN 37831
108. C. E. Olson, Sandia National Laboratories, P.O. Box 5800, Div. 6631, MS 0715, Albuquerque, NM 87185-0716
109. N. Osgood, U.S. Nuclear Regulatory Commission, Office of Nuclear Materials Safety and Safeguards, TWFN 8F5, Washington, DC 20555
110. O. Ozer, Electric Power Research Institute, 3412 Hillview Ave., Palo Alto, CA 94304
111. P. Pacquin, General Nuclear Systems, Inc., 220 Stoneridge Dr., Columbia, SC 29210
112. T. Parish, Department of Nuclear Engineering, Texas A & M University, College Station, TX 77843-3313
113. F. Prohammer, Argonne National Laboratory, 9700 S. Cass Ave., Bldg.308, Argonne, IL 60439-4825
- 114-116. M. Rahimi, 2650 Park Tower Drive, Suite 800, Vienna, VA 22180
117. B. Rasmussen, Duke Power Co., P.O. Box 33189, Charlotte, NC 28242
118. B. Reid, Battelle Pacific Northwest Laboratory, P.O. Box 999, Richland, WA 99352
119. C. Rombough, CTR Technical Services, Inc., 5619 Misty Crest Dr., Arlington, TX 76017-4147
120. T. L. Sanders, Sandia National Laboratories, P.O. Box 5800, Div. 6609, MS 0720, Albuquerque, NM 87185-0716
121. K. D. Seager, Sandia National Laboratories, P.O. Box 5800, Div. 6643, MS 0716, Albuquerque, NM 87185-0716
122. M. Smith, U.S. Department of Energy, Yucca Mountain Project Office, 101 Convention Center Dr., Las Vegas, NV 89190
123. M. Smith, Virginia Power Co., P.O. Box 2666, Richmond, VA 23261
124. K. B. Sorenson, Sandia National Laboratories, P.O. Box 5800, Div. 6643, MS 0716, Albuquerque, NM 87185-0716
125. J. B. Stringer, Duke Engineering & Services, 230 S. Tryon St., P.O. Box 1004, Charlotte, NC 28201-1004
126. F. C. Sturz, Office of Nuclear Material Safety & Safeguards, U.S. Nuclear Regulatory Commission, MS TWFN 8F5, Washington, DC 20555
127. J. Sun, Florida Power & Light Co., P.O. Box 029100, Miami, FL 33102

128. T. Suto, Power Reactor and Nuclear Fuel Development Corp., 1-9-13, Akasaka, Minato-Ku, Tokyo, Japan
129. R. J. Talbert, Battelle Pacific Northwest Laboratory, P.O. Box 999, Richland, WA 99352
130. H. Taniuchi, Kobe Steel, Ltd., 2-3-1 Shinhama, Arai-Cho, Takasago, 676 Japan
131. T. Taylor, INEL, P.O. Box 4000, MS 3428, Idaho Falls, ID 83403
132. B. Thomas, VECTRA Technologies, Inc., 6203 San Ignacio Ave., Suite 100, San Jose, CA 95119
133. D. A. Thomas, B&W Fuel Co., 101 Convention Center Drive, Suite 527, MS 423, Las Vegas, NV 89109
134. J. R. Thornton, TRW Environmental Safety Systems, 2650 Park Tower Dr., Suite 800, Vienna, VA 22180
135. J. Vujic, Department of Nuclear Engineering, University of California at Berkeley, Berkeley, CA 94720
136. G. Walden, Duke Power Co., P.O. Box 33189, Charlotte, NC 28242
137. M. E. Wangler, U.S. Department of Energy, EH-33.2, Washington, DC 20585-0002
138. R. Weller, U.S. Nuclear Regulatory Commission, TWFN 8F5, Washington, DC 20555
139. A. Wells, 2846 Peachtree Walk, Duluth, GA 30136
140. W. Weyer, Wissenschaftlich-Technische Ingenieurberatung GMBH, Mozartstrasse 13, 5177 Titz-Rodingen, Federal Republic of Germany
141. B. H. White, Office of Nuclear Material Safety & Safeguards, U.S. Nuclear Regulatory Commission, MS TWFN 8F5, Washington, DC 20555
142. J. Williams, Office of Civilian Radioactive Waste Management, U.S. Department of Energy, RW-46, Washington, DC 20545
143. M. L. Williams, LSU Nuclear Science Center, Baton Rouge, LA 70803
144. C. J. Withee, Office of Nuclear Material Safety & Safeguards, U.S. Nuclear Regulatory Commission, MS TWFN 8F5, Washington, DC 20555
145. R. Yang, Electric Power Research Institute, 3412 Hillview Ave., Palo Alto, CA 94304